The Use of Hydrogels to Prevent Biofouling on Underwater Sensors

By

Margaret J Smith

A thesis submitted for the degree of

Doctor of Philosophy (Ph.D.)

Department of Mechanical Engineering

Faculty of Engineering, University of Glasgow

2007

UNIVERSITY
of
GLASGOW

Dedicated to my husband Norrie.

Abstract

There is a need for effective biofouling resistant coatings to protect the detection ports of underwater sensors and cameras in order to extend their data collection period without costly intervention for cleaning of the ports and instrument recalibration. This project investigated the use of hydrogel coatings containing surfactants as biofouling resistant coating for these sensors. A study of gas membranes commonly used in gaseous sensors was also carried out to ascertain if the membrane structure affected the biofouling resistance of these materials.

The biofouling resistant coatings of hydrogel containing the cationic surfactants benzalkonium chloride and Arquad 2C-75 both extended the fouling free period in marine temperate waters. In the case of BAC the coating stayed clean for 10-12 weeks and the Arquad 2C-75 for 12-14 weeks. Due to the longer life of the hydrogel containing the Arquad 2C-75 instrument trials were carried out using this material. An effective method of attaching the coatings to the optical and membrane ports of sensors was developed and allows the coating to be either held in either a screw down or bolted polymer ring.

The diffusion coefficient of cationic surfactants in seawater is reduced compared to diffusion coefficients in freshwater. In seawater the diffusion coefficient of benzalkonium chloride was found to be 2.44×10^{-6} cm^2 s^{-1} compared to 7.78×10^{-6} cm^2 s^{-1} in distilled water at 25°C.

Careful choice of gas permeable membrane can result in a slightly longer biofouling lifetime, but only by 1-2 weeks. At 6 weeks all gas permeable membranes had significant fouling which affected their gas permeability. The diffusion rates of ammonia gas, a gas commonly measured in the sea, through PTFE gas sensor membranes varied between PTFE manufacturers with flux measurements ranging from 0.05-1131 μg cm^{-2} h^{-1}

In addition to the hydrogel testing on instruments within this project a variety of external research groups and environmental agencies are currently testing the

hydrogels on their instrument ports. These are Environmental Agency, Wales, UK; Partrac Ltd, Glasgow, UK and University of Wisconsin, Great Lakes Institute, Milwaukee, USA.

Index

Nomenclature

Å-	Ångström
ACT-	Alliance for Coastal Technologies
AF-	antifouling
AFM-	atomic force microscopy
APS-	alkylpyridinium salts
aq-	aqueous
Arquad 2C-75-	dialkyldimethylammonium chloride
AUFS-	attenuated units full-scale
BAC -	benzalkonium chloride
BC-	Before Christ
BTMA-	benzyltrimethylammonium chloride
C-	Centigrade
CA-	cellulose acetate
cm-	centimetre
CMC-	critical micelle concentration
CI-	confidence interval
CO_2-	carbon dioxide
3D-	three dimensional
D-	diffusion coefficient
Dk-	permeability
DO-	dissolved oxygen
EPS-	extracellular polymer secretions
ESEM-	Environmental Scanning Electron Microscope
EU-	European Union
EWU-	equilibrium water uptake
FDA-	fluorescein diacetate
FSD-	full scale deflection
GPa-	Giga Pascals
H^+-	hydrogen ions
HCl-	hydrochloric acid
HDPE-	high density polyethylene
HEMA-	hydroxyethylmethacrylate

Hg-	mercury
HPLC-	high pressure liquid chromatography
hrs-	hours
IC-	ion chromatography
IPD-	indirect photometric detection
k-	solubility coefficient
KCl-	potassium chloride
KCNS-	potassium thiocyanate
kV-	kilovolts
lb-	pound
LED-	light emitting diodes
ln-	natural logarithm
µ-	micro
m-	metre
ml-	millilitre
mm-	millimetre
M-	molar
N-	Newton
N_2-	nitrogen
NaCl-	sodium chloride
NaOH-	sodium hydroxide
NH_3-	ammonia
NH_4^+-	ammonium
nm-	nanometre
O_2-	oxygen
PEEK -	polyetheretherketone
PEG-	poly (ethylene glycol)
pH-	negative logarithm of the hydrogen ion concentration
PHEMA-	poly-hydroxyethyl methacrylate
PMMA -	polymethylmethacrylate
ppm-	parts per million
PTFE-	polytetrafluorethylene
PVC-	polyvinylchloride
QA/QC-	quality assurance and control

redox-	reduction-oxidation
R&D-	research and development
rpm-	revs per minute
RMS-	root mean squared
s-	second
SD-	standard deviation
SEM-	scanning electron microscope
SW-	seawater
TEGDMA-	tetraethylene glycol dimethacrylate
TBT-SPC-	tributyltin self-polishing copolymer paints
TBT-	tributyltin
Tg-	glass transition temperature
UK-	United Kingdom
UMBS-	University Marine Biological Station
USA-	United States of America
UV-	ultra-violet
wt-	weight
w/v-	weight/volume
w/w-	weight/weight
yr-	year
YSI-	Yellowstone Instruments

List of Tables

Chapter 3

Chapter 4

Chapter 5

Chapter 6

Chapter 7

List of Figures

Chapter 2

Chapter 3

Chapter 4

Chapter 5

Chapter 6

Chapter 7

Acknowledgements

Firstly I would like to thank Professor Mike Cowling for beginning me in this process and his continued support and supervision. Without his foresight and belief in me I would not have undertaken such a project. The supervision of Dr Hugh Flowers has been invaluable and I wish to thank him for so willingly sharing his vast scientific knowledge with me, also for his patience throughout and his critical comments.

The encouragement and input of Dr Harry Duncan is also greatly appreciated. His knowledge and wisdom and kept me focused on the goal. Professor John Hancock has advised me on thesis writing and such advice has been crucial to me completing this task and I am extremely grateful to him for this.

I wish to thank numerous technical staff in the departments of mechanical engineering and chemistry whose help contributed to the completion of this project; Mr Alex Torry, Mr Ian Pedan, Mr Alan Birkbeck and Mr Micheal Beglan.

Thanks also go to my wonderful friends, Alexis, Esther, Joan, Joanna, Lynn, Marilyn, Pauline, Alan and Phillip for their continued encouragement and interest throughout the last three years.

Heartfelt thanks goes to my husband Norrie whose great enthusiasm in my work has resulted in the completion of this thesis.

This research was supported by the FP5 Contract EVR1-CT-2002-40023 BRIMOM Biofouling Resistant Infrastructure for Measuring, Observing and Monitoring (2006). Such support was gratefully received.

Chapter 1

Introduction

The purpose of the research, which forms the basis for this thesis, was to investigate the biofouling resistant properties of poly hydroxyethylmethacrylate (PHEMA) hydrogels containing cationic surfactants. The target application was to protect the optical ports of underwater instruments and to prevent fouling on gaseous sensor membranes. These hydrogel coatings were developed mainly for use in the marine environment. However, some testing was carried out on their suitability for fresh water applications. The intrinsic biofouling resistant properties of various gas permeable membranes used on sensors to detect species such as ammonia, oxygen and carbon dioxide were also investigated.

The increased use of marine underwater sensors and cameras in the latter decade of the twentieth century has led to improved and robust instruments which can be deployed in coastal areas from remote buoys and from ocean going research vessels. The data from these instruments are used in weather forecasting, environmental monitoring and to monitor climatic change. The prevention of biofouling on gas and optical ports of marine and freshwater sensors, as well as underwater cameras, is required in order that long-term data acquisition can take place without frequent costly maintenance, which can include boat trips to remote buoys.

The quest for successful antifouling coatings has been on-going for thousands of years. Early Phoenicians and Carthaginians were said to have used pitch and possibly copper sheathing on ships bottoms while wax, tar and asphaltum were used by other ancient cultures. In the 5^{th} century B.C., historians report that coatings of arsenic and sulphur mixed with oil were used to combat shipworms. By the time of the Vikings around the 10^{th} century 'seal' tar was being used and from the 13^{th}-15^{th} centuries pitch was extensively used on boats. Lead sheathing became popular in the 16^{th} century and copper sheathing replaced this by the 17^{th} century. Whole ships were made from iron in the 18^{th} century. The first emergence of antifouling paints was in the 19^{th} century based on the idea of dispersing a toxicant in a polymeric vehicle (Yebra et al., 2004).

Since then to the present day a wide variety of paints to prevent biofouling have been developed probably the most infamous being tri-butyl tin, TBT. In recent years the quest for an environmentally acceptable marine fouling deterrent has continued as all manner of objects immersed in the sea require protection. When considering the protection of optical windows of sensors this deterrent must be transparent and for gaseous ports must not prevent the diffusion of gases so many paints and coatings available are unsuitable for this specific application. One type of coating that has been extensively researched is silicone (Estarlich et al. 2000; Berglin et al., 2003). However, these fail to prevent the adherence of microfouling thus causing problems in sensor detection and output. Wiper blades and chlorine generation across windows have also been investigated and a review by Cloete (2005) details the application of these. The use of hydrogels as biocompatible materials has prompted scientists and engineers (Cowing et al., 2000) to apply their unique chemistry in marine antifouling.

The mechanisms of biofouling have been widely studied in all areas where it occurs. In the case of marine and freshwater fouling the costs to shipping and other industries have resulted in the introduction of paints and coatings that ultimately have had successful but short periods in the market place due to their toxicity to marine life. The quest for prevention of fouling on these instruments has resulted in a vast array of possibilities, which will be discussed in full in chapter 3.

In chapter 2 the history, formation and organisation of biofilms is discussed. The understanding of how biofilms are formed has greatly expanded in the last forty years and in the last decade analytical instrument advances has led to them being studied in greater detail. Examples of typical marine fouling organisms are shown as fouling builds up over time. The manner of initial cell attachment is reviewed via the current literature. The use of antimicrobial agents is discussed as well as the reasons for their success in some cases and failure in others. The development of biofouling-resistant surfaces is also reviewed with its relevance to sensor protection discussed. Future technologies of biofouling-resistant methods and their possible application are also considered.

Chapter 3 looks at the application of underwater cameras and sensors and also the environments in which they are deployed. The properties of sea, brackish and fresh

water are discussed in relation to the sort of conditions in which cameras and sensors are deployed. The parameters sensors measure have implications on how they should be protected from fouling. The geometry of the sensor port has an impact on what type of fouling protection should be applied, as some shapes are more easily protected by a coating than others. The size of the port is also important as smaller ports i.e. less than 30mm in diameter have been shown to foul more (Kerr et al., 2003). The ways in which various parameters can be measured is discussed, as for some measurements there is a choice in which type of chemistry or technique is used. The effects of fouling on optical and detection ports are reported from the limited detail available. This aspect has to be considered by users as only they know the quality of data that is acceptable as output. The deleterious effects of fouling have more profound effects on some measurements than on others and this is discussed. The technologies currently available are reviewed for their usefulness and likely useful lifetime.

In chapter 4 the coatings and membranes with possible biofouling resistant properties are considered. Firstly the history, production and applications of hydrogel coatings are reviewed. In particular poly-(2-hydroxyethylmethacrylate) (PHEMA) hydrogels are reviewed. These hydrogels have found widespread use in biomedical applications due to their properties such as degree of swelling; biocompatibility; permeability and swelling kinetics (Refojo, 1976). Kim et al. (1992) stated that the ability of hydrogels to imbibe bioactive chemicals makes them ideal as carriers/coatings. The antifouling chemicals, cationic surfactants, and their activity when loaded into the hydrogel are discussed. Their properties and mode of action are explained in terms of preventing biofouling. Current analytical methods of quantitatively analysing surfactants are reviewed. The application of gas sensors and the background of their operation is detailed. The physical and chemical properties of the membranes used on the sensor ports are discussed and the effects of biofouling on diffusion are reviewed. The possible forms of biofouling coatings and their required properties are listed.

Chapter 5 is an experimental results chapter. It deals with the hydrogel/surfactant coatings. The method of hydrogel production is evaluated, as are methods of loading the hydrogel with surfactant. The methods of quantitative analysis of cationic surfactants are reported and the difficulties in quantifying the twin-quaternary, Arquad 2C-75 are detailed. A method to measure the liquid diffusion of

benzalkonium chloride is explained and discussed. The effects on the geometry of the hydrogels loaded with surfactants in fresh and seawater in relation to their application are detailed, as are the mechanical properties. Microscopic studies are undertaken to elucidate the structure of the hydrogels using atomic scanning electron microscopy and atomic force microscopy. The surface properties are categorised using contact angle measurement.

The experimental study of the physical and chemical properties of the gas membranes is discussed in chapter 6. Pseudo sensors are developed to measure gas diffusion through the membranes of interest. An extensive microscopic study is reported where the structure of each membrane is imaged. Finally the surface energy of the membranes is measured.

Chapter 7 details the success of a variety of hydrogels in marine field trials where they are exposed as panels. It also discusses the marine trials of hydrogels used to protect instruments ports in both laboratory and field experiments, and evaluates various fixing methods for these. Field trials of gas membranes are reported here and the results related to their structures.

Conclusions of the work are presented in chapter 8. The appendix includes relevant published and submitted journal papers.

Chapter 2

Biofouling

2.1 Biofouling

The marine environment is the single most extensive microbial habitat on the surface of the earth (Wimpenny, 1996). Within this habitat organisms attach to immersed substrates causing biofouling. Biofouling occurs worldwide to the detriment of various industries from oil and gas exploration and recovery to the most commonly known problem of fouling on the hulls of ships. It is also problematic in water systems, implanted medical devices and the food industry to name but a few. Its effects are costly to industry and often cause serious illness due to infections for humans. Here marine and fresh water biofouling is discussed in detail. The effects of fouling on the operation and performance of underwater sensors, particularly at their data collection ports such as optical lenses are detailed in chapter 3.

2.1.1 The History, Formation and Organisation of Biofilms

Representatives of all the phyla living in the sea, from bacteria, through to algae, to invertebrates use sticky materials with permanent or temporary adhesive capabilities at some point in their life histories to attach to substrate (Anderson et al. 2003). Initially there is the formation of a biofilm, it is usually considered to be a prerequisite to fouling (Marshall et al. 1971). What is a marine biofilm? It is a surface accumulation, which is not necessarily uniform in time or space, that comprises of cells immobilised at a substratum and frequently embebbed in an organic polymer matrix of microbial origin (Characklis et al., 1990). They occur at a solid /liquid interface and all objects and structures placed in the sea will foul. Immediately a surface is immersed in the sea a conditioning film of organic molecules forms. This begins after a few seconds of immersion and is considered molecular fouling. In the hours and days that follow bacteria colonise the surface and micro colonies occur. These colonies spread outward and upward to form irregular structures at this stage.

Then other microfouling appear e.g. microalgae and fungi. From these extracellular polymer secretions (EPS) are produced. This EPS is also called the glycocalyx. The biofilm then matures and new species enter and grow, organic and inorganic debris is incorporated and solute gradients develop leading to a spatial heterogeneity. Figure 2.1 shows diagrammatically the development of a biofilm.

At this point three things can occur:

- The biofilm may slough off due the hydrodynamics of the environment
- Organisms may begin to graze on the biofilm
- Larger organisms such as algae and molluscs may establish on it, this is macrofouling.

Costerton et al. (1995) said that direct observations have clearly shown that biofilm bacteria predominate, numerically and metabolically, in virtually all nutrient – sufficient ecosystems. Therefore, these sessile organisms predominate in most of the environmental, industrial and medical problems. They defined biofilms as matrix-enclosed bacterial populations adherent to each other and/or to surfaces or interfaces. The definition included microbial aggregates and flocculates and also adherent populations within the pore spaces of porous media. Different biofilm bacteria respond to their specific microenvironmental conditions with different growth patterns, and a structurally complex mature biofilm gradually develops. The overall strategy of bacteria in oligotrophic environments is to grow in biofilms on surfaces where nutrients are locally available and to persist in nutrient-deprived zones as floating, dormant ultramicrobacteria with the full capacity of returning to the vegetative state when nutrients again become available. These biofilm cells are at least 500 times more resistant to antibacterial agents than planktonic bacteria (Costerton et al. 1995).

Figure 2.2 shows typical fouling that occurs in the marine environment.

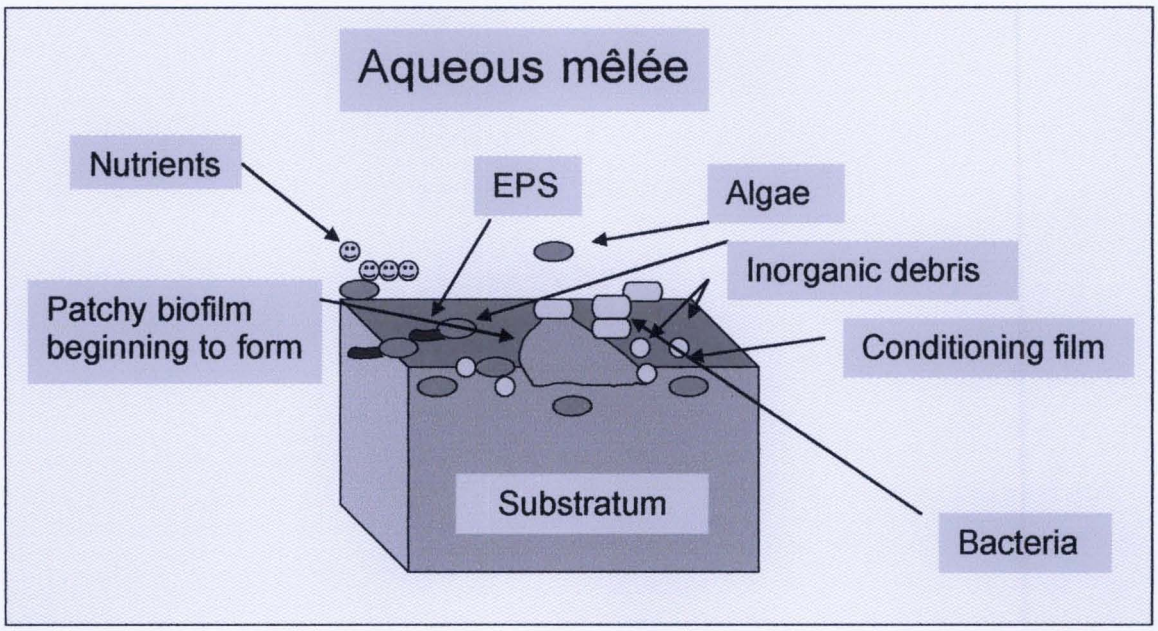

Figure 2.1 A diagrammatic representation of the components that make up a biofilm

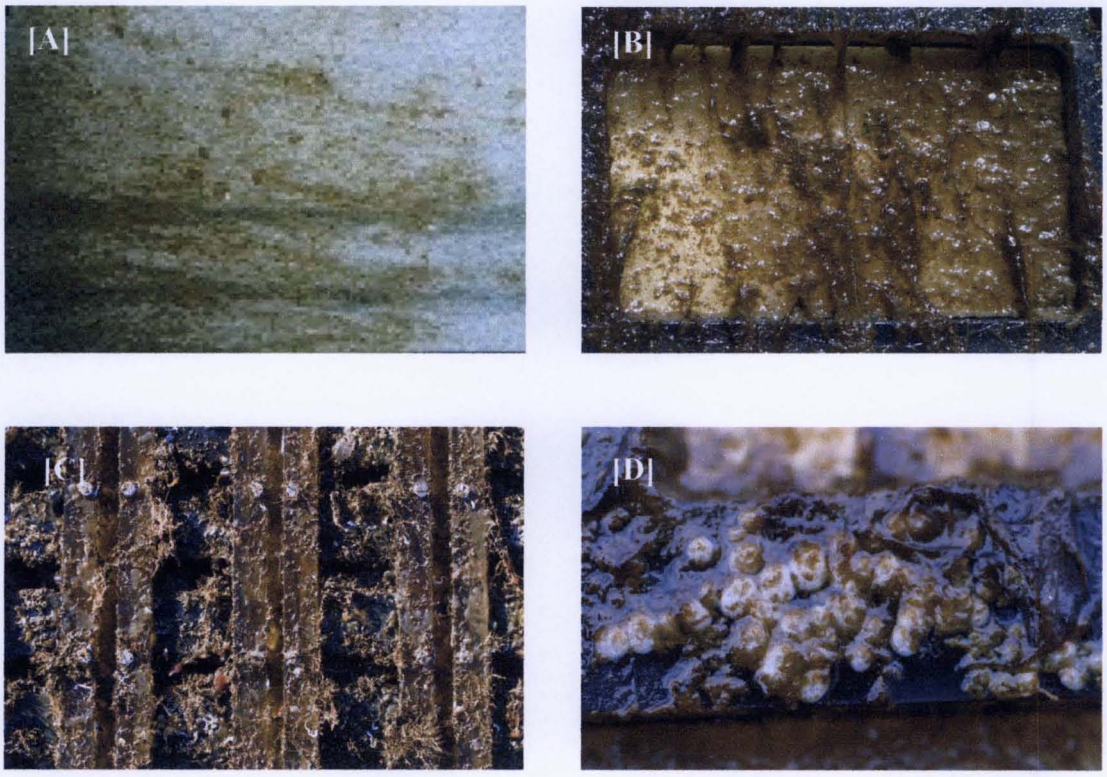

Figure 2.2 Marine biofouling on PMMA test racks. [A] Biofilm with the beginnings of algal growth. [B] The algal growth increasing to a thick coating. [C] A mature mixture of fouling organisms. [D] Establishment of invertebrates and mature plants.

The understanding of biofilm formation began to first be recorded in the 1940's. However, it was two decades later before it became an accepted term after which vast research of the biofilm began and continues at present.

The biofilm time line:

1943	The first recorded mention of biofilm formation was by Zobell. He observed microbial cells 'attached in layers' to bottle walls.
1964-1967	Atkinson and co-workers coined the term microbial or biological film to represent the gelatinous layer of cells and their adherent by-products on bioreactor vessel walls
1971-1972	Topiwala and Hamer and then Howell referred to mucilaginous layers of bacterial cells and their expolymers as 'wall growth'
1973	Characklis wrote a literature review on the basic fundamentals and practical implications of 'microbial slimes'
1984	Characklis termed a biofilm as a collection of microorganisms, predominantly bacteria, enmeshed within a three-dimensional gelatinous matrix of extracellular polymers secreted by the microorganisms
1990	Crarackli et al. summarised a biofilm as "a surface accumulation, which is not necessarily uniform in time or space that comprises of cells immobilised at a substratum and frequently embebbed in an organic polymer matrix of microbial origin"
2000s	In the last few years the instrumentation used in the study of biofilms has made the understanding of them easier as 3-dimensional imaging using confocal laser scanning microscopy (CLSM) allows imaging of living, fully hydrated biological samples (Neu et al. 2003).

The understanding of the structure and properties of biofilms has changed over the years since the 1960's when they were first studied in detail. In 1965 biofilms were considered uniform in structure although permeable to the transport of solute molecules. Bacteria populations were assumed to be uniformly distributed throughout the biofilm. During the 1970's and 1980's researchers recognised that biofilms were structurally irregular. However, what has transpired in the last ten years is an immense explosion in analytical methods and diagnostic tools available to now quantify at the micro and now even molecular scale, many subtle biofilm processes. The structures of biofilms are commonly studied using confocal scanning laser microscopy, nuclear magnetic resonance imaging, scanning electron microscopy and atomic force microscopy.

2.1.2 Attachment of Organisms in Biofilms

Fouling can be divided into two groups, soft and hard foulers. Hard foulers include bryozoans, molluscs, tube worms and zebra mussels while soft foulers include algae, slimes and hydroids.

Marine organisms are of course known for their remarkable adhesive properties, forming very strong bonds under a wide range of conditions of temperature and salinity. Nature appears to have developed strategies to encourage settlement in groups, so called gregarious settlement. The gregarious settlement of barnacle cyprids is induced by a glycoprotein associated with the adult barnacle. It is thought that the cyprids have to make contact with the adult glycoprotein for it to be effective and that the process involves a chemical sense. Little is known about the detailed chemistry of the adhesives produced by the fouling organisms, but it is known that many types of molecules are involved in sticking organisms to surfaces (Callow and Clare, 2003).

The first step of the cell-surface interaction is attachment, in which the cells retain the round shape they had in suspension. Attachment of a cell to a surface is usually followed by a conformational change known as 'spreading' in which the area of the cells in contact with the surface increases. The attachment phase depends on the physical and chemical properties of the polymer surface i.e. interfacial free energy,

hydrophilicity and hydrophobicity, mobility of the polymer chains, and ionic nature (Rosso et al. 2003).

The initial process does not occur in a random fashion. Conditions must be favourable, including pH, humidity and nutrient availability. Nutrient availability is an important factor; bacteria require dissolved organic carbon, humic substances and uronic acid for optimum biofilm growth (Stanczak, 2004). Studies have been carried out with relation to blue mussel attachment in the presence of different chemical elements and the attachment of green mussels *Perna viridis* in relation to chlorine concentrations (Masilamoni et al. 2002). The effects of water turbulence on spores of bacterium *Bacillus thuringiensis* have been studied (Faille et al., 1999). Other aspects such as the composition of the surface to the colour of the organisms have been considered ((Stanczak, 2004). One aspect which has been carefully considered, it has wide application to moving vessels as well as flow past stationary objects, is water flow rate. Bott and Miller (1983) found that maximum development of biofilm created by the bacterium *Pseudomonas fluorescens* occurred at around 1m s^{-1} while zebra mussels (*Dreissena polymorpha*) do not settle at velocities greater than 2 m s^{-1} (Stanczak, 2004). The growth of a biofilm can progress to a point where it provides a foundation for the growth of seaweed, barnacles and other organisms. Microorganisms such as bacteria, diatoms and algae form the primary slime film to which the macroorganisms such as molluscs, seaquirts, sponges, sea anemones, bryozoans, tube worms, polychalets and barnacles attach (Stanczak, 2004).

Callow and Clare (2003) describe the sticking of organisms to surfaces in the marine environment. They stated that organisms are able to attach to a variety of surfaces under a wide range of temperature and salinity. The adhesives produced by organisms are remarkable in their strength and the composition of the glue of *Enteromorpha* spores is a glycoprotein that progressively cures with time. The settlement of barnacle cyprids is induced by glycoprotein associated with adult barnacle. Little is known about the detailed chemistry of the adhesives produced by fouling organisms, but it is known that many types of molecules are involved in sticking organisms to surfaces. However, barnacle adhesive is known to be a hydrophobic protein having a molecular weight of 39kD that crosslinks through cysteine linkages (Naldrett 1993). Mussels secrete byssus threads consisting principally of collagen, but contain a hydrophobic

polyphenolic adhesive protein that crosslinks in an oxidation-reduction reaction involving a polyphenoloxides catalyst (Waite, 1983a; 1983b). These threads attach themselves to solid surfaces in the inter-tidal zone (Anderson, 2003). Diatoms attach to surfaces by producing neutral or acidic polysaccharide mucilages that either encapsulates cells or forms pads, stalks, or tubes (Callow, 1990)

2.1.3 Resistance of Biofilms to Biocides

In aqueous environments, bacteria with the ability to generate glycocalyces abound and less than 0.1% of the bacteria are present in the planktonic form (Morton et al. 1998). Resistance to biocide treatments is increased in bacteria which are attached to surfaces and also to particulate matter within a system. A major role of the glycocalyx is that it constitutes a barrier affording the various constituents of the biofilm partial protection from antibacterial agents and from the possible toxic effects of the substrate upon which the biofilm may form (Costerton et al., 1981; Keevil et al., 1989). The resistance of microorganisms growing within biofilms to antimicrobial agents is well-established compared with the same cells in the planktonic state. Cells on surfaces have different growth rates and nutritional requirements than planktonic cells of the same species and a number of workers have shown that biocide sensitivity can be altered up to 1000 fold by changes in nutrients and growth rates (Morton et al. 1998).

Stewart et al. (2000) stated that one of the hallmarks of the biofilm mode of microbial growth is remarkable resistance to killing by antimicrobial agents. This property frustrates efforts to control detrimental biofouling but it probably also harbours clues to the distinct structures and function of microbial biofilms. Although the diminished susceptibility of microorganisms growing in biofilms to killing by antimicrobial agents is now widely recognised, there is generally no accepted basis for quantifying the degree of this resistance.
The action of an antimicrobial agent against a biofilm involves the complex interaction of multiple processes which must be considered:

1. Bulk fluid flow into and out of the system

2. Consumption of the antimicrobial by reaction with biomasses

3. Substrate utilization

4. Diffusive transport within the biofilm

5. Microbial disinfection

6. Biofilm detachment

Additional processes that might confound the problem include corrosion, accumulation of abiotic particles in the biofilm and mutation or adaptation (Stewart et al. 2000).

Stewart and Costerton (2001) reviewed the mechanisms of resistance to antibiotics and concluded that there were three possible mechanisms. The first hypothesis is the possibility of a slow or incomplete penetration of the antibiotic into the biofilm. The second hypothesis depends on an altered chemical microenvironment within the biofilm. For example, local accumulation of acidic waste products might lead to pH differences greater than one between the bulk fluid and the biofilm interior, which could directly antagonise the action of an antibiotic. A third and still speculative mechanism of antibiotic resistance is that a subpopulation of micro-organisms in a biofilm forms a unique, and highly protected, phenotypic state, a cell differentiation similar to spore formation.

2.1.4 Effects of Biofouling

These are immense and are well documented over a wide range of areas from traditional images of fouling on the bottom of boats to the less well known problems such as sensor fouling, fouling in water systems and indwelling devices in the body. The effects are detrimental in the majority of cases and the amount of fouling tolerated various, depending on application. For example, a little bacterial growth on the hull of a ship would not to especially problematic if it did not include larger organisms, whereas such a bacterial growth on an optical port would adversely affect

the data recorded making it unusable. More specific details of fouling on optical ports of underwater sensors are detailed in chapter 3.

2.2 Biofouling Resistant Surfaces

The study and development of surfaces able to prevent biofouling formation crosses many disciplines and industries. One area where research has focused on is in the biomedical area. The problems caused to patients with long-term indwelling devices such as pacemakers and biliary stents and also those shorter term devices such as contact lenses, catheters and biosensors when these devices become covered in biofilms leading to infections is well documented (Lee & Laibinis, 1998; Ziegelaar et al. 1999; Silver et al, 1999). Due to these problems biomedical research has strived to develop suitable materials with surfaces that would prevent biofilm growth.
The development of paints and coatings for marine vessels and structures has also been greatly studied and these have led to many useful products. Among all the different solutions proposed throughout history of navigation, tributyltin self-polishing copolymer paints (TBT-SPC paints) have been the most successful in combating biofouling on ships. Unfortunately, the TBT-SPC systems adversely affect the environment. This has forced the development of national regulations on its use in countries all over the world (Yebra et al., 2004). Environmental authorities around the world have declared their intention to proscribe toxic coatings as soon as non-toxic alternatives are available, and the need for effective, long-lasting environmentally-benign coatings is urgent (Brady and Singer, 2000). Stanczak (2004) stated that the one of the primary ways to prevent biofouling is to select the appropriate material that would not be welcome to organisms and to accomplish this in coordination with the biological knowledge of biofouling organisms. This has been the focus of much research as a greater understanding of the surface chemistry of surfaces and the chemistry of the foulers has been elucidated.

Surface texture or roughness has been shown to influence bacterial adhesion. Light and electron microscopy studies have shown that surface irregularities serve as preferential starting points for attachment providing niches in which micro-organisms are protected from shear forces. Morton et al (1998) stated that rougher surfaces are

preferentially colonised and the niches can even protect the bacteria from biocide activity. Callow and Clare (2003) stated that rough surfaces accumulate fouling rapidly and that the scientists are trying to create a surface that spores cannot 'recognise' or find inhospitable for settlement. The contribution of surface topography to attachment is believed to be greater than physio-chemical interactions such as surface free energy and hydrophobicity (Taylor et al. 1998). Kiremitci-Gumusderelioglu and Pesmen, 1996) stated that substrate surface properties that can influence adhesion are, surface tension, surface free energy, hydrophilicity-hydrophobicity and texture.

2.3 Future Technologies in Biofouling Prevention

In recent years there have been great advances in the understanding of the mechanisms of fouling (Callow and Clare, 2003). Understanding how organisms are attracted to surfaces and how they attach to these surfaces has led to the development of specific surfaces, which would deter settlement of organisms. Successful biofouling control depends on rationally developed treatment strategies, which are based on information about the specific system (Cloete, 2005).

Traditionally, fouling has been controlled by biocidal antifouling paints, but regulations now require that antifouling paints must not cause adverse effects in the environment and the search is on for 'greener' ways of deterring marine life from attaching to submerged objects (Callow and Clare, 2003).

The only non-toxic method of fouling control that is currently widely available is the use of silicone electrometric coatings, often called fouling-release coatings. International Coatings (UK) pioneered the use of silicone coatings for marine fouling applications and large scale applications with the first product, Intersleek, were started in 1987. Since restrictions on use of TBT-paints on vessels less than 25m were introduced, the development, of fouling release coatings has progressed. The fouling release properties of silicones were mainly attributed to their low surface energy, which makes them non-wettable so that water does not form a surface film but rather falls away from the surface. In addition to low surface energy, other characteristic

such as thickness and compressibility of the coating are also important (Callow and Clare, 2003). The use of non-stick, fouling release coatings are an attempt to prevent the adhesion of fouling organisms by providing a low-friction, ultra-smooth surface on which organisms have great difficulties in settling. Many studies have been performed to elucidate the properties that a coating should possess to resist adhesion.

The main ones are summarised as (Yebra et al, 2004):

- A flexible, linear backbone which introduces no undesirable interactions
- A sufficient number of surface–active groups which are free to move to the surface and impact a surface energy in the desired range
- Low elastic modulus
- A surface which is smooth at the molecular level to avoid infiltration of a biological adhesive leading to mechanical interlocking
- High molecular mobility in the backbone and surface–active chains
- A thickness which can control the fracture mechanics of the interface
- Molecules which combine all the above factors and are physically and chemically stable for prolonged periods in the marine environment

These properties are mainly possessed by two families of materials, fluorpolymers and silicones and belong to a group of materials that are considered non-stick, non-toxic, low energy materials to which many of the new antifouling coatings belong.

Other conventional approaches to limit biofouling that are currently available and are often used in combination (Cloete, 2005):

- Bacteria are chemically killed by application of biocides

- Microbial cells are dislodged from surfaces by dispersant

- The biofilm structure is weakened by enzymes or chelating agents of divalent cations

- Biofilms are removed by a variety of processes

- Biocide efficacy is enhanced by applying an alternating current or ultrasonic sound across the biofilm.

However, there are a large variety of other techniques which have shown promise such as localised chlorine generation (Delauney, 2005); silicone fouling release coatings containing the antifouling chemical zosteric acid (White, 2005) and natural antifouling strategies based on extracts from eukaryotes such as sponges, seaweeds and molluscs (Steinberg, 2005).

2.4 Conclusions

The complex and diverse structures of biofilms make them extremely difficult to eradicate. Ideally prevention of initial formation is more desirable. In order to do this it is important to consider all possibilities of prevention. Many characteristics are attributed to producing the ideal coating and it is important to consider these when testing possible candidate coatings.

Chapter 3

Instrumentation

3.1 Underwater Instruments and Cameras

Many underwater instruments are now made for use in environmental monitoring, climatic and scientific research. The increased use of these underwater instruments and cameras in the latter decade of the twentieth century has led to improved and robust instruments, which can be deployed in coastal areas, from remote buoys and from ocean going research vessels.

Common parameters measured are:

- Chlorophyll *a*
- Conductivity
- Dissolved oxygen
- Fluorescence
- Nutrients such as nitrate and ammonium
- pH
- Salinity
- Temperature
- Transmission
- Turbidity

Cameras are also used to continuously photograph underwater environments as well as underwater structures such as oil and gas rigs.

Figure 3.1 shows two transmissometers commonly used in marine monitoring.

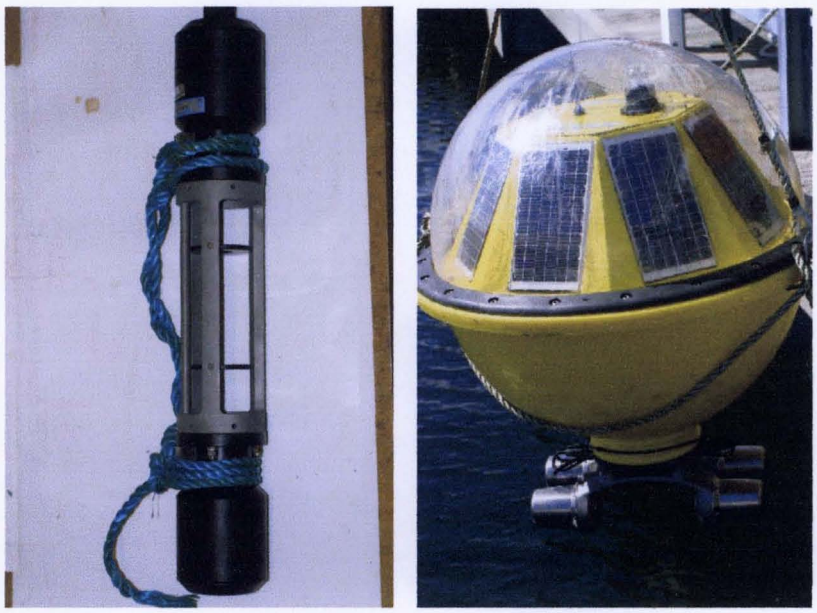

Figure 3.1 The transmissometers shown are the Chelsea Technologies Group transmissometer (AlphatrackaI) and the Optisens transmissometers which are attached to a Seawatch Mini buoy. The solar panels power the electronic storage of data.

3.2 Environments where Underwater Sensors are Deployed

Underwater sensors are commonly deployed in oceans, estuaries, rivers and lakes. This means they are subject to seawater, brackish water and freshwater all of which have different properties and thus have different effects on the deployed sensor body and any antifouling coating used to protect it and the optical or membrane ports. It is therefore important to consider the properties of each medium in which deployment takes place.

Seawater

The oceans are the largest of all ecosystems and cover more than 70% of the earth. They are divided vertically into a number of separate zones. The first is known as the intertidal zone and occurs where the sea meets the land and thus organisms living in this area can be sometimes submerged and sometimes exposed as waves and tides come in and out. Communities in this zone are constantly changing. A diverse array

of organisms live in this zone, such as algae, small animals, molluscs, crabs, sea stars and fish. At the bottom of the intertidal zone, which is only exposed at the lowest tides, many invertebrates, fishes and seaweed can be found (The Aquatic Biome, www.ucmp.berkeley.edu). This accounts from the upper limit of seawater cover down to around 30m in depth. The pelagic zones include those waters further from the land, which would be considered the open sea. These zones are generally cold although there is constant mixing of warm and cold ocean currents. The first of the pelagic zones is known as the epipelagic zone (0-200m) and is the top layer of the ocean where enough sunlight penetrates for plants to carry on photosynthesis. Immediately below this zone is the mesopelagic zone (200-1000m) sometimes known as the twilight zone, a dim zone where some light penetrates, but not enough for plants to grow. Bacteria, salps, shrimps, jellys, octopods, squid and fish are found here, many of which are bioluminescent (Yancy, 2002). The bathypelagic zone (1000-4000m) is the deep ocean layer where no light penetrates. Below this is the abyssal zone (4000-6000m) (Barnes and Hughes, 2002), the pitch-black bottom layer of the ocean; the water here is almost freezing, highly pressured, high in oxygen content, but low in nutritional content. Many species of invertebrates and some fish live in this zone (The Aquatic Biome, www.ucmp.berkeley.edu). The hadopelagic zone (6000-11,000m) is the waters found in the oceans' deepest trenches; here shrimp and anglerfish are found (Yancey, 2006).

There are twelve well-defined geographical zones in the oceans of the world that vary in salinity, clarity, temperature and micronutrients, and the types and numbers of native fouling organisms are different in each of these zones. Figure 3.2 shows the position of the majority of these zones.

The zones are:

1. Arctic Ocean 2. North Pacific 3. North Atlantic 4. Baltic Sea 5. South Pacific 6. Baja California 7. Gulf of Mexico and Caribbean Sea 8. Mid-Atlantic 9. Mediterranean Sea 10. South Atlantic 11. Indian Ocean 12. Antarctic Ocean

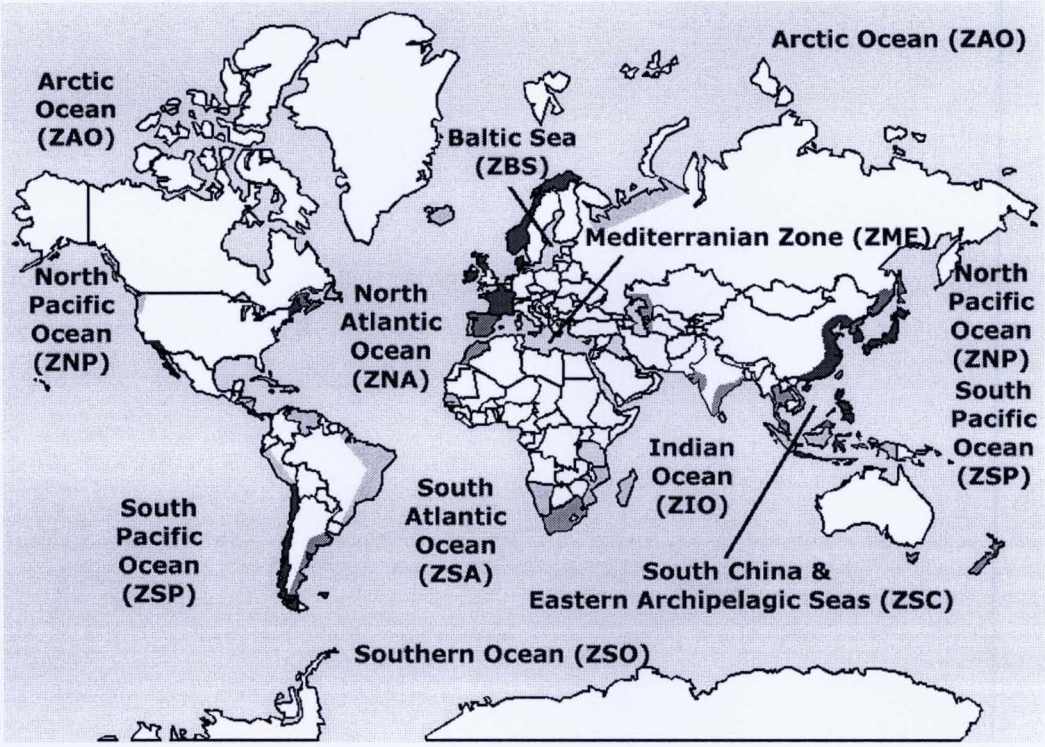

Figure 3.2 Map showing the world oceans

reference to source

The globally accepted value to describe salinity of seawater is 3.5wt. %. (Yebra et al., 2004). There is a higher variance of salinity near the surface which is mainly due to rainfall and evaporation. Also the immediate area where a river enters the sea will have a slightly lower salinity. The salt content of the open sea is normally in the range 3.3-3.8 wt. %. Table 3.1 shows the major constituents of seawater.

Ions	g kg^{-1}
Total salts	35.7
Sodium	10.77
Magnesium	1.30
Calcium	0.409
Potassium	0.338
Strontium	0.010
Chloride	19.37
Sulphate as SO_4	2.71
Bicarbonate	0.14
Bromide	0.065
Boric acid	0.026
Dissolved organic matter	0.001-0.0025g
Oxygen in equilibrium with atmosphere at 15°C	5.8cm^3 l^{-1}

Table 3.1 The major constituents of seawater.

The temperature of the surface waters of the oceans tends to vary directly with the latitude, and the range is from about -2°C at the poles to 28°C right on the equator (Pickard and Emery, 1982). In temperate zones the seasonal variations amount to around 10°C and up to 18°C in areas under continental influences or 2°C in equatorial and polar regions (Capurro and Griffith, 1970). The diurnal variations of temperature in the open sea are hardly ever bigger than 0.4°C.

Seawater is normally alkaline and the pH of the surface layers of the ocean, where the water is in equilibrium with carbon dioxide of the atmosphere, lies between 8.0 and 8.3, and in the open ocean it is, again, a very constant property. A basic assumption is that surface water is saturated with the atmospheric gases (mainly, O_2, N_2 and CO_2),

but biological processes such as respiration and photosynthesis can alter their concentration. In areas with considerable microbiological activity, there may be some variations due to production of hydrogen sulphide (lower pH) or removal of CO_2 by algae (rise in pH) (Yebra et al. 2004).

Brackish Water

The Longman Dictionary of Environmental Science defines brackish water as "water with a salinity of between 0.5 and 30 parts per thousand total dissolved solids". This means that there is a wide variety of conditions possible in brackish water. Consider an estuary where the salinity will reduce the further up the estuary you move.

Freshwater

Freshwater is defined as having less than 0.5 parts per thousand salts. Freshwater environments such as lakes, ponds and rivers vary greatly in temperature. Diurnal and seasonal temperature changes are therefore less drastic in the aquatic environment than the terrestrial environment. Temperature has traditionally been recognised as a key environmental factor in freshwater ecosystems, affecting, for example, distribution patterns, behaviour and metabolic rates of freshwater organisms. Freshwater organisms are poikilothermic, which means that their internal temperature varies with environmental temperature and thus, environmental temperature is a very important factor in their life (Brönmark and Hansson, 1999). The density of water changes as temperature changes. Many lakes stratify during the summer months with lighter, warm water at the top and heavier cooler water underneath. Some lakes such as Loweswater and Ullswater in the UK were found to have a difference of over 10°C between the top and bottom during summer. (www.environment-agency.gov.uk).

Lakes and ponds show regional differences in pH due to differences in geology and hydrology of the catchment area, input of acidifying substances, and productivity of the system, but the pH in the majority of lakes on earth is between 6 and 9 (Brönmark and Hansson, 1999).

These regions range in size from just a few square metres to thousands of square kilometres.

3.3 Application of Commonly used Sensors

3.3.1 Optical Sensors

Chlorophyll a sensors

The measurement and distribution of microscopic living plant matter commonly referred to as phytoplankton or algae, have been of interest to scientists, researchers, and aquatic resource managers for decades. An understanding of the phytoplankton population and its distribution enables researchers to draw conclusions about a water body's health, composition, and ecological status (YSI Corporation Literature). Chlorophyll *a* concentrations above 0.5mg m^{-3} are thought to be the threshold for marine eutrophication. Chlorophyll *a* sensors are used in ocean, coastal, lake and reservoir management to investigate the distribution and growth of phytoplankton and observe the algal population and distribution.

Fluorimeters

These are used to monitor photosynthetic parameters in phytoplankton in oceanographic, estuarine, limnological and riverine studies. These are produced by many instrument companies and are one of the most commonly used sensors. One example is manufactured by the Chelsea Technologies Group, the 'MinitrackaI' fluorimeter; it is shown in figure 3.3. These instruments are capable of measuring a wide range of compounds, such as chlorophyll *a*, fluorescein, phycocyanin, amido rhodamine and phycoerythrin. When measuring fluorescein these instruments have an excitation wavelength of 470nm and a fluorescence wavelength of 685nm. The fluorescence wavelength is detected at right-angles to the excitation wavelength.

Figure 3.3 MinitrackerI fluorimeter made by the Chelsea Technologies Group, UK

Transmissometers

Transmissometers are able to measure turbidity, suspended mass transport, visibility and light attenuation. These instruments measure at a variety of wavelengths such as 470, 565, 590, 660nm, these reflect blue green and red light. Figure 3.4 shows a drawing of the Optisens instrument (Oceanor, Trondheim, Norway). The output of the instrument is presented as transmittance through the length of the beam path (250mm). The three light sources are light emitting diodes (LED) (red 660 nm and green 525nm with 25 nm bandwidths, and blue 470 nm with 20 nm bandwidth). The Optisens has a reference diode and a transmittance diode, which measure the intensity of incident and transmitted light respectively. The reference photodiode compensates for the usually occurring drift ("ageing") in the light output from LEDs during use. Figure 3.4 shows a schematic of the Optisens transmissometer.

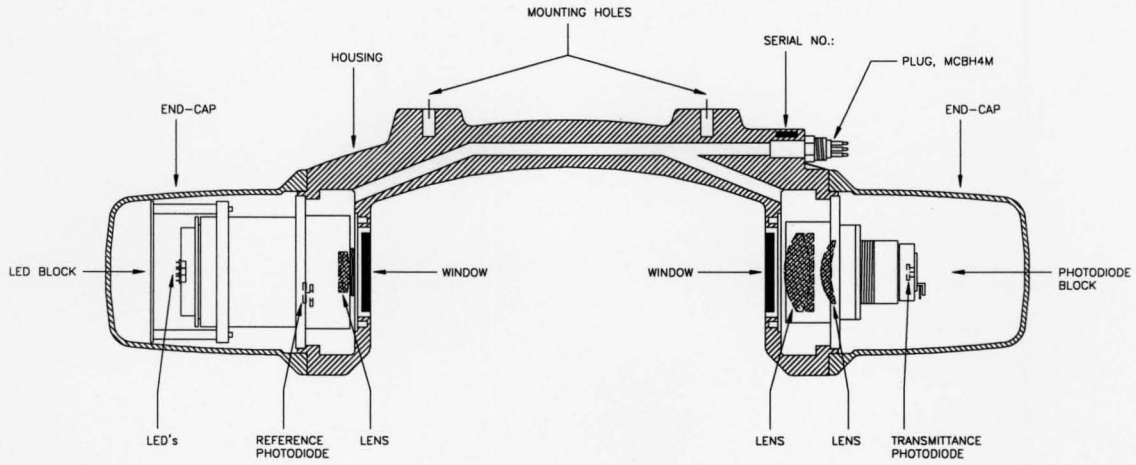

Figure 3.4 Schematic diagram of the Optisens transmissometer transmissometer (Courtesy of the BRIMOM project)

Another commonly used transmissometer is the Fasttracka made by the Chelsea Technologies Group. It operates in a similar way to the utilising a 660nm light source and a 250mm path length.

3.3.2 Gas Sensors

The level of gases in the fresh and marine water environments is frequently measured and those commonly measured are ammonia, carbon dioxide, and oxygen.

Ammonia sensors

Ammonia is an excellent indication of the presence of animal or plant microbiological decay in water. The presence of ammonium is essential for nutrient cycling in estuaries, rivers and open seas. Ammonium–nitrogen NH_4^+ is the preferred N species for uptake by photoplankton and bacteria. However, large input of plant nutrients often results in phytoplankton blooms of such intensity that the sea becomes discoloured. Careful monitoring of run-offs from farmlands is essential as high levels often result in unwanted algal blooms in water bodies. Therefore continuous monitoring of ammonia allows these changes to be monitored.

Oxygen sensors

The measurement of dissolved oxygen (DO) in oceans, estuaries and rivers is probably the most common parameter measured

There are two main sources of DO in water: the atmosphere and photosynthesis. Waves and tumbling water mix air into water where oxygen readily dissolves until saturation occurs. Aquatic plants and algae also produce oxygen as a by-product of photosynthesis. Over fertilization (from run-off from the land) results in extravagant growth of plants and the bacterial decay of dead plant material may result in oxygen depletion.

Oxygen sensors monitor the changes in oxygen levels that can, when decreased, reflect high bacterial growth or algal blooms. If oxygen drops below 1.5mg l^{-1} anaerobic bacteria can oxidise organic molecules resulting in end products that include compounds such as hydrogen sulphide, ammonia and methane which are toxic to many organisms. The lower level of a lake, called the hypolimnion, can become devoid of oxygen if the lake is stratified. The dwell time of a body of water without adequate mixing is an important consideration and especially applies to estuaries that are subject to regular upstream and downstream alterations of flow, and any body of water passes slowly through it to the sea. Organic wastes in the water have a long 'residence time' and bacterial degradation is slow, resulting in severe oxygen depletion or even anoxic conditions (Clark, 2002)). Lakes also suffer from oxygen depletion especially in areas where rivers run into them from farmlands. Figure 3.5 shows a photograph taken in August 2003 of Bardowie Loch, north of Glasgow, UK and gives an indication of the extent of an algal bloom at that time. This particular loch has farmlands surrounding it. Figure 3.6 shows a sample of the water collected at that time showing the density of the algae in the water. Rivers are continually flowing in one direction and therefore a body of water moves relatively quickly preventing a long 'residence time' and in oceans there is continually mixing due to wave action so oxygen depletion is less of a problem, although sometimes there can be stratification in seas and oceans. However, the dumping of raw sewage in open seas has now been prohibited but for many decades, this was the method of disposal of waste from major

towns and cities. This method of disposal caused high nutrient levels around the dumping ground.

Figure 3.5 Bardowie Loch exhibiting an algal bloom in August 2003.

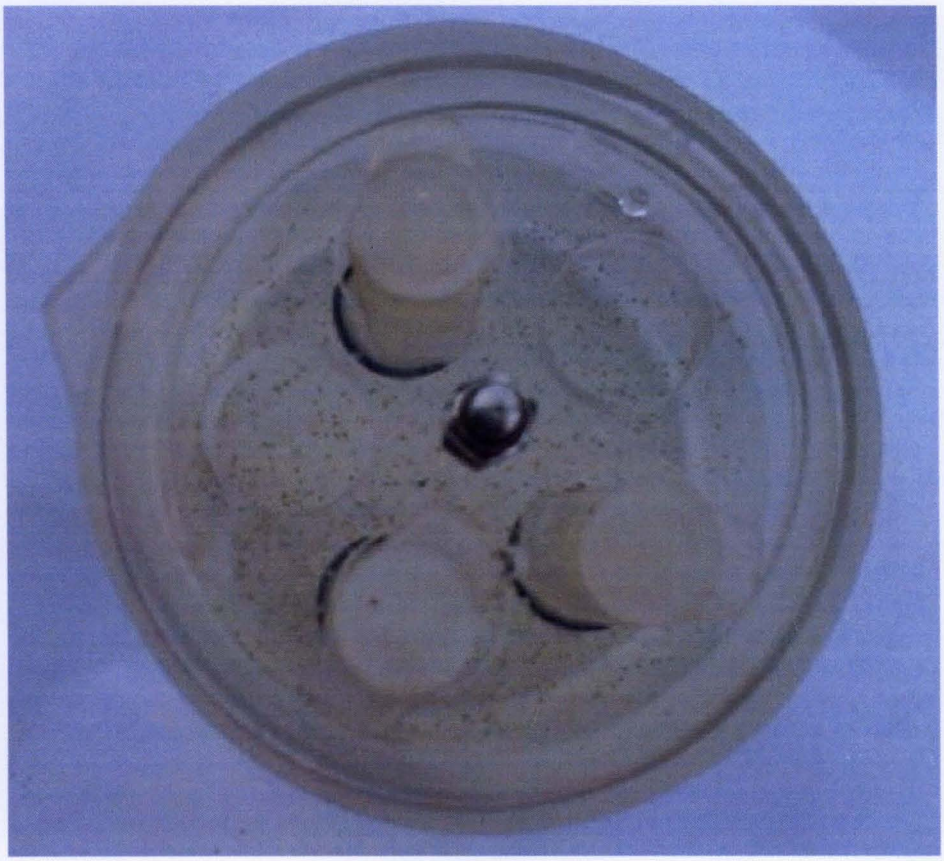

Figure 3.6 Sample of water from Bardowie Loch showing the density of algae.

Oxygen does not react with water. Dissolved Oxygen (DO) is really a physical distribution of oxygen molecules in water. Dissolved Oxygen can be measured using the polarographic (Clark Cell) and this is the most common type of method used to measure oxygen in real-time for nearly 50 years. The concentration is usually expressed in milligrams of oxygen per litre (mg l^{-1}) or in parts per million (ppm). These electrode type sensors actually measure the partial pressure of oxygen in water. There are various disadvantages associated with these electrodes; oxygen consumption during the measuring process, long measurement times and easy poisoning by hydrogen sulphide (Xiao et al., 2003).

The Clark type oxygen electrode is a specially designed electrochemical cell containing a silver anode and gold or platinum cathode immersed in an electrolytic solution such as potassium chloride. When a polarising voltage is applied a series of electrochemical reactions consume oxygen from the electrolyte. The current that flows through the electrode is directly related to the rate of these reactions and thus related to the oxygen concentration of the electrolyte. A thin oxygen permeable membrane is placed above the electrolyte and oxygen diffuses through this from the sample at a rate proportional to the oxygen tension in the sample. However, the introduction of optical oxygen sensors such as the Aanderaa oxygen optodes (Aanderaa Data Instruments AS, Bergen, Norway) are becoming increasingly more used as they do not have the problems with output, that the polarographic sensors have, such as rupture and leakage. The Aanderaa oxygen optodes are based on their ability of selected substances to act as dynamic fluorescence quenchers. The fluorescent indicator is a special platinum porphyrin complex embedded in a gas permeable foil that is exposed to the surrounding water. A black optical isolation coating protects the complex from sunlight and fluorescent particles in the water. This sensing foil is attached to a sapphire window providing optical access for the measuring system from inside watertight titanium housing. The foil is excited by modulated blue light, and the phase of a returned red light is measured. By linearizing and temperature compensating, with an incorporated temperature sensor, the absolute O_2 concentration can be determined. The principle of measurement is based on the effect of dynamic luminescence quenching (lifetime based) by molecular oxygen. Figure 3.7 shows an Aanderaa oxygen optode.

The manufactures claim that it has the following advantages over the traditional polarographic oxygen sensors

- Not stirring sensitive (it consumes no oxygen)
- Less affected by fouling
- Measures absolute oxygen concentrations without repeated calibrations
- Better long-term stability
- Less affected by pressure
- Pressure behaviour is predictable
- Faster response time.

Figure 3.7 An Aanderaa Oxygen Optode which has an optical detection port

pH sensors

The traditional approach to pH measurement is the use of a proton-selective glass membrane electrode. The core of this device is the glass membrane, consisting of a specially formulated, ultra thin glass (Whelan and Regan, 2006). The pH of open oceans is around about 8.2. Obviously there are areas where there are slight variations of this but these would be very rare. In the event of a major acid or alkali spill the pH of the immediate area would change and cause huge toxic problems for the organisms in this area. pH sensors would also detect small changes in pH indicative of emerging problems in rivers and estuaries such as the production of hydrogen sulphide or the depletion of carbon dioxide by algae. Therefore pH can give a good indication of how productive a lake is.

Cameras

Video and still underwater cameras are used for many purposes in oceans, lakes estuaries and rivers. Examples of uses are for inspection of rigs and piers, exploration, surveillance, climate monitoring and marine biological research. They are thus often used on fixed submerged installations, underwater vehicles, diver systems or when used in coastal, estuary or river monitoring can be deployed as single fixtures. For the majority of applications the deployment of the camera systems has, historically, been for fairly short durations that can be measured in hours or sometimes days, but rarely long enough to induce the formation of biofouling. There has, however, been a steady increase in the demand for video cameras on static long term installations such as harbour surveillance (BROS Project MAS3-CT95-0028/B1.2, 1997).

These cameras come in many shapes and forms and again their main drawback is their limited deployment times due to biofouling accumulation on their optical windows. Figure 3.8 shows two cameras. One is produced by Outland Technology (USA) Model UWC-185 and the other by Kongsberg Simrad (UK). The Konsberg Simrad model OE1366 colour zoom CCD video camera and is capable of operating at depths up to 3,000 metres at temperatures ranging from -5°C to +40°C and has an optical windows with a diameter of 50mm. The Outland Technology camera has a body constructed from hard coat anodized aluminium, a 8-80mm f1.6 lens, a resolution for

colour of 470 horizontal lines, a lens diameter 195mm and is capable of working to a depth of 1000m.

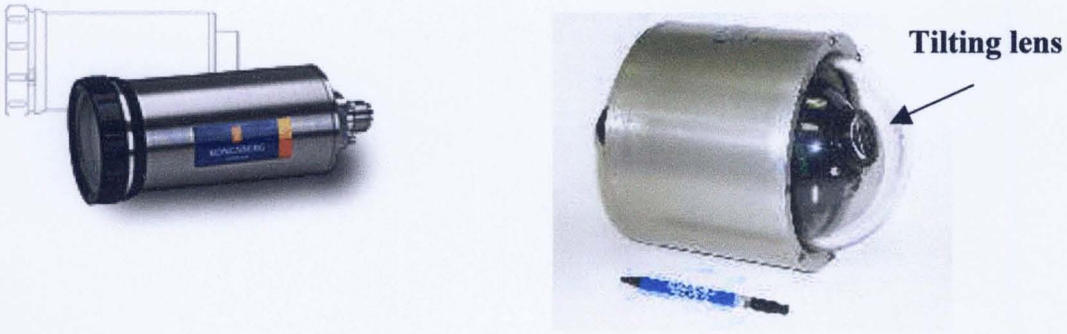

Figure 3.8 A video camera (Kongsburg Simrad, UK) and a video pan/tilt camera (Outland Technology, USA).

3.4 Effects of Fouling on Sensors

The way in which biofouling accumulation on optical and detection ports of sensors affects them is clearly dependant on the parameter being measured and the quality of data required. However, it is certainly detrimental to some extent in some, while to others the effects result in data being completely useless to the end user. When trying to pinpoint exact points in time when data are no longer valid it is important to understand what output the user is expecting. Although practically all users of underwater sensors complain about the adverse effects of biofouling on their data collection few are able to quantify these effects. However, it appears that in normal temperate marine waters, even in winter, degradation of the optical performance in the visible spectrum is observed within 15 days (Lemoine, 1993).

It is useful to consider the effects of fouling on all types of sensors used in a variety of environments such as industrial and medical as the problems faced by these users are comparable to those using underwater sensors and the problems caused by fouling on *in vivo* medical sensors is widely researched and published. Due to the lack of data on fouling effects on underwater sensors comparison have to be made to biosensors. Chapter 4 section 4.3.1 details some biofouling problems faced by biosensors as well

as details of the limited information on fouling effects on optical ports of underwater sensors.

Here each instrument is considered separately and how biofouling on its detection or optical port affects its output considered.

Transmissometers

These instruments operate using light sources of specific wavelength. The optical pathways tend to be around 250mm and the beam must pass through a quartz window at each end of the optical path. The light beam is very well defined and any deviation from the path caused by obstacles leads to a loss of measured transmission. Figure 3.9 shows the measuring principles of a typical transmissometer.

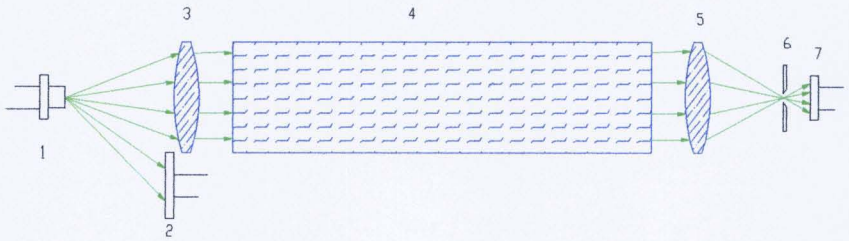

1- LED assembly, 2 – Reference diode, 3 – Lens, 4 – Water layer, 5 – Lens, 6 – pinhole, 7 – Transmittance photodiode,

Figure 3.9 Measuring principles of a typical transmissometer (Courtesy of the BRIMOM project)

Figure 3.10 shows the loss in signal to a transmissometer over time caused by a Skeletonema bloom.

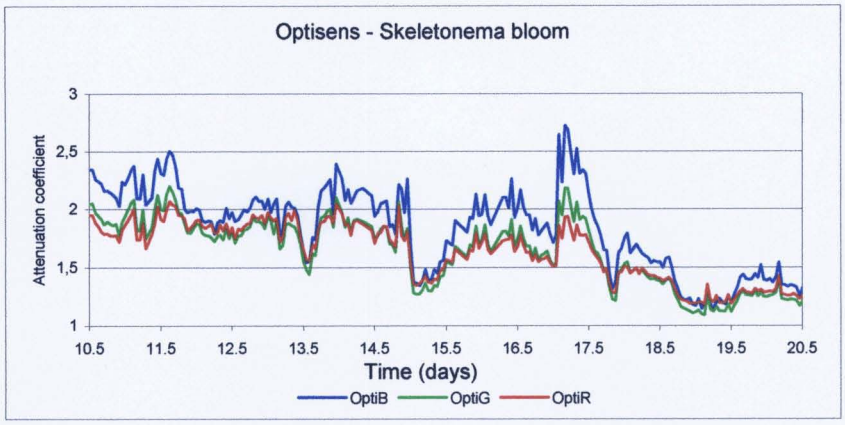

Figure 3.10 Example of the output from a transmissometer (Courtesy of the BRIMOM project; 2006)

Kerr et al. (1998) found that fouling on transmissometer windows had two distinct effects. Firstly, it obstructs the light path, causing the light beam to be scattered. This form of attenuation is common to all particulate matter. The second form of light attenuation is absorption. In this, the light is turned into other forms of energy and this can cause uneven disruption across the spectrum, as only one region of the spectrum may be absorbed while other wavelengths are undisturbed. They also concluded that bacterial fouling is a major contributor to the initial deterioration in the performance of optical marine sensors. Also, that the deterioration of results with fouling is not linear. Initial fouling has little effect on the performance of sensors, but once the fouling limit is exceeded, subsequent fouling has a disproportionate effect on the instruments and found that the fouling limit for these trials was a bacterial population of 10^5 mm^{-2}. Figure 3.11 shows fouling on the optical port of an Optisens transmissometer after 12 weeks deployment in Trondheim Fjord.

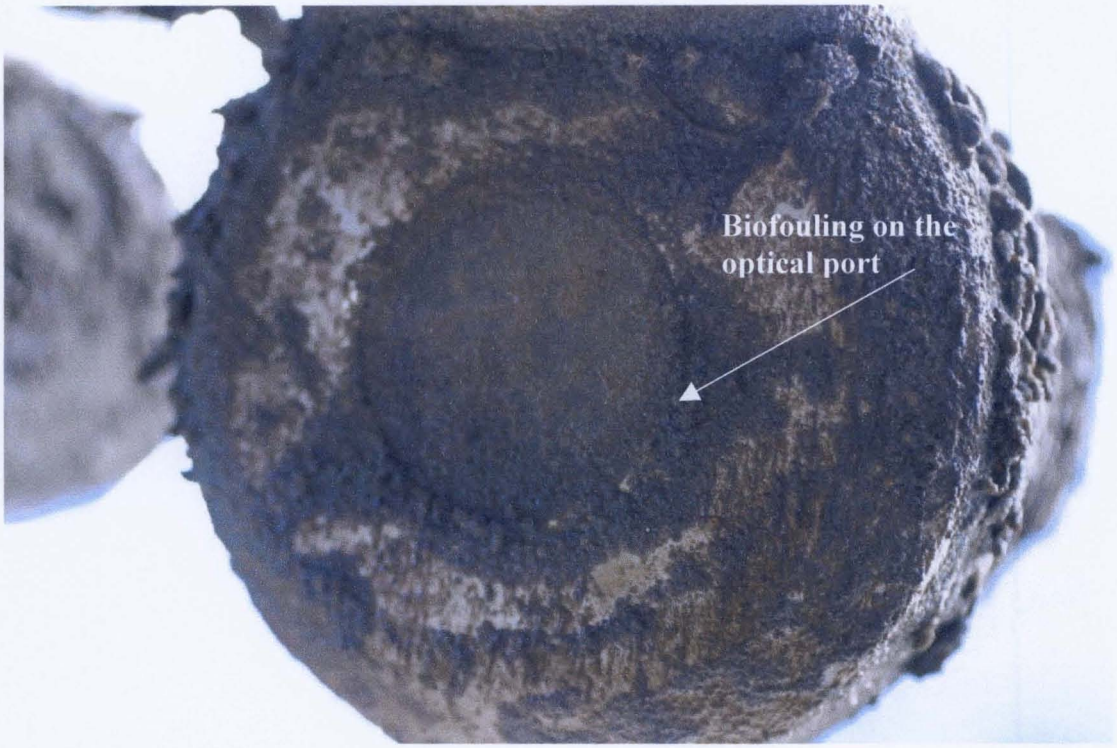

Figure 3.11 An Optisens transmissometer port with biofouling after 12 weeks marine deployment

Cameras

When considering the various optical degradations on underwater camera lenses it is important to consider the camera's angle of view. At a wide-angle setting the camera has a large depth of field and a small entrance pupil, making non-uniformities and surface irregularities on the camera window readily visible as blotches on the image, while refractive effects (such as due to poor surface flatness) are seen as localised geometric distortion. Conversely at a narrow-angle setting, the camera has a small depth of field and a large entrance pupil so that non-uniformities and surface irregularities tend to average out, while refractive effects can severely diminish the camera's resolution of fine detail (BROS Project MAS3-CT95-0028/B1.2, 1998). Cowling et al. (1998) stated that in the untreated state the normal progression of micro and macrofouling leads to deterioration in the performance of instruments. In optical applications the effects of fouling will depend on the wavelength of the radiation. They found that the lens of an unprotected camera after 4 weeks deployment, in the

Firth of Clyde Scotland, UK, produced an image that was severely degraded due to very low contrast and after 5 weeks the image under capture was barely discernible.

3.5 Current Oceanographic Instrument Manufacturers and Suppliers

The BRIMOM Project Contract EVR1-CT-2002-40023 (EU Framework 5) concluded that at the time of writing the majority of European oceanographic instrumentation manufacturers are small companies employing less than 20 members of staff and often their technology is focused on marine science requirements. However, as the market for in situ instruments changes with an emphasis on long term deployment and extended data sets instrument manufacturers require to respond with a new generation of instruments specially designed to meet these new requirements.
Recent legislation and initiatives demonstrate the need for long term marine monitoring systems. During the 1990s various pieces of legislation came into force such as in 1994 'The United Nations Convention on the Law of The Sea' part of which states that countries have an obligation to preserve and protect the marine environment. In 1992 the United Nations Conference on Environment and Development agreed that 'protection of the oceans, all kinds of seas, including semi-enclosed areas and coastal areas and the protection, rational use and development of living resources'. Then in 2000 the Water Framework Directive (2000/60/EC) was introduced which applies to all waters in the natural environment including estuaries and coastal waters. Also the EU Bathing Water Directive (76/160/EEC) which sets down legislation on the quality of bathing waters which has 9 physical, chemical and microbiological parameters and requires countries to monitor these water regularly. Environmental agencies monitor seas, river and estuaries and report on a huge variety of measurable parameters.

3.6 Requirements of Sensors

Due to the diverse requirements of those wishing to monitor the physical, chemical and biological parameters of the seas it has been useful to set up partnerships of scientists, engineers, instrument manufacturers and users to produce guidelines for

future development and uses of instrumentation. One such group is the Alliance for Coastal Technologies (ACT), which is a partnership of research institutions, state and regional resource managers and private sector companies interested in developing and applying sensor technologies for monitoring and studying coastal environments. This organisation produces many reports and reviews on all aspects of sensor technology. In 2003 they produced a report entitled 'Biofouling Prevention Technologies for Coastal Sensor/ Sensor Platforms (UMCES Technical Report Series) which detailed the antifouling requirements for the protection of instruments, reviewed the current technology, listed the huge variety of instruments used and suggested technologies which may prove useful in the future. The report begins by listing the important operation and technical conclusions:

- Monitoring systems are moving toward longer instrument deployments that exacerbate biofouling effects on operations
- Battery needs and data storage issues in observing systems have been in part overcome, thus making biofouling the major impediment to longer deployments
- Maintenance costs due to biofouling are high, about one half of most operational costs

The technical conclusions were:

- A range of sensor type-specific biofouling solutions are needed
- The coating technologies developed and optimised for the shipping industry need to be optimised or modified through R&D for sensors
- Much of the developing technologies are being developed by the sensor instrument companies themselves
- One of the most promising new areas of biofouling control is localised sterilization systems such as UV and chlorine generation
- The effects of biofouling on QA/QC data have not been tested or quantified to an adequate degree

Biofouling inhibits sensor operations and diminishes performance by interfering with membrane and electrode sensors, interfering with water flow through orifices and hoses, adding weight to the instrumentation, adding hydrodynamic drag, and inhibiting the mechanical movement of some sensor types.

The report then goes on to discuss the particular requirements of optical, electrode and membrane sensors.

Optical sensors:

- Three month to one year deployments are required
- Zero tolerance for fouling
- Mechanical in-situ wiper systems are effective but can cause damage due to abrasion
- The mechanical wipers can become inoperable due to biofouling
- Clear AF coatings do not exist
- Data degradation usually occurs immediately with no biofouling protection.
- Instrument calibration as biofouling degradation occurs is an important concern that has not been addressed
- Traditional AF coatings can be used to protect the housing elements of the systems
- Hazardous materials issues are a common concern for manufacturers servicing instruments returned to them with unknown AF coatings applied to the instrument housing

Electrode type sensors:

- Three month to one year deployments are required
- Of all sensor types sensors incorporating electrodes and membranes are the most susceptible to inoperability and data degradation due to biofouling
- For worst case scenarios, electronic and membrane sensors can require daily maintenance

- Cannot coat electrodes with conductive metal based biocides as it will disturb the instrument calibration
- Electrode devices can suffer for weight and drag issues for biofouling accumulation
- Wiper mechanisms can become inoperable due to biofouling
- Membranes cannot be coated
- For systems requiring circulation and pumping, clogging and filtration is an issue
- Hazardous materials issues are a concern for manufacturers servicing instruments returned to them with unknown AF coatings applied to the instrument housing

These problems listed in the ACT report cover the main problems that sensors suffer with fouling. Some are common to all types of sensors while others are unique to sensor type either optical or membrane.

The report then lists what it terms 'candidate technologies for intermediate and long term implementation' which are:

- Advanced shutter systems
- Advanced peel away coatings
- Harder materials for acoustic transducers
- Ultrasonics
- UV sterilization
- Localised chlorine generation
- Rotating turrets- biofouled heads replaced by a fresh sensor head
- Smooth surfaces
- Increased use of foul release coatings
- Red pepper formulations
- Self-polishing surfaces
- Optically clear biocides
- Advanced co-biocide copper based paints
- TBT collars

- Self calibrating instrumentation to account for biofouling

Many of these technologies are at present used on sensor windows. However, there are still inherent problems with them due the mechanical components in shutter systems and rotating turrets. Ultrasonics, UV sterilization, local chlorine generation all require the use of additional power supplies as well as significant adaptation of the instruments. The use of coatings such as foul release coatings and optically clear biocides offer more simple solutions as they do not require power and they can be attached to the ports fairly easily either by being painted, sprayed or modifying the optical glass before fitting. However, the extension of the biofouling resistant lifetime has not been widely published as most of these coatings are still at the research stage and the results mainly apply to panel trials in laboratory conditions and often against single strains of organisms. Lee and Laibinis (1998) found that coating glass and metal oxide surfaces with oligo (ethylene glycol) – terminated alkyltrichlorosilanes made then resistant to certain proteins. They concluded that the oligo(ethylene glycol)-siloxane coatings offer performance advantages over available systems and could easily provide a direct and superior replacement in protocols that presently use silane reagents to generate hydrophobic, 'inert' surfaces. Sawada et al. (1997) looked at the antibacterial activity of fluoroalkylated allyl- and diallyl-ammonium chloride oligomers. Antibacterial activity was found to be sensitive to the structure of these fluoroalkylated oligomers. They concluded therefore, that these fluoroalkylated oligomers are new attractive functional material possessing not only unique properties imparted by fluorine but also antibacterial activity. Clarkson and Evans (1993) prepared test coupons using 3-(trimethoxysilyl)-propyloctadecyl-dimethyl ammonium chloride bound to glass surfaces. The test coupons were subject to *A. coffeaeformis* in artificial seawater conditions. The coated glass surfaces were found to be toxic to the majority of the settling cells, killing a mean of 99.93% of the cells. Faimali et al. (2003) tested compounds isolated polymeric 3-alkylpyridium salts from the Mediterranean sponge, *Reniera sarai*, for their toxicity to the cyprids and nauplii of *Balanus amphitrite*; the microalgae *Tetraselmis suecica* and lavae of the mussel *Mytilus galloprovincialis*. They found that the extracts, when compared with commercial booster biocides, were less effective at inhibiting cyprid settlement and had a very low toxicity against organisms used in the toxicity bioassays. They

concluded that although encouraging, the results are not enough to warrant the use of poly – APS as a commercial antifoulant.

3.7 Conclusions

The use of underwater sensors has rapidly increased in the last decade. However, the problem of biofouling on their detection ports reduces their useful deployment time resulting in cleaning and replacement costs. A variety of methods to deter fouling have been used but these are often only partially successful. Some of these solutions are mechanical and also require a power source making them both open to failure and requiring additional energy. Ideally a coating that is able to deter fouling would offer a more simple solution.

Chapter 4

Hydrogels and Gas Membranes

4.1 Hydrogels

4.1.1 Background and History

The original hydrogel patents were placed by Wichterle and Lim (1960) and encompassed the formation of sparingly cross-linked soft and elastic hydrogels both by polymerisation of hydrophilic monomers and alternatively by the cross-linking of preformed hydrophilic polymers. These hydrogels are particularly useful in the field of ophthalmology because they are soft, easily cast to any shape, and can be made transparent. The permeability of hydrogels to water and to low molecular weight water-soluble substances is a very important property when they are considered for use as prostheses (Refojo, 1965).

Hydrogels consist of two components, the polymer network and the aqueous phase. At equilibrium swelling the chemical potentials of the water in the gel and the water surrounding the gel are equal (Refojo, 1976). Hydrogels have four key properties, swelling degree, biocompatibility, permeability and swelling kinetics. These characteristics have made them useful as contact lenses material, agents for drug release and as prostheses.

The hydrogels used in this research were prepared from the monomer hydroxyethylmethacrylate (HEMA). The resultant polymer is poly-(2-hydroxyethylmethacrylate) (PHEMA) and is a transparent lightly cross-linked material containing water. Both heterogeneous and homogeneous hydrogel can be prepared and this is dependant on the polymerization medium. Heterogeneous hydrogels are formed when HEMA is polymerised in aqueous solution with a high water content or water alone with a redox initiator system, whereas homogeneous hydrogels are formed when HEMA is polymerised in a medium, which is a good solvent for both the monomer and the polymer such as ethylene glycol-water

solutions. This resultant polymer is transparent from freezing to boiling temperature in water and has a remarkable shape and volume stability. The amount of water can be varied depending on the final use of the hydrogel. When a transparent hydrogel is required the water content should not exceed 40% (Refojo and Yasuda, 1965).

4.1.2 Physical and Chemical Properties of Hydrogels

Hydrogels are three-dimensional, hydrophilic, polymeric networks capable of imbibing large amounts of water. The presence of chemical crosslinks or physical crosslinks makes them insoluble regardless of the solvent. Hydrogels are called 'permanent' or 'chemical' gels when they are covalently-crosslinked networks. In the crosslinked state, crosslinked hydrogels reach an equilibrium swelling level in aqueous solutions that depends mainly on the crosslink density. Another way of classifying the hydrogel is by crosslink ratio. This is defined as the ratio of moles of crosslinking agent to the moles of polymer repeating units. The higher the crosslinking ratio, the more crosslinking agent is incorporated in the hydrogel structure (Peppas et al., 2000). Figure 4.1 shows the covalent junctions that 'tie' the polymer chains. The maximum amount of water which can be maintained in homogeneous polymeric hydrogels depends on the hydrophilicity of the polymer, and thus on the hydrophilicity of the monomer. The water present within a hydrogel is described as being in three different forms, bulk water, interfacial water and bound water. The bulk water has properties similar to those of water in an aqueous solution. The bound water is strongly associated with the polymer and the interfacial water is less strongly associated (Peppas and Moyniban, 1987). Hoffman (2002) described it as primary bound water and secondary bound water combining to simply be called 'total bound water' and free or bulk water. Another property of hydrogels, which is relevant to their application as a coating, is their glass transition temperature (Tg). There appears to be two glass transition temperatures of hydrogels -143 and -113°C (Kyritis et al.1995) that they attribute to two different types of water in the sample. Meakin et al. (2003) found the glass transition temperature of hydrogel to be -146°C.

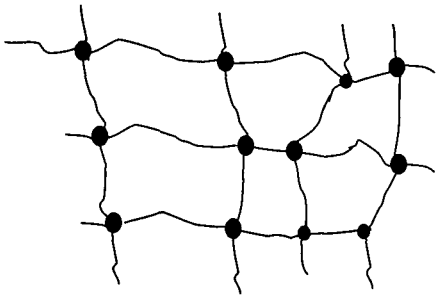

● Covalent junctions – PHEMA hydrogels

Figure 4.1 A diagrammatic representation showing the covalent junctions between chains.

Hydrogels then consist of two components, the polymer network, which is a constant quantity and the aqueous component, which is variable. The swelling behaviour was explained by the Flory-Rehner's equation (1943) which states that the volume of a gel is influenced by osmotic pressure, π,

$$\pi = \pi_{mix} + \pi_{el} + \pi_{ion}$$

Where, π_{mix} is the polymer-polymer affinity

π_{el} is the rubber elasticity

π_{ion} is the hydrogen-ion pressure

The polymer-polymer affinity is the interaction between the polymer strand and the solvent and is always a negative pressure. Such interactions can be either attractive or repulsive, depending mainly on the electrical properties of the molecules. Where the interaction is attractive the polymer can reduce its total energy by surrounding itself with solvent molecules. When the interaction is repulsive the solvent is excluded. The rubber elasticity derives from the elasticity of the individual polymer strands i.e. from the resistance the strands offer to either stretching or compression. Between a stretched polymer and a crumpled polymer there must be some end-to-end distance

where the average force is zero and the strand is neither in tension nor in compression, mathematically this is equilibrium (Tanaka, 1981). The hydrogen ion pressure is associated with the ionisation of the polymer network, which releases an abundance of positively charged hydrogen ions (H^+) into the gel fluid; this is probably more applicable to ionic gels such as polyacrylamide gels which have a large π_{ion} contribution, whereas, non-ionic hydrogels such as PHEMA contribute negligible π_{ion} to the total osmotic pressure. An essential principle is that whenever possible a gel will adjust its volume so that the total osmotic pressure is zero.

Refojo (1976) defined the osmotic pressure attributed to a polymer network (π) as the driving force of swelling. The swelling process distends the network, and is counteracted by the elastic contractibility of the stretched polymer network (p). Hence the swelling pressure of non-ionic gels hydrogels (P) is the result of the imbibition of solvent driven by an osmotic pressure, counteracted by the contractibility of the network which tends to expel the solvent resulting in the equation

$$P = \pi - p$$

At equilibrium, $\pi = p$, and the swelling pressure is zero (P=0).

In order to measure volume swelling of discs of hydrogels experimentally the swelling ratio (X) is defined by:

$$X = V/Vo = (D/Do)^3$$

Where V and Vo are the volumes after treatment and at zerotime, respectively and D and Do are the diameters of the hydrogel discs after treatment and at zerotime, respectively (Ilavsky, 1982).

4.1.3 Diffusion of Analytes in Hydrogels

Two mechanisms describe the solute transport through polymers, pore mechanism and partition mechanism.

Hydrophilic solutes diffuse primarily via a 'pore' mechanism and permeation occurs through the bulk water fraction of the hydrogel (Mack et al, 1987).
The parameters that affect drug permeability in hydrogels are dependant on:

- Type of releasing agent
- Water content in hydrogel
- Cross-linking density
- Polymer composition

The interaction among solutes, gel polymers and solvents has an important effect on the diffusion process (Peppas et al. 2000).

Refojo (1965) stated that the transport process in hydrogels is undoubtedly predominantly viscous flow through the pores of the membranes. Numerous experimental and theoretical analyses have determined that solute diffusion in water-swollen hydrogels occurs mainly through the water filled pores of the matrix (Yasuda et al. 1968 and 1969).

The use of hydrogels as drug reservoirs in biomedical systems is due to the presence of the pores within the material. The term pore is slightly misleading as Swan and Peppas (1981) classified hydrogels as nonporous membranes as their pores are at a molecular level. PHEMA pores are 30-50Å. They were also described by Peppas and Reinhart (1983) as nonporous gel membranes, which are swollen polymeric networks with 'pores' of molecular size, usually between 20-100 Å. However, the use of 'pore' to describe these spaces is probably commonly accepted.

The average pore size, the pore size distribution and the pore interconnections are important factors of a hydrogel matrix that are often difficult to quantify and are usually included together in a parameter called 'tortuosity', which is the pathway the solutes travel to diffuse through the hydrogel. This can be defined as the ratio of the distance achieved/distance travelled (figure 4.2 shows this diagrammatically).

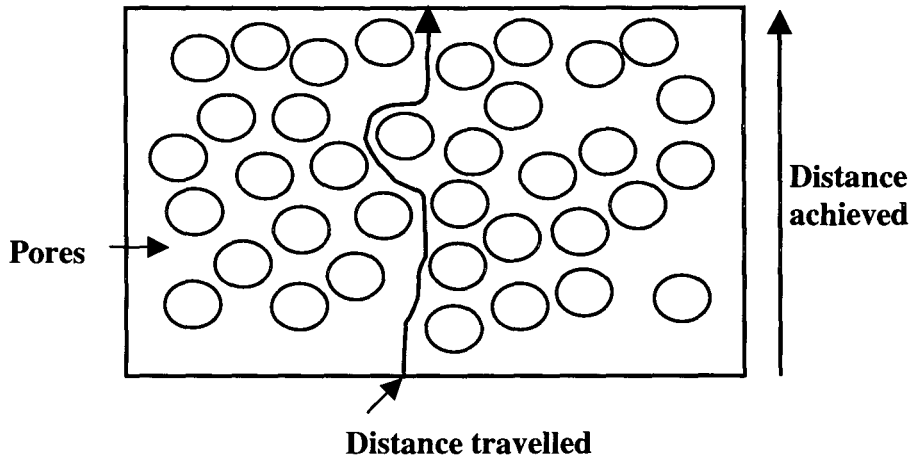

Figure 4.2 Diagrammatical representation of tortuosity

Hoffman (2002) defined the effective diffusion path length across a hydrogel is estimated by the hydrogel thickness times the ratio of the pore volume divided by the tortuosity.

Two important factors, which influence the diffusion characteristics of solutes through hydrogels, are the cross-linking density of the polymer (the nature of the cross-links) and the organisation of water within the hydrogel (crudely represented by the degree of swelling) (Peppas and Moynihan, 1987).

McNeill and Graham (1992) stated that it was reasonable to assume that the free volume of water present in the hydrogel is available for diffusion of water-soluble solutes.

Equations describing the release of water soluble solutes uniformly distributed in the matrix of a fully hydrated hydrogel into aqueous sink have been derived by Crank and Park (1968) from Fick's Laws for diffusion. A simplified form of a complex mathematical equation valid for the first 60% of the total release from a thin slab of constant dimensions is shown to be:

$$Mt/M\infty = kt^n$$

where M(t) = mass of penetrant sorbed at time t.

$M(\infty)$ = mass of penetrant sorbed at equilibrium

and k and n are curve-fitting constants.

If n=0.5 the diffusion is Fickian; n=1 diffusion is termed Case II transport and where ½<n<1 diffusion is described as being anomalous transport.

However, the equation described by Vaidyanathan and Nye (1966) better fits the system of diffusion from a single exposed surface of the hydrogel. The equation from which calculations can be derived is:

$$M_t = 2(C_1 - C_2)\sqrt{(D)t/\pi}$$

where M_t = the amount of penetrant lost per unit area at any given time,t.
C_1 = the initial concentration of penetrant in the hydrogel at zero time
C_2 = is zero as it represents the concentration of penetrant at the sink
(D) = the effective bulk diffusion coefficient in the polymer

Therefore a reduced equation can be used:

$$M_t = 2(C_1)\sqrt{(D)t/\pi}$$

4.1.4 Effects of Solutes on Hydrogel Structure

The biofouling resistant application of hydrogel coatings in the marine and freshwater environments requires them to be firstly loaded with cationic surfactant and then exposed in both fresh and marine waters. The influence of solutes on the structure of hydrogel has to be considered.

Due to their application in the biomedical field, studies have looked at the effects of a variety of chemicals on hydrogels. In principle, changes in swelling behaviour due to the presence of salt can affect the mechanical properties of the material as well as the 'tortuosity' of the matrix which gives rise to different diffusion coefficients of drug

release (Huglin and Rego, 1991). Roorda et al. (1987) stated that the water and the polymer in the gel form a coherent, integral structure, in which there is essentially no place for solute compounds. Absorption of solutes is possible as far as the solutes can disrupt the integral structure of the gel. Disruption of the structure allows further relaxation of the macromolecular chains, which leads to increased water sorption and swelling of the gels. If solutes cannot enter the gel significantly, their presence in the surrounding medium causes a disturbance in the swelling equilibrium, due to increased osmotic value of the outside medium. This leads to a decrease in water content, so to de-swelling of the gel. The effects of the marine environment on PHEMA hydrogels have not been specifically studied. However, the effects of a variety of salts have been investigated in terms of hydrogel swelling have been reported. Huglin and Rego (1991) reported the effects of a variety of concentrations of potassium thiocyanate (KCNS) on hydrogels. They found at low concentrations 0.6 M that the entrance of water into the gel was favoured with respect to the entrance of the salt. At concentrations greater than 0.6 M the entrances of water and salt are equally favoured. Hydrogel swelling occurred to some degree over the entire concentration range investigated 0-1.8 M KCNS. Roorda et al (1987) stated that the presence of solutes in the surrounding aqueous medium has a profound influence upon the swelling behaviour of the hydrogels. Hydrogel cylinders were soaked in 0.5M, 1.0M and 2.0M sodium bromide, sodium chloride, sodium fluoride and sodium iodide solutions for 1 week and the changes recorded. Only the hydrogel soaked in the sodium iodide absorbed water while all of the hydrogels absorbed the salts at all concentrations. They also looked at the effects of organic solutions, urea and antipyrine at 0.5M on hydrogels. The hydrogels both swelled and absorbed these solutes. Xerogels were soaked in aqueous solutions of various sodium chloride (NaCl) solutions ranging from 0-5wt%. As the ionic strength of the NaCl increased, the equilibrium water content (EWC) of the hydrogel decreased and the polymer fraction increased accordingly. This was explained by the fact that the increasing ionic strength would enhance polarity of swelling medium, strengthening hydrophobic bonding, and polymer-polymer interactions would also become improved. Refojo and Yasuda (1965) found that PHEMA hydrogels equilibrated in 0.9% NaCl decreased in water content to 38% from 40% (in distilled water), but when the concentration of the NaCl was increased to 1.4% the amount of water in the hydrogel also increased markedly to 46%.

In the marine environment the salt concentration can be considered to 3.5%. However, in brackish water the salt concentration will vary greatly. In the application of hydrogel coatings to sensors any swelling of shrinkage has to be considered due to the effects on the integrity of the coating.

4.1.5 Hydrogel Production Techniques

The most important processes for the synthesis of hydrogels are bulk, solution and suspension polymerizations. In general, bulk and solution polymerization are the most appropriate for preparing hydrogels since a hydrogel of any geometry can be made by casting it in a suitable mould.

In bulk polymerization the crosslinker and the initiator are dissolved in the liquid monomer before the solution is poured into the mould. Solution polymerization requires the reactant to be dissolved in a suitable solvent (in the case of PHEMA hydrogels ethylene glycol or water). The solution is then degassed under vacuum and /or sparged with an inert gas such as nitrogen or argon prior to initiation. Typical moulds are made from nylon, polypropylene and polymethylmethacrylate, also flat coatings can be polymerised between sheets of glass. The surface of the resultant hydrogel reflects the surface of the mould that it is prepared in therefore is important to consider this aspect when attempting to produce a smooth-surfaced hydrogel. Dry, glassy hydrogels can be machined to precise tolerances, but the expense is much higher than moulding, even assuming a much higher rejection rate of moulded pieces (Gehrke and Lee, 1990).

The clean up process of hydrogels after production involves soaking them in large volumes of distilled water which should be changed daily until the equilibrium water content of the hydrogel remains constant. The soaking period removes excess initiators as well as any uncrosslinked water-soluble material such as unreacted monomer present. In general the polymerisation of HEMA to PHEMA results in a nearly 100% conversion (Huglin and Rego, 1991). The time period required to leach all impurities varies depending on the size and geometry of the hydrogel and within the literature ranged from one week to two months (Compañ et al. 1999; Huglin and Rego, 1991).

There are three major problems that commonly develop in bulk or solution polymerisation, these are heat removal, shrinkage and incomplete monomer conversion. Heat removal is the most serious problem it results from a combination of highly exothermic heats of reaction and the low thermal conductivity of the polymers. These problems frequently cause inhomogeneities, opacity, bubble formation and surface shrinkage marks. As a result of this, uniform hydrogel samples are only easily prepared for a thickness of a few millimetres. During bulk polymerisation from the monomer to the polymer the volume contracts by about 20% (Gehrke and Lee 1990).

4.1.6 Surface Properties of Hydrogels

The surface properties of potential biofouling resistant materials are widely studied as they can predict the ability of materials to interact with their environment. The response of synthetic materials to marine biofouling is a much investigated process and its complexity has led to many theories on what type of material would present the 'ideal' surface to prevent fouling. The precise requirements for an effective fouling resistant surface remain uncertain although smoothness, flexibility and low surface energy have been implicated (Estarlich et al., 2000). Berglin et al. (2003) stated that mechanisms controlling fouling release behaviour are not fully understood but the generally accepted design criteria for fouling-release coatings are low surface free energy materials; high molecular mobility (e.g. low glass transition temperature, Tg) to minimize mechanical locking; a low modulus material for facilitating breaking of adhesive joints and chemical and physical stability upon long-term water exposure to prevent an increase in surface free energy and to avoid loss of mass and the development of surface roughness. Predominantly, research has been focused on materials that exhibit low surface energy properties such as silicones, fluorosilicones and PTFE as they have good water repellence (Schmidt et al., 2004; Berglin et al., 2003; Ista et al., 2004; Barbu et al., 2002). Estarlich et al. (2000) studied silicone and fluorosilicone elastomers resistance to biofouling in seawater and found progressive changes in contact angles for water droplets and for air bubbles on immersed surfaces and attributed this to the slow absorption of water and /or changes in the molecular conformations of the siloxane chains. These conformational changes modify the surface-energy characteristics of the coatings and this may alter their surface attractions of organic solutes forming the conditioning layer and also their ability to

act as secure substrates for sessile marine organisms. All these coatings reviewed have properties very different to hydrogels. However, it has been shown that very hydrophilic surfaces, as well as very hydrophobic surfaces, do not promote bioadhesion (Hermitte et al., 2004). Berglin et al. (2003) said that the use of hydrophilic surfaces to discourage bacterial adhesion has been explored and an adaptation of such an approach against marine fouling remains an interesting possibility. Hydrogels, although not strictly hydrophilic, certainly exhibit hydrophilic properties in a polar environment. Kodjikian et al. (2002) tested five different materials against *Straphylococcus epidermidis* and found hydrogel to have the best bioadhesion resistance while the silicone coating was the poorest. Holly and Refojo (1975) stated that refined knowledge at the molecular level will allow a better understanding of the mechanisms of cell adhesion on hydrogel polymers.

Hydrogels such as PHEMA are able to exhibit both hydrophobic and hydrophilic properties depending on their environment. Figure 4.3 shows the hydrophilic hydroxyl group attached to the ester portion and the hydrophobic backbone of the polymer.

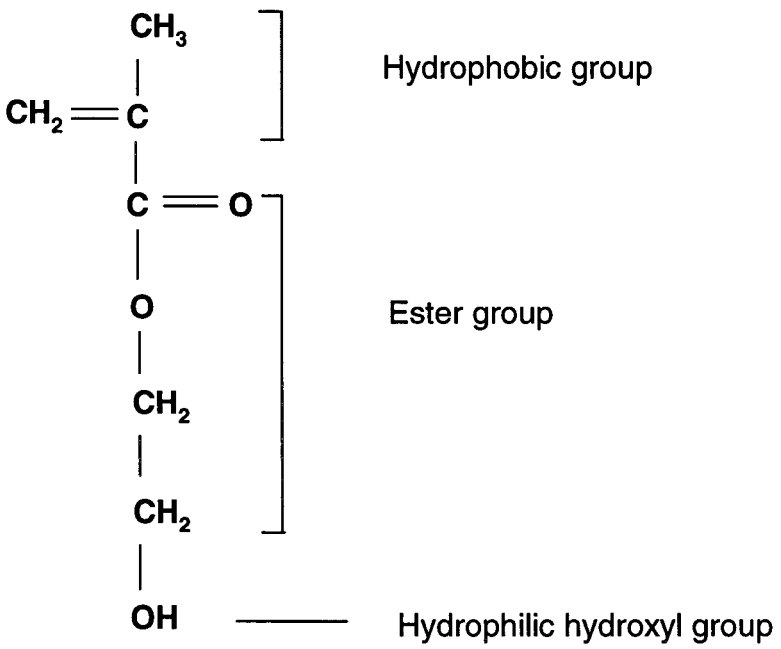

Figure 4.3 Structure of the PHEMA, showing the hydrophobic and hydrophilic portions.

The process of wetting any surface with a liquid film is a complex one, polymer surfaces are particularly mobile and the molecular orientation of the surface at any point in time may be modified in response to the surrounding environment.
The surface of a PHEMA hydrogel surface changes depending on the medium it is being exposed to. When materials such as poly [2-hydroxyethylmethacrylate] are exposed to air their hydrophobic methyl groups become directed towards the air interface by a process of chain rotation, leading to a minimised interfacial tension and consequently lower surface free energy. However, upon exposure to polar liquids, such as water, they demonstrate a higher surface energy by reorienting their hydrophilic groups towards the water phase (Tonge et al., 2001). Figure 4.4 shows the orientation of molecules in water and air.

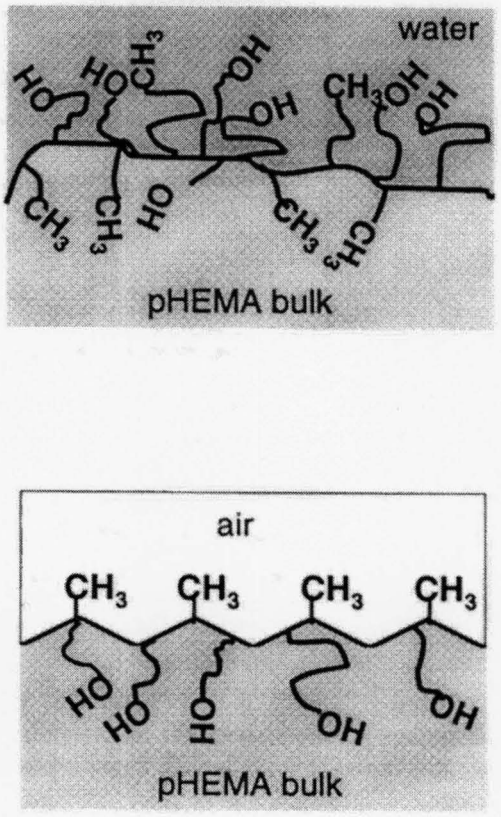

Figure 4.4 Diagrammatical representation of the surface molecular orientation of hydrogel in water and air (Opdahl et al., 2003).

Hydrogels have been studied using various microscopic techniques such as scanning electron microscopy (SEM) and atomic force microscopy (AFM). In general little topography has been found to be visible using these methods.

4.1.7 Measurement of Surface Tension

The measurement of contact angles yield data, which reflect the thermodynamics of a liquid/solid interaction. To characterise the wetting behaviour of a particular liquid/solid pair it is only necessary to report the contact angle (Fletcher et al. 1994). Contact angles are determined by the upper two or three monolayers of molecules, this thin layer, only 5 to 10Å thick, is what determines adhesion, electrical properties etc (www. firsttenangstroms.com).

The shape of a liquid drop or gas bubble placed at a homogeneous, rigid solid surface is controlled by the free energy of the three interfaces, solid/liquid, solid/vapour, liquid/vapour and by the solid topography. The angle between the tangent of the liquid and solid surface (contact angle), a characteristic parameter of the three-phase system, is used to describe the lyophobic/lyophilic properties of the solid surface and its quality (Drelich et al., 1996). Figure 4.5 shows the forces that control the wetting of a surface.

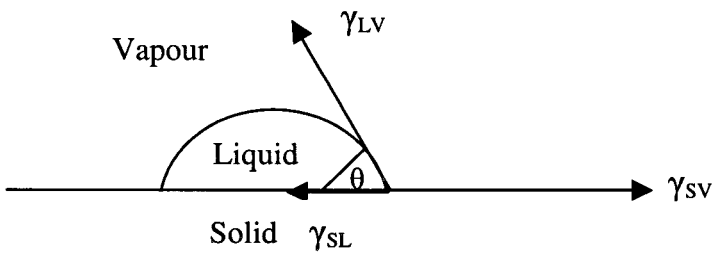

Figure 4.5 Forces that control the wetting of a surface.

At equilibrium Young's equation can be used to calculate the interfacial tension.

$$\gamma_{SV} = \gamma_{SL} + \gamma_{LV} \cos\theta \qquad \text{- Young's Equation}$$

Where γ_{SV} is the tension force between the solid and the vapour

γ_{SL} is the tension between the solid and the liquid

γ_{LV} is the tension between the liquid and the vapour

θ the angle between the bubble and the surface at the point of contact

Characterising the wetting behaviour of surfaces can be measured in a variety of ways:

- Sessile drop- where a drop of liquid is dropped on to the surface of interest and the subsequent angle measured. This is known as a liquid in air measurement.
- Captive bubble- where an air bubble is introduced to a surface immersed in a liquid. This is known as air in liquid measurement
- Wilhelmy plate- a micro-balance is used to measure the weight of the sample as it is moved into and out of the liquid.

Measurements of contact angles using the sessile-drop and captive-bubble techniques are among the most popular methods used in surface chemistry laboratories for this purpose, especially due to their simplicity and small amount of liquid and solid sample required (Drelich et al., 1996)

Contact angles may be advancing or receding. The advancing angle being that of the liquid or gas as it hits the surface and the receding being the angle as the liquid or the gas as it is removed. Advancing contact angles are a measure of the hydrophobicity of a material whereas, receding contact angle measurement are a measure of the material's hydrophilicity. A measure termed hysteresis which is calculated by subtracting the receding contact angle from the advancing contact angle indicates a changing of the surface properties of the material under test.

Hydrogels are not strictly hydrophilic as their contact angle is not zero; this is due to their dual properties, the hydrophobic part ($CH_3 - C = CH_2$) and their hydrophilic hydroxyl group. The wetting angle of a liquid is inversely proportional to the wettability of the solid being tested, it would have been expected that PHEMA hydrogels would exhibit a fairly low water contact angle. However, PHEMA appears to have a hydrophobic surface even when the hydrogel is fully hydrated. Hermitte et al. (2004) found, using the captive bubble method, that a 38% water content PHEMA hydrogel had a contact angle of 33.1°. Figure 4.6 shows the behaviour of an air bubble introduced to a hydrophilic surface through to a hydrophobic surface in a water environment. The lower the angle measured the more hydrophilic the surface.

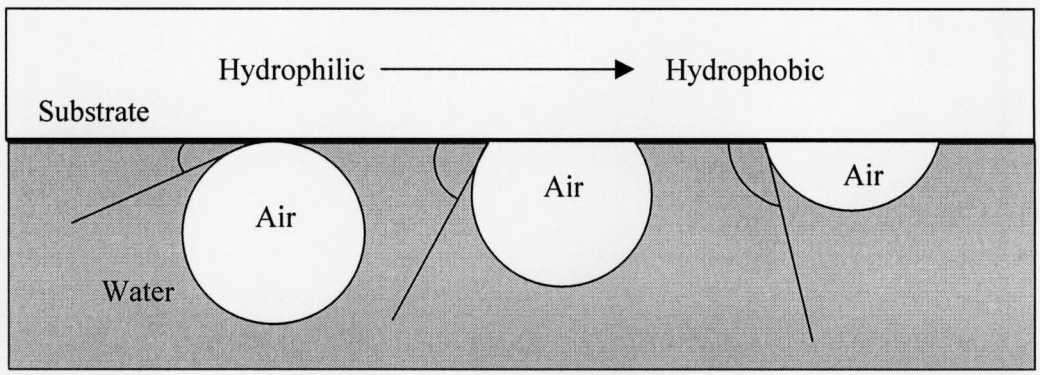

Figure 4.6 The change in bubble shape as the material under test becomes more hydrophobic.

4.1.8 Mechanical Properties of Hydrogels

The mechanical behaviour of hydrogels is best understood using the theories of rubber elasticity and viscoelasticity. These theories are based on time independent and time-dependant recovery of the chain orientation and structure, respectively. Rubbers are materials that respond to stresses with nearly instantaneous and fully reversible deformation. In their swollen state most hydrogels satisfy these criteria for a rubber material. When a hydrogel is in the region of rubber like behaviour, the mechanical behaviour of the hydrogel is dependent mainly on the architecture of the polymer network. General characteristics of rubber elastic behaviour include high extensibility generated by low mechanical stress, complete recovery after removal of the deformation, and high extensibility and recovery (Anseth et al., 1996). Common methods for measuring mechanical properties of hydrogels include tensile testing. For

most uniaxial tensile testing, dumbbell-shaped samples of polymer are placed between two clamps and one end of the material is pulled away from the other at varying loads and rates of extension.

4.2 Cationic Surfactants

Cationic surfactants are a well known group of chemicals which are used in a wide variety of areas. They have both antimicrobial and antistatic properties. Their antimicrobial properties are utilised in products such as eye drops, mouthwashes and laundry agents. Their surface-active properties are important as lubricators, constituents for polishes and in corrosion inhibition. The surfactant benzalkonium chloride has been shown to prevent growth of a variety of marine diatoms (Beveridge et al., 1998).

4.2.1 Properties

Cationic surfactants have unique properties, a positively charged head and a hydrophobic tail, which allow them to align themselves at interfaces. This occurs because the hydrophobic alkyl groups (usually range from C_8 to C_{22}) orient themselves at surfaces and interfaces while in the body of the solution they form micelles. Micelles are groups of 50-100 molecules (Clint, 1994), and are formed when the critical micelle concentration (CMC) is reached. Initially they are spherical in shape but as the concentration of the surfactant increases the shape of these micelles changes and becomes cylindrical, then hexagonal and lastly lamellar, in order to conserve space (Moroi, 1992) In a polar solution such as seawater the hydrophobic tail of the surfactant will be in the centre of the sphere, while the charged head will be on the outside, attracted by the polar environment. They therefore have two properties ideally thought to prevent microbial development. The charged head has antimicrobial properties and the tail has surface-active properties.

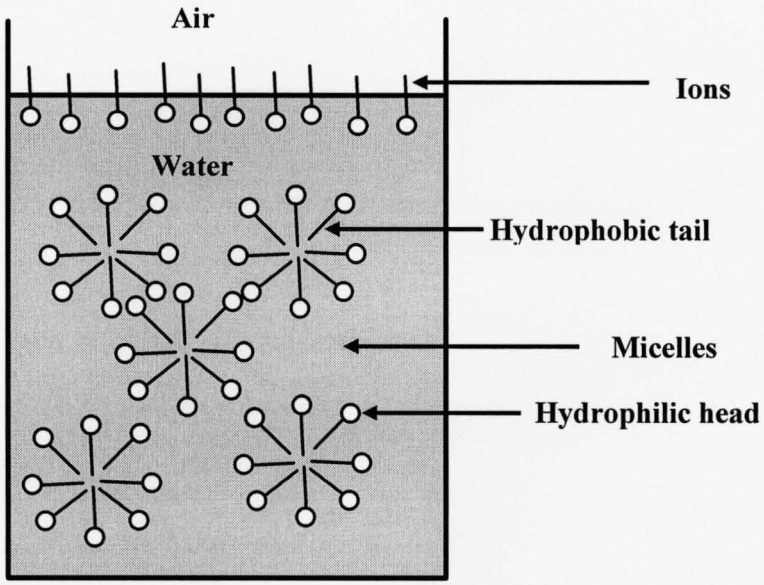

Figure 4.7 Arrangement of surfactant ions and micelles in water and at the air/water interface.

If a cationic surfactant is added to water the arrangement of the molecules within the water can be diagrammatically represented by figure 4.7. It can therefore be assumed that the arrangement of a surfactant within the water portions of a hydrogel would be broadly similar.

4.2.2 Mode of Action

The germicidal activity of cationic surfactants is directly related to their chemical properties. Those properties include a reduction in surface tension and formation of ionic aggregates, which results in changes in conductivity and solubility. Since cationic surfactants are positively charged, the cations are attracted to negatively charged materials such as bacterial proteins (Fredell, 1994). Hugo (1965) lists the five possible modes of cidal action of cationic surfactants as:

- Direct effects on proteins: denaturation and disruption
- Effects on metabolic reactions
- Effects on cell permeability and membrane damage
- Stimulatory effect on the glycolysis reactions

- Effect on the enzyme system, maintaining a dynamic cytoplasmic membrane

Merianos (2001) states that the most important site of adsorption is the cytoplasmic membrane of bacteria and the extent of bacterial death is governed by six factors:

- Concentration of antiseptic or disinfectant
- Nature of bacterial cells and density
- Time of contact
- Temperature of the medium
- pH
- Presence of foreign matter

The lowest concentration of the antiseptic that induces bacterial death also brings about leakage of cytoplasmic constituents of low molecular weight. The most immediately observed effect is loss of potassium ions. The increased permeability is a sign of changes in the membrane that are initially reversible but become irreversible on prolonged treatment. The necessary characteristic of an antiseptic is its bactericidal action, but there is often a low and rather narrow concentration range in which its effect is bacteriostatic. At this low concentration, certain biochemical functions associated with the bacterial membrane may be inhibited (Merianos, 2001). He also reviewed the most reliable evidence on the mode of action of cationic antiseptics suggested the following generalisations which elucidates Hugo's (1965) explanation.

1. Adsorption of compound on the bacterial cell surface
2. Diffusion through the cell wall
3. Binding to the cytoplasmic membrane
4. Disruption of the cytoplasmic membrane
5. Release of potassium ions and other cytoplasmic constituents
6. Precipitation of cell contents and the death of cells

4.2.3 Quantitative Analysis of Cationic Surfactants

Cationic surfactants which contain an aromatic ring are predominantly analysed using high performance liquid chromatography (HPLC) combined with an ultra-violet (UV) detector. Benzalkonium chloride falls into this category and exhibits absorbances at a variety of wavelengths, 214nm showing the greatest absorbance and therefore the most sensitive detection wavelength.
Cationic surfactants which are aliphatic and therefore have no chromophore cannot be detected using direct UV but can be detected indirectly or by ion-pair chromatography. Refractive index and conductivity detectors can also replace UV for the detection of these ions (Suortti and Sirviö, 1990; Nakamura and Morikawa, 1982)). Another method of detection of these compounds is by ion chromatography (IC) using suppressed conductivity detection. Gas chromatography has also been used (Choi et al., 1979).

The principles of HPLC were put into practice during the 1970's when these instruments replaced titration and spectrophotometers for quantitative analysis of compounds. HPLC has its origins in classic chromatography dating back to 1920's when open glass columns were filled with silica or alumina and a sample introduced from the top in a suitable solvent. This solvent 'carried' the sample down through the glass column and separation of the compound could be seen as coloured bands. In order to extract each component the packing material had to be removed and the component extracted from it. These original components have been replaced by stainless steel columns filled with appropriate silica, pumps which are able to pump solvent through the columns at high pressures allowing the compound of interest to be carried to a detector from which an output is recorded for quantification. HPLC is a robust and commonly used technique for the quantitative analysis of surfactants.

4.3 Gas Sensors

Gas sensing probes have found widespread use in the determination of dissolved gases in water systems. These sensors are used for both discrete measurement and continuous monitoring and are deployed in rivers, estuaries, coastal areas and oceans. They can be deployed singularly or as part of sensor pack. The manner in which they

are employed varies from floating buoys to towed vehicles. A variety of gases are measured but the gases, which are most frequently measured, are oxygen, ammonia and carbon dioxide.

4.3.1 Background of Sensor Measurement

Ammonia and carbon dioxide sensors are potentiometric gas-sensing probes and essentially they are ion-selective electrodes. Oxygen sensors are usually Clark-type cells. They are constructed within a tube that contains a reference electrode, an ion selective electrode and an electrolyte solution. A thin, replaceable gas-permeable membrane is attached to the end of the tube and this serves two purposes; to serve as a barrier between the internal and analyte solution and to allow the flow of gaseous species through from the measuring medium. The gas permeable membrane is fabricated from a hydrophobic polymer and is highly porous with a pore size in the region of 1μm and a thickness of about 0.1mm.

These sensors measure the gas species of interest by diffusion of the gas across the membrane until a reversible equilibrium is established between the gas level in the bulk solution and the internal filling solution. In the case of ammonia measurement hydroxide ions are formed as the ammonia diffuses in and the internal electrode measures the pH and this level is directly proportional to the ammonia level. Table 4.1 shows the electrode filling solutions and electrodes for oxygen, ammonia and carbon dioxide detection.

Gas	Filling Solution	Electrode	Ref. Electrode
Ammonia	Ammonium chloride	pH	Silver/Silver chloride
Carbon dioxide	Sodium hydrogen carbonate	pH	Silver/Silver chloride
Oxygen	Potassium chloride	Gold/ Platinum	Silver

Table 4.1 Typical conditions for the measurement of gases present in water.

The measurement of oxygen in water is affected by a variety of factors (Thermo Russell, technical information sheet). Whenever air comes in contact with water, the oxygen in the air will dissolve in the water, at what rate this happens depends on whether there is adequate time and adequate mixing to fully saturate the water, the water temperature, the air pressure and whether there are substances in the water which consume the oxygen. The same applies to other dissolved gases.

4.3.2 Effects of Membranes on Gas Diffusion

Free diffusion coefficients in water of the gases of interest such as ammonia, carbon dioxide and oxygen are 1.5×10^{-5}, 2.5×10^{-5} and 2.01×10^{-5} $cm^2 s^{-1}$ respectively, at 20°C (The CRC Handbook of Chemistry and Physics (2005) Data Book). These diffusion rates are slowed down as the gases move through gas membranes (PTFE) on sensors. However, when equilibrium is reached this does not affect measurement. Tarsiche and Ciurchea (1997) found that the diffusion coefficient of ammonia through PTFE membranes was reduced two-fold compared with diffusion in water and that the concentration had an affect on diffusion, increasing as concentration increased, finding it to be 1.2×10^{-7} and 5.90 $cm^2 s^{-1}$ for 10^{-5}M and 5×10^{-3}M respectively at 20°C. The diffusion of oxygen across a PTFE membrane was found to be 2.8×10^{-7} $cm^2 s^{-1}$. Mirtaheri et al. (2004) stated that for PTFE, the diffusion coefficient is

variable and dependent on the nano-porous structure of the material. The estimated value for carbon dioxide is between 5 $x10^{-6}$ and 5 $x10^{-5}$ cm^2s^{-1} for typical PTFE membranes, although these were at 37°C (Cunningham and Williams, 1980). Mirtaheri et al. (2004) found that for a planar sensor the calculated response time for carbon dioxide diffusion through a PTFE membrane was 50 seconds. Therefore the type, thickness and structure of membranes affect the diffusion of gases, as would any biofouling protective coating.

4.3.3 Gas Membranes - Effects of Biofouling

The deleterious effect that biofouling has on sensor stability is a serious impediment to the development of long-term deployment of underwater instruments. Fouling can affect a sensor in a variety of ways such as component-based failures, electrical shorts, membrane degradation, and membrane biofouling (Wisniewski and Reichart, 2000). However, it is the effects of membrane biofouling that will be studied here and to a lesser extent membrane degradation. In order to be detected by a sensor the gas of interest must be able to freely diffuse through the membrane therefore any fouling on the membrane will reduce its diffusion. Biofilms are dynamic and heterogeneous and will affect the diffusion of gases in a number of ways. Firstly it will increase the thickness and thus increase the diffusion path length for the species, it will also present a higher resistance to the species of interest and thus increase the response time of the sensor. The solution contained within the biofilm will create a buffering capacity, which will also increase the response time (Munro et al., 1996). The reaction of the gaseous species with the biofilm may also cause an erroneous result. Fraher and Clarke (1998) found that fouling on the membrane of an oxygen sensor caused the "gain" to be reduced and the resultant dissolved oxygen was lower than the actual level. Marshallsay (1989) found that biofilms on pH electrodes increased the response time from 14 seconds to nearly 3 minutes for a step change of 8 to 9.5 pH units after 3 weeks in situ at a water treatment plant. Munro et al. (1996) found that fouling on a pH electrode caused the response time to increase in a linear manner with increasing attached biomass and biofilm optical absorbance. Wisniewski et al. (2000) and Wisniewski and Reichart (2000) have published extensively on the effects of membrane fouling on implantable biosensors and reviewed various methods to prevent it. The effects of biofouling on the membranes of implantable glucose sensors

are very similar to marine biofouling on gas sensors membranes and so consideration of the methods of prevention for implantable sensors may result in a useful method for deterring biofouling on marine underwater sensors.

When considering how to prevent fouling on gas sensor membranes it is important firstly to look at the available membranes, their structure and properties as often these are chosen through habit or ease of access when more careful consideration of what material it had been made from may reduce the fouling to a more acceptable level. Most membranes for gas sensor membranes are made from polytetrafluoroethylene (PTFE) and some from high-density polyethylene (HDPE). Figure 4.8 shows the structure of the repeating unit in these polymers.

$$- (CF_2CF_2) - \qquad\qquad - (CH_2CH_2)-$$

Figure 4.8 The structure of the repeating units of PTFE and HDPE.

Both the PTFE and HDPE membranes vary in structure and thickness depending on their production method. It has been shown that choosing a PTFE membrane with a small pore size can reduce fouling. Brauker et al. (1995) showed that implanted 5μm pore-size PTFE membranes had 80-100 fold more vascular structures in close proximity to the membrane than did implanted 0.02μm PTFE membranes. Simple surface modifications have also been considered (Ratner, 1995) such as creating functionalities like hydroxyl, carboxyl, amine, sulphonate or phosphate groups. Glasspool and Atkinson (2003) carried out a study to evaluate the characterisation of membrane materials suitable for dissolved oxygen sensors. They tested three membranes, cellulose acetate (CA), PTFE and polyvinylchloride (PVC). The membranes had thicknesses of 9, 5 and 8μm and response times to oxygen detection in tap water of 3 minutes for the PTFE and cellulose acetate and 5 minutes for the PVC. After 4 hours white deposits were noted the main constituent of which was calcium. These deposits on the CA reduced the current to 4% of its initial value; no decrease was noted for the other two membranes.

They concluded that the flow sensitivity of each membrane to oxygen diffusion can be attributed to differences in membrane thickness and to their oxygen permeability coefficients.
However, due to the diversity of marine biofouling it is unlikely that any of these modifications alone would be able to prevent biofilm formation.

4.3.4 Materials used to Protect Sensor Membranes

There has been little work in the area of biofouling prevention protection of underwater gas sensing instruments except for the use of mechanical mechanisms such as wipers and water jetting. Therefore comparisons of coating technologies can only be made to the protection of biosensors where a great deal of research, using a variety of techniques, has been done.

Wisniewski and Reichert (2000) reviewed a variety of methods for the reduction of biofouling on biosensor membranes. They stated that anything that raises or lowers capillary perfusion or analyte diffusion can affect sensor performance and also that membrane materials are generally chosen out of convenience.

When modifying a surface to prevent biofouling it can usually be grouped into two broad categories:

1. Chemically or physically altering the atoms or molecules in the existing surface (treatment, etching, and chemical modification).
2. Coating over the existing surface with a material having a new composition (solvent coating or thin film deposition by chemical vapour deposition, radiation grafting, chemical grafting or RF-plasmas) (Ratner 1995).

Hydrogels such as PHEMA and poly (ethylene glycol) (PEG) have been used as overlays for some implantable biosensors. These can produce a hydrophilic interface between the solid surface and aqueous bulk. Several problems have been encountered in applying hydrogels to the sensor surface such as poor adherence, less than acceptable mechanical stability, the monomer and solvent may have a detrimental

effect on the enzyme being measured and the hydrogel may limit the diffusion into the sensor. However, studies have successfully applied PHEMA to sensors and these have been shown to reduce clotting, reduce protein adsorption and enhance electrode stability (Wisniewski and Reichert 2000).
However, any surface modification must maintain appropriate gaseous diffusion through the coating as the sensor must be able to respond to fluctuations in gas concentrations over the monitoring period. The permeability of hydrogels to water is important in the transfer of the gaseous species and values for permeability at 27° C of around 30,000 g mm m^{-2} day^{-1} are quoted (Refojo and Yasuda, 1965) compared with values for polyethylene and nylon, 5 and 280 g mm m^{-2} day^{-1} respectively. Therefore highly swollen surface hydrogels should not prevent the diffusion of small gaseous species.

4.3.5 Characteristics Required of a Coating to Prevent Biofouling on Gas Membranes

Any coating chosen must adhere well to the existing gas permeable membrane and must not have a deleterious effect on the diffusion of the gas being monitored (Quinn et al. 1995). It is also important that the coating does not interfere with the parameter being measured i.e. significantly prevent or reduce or increase the diffusion of the gas being detected or react with the measured parameter altering the end product. It also requires to be robust for its application and so its physical properties in applicable environments must be considered to ensure there is no drastic change in the behaviour of the coating which in turn would change the diffusion through it.

Polymeric materials that are used in the manufacture of *in vivo* biosensors and medical devices must satisfy requirements for performance, biointeraction and biocompatibility; these requirements would be less relevant for a hydrogel being used as a coating in the marine and freshwater environments. The understanding of structure-property relationships in polymers is sufficiently advanced so that the desired mechanical properties, durability and functionality can be achieved. Biological responses to biomaterials, on the other hand, are associated with surface chemistry and structure. Thus, the rationale for the surface modification of biomaterials is straightforward; retain the key physical properties while modifying

only the outmost surface to influence biointeraction. With well engineered surface modification, the mechanical properties and functionality of the device will be unchanged, but the biocompatibility, biorecognisability or biofunctionality will be enhanced (Ratner, 1995).

4.3.6 Gas Diffusion through Hydrogel Membranes

The use of hydrogels as contact lenses has prompted study of oxygen diffusion through them. This is usually termed oxygen permeability (Dk) which is defined as the product of the diffusion coefficient, D and the solubility coefficient, k. The term D indicates the speed with which oxygen molecules pass through the material while k describes the ease with which oxygen dissolves in the material (Fletcher et al., 1994) In order for hydrogels to be successful as lenses the amount of oxygen reaching the eye must be sufficient to maintain corneal function. The permeability coefficient is known to increase with increasing membrane thickness due to boundary layer effect (Compañ et al.1999). Compañ et al. (1992) also stated that oxygen permeability is a characteristic of the lens, which depends on temperature, pressure, water content and thickness. They also found that oxygen permeability is found to be exponentially dependent on water content rather than on the chemical composition of hydrogel. The oxygen permeability through the stroma of the eye is around 300 $x10^{-10}$ cm^2 ml O_2 s^{-1} ml^{-1} $mmHg^{-1}$ (Tighe, 1992). The permeabilities of a variety of hydrogel materials used as contact lens are available in the literature. Table 4.2 shows the range of measured oxygen permeabilities and diffusion of contact lenses with water content of around 40%. Wichterlová et al. (2005) studied permeability and diffusion of oxygen through PHEMA material with a water content of 38% over a range of thicknesses (0.1mm – 3.2mm) and found that permeability ranged from 13.6 x 10^{-11} cm^2 ml O_2 s^{-1} ml^{-1} $mmHg^{-1}$ for 0.1M KCl electrolyte to 10.5 x 10^{-11} cm^2 ml O_2 s^{-1} ml^{-1} $mmHg^{-1}$ for 0.5M KCl electrolyte when measured at 34°C. This type of data shows that gaseous diffusion is not prevented by hydrogels but it does not elucidate the response times in terms of sensors or whether these times would be relevant over long term deployment periods.

Contact Lens (EWC)	**Temp** (°C)	**Diffusion Coeff.** ($cm^2\ s^{-1}$)	**Permeability Coeff.** (cm^2 ml $O_2\ s^{-1}\ ml^{-1}\ mmHg^{-1}$)
Sequence (38%)[1]	35		10.5×10^{-11}
Sequence (38%)[1]	35		9.0×10^{-11}
Sequence (38%)[1]	35		8.4×10^{-11}
PHEMA (40%)[2]	37		8.0×10^{-11}
Softlens (38.6%)[3]	20	2.71×10^{-7}	11.2×10^{-11}
Lenticon (40%)[3]	20	2.52×10^{-7}	12.1×10^{-11}
HEMA (39%)[4]	25		7.5×10^{-11}
HEMA (39%)[4]	34		14.5×10^{-11}

Table 4.2 Oxygen permeabilities through a variety of contact lens hydrogel materials. (1. Compan et al. 1999. 2. Weissman and Fatt, 1991. 3. Compan et al. 1992. 4. Ng and Tighe, 1976)

The fact that oxygen does diffuse through hydrogels, although they reduce the diffusion, when compared with that through the stoma of the eye, indicates that they have possible application to gas sensors.

4.4 Summary

4.4.1 Hydrogels

The use of hydrogels as biocompatible materials has shown them to be successful in preventing biofouling. They have great potential in the application of antifouling coatings for sensor ports due to their properties such as, ease of polymerisation, ideal reservoirs for bioactive substances, transparency and ease of producing them in any geometry. They have been shown to prevent marine biofouling when loaded with the cationic surfactant benzalkonium chloride (Parr et al. 1998) and Arquad 2C-75 ([a]Smith et al. 2002).

4.4.2 Gas Membranes

The study of the physical and chemical properties of gas membranes shows them to vary considerably. Careful considerations of their properties and applications may lead to increasing the fouling free lifetime. The addition of thin hydrogel overlays seems to be a feasible way of protecting these membranes further.

Chapter 5

Hydrogels - Experimental Work, Results and Discussion

5.1 Production Techniques - Production Method Development

The problems of producing a high quality hydrogel are detailed in chapter four. In the preparation of the hydrogel it is crucial to produce a bubble free material and a flaw free surface. Any such flaws are detrimental to optical and gaseous diffusion measurements as well as having a tendency to increase the biofouling accumulation.

5.1.1 Method

The hydrogels are produced using thoroughly degassed solutions, as oxygen in the system will slow down polymerisation. Degassing is also important as the polymerisation process is exothermic and can result in bubble formation within the hydrogel during curing. Considerable method development was carried out to create a hydrogel suitable for coating optical sensors. The resultant polymer is poly - (hydroxyethylmethacrylate) (PHEMA) and is a transparent lightly cross-linked material containing 40% water. These hydrogels exhibit a high degree of chemical and mechanical stability and are generally considered to be inert making them ideal as materials for contact lenses, medical implants and coatings for a variety of surfaces. The hydrogel coating is fabricated in sheet form by solution polymerisation. The sheets produced are 250mm x 250mm x 1mm and can be cut to size using precision-machined cutters.

Table 5.1 shows the chemicals used and proportions of each required to produce a hydrogel with a water content of 40%. The monomer 2-hydroxyethylmethacrylate (HEMA) was used without further purification. The cross-linker used was tetraethylene glycol dimethacrylate (TEGDMA) and the catalysts were 6 %(aq) ammonium persulphate ($(NH_4)_2S_2O_8$) and 12%(aq) sodium metabisulphite ($Na_2S_2O_5$) (Refojo, 1965).

Solution/Solvent	Quantity/Proportion	Storage
Distilled water	X/2	Freshly generated
Ethylene glycol	X	Room-temperature
2-hydroxyethylmethacrylate	X	Refrigerate
Tetraethylene glycol dimethacrylate	X	Refrigerate
6%(aq) ammonium persulphate	X/10	Refrigerate salt
12%(aq) sodium metabisulphite	X/10	Room temperature

Table 5.1 The chemicals and their proportions used in hydrogel production.

The catalyst solutions were dissolved in distilled water. All the solutions were degassed before used. The hydrogels were polymerised in an oven at 60° C for 24 hours then removed and cooled to room-temperature before being removed from their moulds. The hydrogels were then soaked in distilled water to remove the ethylene glycol, any excess initiator and unpolymerised monomer. The water was changed twice daily for 3-4 days and the hydrogels were then stored in distilled water at room-temperature until required. The hydrogel produced has a cross-link ratio of 3.9×10^{-3}. The mole percentage crosslinker is 0.37% and from this value it would be assumed that diffusion through this hydrogel is mainly via a pore mechanism (Wisniewski et al. 1976).

5.2 Loading the Hydrogel with Cationic Surfactant

The two cationic surfactants used were benzalkonium chloride (BAC) supplied by Sigma-Aldrich, UK, and was considered to have a purity of >98%. The second surfactant was dialkyldimethylammonium chloride (Arquad 2C-75) and was a gift from Akzo Nobel, Littleborough, UK. It was supplied at a concentration of 75% surfactant, 15% 2-propanol and 10% water. The structures of these surfactants are shown in figure 5.1.

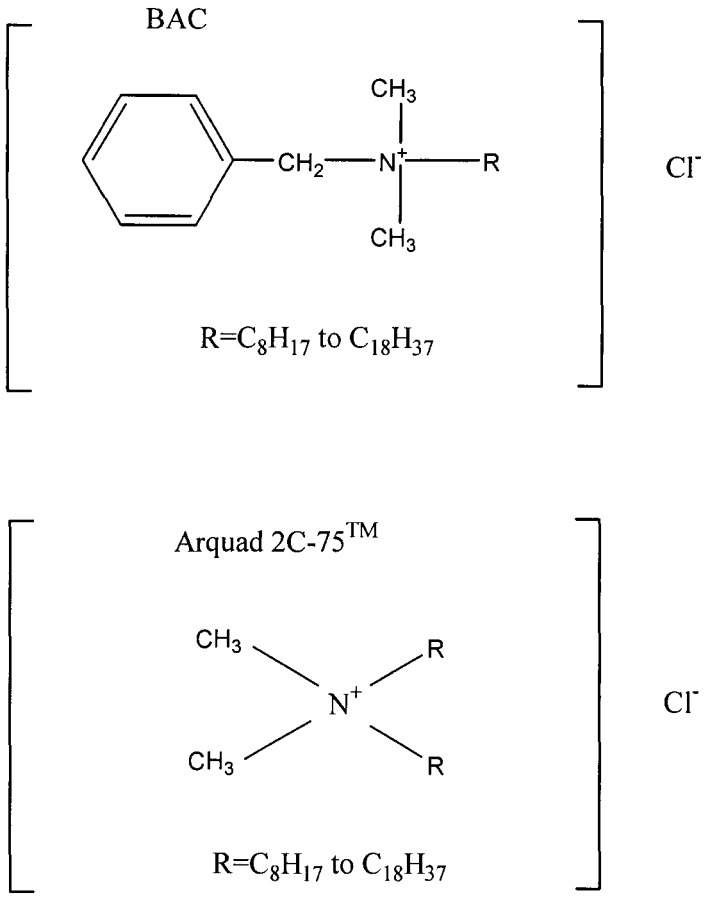

Figure 5.1 The structures of benzalkonium chloride (BAC) and dialkyldimethylammonium chloride (Arquad 2C-75).

5.2.1 Method

Quantitative analysis and method development of both the surfactants used is detailed in section 5.3.

5% w/v solutions of the surfactants were prepared and these were clear in the case of BAC and translucent in appearance in the case of Arquad 2C-75. The hydrogels were soaked in sheet form as prepared; this was a size of 250 x 250 x 1mm. The surfactant volume, 330ml per sheet, ensured that there was always an excess of volume, at least 10 to 1. Hydrogel discs were sampled at various time points and quantitatively

analysed for surfactant content. Gehrke and Lee (1990) stated that when drugs were being absorbed by hydrogels, loading was normally established after 24 hours. However, this was due to loading being carried out in a 50/50 ethanol/water mix, which causes the hydrogel to swell substantially more, causing loading to occur at a faster rate. However, as the hydrogel was being deployed in the marine environment for months at a time it was considered prudent to reduce the swelling/shrinking process as much as possible as it may have ultimately had a negative effect on the mechanical strength of the hydrogel coating.

5.2.2 Results and Discussion

Figure 5.2 shows the amount of BAC absorbed over time. Initially a substantial amount of BAC is absorbed and although the amount absorbed continued to increase, by 3 weeks 75% of the final amount at 12 weeks had already been absorbed. Previous work (BROS Report, 1998) had shown around 5% BAC to be an ideal amount as it prevented fouling, allowed the hydrogel to retain enough mechanical strength to be easily handled and the hydrogel remained transparent at this level. Loading with higher levels resulted in the hydrogel becoming translucent and with even higher levels (20%) becoming opaque. The loading was therefore considered to be complete after 2-3 weeks.

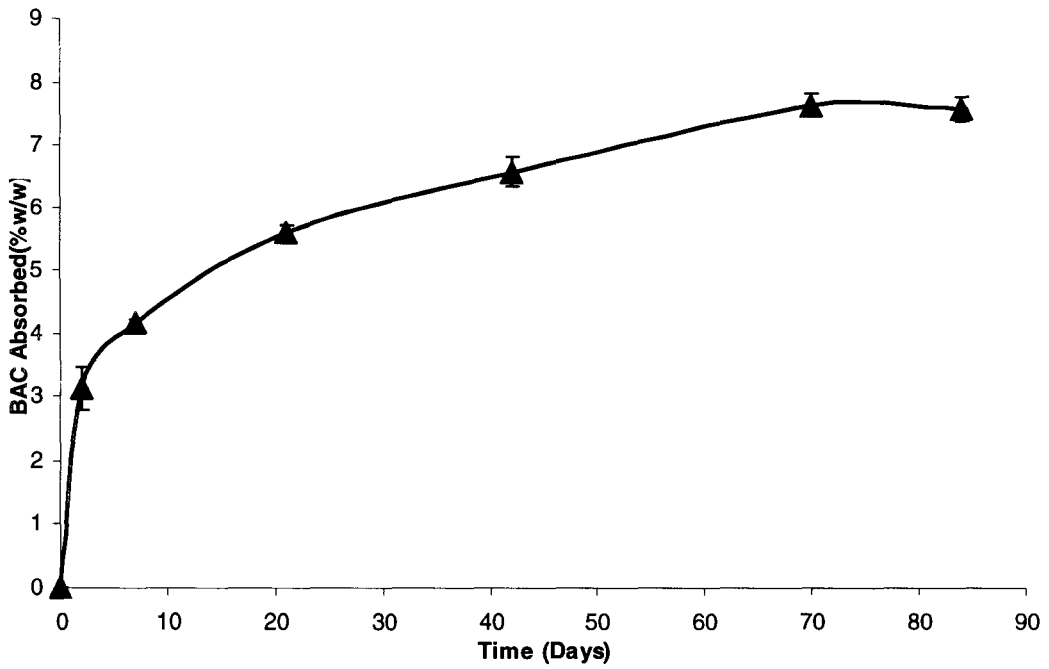

The absorption of Arquad 2C-75 was also measured over time. The amount of Arquad 2C-75 absorbed from a 5% solution was rapid over the first 7 days resulting in around 50% of the 1.4% absorbed after 72 days, figure 5.3 shows this. The amount absorbed continued to increase but to a much lesser extent. Again as with the BAC hydrogel which had been soaked for around 3 weeks was considered to be useful for application as by that time it had absorbed around 1% of surfactant.
The amount of Arquad 2C-75 after 3 weeks was approximately 20% of the amount of BAC absorbed over the same time.

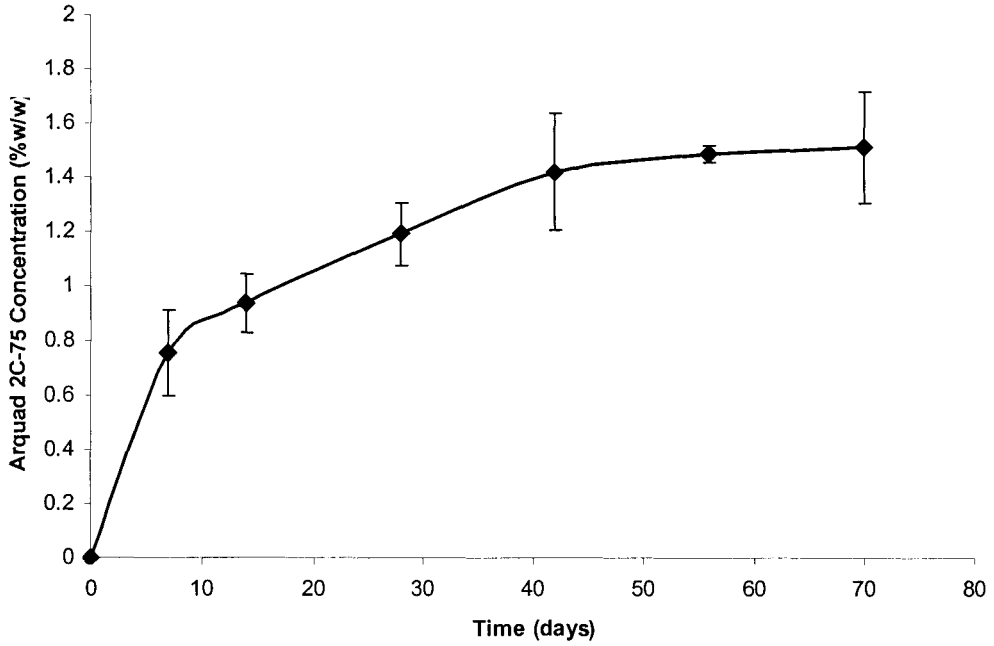

Figure 5.3 Arquad 2C-75 absorbed by hydrogel over 12 weeks, (± SDs are shown).

The absorption is a diffusion controlled process. Both surfactants, after an initial phase, follow non-steady state diffusion into the hydrogel as can be seen by figures 5.4 and 5.5. Hoch et al. (2003) found that water diffused through hydrogel following Fickian diffusion, as did Gehrke et al. (1995).

1994 in lit

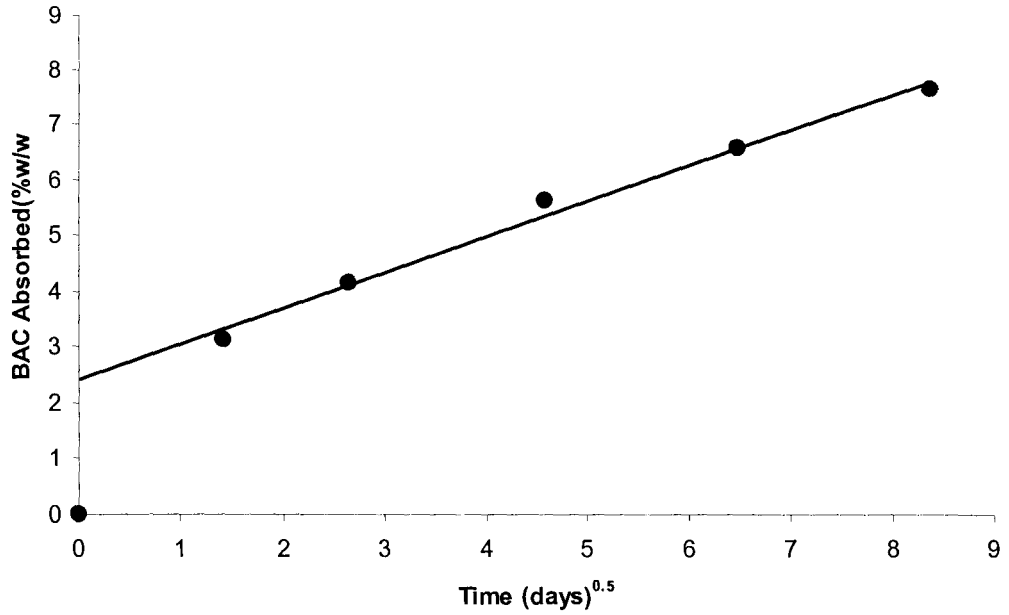

Figure 5.4 Absorbance of BAC in hydrogel versus the square root of time, demonstrating Fickian behaviour.

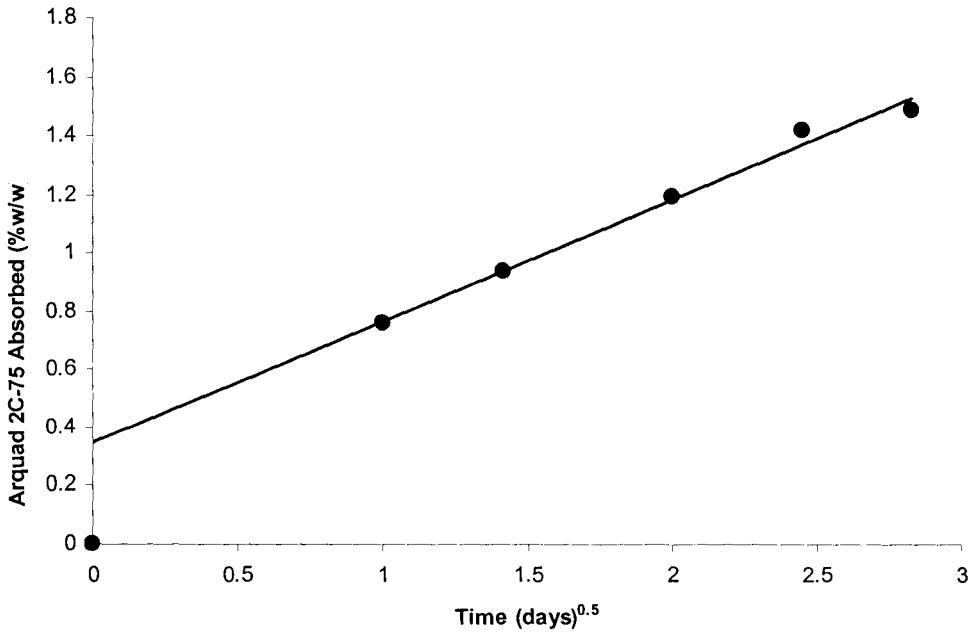

Figure 5.5 Absorbance of Arquad 2C-75 in hydrogel versus the square root of time, demonstrating Fickian behaviour.

Absorption of Surfactants by Hydrogel – Gravimetrically

The amount of surfactant absorbed by the hydrogel can also be calculated using the equation

$$\text{Surfactant Loading} = (D_l - D_{water})/ D_l$$

Where D_l is the dry weight of loaded hydrogel and D_{water} is the wet weight of the unloaded hydrogel.

Discs of hydrogel (20mm diameter) were cut from a sheet, which had been soaking in distilled water and dried at 60°C for 24 hours; these were considered the unloaded dry weights. The discs were then placed in 30ml of 5% BAC, 5% Arquad 2C-75 and distilled water (4 replicates of each). The weights of the discs were recorded at 1, 3, 7, 14 and 21 days. The hydrogel discs were then dried as described and their weights recorded. Figure 5.6 shows the increase in wet weight over the time period.

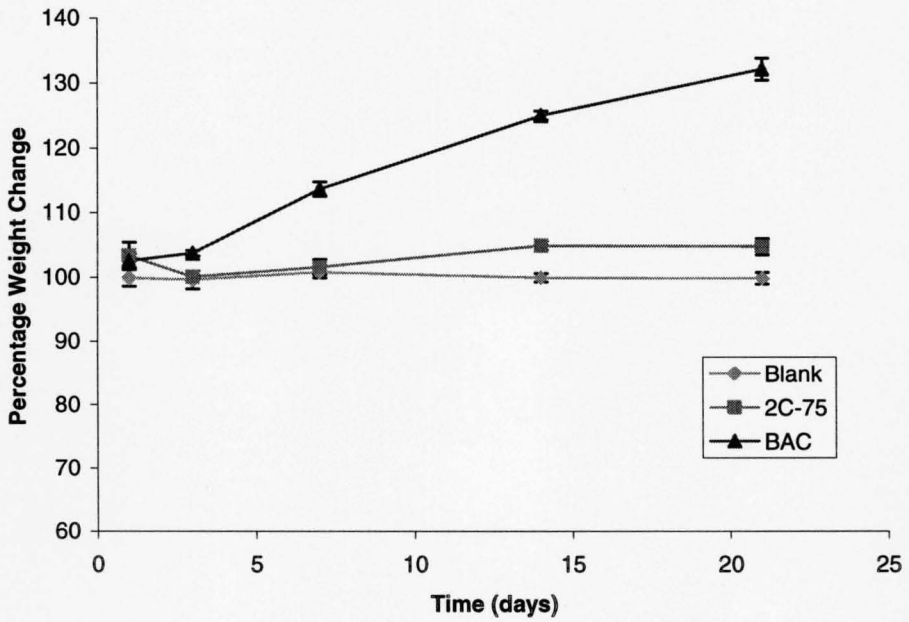

Figure 5.6 The percentage wet weight change of hydrogel discs in distilled water (Blank), 5% BAC and 5% Arquad 2C-75.

The equation above was used to calculate the amount of BAC and Arquad 2C-75 adsorbed by the hydrogel. After the 21 days soaking the concentration of BAC was 12 ±0.16 %w/w and in Arquad 2C-75 was 2.9 ±0.36%w/w. These amounts are higher by roughly by a factor of 2 than the amounts absorbed by soaking the wet hydrogel in the surfactant solution. Due to the increased absorption this method warrants further study. However, the effects on the structural properties of the hydrogel have not been fully studied and it was decided to continue to load the hydrogels in their wet state, as described in section 5.2.1.

5.3 Quantitative Analysis of Cationic Surfactants

Benzalkonium chloride can be measured using high performance liquid chromatography (HPLC) with ultra-violet (UV) detection. A method described by Guilfoyle et al. (1990) was modified and used in this work.

The quantitative measurement of the twin-quaternary compound Arquad 2C-75 is problematic as it is an aliphatic and does not have a chromophore as the aromatic BAC has. Various methods were investigated and these are reported in section 5.3.2.

5.3.1 Quantitative Analysis of Benzalkonium Chloride

Sample discs were taken using a cork borer with a diameter of 20mm. Three replicates were cut from each hydrogel at each time point. The discs were weighed and put into 30ml of methanol (HPLC grade) to swell and allow the BAC present in the hydrogel to be released. The hydrogel discs were cut into small pieces to increase the surface area exposed to the methanol. The hydrogel was left in the methanol for 24 hours and then crushed using a mortar and pestle to ensure all the BAC was released. It was then returned to the methanol and this was filtered through Whatman No.1 filter paper into 100ml volumetric flasks, which were made up to the mark using methanol. The samples were analysed using the method described.

The HPLC conditions were:

Instruments	Datajet Integrator, Thermo Separating Products (TSP)
	Spectra Series UV100, TSP
	Constametric III metering pump, LDC / Milton Roy
Column	Techsphere 5CN (250mm x 4mm), HPLC Technology, UK
Column Temp	Ambient
Flow Rate	2.00 ml / min
Mobile Phase	Acetonitrile / 0.06M NaH_2PO_4 80 / 20 pH = 7.00
Wavelength	214nm
Detection	0.5AUFS

5.3.2 Method Development for the Analysis of Arquad 2C-75

Two main detection types were used to try to develop a method to quantify the twin-chain cationic surfactant Arquad 2C-75, high performance liquid chromatography HPLC and suppressed conductivity detection (IC). However, a variety of other methods from the literature were tried and assessed for their usefulness.

In the literature there are very few methods published. However, two HPLC/UV methods were utilised. The first by Larson and Pfeiffer (1983) is a photometric chromatographic procedure for the determination of aliphatic ammonium salts in which an aromatic quaternary salt is employed as a UV absorbing species. Inverted peaks are observed in an elevated baseline as the UV absorbing ion selectively displaces the transparent sample ions from the column. The second method was described by Helboe (1983) and involves reversed-phase ion-pair liquid chromatography using ultraviolet- absorbing counter ions.

An HPLC/conductivity method was published by Wee (1984) and it was tested for its suitability.

A potentiometric (titration) was also utilised, this was used courtesy of Metrohm, UK.

HPLC/Conductivity Detection

This equipment was used at Akzo-Nobel, Littleborough, England. Analysis was carried out using a method that they had developed. This has shown to be a robust method, which operates using a cyano-nitrile column. The samples must be prepared in the mobile phase which is chloroform:methanol in the ratio 92:8. The extraction of Arquad 2C-75 from hydrogel is done in methanol, approximately 50ml. The sample has to be reduced (steam bath) and made up in a small quantity of the mobile phase e.g. 5ml or 10ml. The method is linear over the range of interest. However, this method is only applicable to samples at zerotime i.e. before immersion in seawater, as seawater ions would interfere with the analysis.

Potentiometric Titration

The marine samples were prepared in 50ml methanol and a 5ml aliquot of this was titrated. Zero time, 1 week and 4 week samples were analysed. The end-point was easily detected on the zero time and 1 week samples but the method found it more difficult with the four week sample. This method appeared to be useful at higher concentrations e.g. 500mg l^{-1}. To improve the analysis the sample could be evaporated and re-dissolved in a small volume (5ml), or a larger volume of sample could be titrated.

It was useful to see this method demonstrated (Metrohm UK Ltd, Buckingham, England) and it also gave results, which were comparable to those subsequently obtained from the ion chromatography. However, due to the various limitations this method was not pursued further.

HPLC/UV Using an Ion-pairing Agent

A method developed by Helboe (1983) was investigated. The method operates by pairing the active substance (Arquad 2C-75) with an UV absorbing anion, in this case p-toluene sulphonic acid. The absorbing wavelength was 254nm as this resulted in the greatest detection.

The method worked well for quantitative detection at high concentrations, above 1000 mg l^{-1}. It splits the alkyl chains and gives a homologue percentage distribution. However, even when the extracted sample (from hydrogel) is reduced to a white residue and made up in a small volume of mobile phase it was difficult detecting any Arquad 2C-75 after only one week in marine trials.

It would be of more use in studying the effects of the absorbance and release of the alkyl chain lengths than for quantitative analysis. (The method was originally developed for the analysis of cetrimide (a single chained cationic surfactant with no chromophore) but it appears to be useful for Arquad 2C-75.)

HPLC/UV using Indirect Photometric Detection

The method described by Larson and Pfeiffer (1983) was used 'as is' and also with various changes to the parameters to attempt to improve the detection.

The method operates by using an aromatic quaternary ion as the UV absorbing species. This ion is then displaced when the aliphatic quaternary ion i.e. 2C-75 is eluted and a negative peak results which indicates the amount of 2C-75 present in the injection. The method is referred to as Indirect Photometric Detection (IPD).

The mobile phase contains 1% acetic acid. The pump supplier states that 10% acetic acid in the mobile phase should not cause problems to the pump components and therefore this particular mobile phase should not be detrimental to the pump.

The samples and standards must be prepared in either acetonitrile:water, 70:30 or in the mobile phase.

Table 5.2 shows the variations to the method. 1 is the method described by the Larson and Pfeiffer and 2-5 the variations in mobile phase and columns tried.

	1	2	3	4	5
Conditions					
Column	4.6 x 250mm Partisil – 10 SCX	4.6 x 250mm Partisil – 10 SCX	4.6 x 250mm Partisil – 10 SCX	Spherisorb C8	Techsphere 5CN
Mobile phase	70 acetonitrile 30 water 0.01M BTMA 1% acetic acid	70 acetonitrile 30 water 0.005M BTMA 1% acetic acid	70 methanol 30 water 0.005M BTMA 1% acetic acid	70 methanol 30 water 0.005M BTMA 1% acetic acid	70 methanol 30 water 0.005M BTMA 1% acetic acid
Flow rate	2ml min^{-1}	2ml min^{-1}	2ml min^{-1}	2ml min^{-1}	1ml min^{-1}
Wavelength	268nm	268nm	268nm	268nm	268nm
Sample eluent	70 acetonitrile 30 water	70 acetonitrile 30 water	70 acetonitrile 30 water	70 acetonitrile 30 water	70 acetonitrile 30 water

Table 5.2 Conditions based on the Larson and Pfeiffer method. (BTMA - benzyltrimethylammonium chloride)

However, none of these variations improved the analysis. There was no peak detection of the Arquad 2C-75. This method was therefore not useful.

Gas Chromatography

This method (Metcalfe, 1963) is not useful for the analysis of dialkyldimethylammonium ions as they are not volatile enough and they cause column damage after only two or three injections. The peaks tail and therefore quantitative analysis is very inaccurate.

Ion-Pair Chromatography with Suppressed Conductivity Detection Dionex DX500 Chromatography System

A method of surfactant detection (Dionex (UK) Ltd. Technical Note 12) was tried for Arquad 2C-75. This method combined mobile-phase ion chromatography (MPIC)

with ion-pair chromatography. It used methanesulphonic acid as the counter ion in the mobile phase (90% acetonitrile and water) with a gradient elution.
The HPLC conditions were:

Instruments	Dionex DX500 Chromatography System
	Dionex GP40 gradient pump
	Dionex ED 40 electrochemical detector
Column	IonPac® CS17 Cation-Exchange Column
Temp	Ambient
Flow Rate	1.00 ml / min
Injection Volumes	25µl
Mobile Phase	Gradient elution
	100mM methanesulphonic acid 5% to 40%
	Water 55% to 20%
	90% acetonitrile 40%
Detection	Suppressed conductivity CSRS, external water mode

No peaks were eluted using this method it could have been that the surfactant was binding to the column and not being eluted. It was decided not to pursue this method as variations in mobile phase composition did not help

Flow Injection Dionex DX500 Chromatography System

A flow injection system was developed that allowed the Arquad 2C-75 to be detected. This method used water as the eluent which was pumped by a Dionex GP40 gradient pump at 1ml min^{-1} into a 100µl loop. The liquid then flowed through a 1m length of PEEK tubing with a 0.5mm diameter to ensure good peak shape before reaching the cation self-regenerating suppressor (CSRS II) and then the conductivity detector. The data was analysed by a Dionex software package, Peaknet 4.3. Figure 5.7 shows a schematic of the set-up.

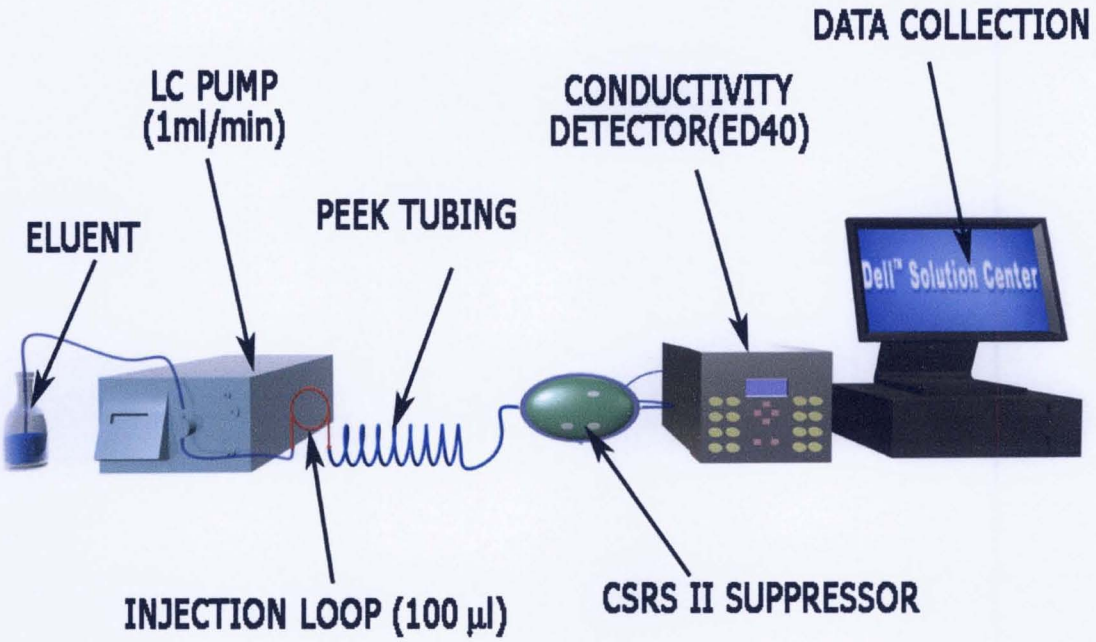

Figure 5.7 Schematic of the flow injection system

This method detected cations and was only applicable when the cation level of the other solution present in the hydrogel was very small. Background samples of methanol and blank hydrogel were run and subtracted from the peak area of the Arquad 2C-75. Therefore this method was only useful for absorbance of the surfactant into the hydrogel where there were no major competing cations. Release studies in seawater resulted in the ions from the seawater (present in the pore water) interfering in the analysis and thus making the method inapplicable to monitor release in seawater studies.

5.3.3 Discussion and Conclusions

The quantitative analysis of twin-chained quaternary ammonium compound has proved to be extremely difficult, this is primarily due to the compounds having no chromophore. No one method was robust for all the applications. The interference of seawater ions prevented traditionally used conductivity methods being used to monitor release of the Arquad 2C-75. The flow injection system using ion chromatography was useful for absorbance studies and was used for this purpose as it proved to be the most robust method of those considered.

5.4 Measuring Diffusion of Cationic Surfactants

The diffusion coefficients of benzalkonium chloride were measured using the following methods.

5.4.1 Diffusion Measurement

A method to measure the free diffusion of cationic surfactants in water and seawater was adapted and developed from a method originally described by Stokes (1950) and later developed by Blurton and Riddiford (1967). Benzalkonium chloride was the cationic surfactant used in this work.

5.4.1.1 Diffusion Cell

A diffusion cell was prepared using a Pyrex cell with a glass sinter with porosity No. 4. The diameter was 40mm and the thickness of the sinter membrane was 4mm. The upper and lower compartments were stoppered using silicone stoppers and each compartment volume was approximately 60ml, an accurate volume for each cell was measured for use in the calculations. The upper stopper had two holes drilled in it to house lengths of polyether-ether ketone (PEEK) tubing, one being the air hole and the other the sample point. The lower stopper has one hole drilled to house a small length of PEEK tubing with a stopcock this allows excess liquid to be expelled during the filling process as well as releasing any trapped air. In order to stir the contents of each compartment a novel stirring device was fabricated. A glass rod was held from the stopper (ground glass sleeve containing a silicone stopper) which supported a hollow glass cross piece. One arm of the crosspiece contained a cylindrical magnet, which filled the crosspiece from end to end. The glass crosspieces were held 2-3mm from the membrane to prevent rubbing and thus cause damage to the membrane. When the cell was held vertically into the insulated water tank it was ringed by six magnetic coils, which created a rotating electromagnetic field. The coils were housed in a ring of silicone to keep them watertight. A 4mm hole was drilled in the PMMA tank lid for the wire to power the magnetic coils. The speed at which the device turned could be varied between 120-150rpm. Figures 5.8 and 5.9 show a photograph of the cell and a diagrammatic representation of it.

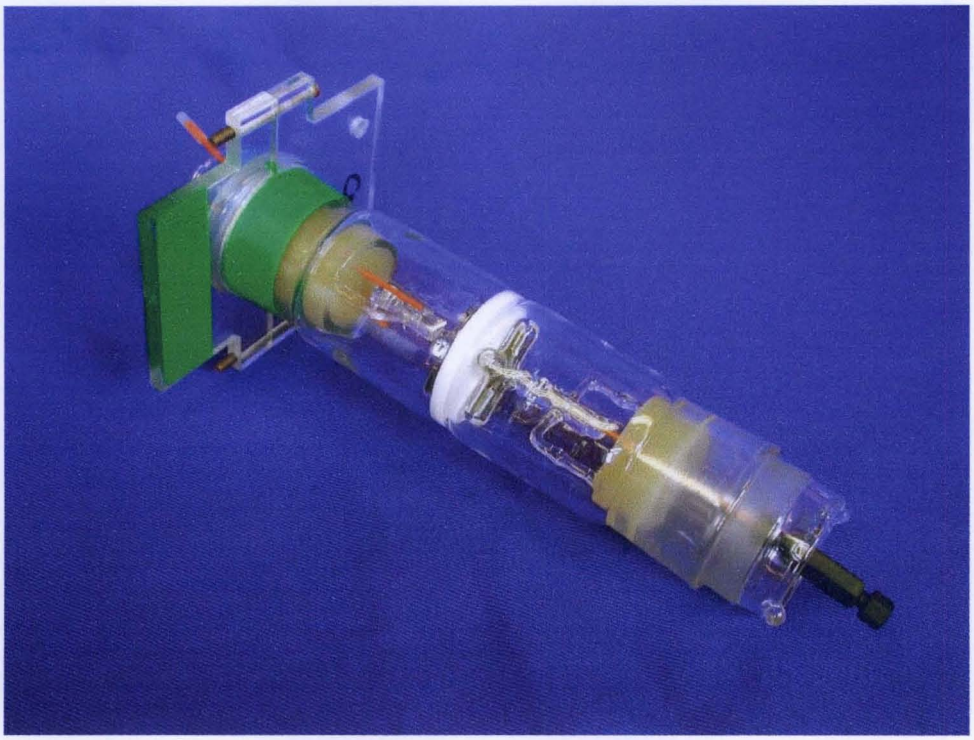

Figure 5.8 Glass diffusion cell

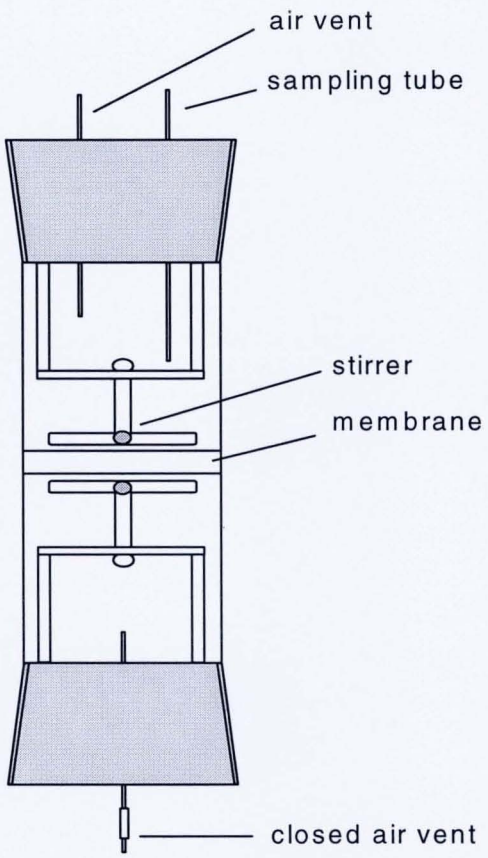

Figure 5.9 Schematic diagram of a diffusion cell.

5.4.1.2 Tank Set-up

To control the temperature the cell was held in a 10 litre PMMA tank and the tank was placed in a wooden insulate box. This was placed into another insulated box to ensure that external changes in the laboratory temperature of would not affect the diffusion runs. A 10mm PMMA lid was screwed down onto the outer insulated box. The tank was able to hold two diffusion cells in a vertical orientation. Figure 5.8 showing the photograph of the diffusion cell also shows a PMMA collar that held the cell in place in the tank. It was important to ensure that the diffusion cell was level to prevent errors caused by bulk flow. A Technicon temperature controller was used to control the tank temperature. Figure 5.10 shows the instruments and equipment used

for the diffusion measurements. Two thermometers were used to monitor the temperature at 30 minute intervals, throughout each diffusion run.

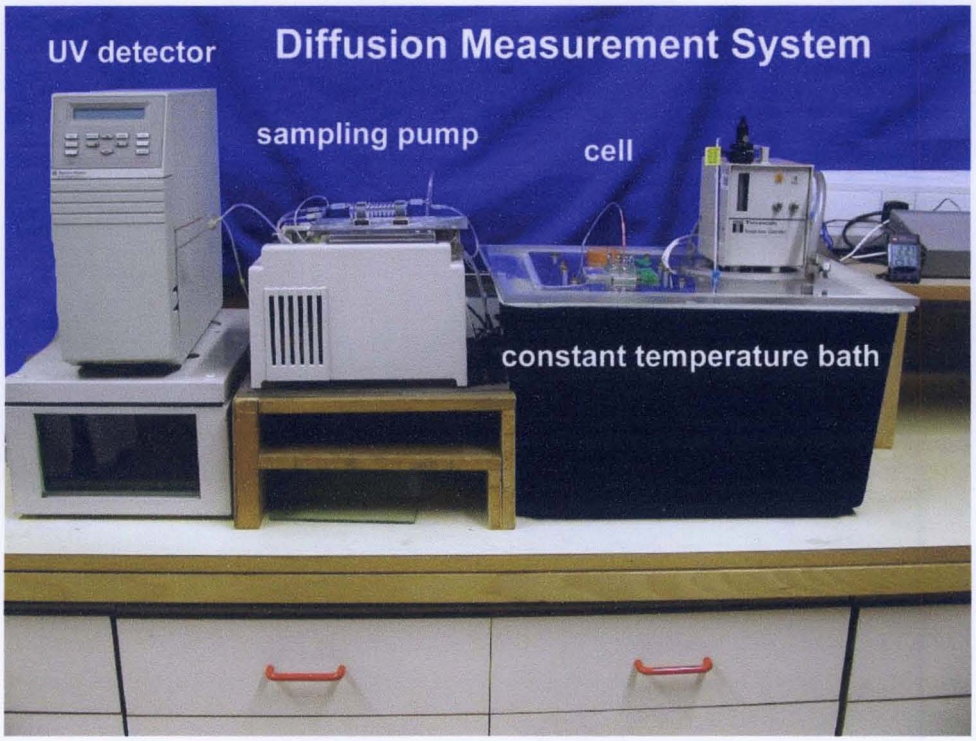

Figure 5.10 The instrumentation for measuring the diffusion coefficients

5.4.1.3 Calibration of the Diffusion Cell and Diffusion Coefficient Calculation

The volumes of the upper and the lower compartments of the cell and the membrane and the concentrations in the compartments at the starting conditions (time 0 s) and at any time (time = t s) are shown in figure 5.11.

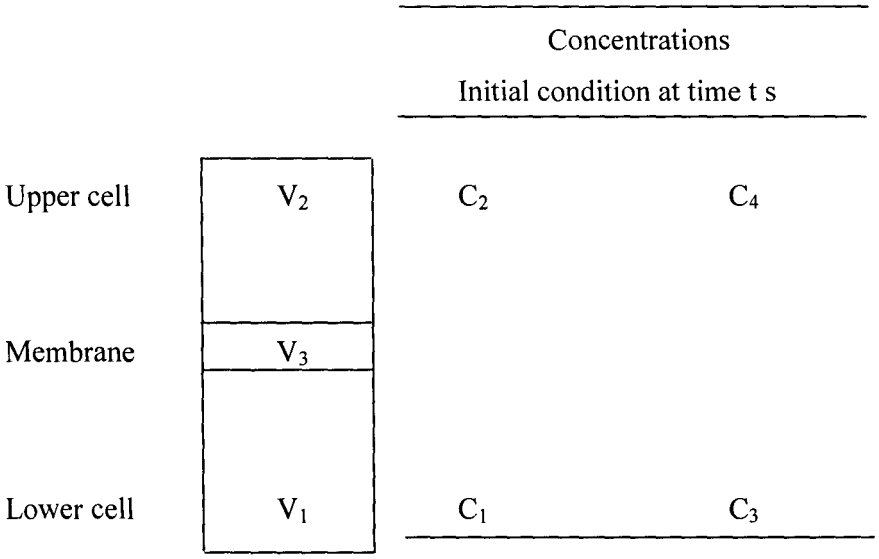

Figure 5.11 Definitions of volumes and concentrations at beginning and end of run

Where

C_1 initial concentration (calculated by mass balance at end of equilibrium period)

C_2 0

C_3 final value at the end of the experiment (calculated by a mass balance)

C_4 final value at the end of the experiment (measured)

V1 volume in the bottom half of the cell

V2 volume in the top half of the cell

V3 volume in the membrane

The diffusion coefficient is given by Stokes (1950)

$$\overline{D} = \frac{1}{\beta t} \ln\left(\frac{C_1 - C_2}{C_3 - C_4}\right) \qquad \ldots\ldots 1$$

where β is the cell constant given by

$$\beta = \frac{A}{l}\left(\frac{1}{V_1} + \frac{1}{V_2}\right) \qquad \ldots\ldots 2$$

Where, A = total effective cross-section of the diaphragm pores

l = length along the diffusion path

V_1 = volume in the bottom half of the cell

V_2 = volume in the top half of the cell

According to equation 1 a plot of $\ln[(C_1-C_2)/(C_3-C_4)]$ against time gives a straight line of gradient $\overline{D} * \beta$. Thus the membrane-cell integral diffusion coefficient ($\overline{D}$) for BAC can be obtained. $\overline{D}$ calculated from equation 1 is a complex concentration-averaged and time-averaged value, termed the membrane-cell integral diffusion coefficient, which is not easy to convert into the fundamental diffusion coefficient D (Stokes, 1950; Robinson and Stokes, 1968)

However, in order to calculate $\overline{D}$ from the slope, the cell constant β must be known for each cell. It cannot be calculated directly from equation 2 as A and l are not easily measured but may be calculated by measuring the diffusion coefficient of a solution with a known diffusion coefficient (Stokes, 1950). Cell calibration to determine β was carried out using KCl for which D is known as a function of concentration. Stokes (1951) and Robinson and Stokes (1968) have tabulated values of $\overline{D}^0(c)$ for KCl at 25°C. $\overline{D}^0(c)$ is the average D with respect to concentration over the range zero to the final concentration (in the top cell 0 to C_4)

The membrane-cell integral diffusion coefficient $\overline{D}$ corresponding to the range of concentrations in the experiment was calculated from these tabulated values using equation 3 (Robinson and Stokes, 1968):

$$\overline{D} = \left[\overline{D}^0(Cm^b) - \frac{Cm^t}{Cm^b}\overline{D}^0(Cm^t)\right] \Big/ \left(1 - \frac{Cm^t}{Cm^b}\right) \qquad \ldots\ldots 3$$

Where

$$Cm^b = \frac{C_1 + C_3}{2} \qquad \text{and} \qquad Cm^t = \frac{C_2 + C_4}{2}$$

In order to determine the cell constant using the diffusion of KCl, the bottom of the cell is filled with 0.1M KCl and C_4 is measured over time (corrected for removal). According to equation 1 a plot of $\log_e[(C_1-C_2)/(C_3-C_4)]$ against time gives a straight line of gradient $\overline{D} * \beta$. Using $\overline{D}$ calculated from equation 3 , β can be obtained from the gradient (figure 5.12).

Two cells were used for the determination of BAC diffusion. The cell constant of each of these was determined

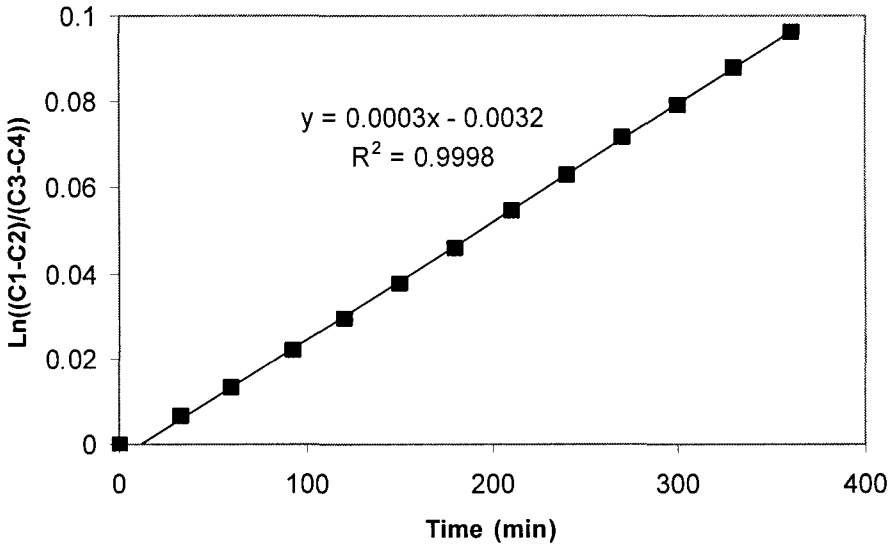

Figure 5.12 Plot of ln $(C_1 - C_2/C_3 - C_4)$ v time for diffusion of KCl for determination of cell constant

In order to measure the diffusion of BAC, the bottom of the cell is filled with 0.05M BAC and C_4 is measured over time (corrected for removal). As β is now known $\overline{D}$ is calculated from the slope of the plot of $\ln[(C_1-C_2)/(C_3-C_4)]$ against time (figure 5.13).

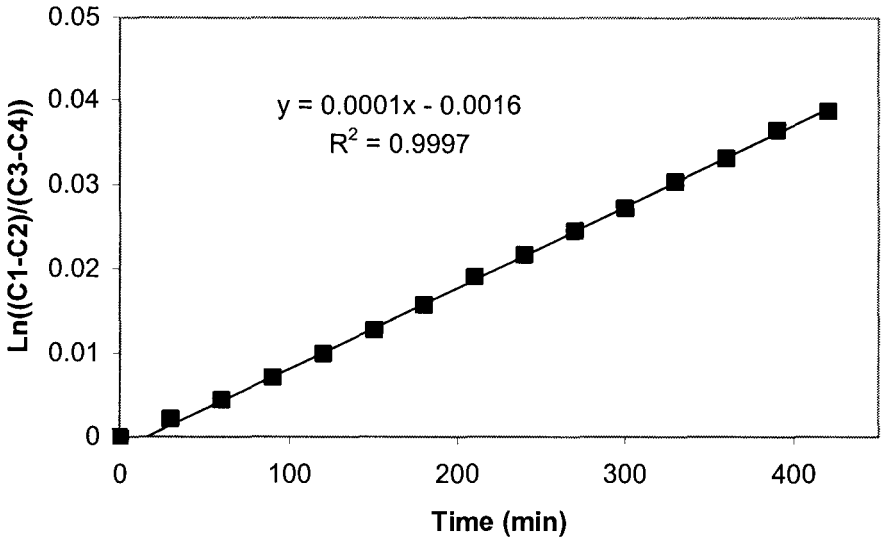

Figure 5.13 Plot of ln ($C_1 - C_2/C_3 - C_4$) v time for diffusion of BAC

5.4.1.4 Method for Measuring Cell Constant

The cell constant was measured by determining the diffusion rate of KCl for which there are published values. The bottom compartment of the diffusion cell was filled with degassed 0.1 M KCl and the top compartment with degassed water. Following equilibration for 3 hours the top compartment was emptied, rinsed 3 times and filled with deionised water. The top compartment was sampled using a peristaltic pump for 2 minutes at a flow rate of 0.05 ml min^{-1} and the chloride concentration measured using an automated mercuric-ferric thiocyanate colorimetric method (Greenberg et al, 1992) adapted for a sample flow rate of 0.05 ml min^{-1} and standard solutions covering the range 0 to 200 mg l^{-1}.

5.4.1.5 Preparation of the Cationic Surfactant Benzalkonium Chloride

It was important to completely degas the solutions being used to fill the compartments of the cell as any air bubbles forming in the bottom compartments will sit on the membrane preventing diffusion at that point. When preparing the 0.05M BAC, the distilled water was thoroughly degassed using helium. The BAC was then added and dissolved and the resultant solution was degassed using an ultra-sonic bath with the

BAC solution kept under vacuum. The KCl, distilled water and artificial seawater were degassed using helium.

5.4.1.6 Setting-up the Diffusion Cell

The diffusion cell was stored in distilled water prior to use in order that the membrane remained air free. In order to fill the cell compartments efficiently the top was filled and stoppered and the bottom filled and stoppered. The top half was then emptied and refilled. This process prevented leakage through the membrane and loss of solution. The stopper with the stirring spindle attached was then put in place. The top was then filled with seawater and the stopper put in place. The cell was then placed in the water tank and left for three hours to equilibrate. Test runs had found this time to be required time for the equilibrium to be reached. A sample was quantitatively analysed at the end of the equilibrium period in order that a true concentration value for the initial BAC present at the beginning of the diffusion run be determined. After this time the seawater from the top-half of the cell was carefully removed using a syringe and the compartment rinsed with seawater three times to remove any BAC. During the cleaning process the cell was not removed from the water tank. The top compartment was then filled with fresh seawater and the timer started for the diffusion run, typically a diffusion run was of the order of six hours.

5.4.1.7 Method for Quantifying Benzalkonium Chloride

The amount of BAC diffusing was measured at fixed intervals. Sampling from the cell was done for 2 minutes at a flow-rate of 0.05ml/min i.e. 0.1ml per sample point; the sample was diluted into a flowrate of water at 2.9ml/min. The BAC was detected using a Spectra Physics UV100 detector set at a wavelength of 214nm. The signal was recorded using a chart recorder. A calibration graph was prepared at the beginning of each diffusion run. Standards ranged from 10mg/l to 90mg/l to encompass the change in concentration throughout the diffusion run. A linear equation was fitted to the calibration curve. This equation was then used to quantify the amount of BAC at the fixed time intervals throughout the diffusion run.
Figure 5.14 shows a typical calibration graph for BAC in seawater.

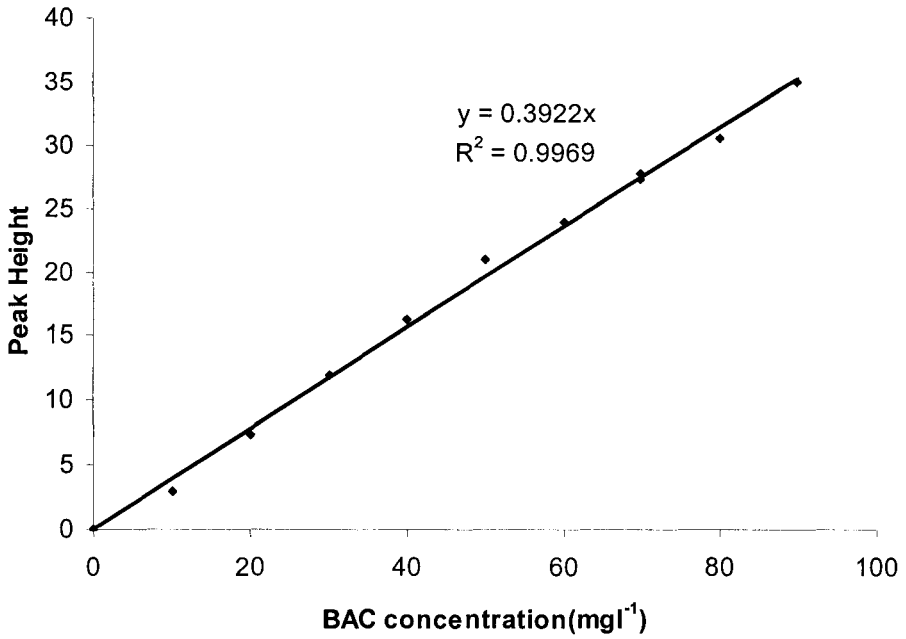

Figure 5.14 A typical calibration graph of BAC in seawater.

5.4.2 Diffusion of Benzalkonium Chloride in Synthetic Seawater

5.4.2.1 Method

The diffusion of BAC in seawater was measured at 25°C as described in section 5.4. Four replicate runs were carried out.

The synthetic seawater used was prepared in the laboratory in 5 litre quantities, table 5.3 shows the quantities used.

Salt	Weight (g)
Sodium chloride	122.33
Sodium sulphate	20.49
Potassium chloride	3.77
Sodium hydrogen carbonate	1.00
Magnesium chloride hexahydrate	55.37
Calcium chloride dehydrate	7.76

Table 5.3 Salts used to produce seawater with a salinity of 3.5%.

5.4.2.2 Results and Discussion

A typical graph of ln $(C_1 - C_2/C_3 - C_4)$ v time is shown in figure 5.15. Initially there is a lag period as the diffusion of the BAC reaches the non-steady state diffusion and the gradient is taken from 120 to 240 minutes in order to avoid the lag period.

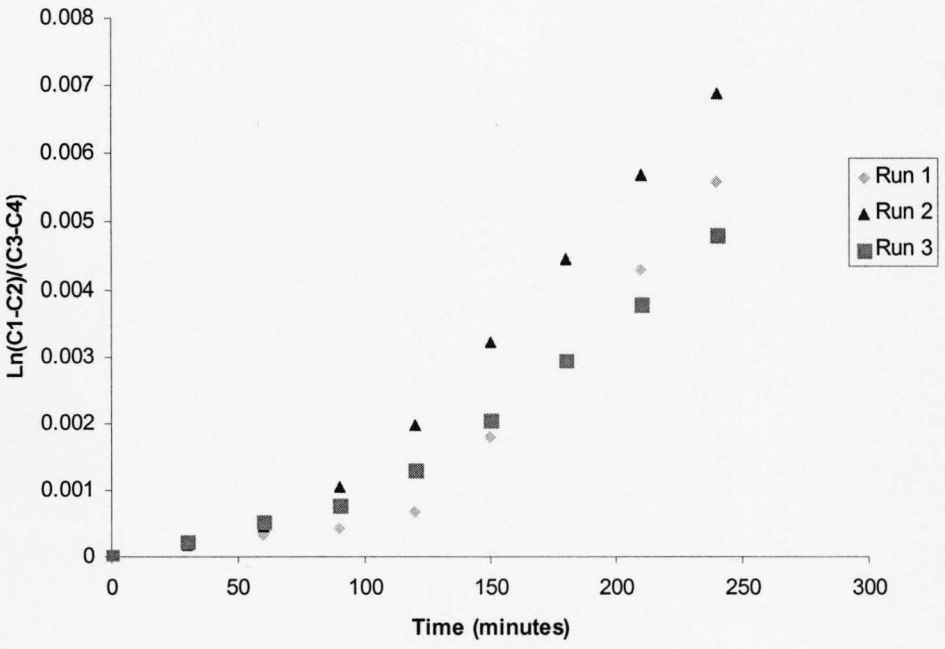

Figure 5.15 A graph of ln $(C_1 - C_2/C_3 - C_4)$ v time of BAC diffusion in seawater.

Diffusion measurements of BAC in seawater at 25±0.1°C gave an average diffusion coefficient of 2.44 x 10^{-6} cm^2 s^{-1} (95% confidence intervals 1.89-2.99), 4 replicates were used.

In the literature there appeared to be no quoted value for diffusion of BAC in seawater. However there are values of BAC in distilled water. [b]Smith et al. (2002) found the diffusion coefficient of BAC in distilled water at 25°C to be 7.78 x 10^{-6} cm^2 s^{-1}. Saltzman and Tena (1991) quoted values ranging from 3.2 - 4.4 x 10^{-6} cm^2 s^{-1} and Stewart et al. (2000) 4.3 x 10^{-6} cm^2 s^{-1}. The CRC Handbook of Chemistry and Physics (2005) Data Book gave a value of 9.21 x 10^{-6} cm^2 s^{-1}. The most valid comparison is the value found by [b]Smith et al. (2002) as it was directly measured whereas the method quoted by Stewart et al (2000) was a derived value based on work done on correlation of diffusion coefficients by Wilke and Chang (1955). In that case the diffusion in seawater is approximately one third of that in distilled water. This reduction in diffusion can be explained by the fact that in seawater there will be more micelle formation and therefore less ion availability. The critical micelle concentration (CMC) in seawater will be lower than in distilled water. Varade et al. (2005) found that the CMC of the cationic surfactant cetylpyridinium chloride decreased with increasing salt concentration and stated that ionic micelles undergo the salt induced sphere-to- rod transition, when sodium chloride or sodium bromide is added across a certain threshold salt concentration. Lindman et al. (1980) stated that in salt solutions micelles favour forming rod-shaped species. The change in micelle shape can help to explain the reduced diffusion found, as rod shaped micelles would diffuse less freely than spherical micelles. More detailed descriptions of micelles can be found in chapter 4 section 4.2.1.

5. 5 Hydrogel Weight and Swelling Changes

A variety of experiments were carried out to look at the changes in the hydrogel when it was loaded with the surfactant and when the unloaded hydrogel and the surfactant loaded hydrogel discs were transferred to freshwater or seawater. When loading with surfactant it was important to find an optimum time period to load the hydrogel. The effects on the physical character of the hydrogel in seawater and freshwater can be

elucidated by measuring them gravimetrically and also monitoring volume changes over time.

5.5.1 Weight Changes in Benzalkonium Chloride and Arquad 2C-75

5.5.1.1 Method

A sheet of hydrogel that had been stored in distilled water was cut into discs, 20mm in diameter, using a cork borer (No.11). These discs were then soaked in 5%w/w BAC and 5%w/w Arquad 2C-75 and weighed at regular time periods. The discs were weighed after 1, 3 and 7 days, then 2 and 3 weeks soaking. All the work was carried out at ambient temperature.

The swelling ratio was also calculated using the equation:

$$X = V/Vo = (D/Do)^3$$

Where V and Vo are the volumes after treatment and at zerotime, respectively and D and Do are the diameters of the hydrogel discs after treatment and at zerotime, respectively (Ilavsky, 1982). The diameters were measured using a Mitutoyo Profile Projector Type PJ-300.

5.5.1.2 Results and Discussion

The hydrogel soaked in the 5% Arquad 2C-75 increased in weight over the 21 days. The hydrogel also increased in volume over this period. Initially there was a sharp increase in weight over the first 24 hours. The weight continued to increase, although less rapidly until 14 days after which time there was little further weight increase noted. The hydrogel soaked in 5% BAC increased in weight sharply over the first 24 hours and continued to increase although less dramatically throughout the experimental time scale. From the graph shape it can be seen that the weight increase was still continuing at 21 days. Figures 5.16 and 5.17 show the weight increase in hydrogel disc when soaked in 5% Arquad 2C-75 and 5% BAC.

Figures 5.18 and 5.19 show the swelling ratio of hydrogel in 5% Arquad 2C-75 and BAC.

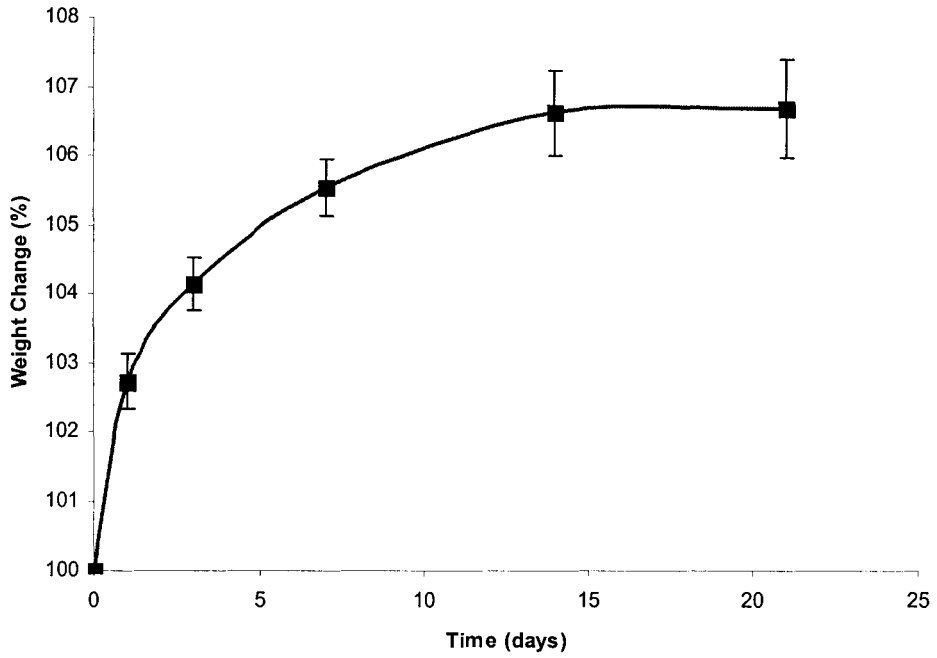

Figure 5.16 Weight changes over time of hydrogel discs soaked in 5% Arquad 2C-75.

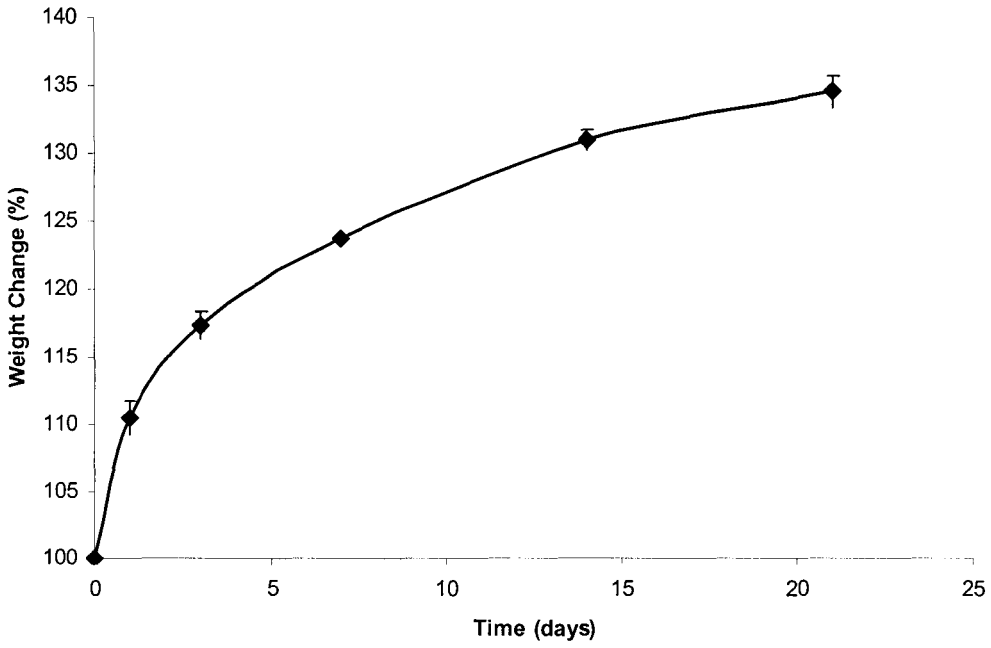

Figure 5.17 Weight changes over time of hydrogel discs soaked in 5% BAC.

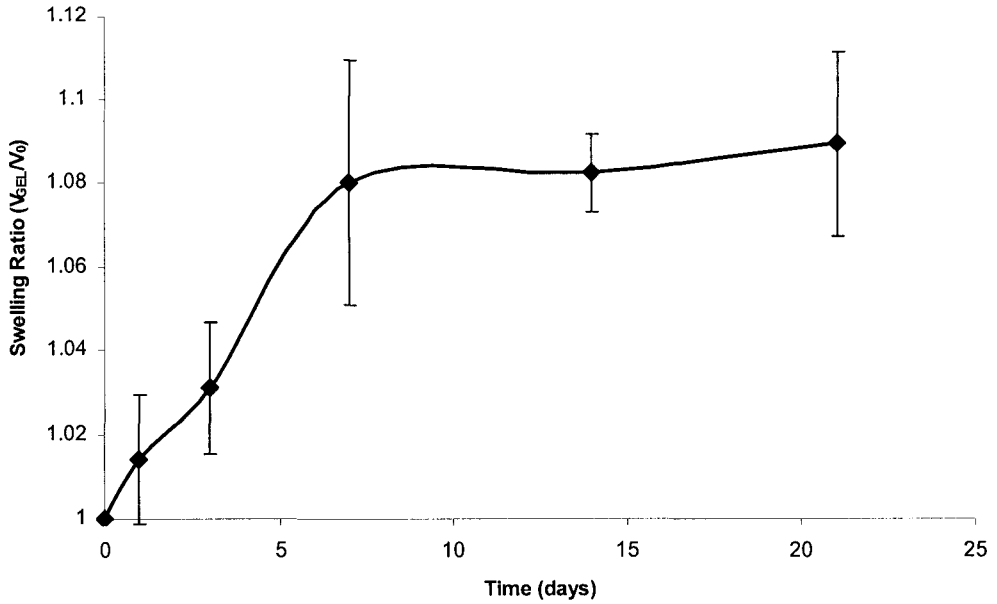

Figure 5.18 Swelling ratio changes over time of hydrogel discs soaked in 5% Arquad 2C-75.

The increase in weight was reflected in the increase in swelling in both experiments. The swelling ratio for hydrogel discs in 5% BAC was 1.37 and for discs in 5% Arquad 2C-75 it was 1.09 at the 21 day time point.

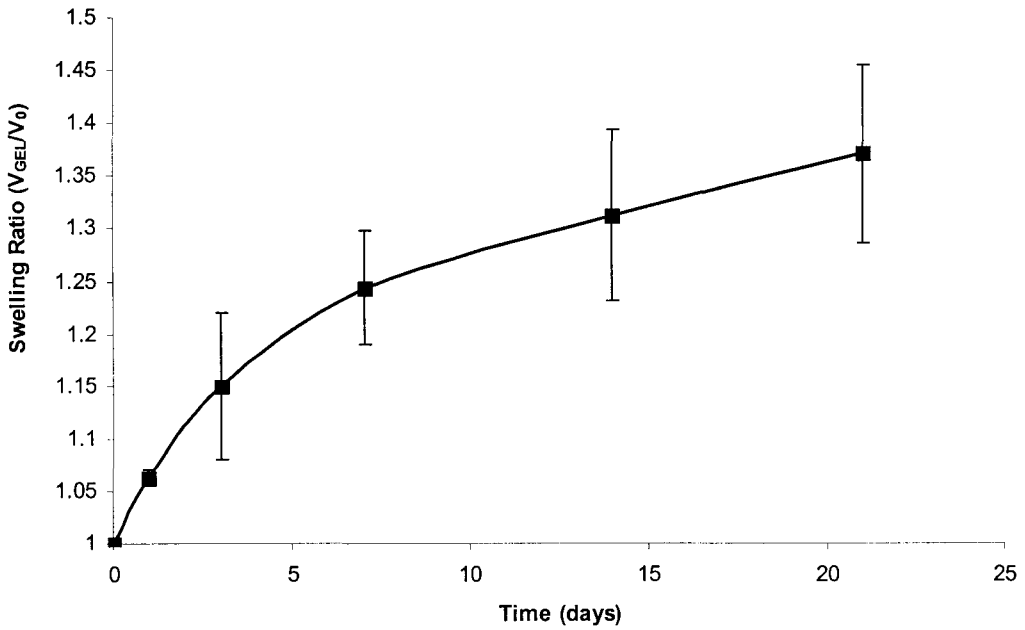

Figure 5.19 Swelling ratio changes over time of hydrogel discs soaked in 5% BAC.

5.5.2 Weight Changes of Hydrogels in Various Salinities

The application of hydrogel coating to marine, brackish and freshwater environments necessitate its behaviour in these environments to be elucidated.

5.5.2.1 Method

A sheet of hydrogel which had been loaded with BAC was cut into discs of 14mm diameter using a cork borer (No.8). Each disc was weighed before the experiment was begun. Distilled water and water with salinities of 4g l^{-1} and 35g l^{-1} solutions were prepared using Instant Ocean and 20ml of the solutions added to 30ml screw top bottles, 3 replicates were used for each water condition. A disc was added to each bottle and weighed at regular intervals up to 17 days. Both the distilled and water with salinities of 4g l^{-1} and 35g l^{-1} were replaced regularly to mimic sink conditions.

5.5.2.2 Results and Discussion

Figure 5.20 shows the weight changes with time in the different waters. The hydrogel/BAC soaked in the distilled water showed a weight increase after 24 hours. This is due to mass flow of water being drawn into the hydrogel by osmotic pressure resulting in an increase in weight. It returns to its original weight after 48 hours due to diffusion of BAC in water out of it. This is followed by a reduction in weight due to the diffusion of BAC over time. From figure 5.16 it can be seen that hydrogel/BAC discs shrink to a similar amount after 17 days in both distilled and water with a salinity of 4g l^{-1}. However, in water with a salinity of 35g l^{-1} the hydrogel/BAC disc shrunk more than in the other solutions. The behaviour of the hydrogel/BAC discs in the 35g l^{-1} saline solution showed a dramatic decrease in weight at day 1 with practically no more decrease in weight over the 17 days. Again this weight loss is due to osmotic pressure as there is a flow out of the hydrogel/BAC that has a concentration of 0.15M to the higher concentration of 0.6M salt concentration of the seawater. At 17 days the discs in distilled water had reduced to 84% of their original weight while those in water with a salinity of 4g l^{-1} reduced 83% and those in 35g l^{-1} reduced to 80%.

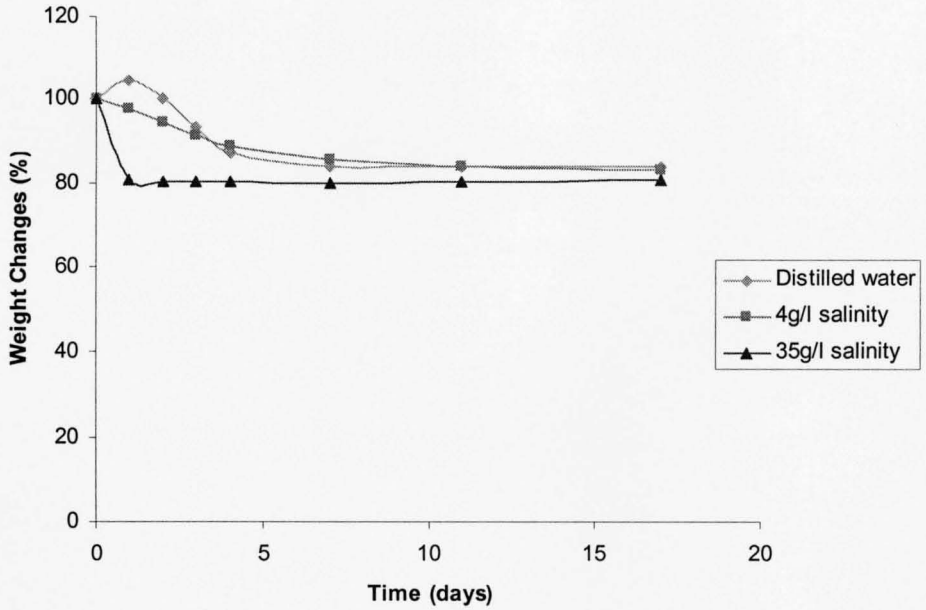

Figure 5.20 The weight changes of hydrogel/BAC discs in distilled water and water of 4g l^{-1} and 35g l^{-1} salinity.

In order to try and understand the results more fully a more comprehensive experiment was carried out which included unloaded hydrogel, BAC and Arquad 2C-75 loaded hydrogel. Hydrogel discs were cut as described (20mm diameter) and soaked in distilled water and seawater with a salinity of 35g l^{-1}. In this experiment the swelling ratio was also recorded to establish if weight change was correlated with an increase in size.

Figures 5.21 and 5.22 show the weight and volume changes over 21days. The hydrogel containing BAC again demonstrated changes in weight and swelling ratios when transferred from its BAC soaking solution to distilled water and seawater. In distilled water there was an initial increase after 24 hours in the weight and volume. This was followed by a decrease and at 7 days the weight and volume reached around 70% of the original values and did not change again over the 21 day measuring period. The hydrogel containing Arquad 2C-75 reduced slightly in weight and volume after 24 hours in distilled water; the weight to around 97%, a value it remained at over the time period of the experiment. In seawater the hydrogel decreased to around 92% after 24 hours and then increased gradually to around 101% of its original value. The

weight and swelling of the unloaded hydrogel (blank) did not change in distilled water as expected. In seawater both the weight and the swelling decreased initially over the first 24 hours and then both weight and swelling began increasing to greater than the original weight and volume. At 21 days the swelling ratio in seawater for the unloaded hydrogel was 1.05, for BAC/hydrogel it was 0.73 and for Arquad 2C-75 it was 1.04 showing that neither the unloaded nor the Arquad 2C-7/hydrogel had changed in volume at 21 days whereas the BAC/hydrogel had shrunk from its initial volume. In distilled water, which would equate approximately to freshwater, the swelling ratios were 1.00 for the unloaded hydrogel, 0.76 for the BAC/hydrogel and 0.96 for Arquad 2C-75/hydrogel again showing that the only marked change was the shrinkage of the BAC/hydrogel.

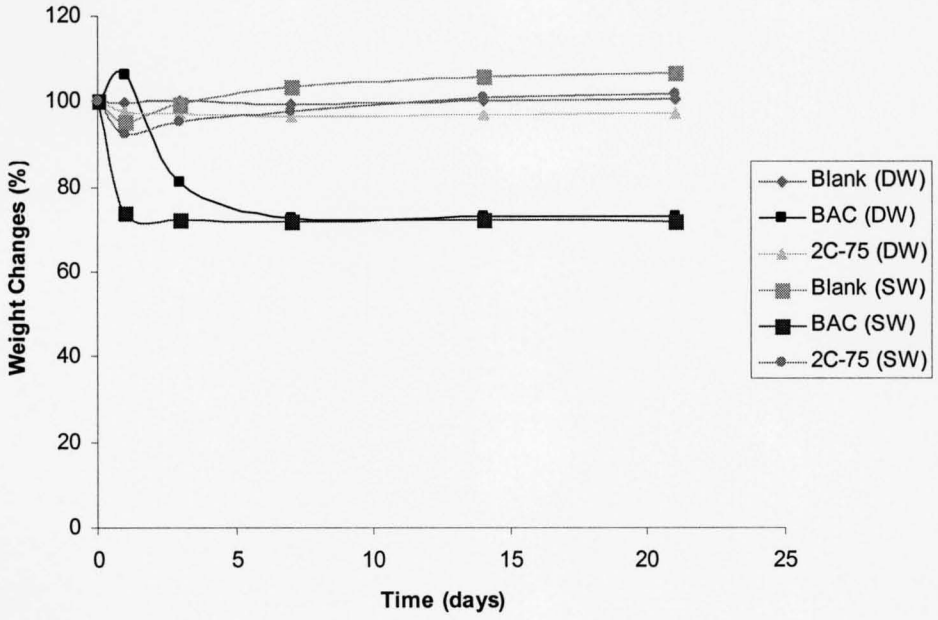

Figure 5.21 Percentage weight changes of hydrogel discs in distilled water and seawater.

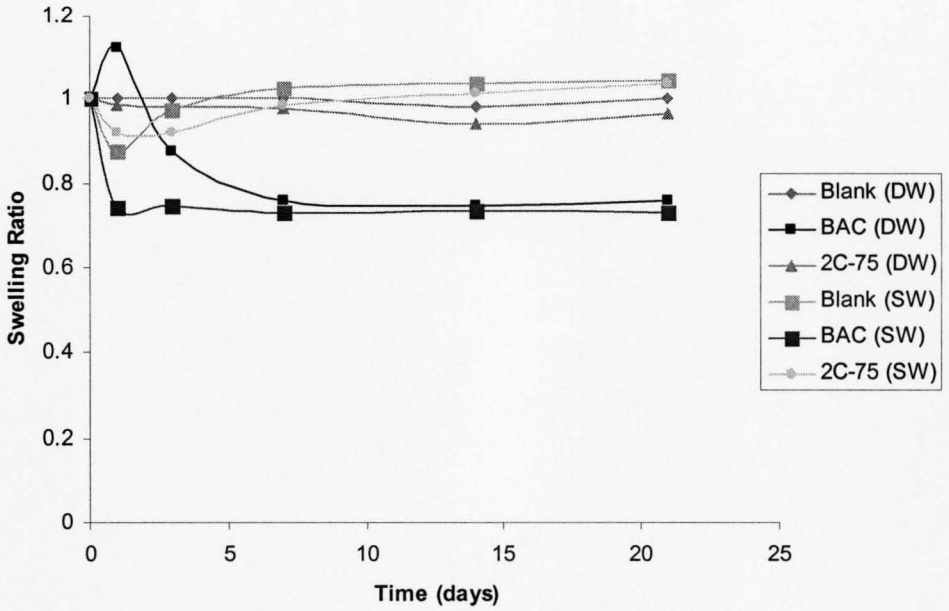

Figure 5.22 Swelling ratios of hydrogel discs in distilled water and seawater.

The weight changes were mimicked in the volume changes for all the hydrogel discs. From the weight changes shown in section 5.5.1 it is known that as the hydrogel imbibes BAC its weight increases, as does its volume. However, this does not occur when the hydrogel imbibes Arquad 2C-75. Thus when hydrogels containing BAC are put into distilled water and seawater, when the BAC begins to release the hydrogel begins to return to its original structure.

The structure of the hydrogel is altered when soaked in BAC and this can be seen using light microscopy. Figure 5.23 shows a blank hydrogel where there is no visible structure whereas figure 5.24 shows a hydrogel loaded with BAC. The hydrogel was viewed using an Olympus BH2 microscope (Southall, Middlesex, UK)

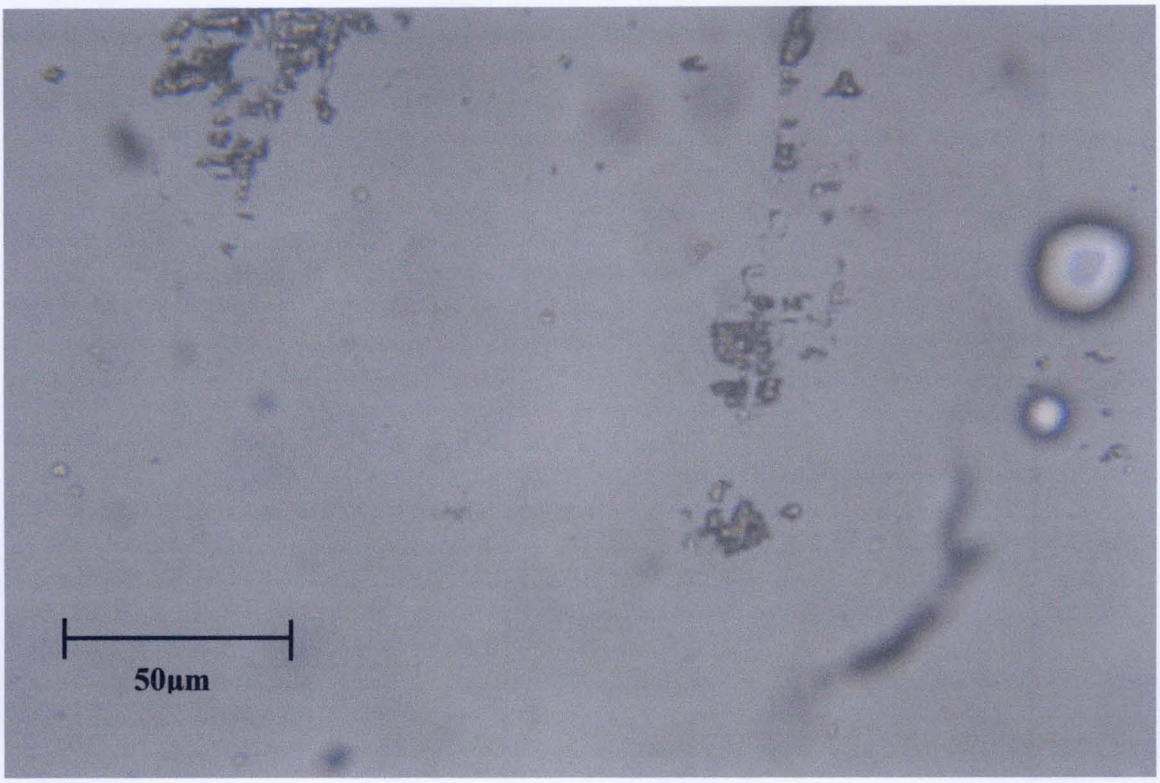

Figure 5.23 Image of a blank hydrogel which had been stored in distilled water.

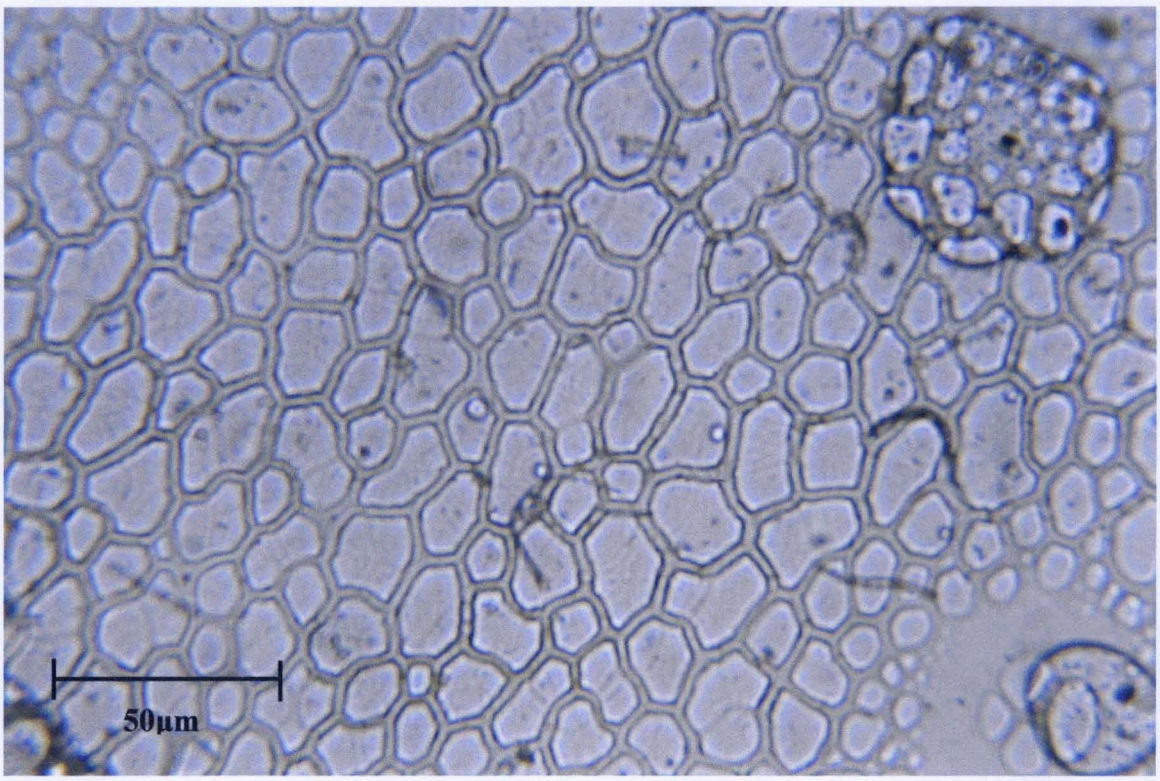

Figure 5.24 Image of a hydrogel loaded with BAC showing the affect on structure.

Hydrogel samples containing BAC, which had been in distilled water and seawater for 21 days where photographed on the Mitutoyo Profile Projector Type PJ-300. This enabled the whole disc to be imaged showing the change in structure in the disc in distilled water as the BAC leached out. The disc in seawater leached out to a lesser extent and the honeycomb type structure is still visible, whereas the disc in distilled water shows a patchy appearance as the honeycomb structure caused by the BAC begins to disappear and the hydrogel begins to return to its usual featureless appearance. The diffusion coefficient of BAC in seawater is approximately 33% of the diffusion coefficient in distilled water at 25°C, thus these physical differences in the hydrogel structure would be expected as leaching from the hydrogel in distilled water would occur more quickly.

The images of hydrogel/BAC discs after 21 days in distilled water and seawater are shown in figures 5.25 and 5.26.

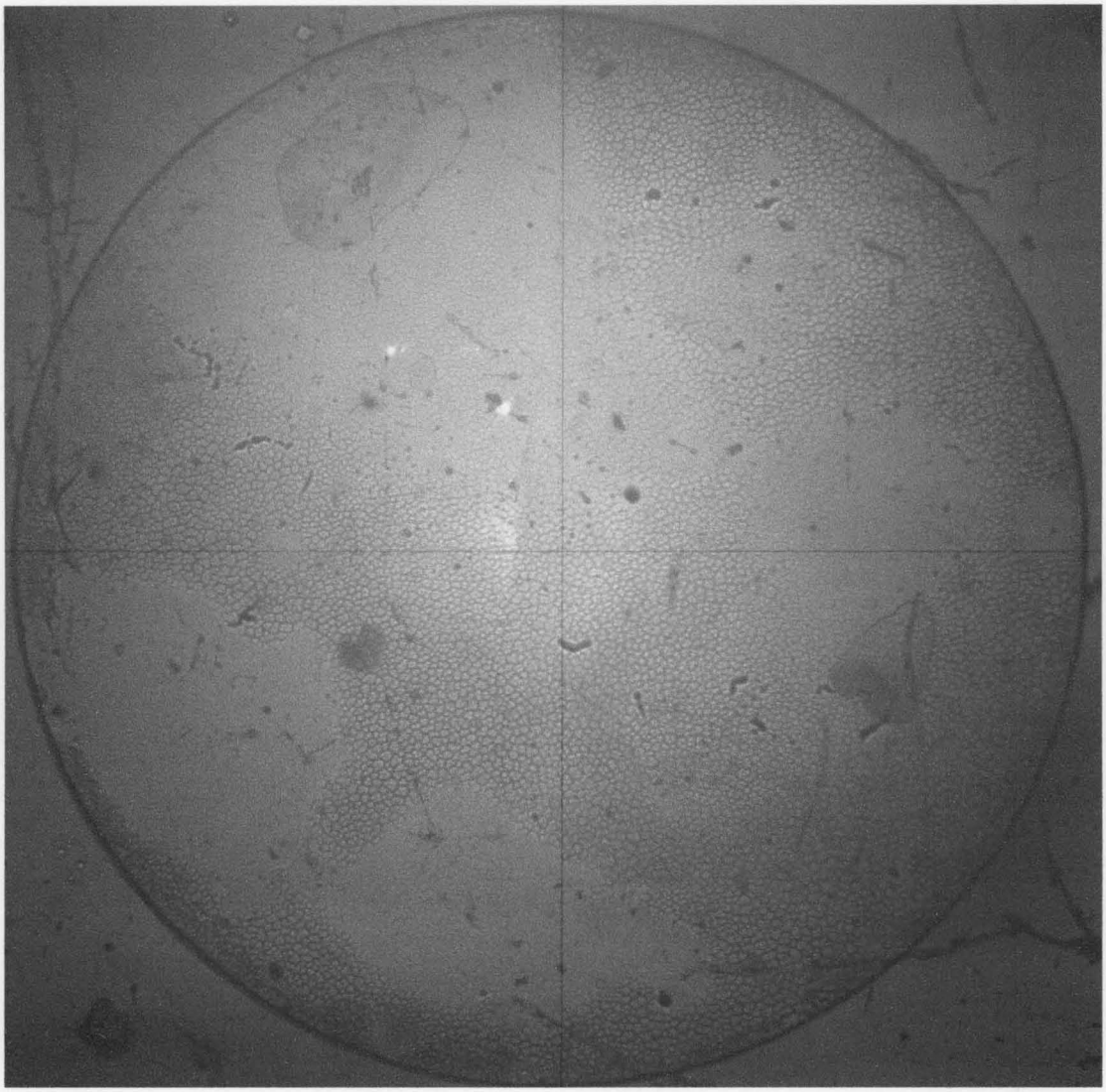

Figure 5.25 Hydrogel containing BAC that had been leached in distilled water for 21 days (hydrogel diameter 20mm).

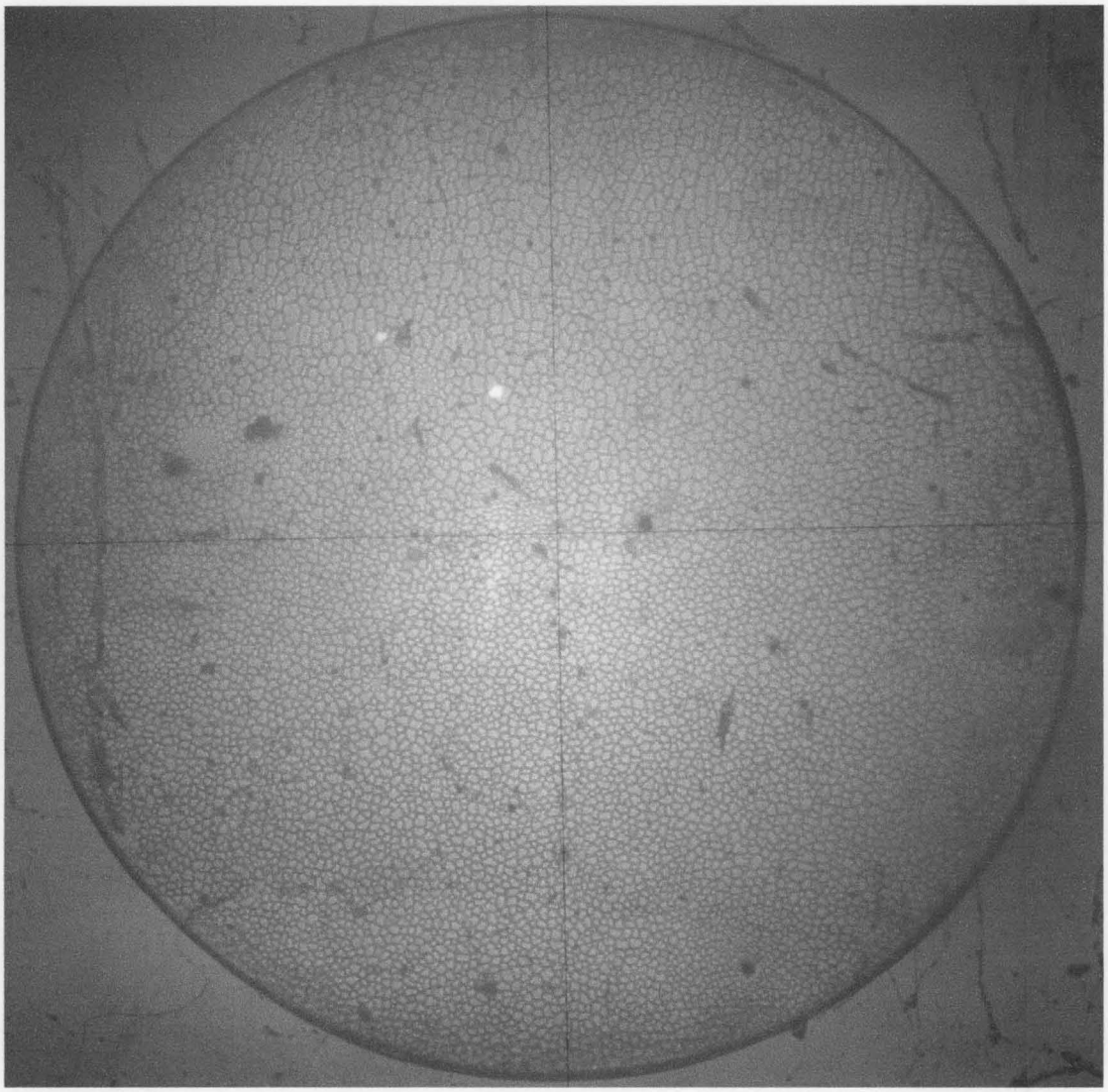

Figure 5.26 Hydrogel containing BAC that had been leached in seawater for 21 days (hydrogel diameter 20mm).

The behaviour in different mediums of hydrogel is shown diagrammatically in figures 5.27 and 5.28.

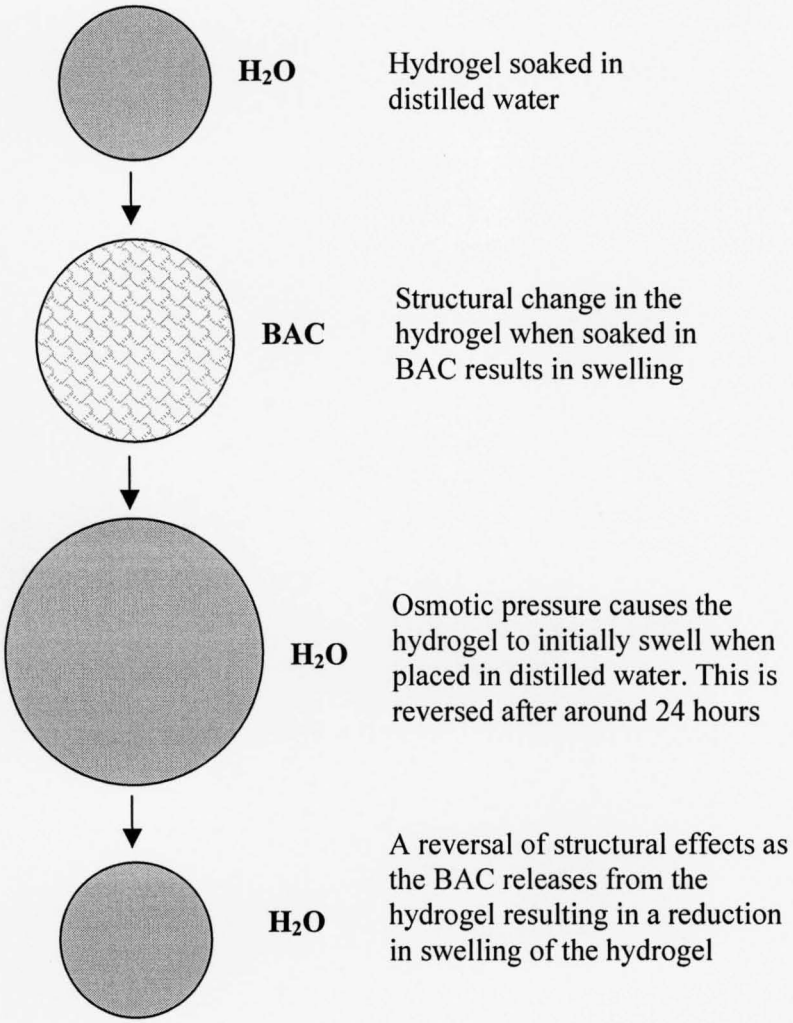

Figure 5.27 Swelling and shrinkage of hydrogel discs when transferred from distilled water to BAC and then into distilled water.

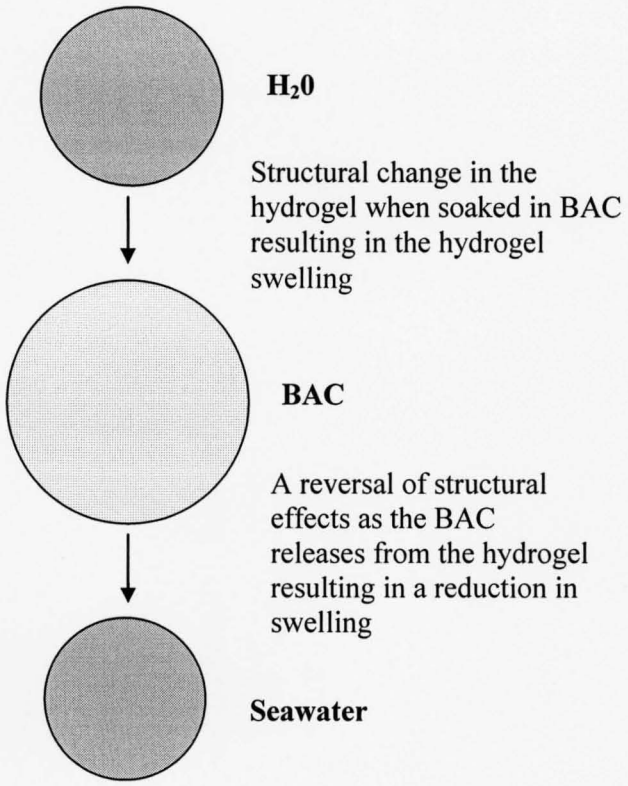

Figure 5.28 Swelling and shrinkage of hydrogel discs when transferred from distilled water to BAC and then into seawater.

Despite the effects of both fresh and seawater on hydrogel which was swollen with BAC these coatings proved successful in marine trails (full details in chapter 7). Ideally, coatings would change their dimensions little in freshwater and seawater, as was the case with the unloaded hydrogel and the hydrogel loaded with Arquad 2C-75.

5.5.3 Equilibrium Water Uptake of Hydrogel

The equilibrium water uptake (EWU) of hydrogels can be calculated by the equation and is expressed as a percentage

$$EWU = \left(\frac{Ww - Wd}{Ww} \right) \times 100$$

Where W_w is the wet weight of the hydrogel and W_d is the dry weight of the hydrogel.

This method is commonly used to express water content of hydrogels.

5.5.3.1 Method

Oven dried weights of unloaded hydrogel and hydrogel loaded with surfactant were recorded. The difference in weight between the wet and dry hydrogel is used to calculate the equilibrium water uptake (EWU).

5.5.3.2 Results

After 6 days there was little change in the weight resulting in blank hydrogel, BAC/hydrogel and Arquad 2C-75 having EWUs (water/solution) of 41.1%, 41.0% and 41.4% contents of respectively.
Figure 5.29 shows the increase in EWC as the hydrogel dries out over time.

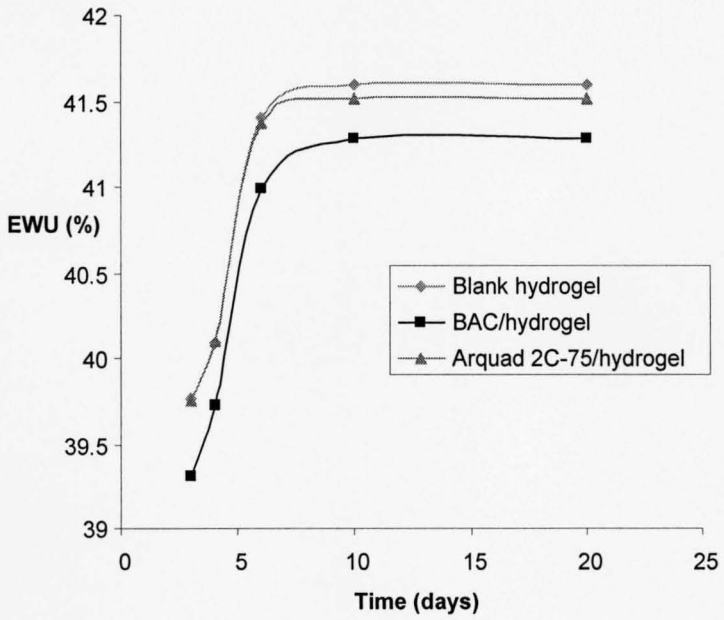

Figure 5.29 EWU of hydrogels in water, BAC and Arquad 2C-75

5.6 Mechanical Properties of Hydrogels

The mechanical properties of hydrogels were examined using tensile strength measurements. From these measurements the Young's Modulus (Elastic Modulus) is calculated which measures the resistance of a material to elastic deformation under load. These properties are important as they directly relate to the visual performance and durability of these coatings.

5.6.1 Method

The hydrogels were prepared as described in section 5.1. They were then either kept in distilled water (blank) or soaked in BAC or Arquad 2C-75 for three weeks prior to testing. The blank and surfactant loaded hydrogels were also soaked in seawater for seven days and tested in order to mimic conditions after marine deployment. All hydrogels were prepared to a thickness of around 1mm. A series of tensile tests were carried out on samples cut using a specially prepared stainless steel die in the traditional dumb-bell shape. A dumbbell shape is desirable because it prevents samples from breaking at the clamps where the stress concentration would otherwise be high in a uniform strip (Anseth et al. 1996). The tests were carried out using a Lloyd L10000 materials testing machine using a 50N load cell. A clamping system was purchased suitable for softer materials. It incorporated rubber grips to prevent the grips cutting into the hydrogel. The tests were carried out at a crosshead speed of 60mm min^{-1}. The gels were loaded to failure. During the tests the hydrogels were prevented from drying out by spraying them with a fine spray of distilled water (Cauich-Rodriguez et al. 1996). Eight replicates for each condition were tested. All work was carried out at ambient temperature.

Specimens as-cut had a thickness of 1mm, a width of 5mm and a gauge length of 25mm (British Standard; EN 10002-1:2001). The thickness was measured at three points on the gauge length using Vernier callipers and the mean value used in tensile calculations. The specimens were held in clamps that were tightened sufficiently to prevent slippage but not to cut the hydrogel. Slippage during testing would have been

noted as a drop in force, this was not noted during the testing. Figure 5.30 shows a hydrogel sample held in the clamps.

The following parameters were calculated:

1. Elastic modulus
2. Ultimate tensile strength
3. Percentage elongation at failure

The output of the instrument plots the Force (N) against the elongation of the sample in mm. This is converted to stress against strain by the following relationships from which the modulus of elasticity can be calculated.

$$Stress = \frac{Force(N)}{Cross-sectional\ area(mm^2)}$$

$$Strain = \frac{Elongation}{Gaugelength}$$

$$Modulus\ of\ Elasticity = \frac{Stress\ (Nmm^{-2})}{Strain}$$

The modulus of elasticity gives a measurement of the elasticity of the material. A measurement of the gradient on the stress/strain curve is used to determine the modulus. (1GPa = 1000 N mm^{-2}).

The ultimate tensile strength (UTS) (load at break) is calculated using the following equation

$$UTS = \frac{Load\ at\ break(N)}{Cross-sectional\ area(mm^2)}$$

The percent elongation is the specimen's failure strain expressed as a percentage and is calculated using the following equation

$$Percentage\ elongation = \frac{Lf - Lo}{Lo} x100\%$$

Where L_o is the original gauge length and L_f is the length at failure.

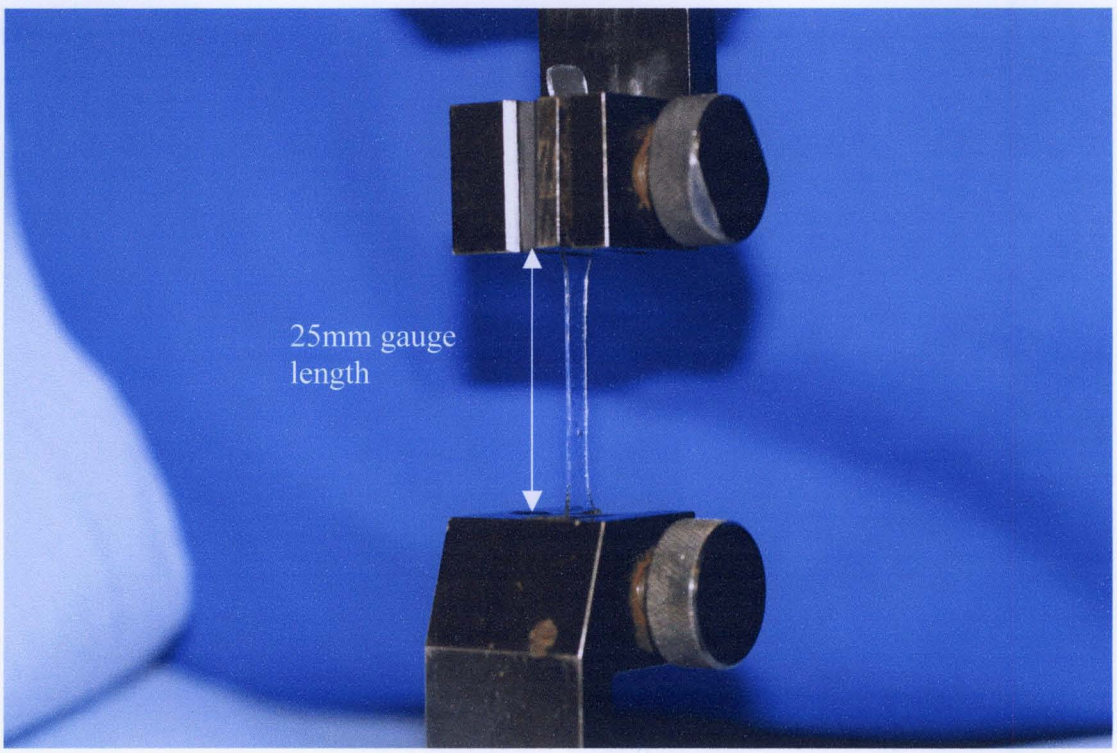

Figure 5.30 Hydrogel sample held in clamps during tensile testing.

5.6.2 Results and Discussion

The hydrogels were capable of stretching to 250-750% of their original size. Figure 5.31 shows a hydrogel during a test.

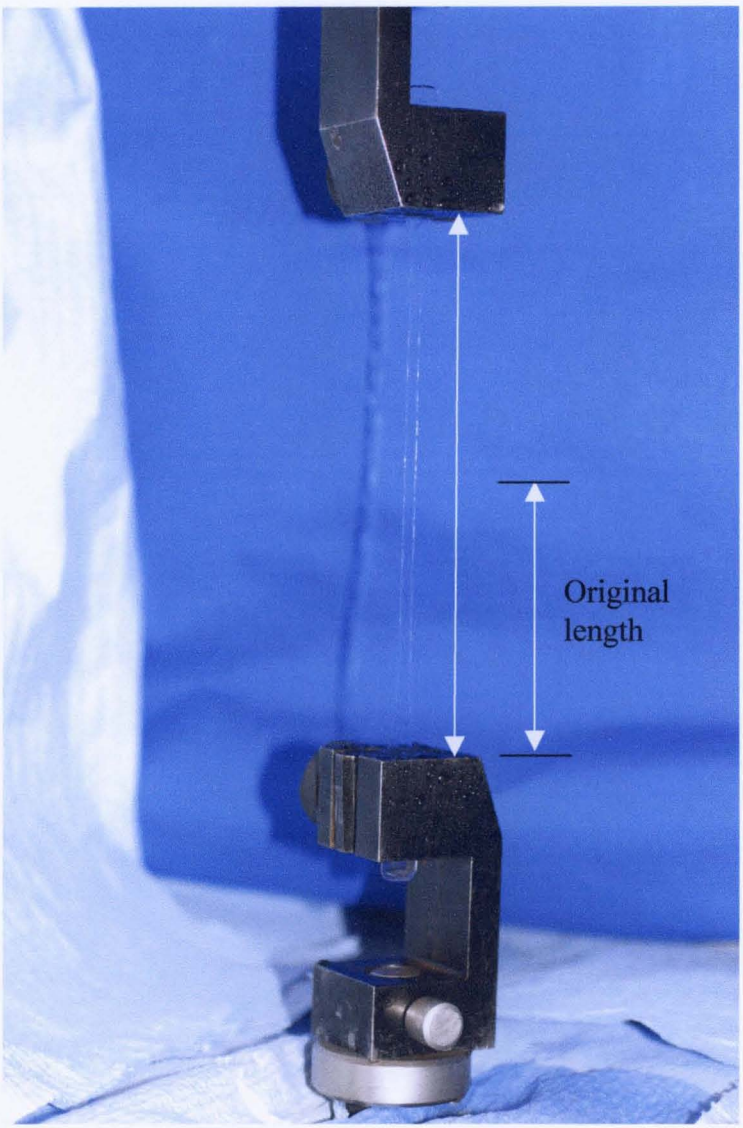

Figure 5.31 Hydrogel during a tensile test.

Figure 5.32 shows the percentage elongation at failure for the hydrogels. The extent of elongation varied from 256% for the BAC hydrogel to 712% for the BAC hydrogel after seawater treatment. There was no significant difference between the blank hydrogel before and after seawater treatment or between the Arquad 2C-75 hydrogel before and after treatment. Before treatment the BAC hydrogel elongated significantly less than blank hydrogel and Arquad 2C-75 hydrogel.

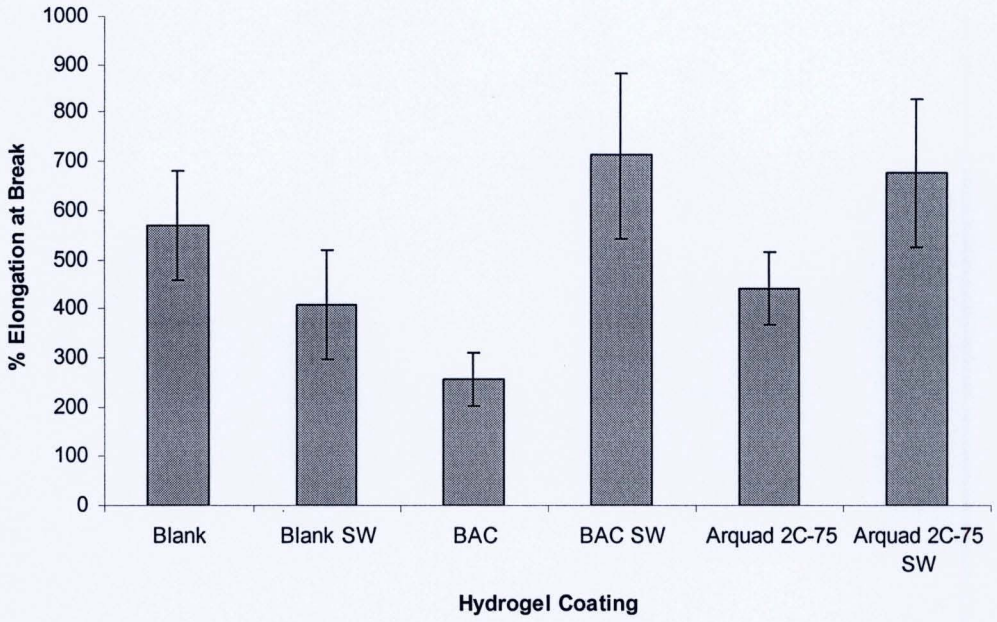

Figure 5.32 Extension at maximum load of the hydrogels, (±SD shown) (SW- seawater)

The blank hydrogel and the hydrogel loaded with Arquad 2C-75 samples all broke within the gauge length. However, the hydrogel loaded with BAC was more difficult to test as the samples were more swollen than the others and these either slipped out of the grips or broke at the radius. The samples that did break within the gauge length had lesser tensile strength than the blank hydrogel and the hydrogel containing Arquad 2C-75. Figure 5.33 shows the specimens after failure.

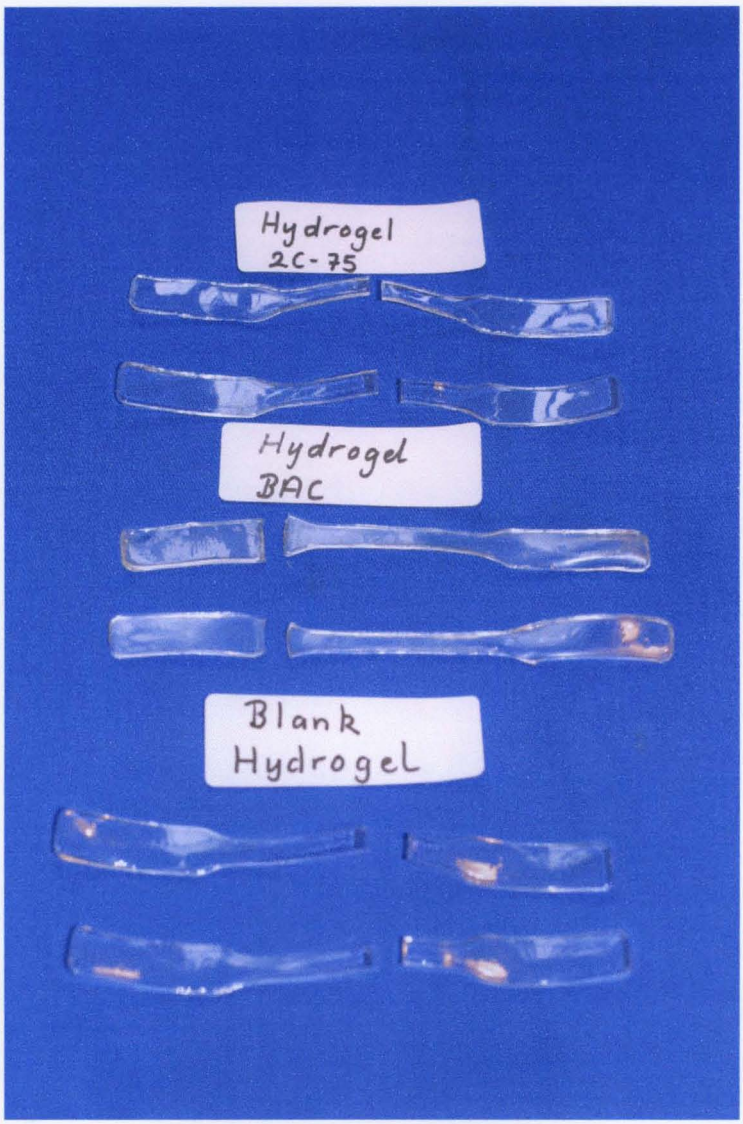

Figure 5.33 Specimens after failure showing the position of a typical failure on the hydrogels.

Figure 5.34 shows a typical stress/strain curve for the hydrogel material. The modulus was calculated between the 0.08-0.16 Nmm^{-2}.

Maldonaldo-Codina and Efron (2004) found that the shape of the stress/strain curve showed that the hydrogels behaved in a Hookean manner i.e. there is no plastic deformation.

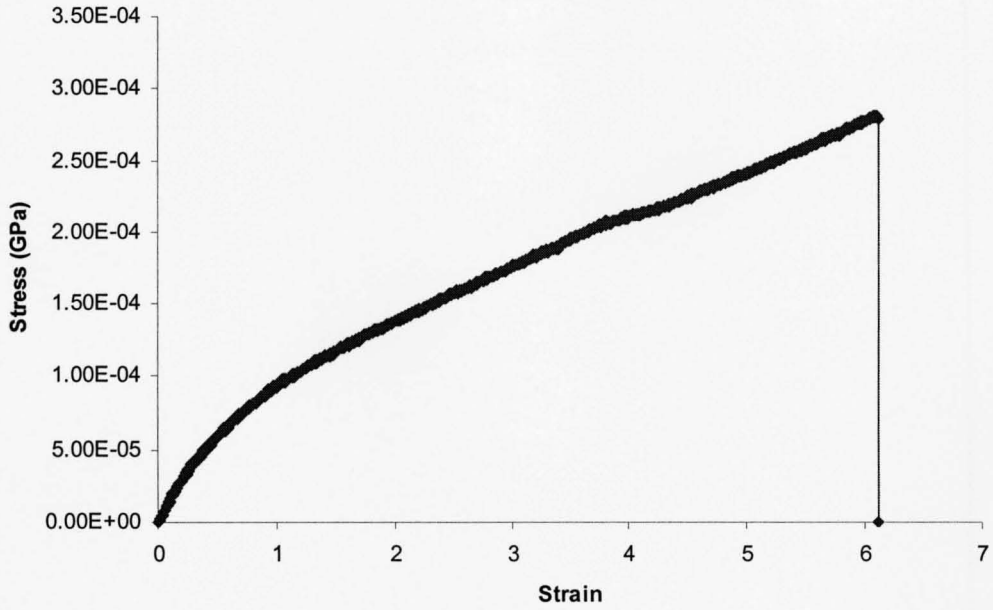

Figure 5.34 A typical stress/strain curve obtained from a hydrogel specimen

Figures 5.35 and 5.36 show the UTS and the moduli of elasticity of the hydrogel samples before and after being in seawater.

Before treatment in seawater the blank hydrogel and the Arquad 2C-75 hydrogel both had significantly higher tensile strengths than the BAC hydrogel
The tensile strength of both the blank hydrogel and the Arquad 2C-75 loaded hydrogel and that of the blank hydrogel and the Arquad 2C-75 loaded after the 7 day seawater treatment were not significantly different. However, the tensile strength increased in the BAC loaded hydrogel after the 7 day seawater treatment.

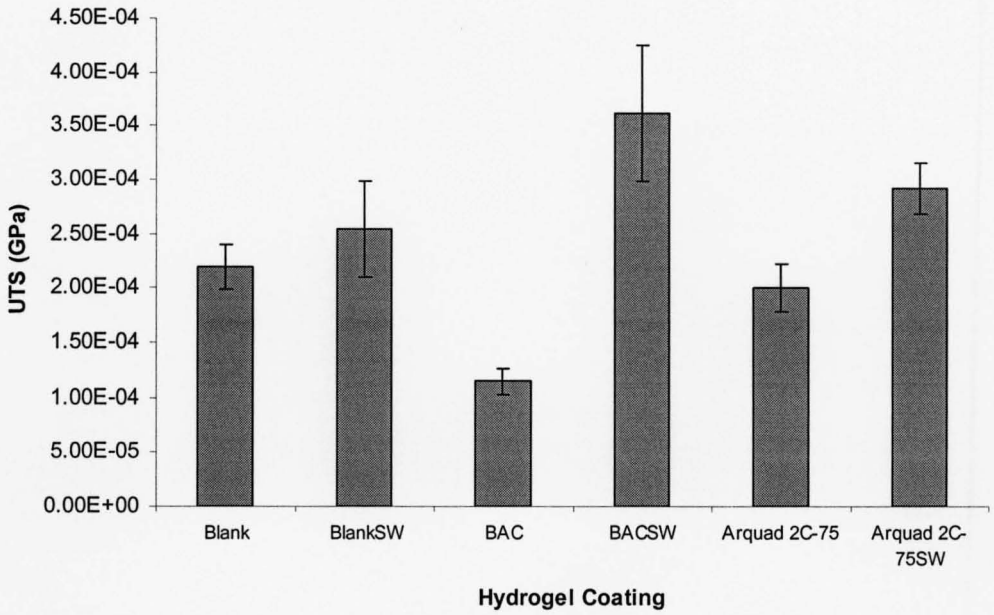

Figure 5.35 The ultimate tensile strength of the hydrogels, (±SDs are shown). (SW- seawater)

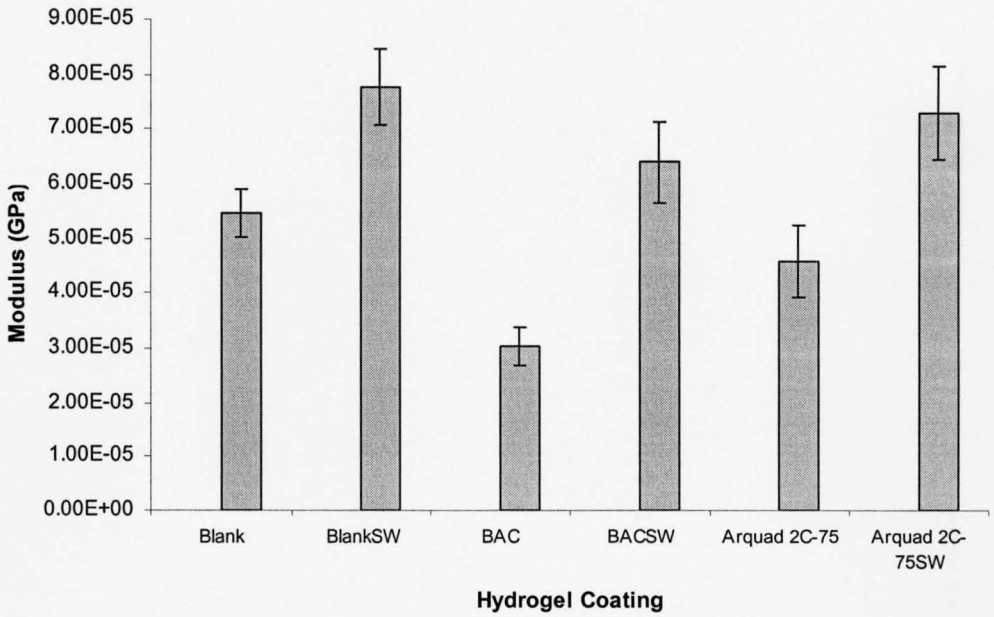

Figure 5.36 The moduli of elasticity of the hydrogels, (±SDs shown). (SW –seawater)

The elastic modulus of the hydrogel containing BAC was the lowest of all those tested. This material also had the highest water content. Opdahl et al. (2003) stated that in general as the water content of the hydrogel increased the modulus decreased. The elastic modulus is related to fouling and Yebra et al (2004) listed a low modulus as one of the properties a coating should posses to resist fouling. Brady and Singer (2000) found that minimum adhesion coincides with the lowest value of elastic modulus tested. They found that poly(dimethylsiloxane) with an elastic modulus of 0.002GPa was the material, out of a variety of polymers tested, to which adhesion was the least. Poly(tetrafluoroethylene) with an elastic modulus of 0.5GPa also was considered to have fairly low adhesion. However, these polymers were chosen as they were considered to be fouling resistant also due to their low surface energy. The hydrogels are not in this category as hydrogels have relatively high surface energies. Maldona-Codina and Efron (2004) found that contact lenses produced by cast moulding had an elastic modulus of around 1N mm^{-2} (0.001GPa). However, these tests were carried out in saline solution in a uniaxial extension at a rate of 2mm min^{-1}. The speed of the testing has an effect on the result. Due to the limitations of the system used, in that it was not possible to test the hydrogel coatings in solution, a faster speed was chosen to prevent the hydrogels drying out.

5.7 Microscopic Study of Hydrogels

5.7.1 Methods- Scanning Electron Microscopy and Atomic Force Microscopy

Both dehydrated and hydrated hydrogels were studied using scanning electron microscopy (SEM). Three instruments were used for their study. The samples were firstly studied using a Philips XL30 Environmental Scanning Electron Microscope that is capable of operating under low-vacuum for the imaging of 'wet' and non-conductive samples. Secondly they were examined using a Hitachi S4 1000 field emission microscope and thirdly they were imaged using the FEI 200F Quanta Environmental Scanning Electron Microscope which can also operate at low vacuums and look at samples in their 'wet' state.

Philips XL30 Environmental Scanning Electron Microscope-

Unloaded and hydrogel loaded with benzalkonium chloride (BAC) were initially examined in their hydrated state, both the surface and cross-section were viewed and photographed.

Hitachi S4 1000 Field Emission Microscope –

Unloaded hydrogel pieces which had been soaked in distilled water or seawater were air dried then they were gold coated.

FEI 200F Quanta Environmental Scanning Electron Microscope-

Unloaded and hydrogels loaded with benzalkonium chloride were viewed in their hydrated state.

Atomic force microscopy (AFM) is a technique that creates a topographic image of a surface by analysing minute force (10^{-9}N) differences between the atoms of the surface and the cantilever. AFM has opened whole new horizons for explaining biomaterial as it is able to image non-conducting materials. This method had been used to show the surface of hydrogels (Grobe et al. 1996; Maldonado-Codina and Efron, 2005).

Discs of 20mm diameter were cut from hydrogel that had been soaking in distilled water, 5%BAC and 5% Arquad 2C-75. The discs were examined using a Digital Instruments Dimension 3100 AFM (Vecco, USA). The samples were held in a chamber of distilled water to prevent hydration. Several images were recorded on different locations to verify the reproducibility of the observed features.

5.7.2 Results and Discussion

5.7.2.1 Scanning Electron Microscopy

Philips XL30 Environmental Scanning Electron Microscope-

Figure 5.37 shows the surface of the hydrogel and figure 5.38 shows the cross-section. There is no obvious visible structure apparent on the surface or on the cross-section. A piece of hydrogel was then freeze-dried and looked at in cross-section, figure 5.39 shows this image. Some structure is visible on the freeze-dried sample showing what could be pores within the polymer.

Hydrogel loaded with BAC was looked at in its hydrated state and then dried in the chamber. Figure 5.40 shows the surface of the hydrogel containing BAC viewed in its hydrated state. The white patches may be due to BAC drying on the surface. Again no structure is visible.

Figure 5.37 Surface of unloaded hydrogel in the hydrated state.

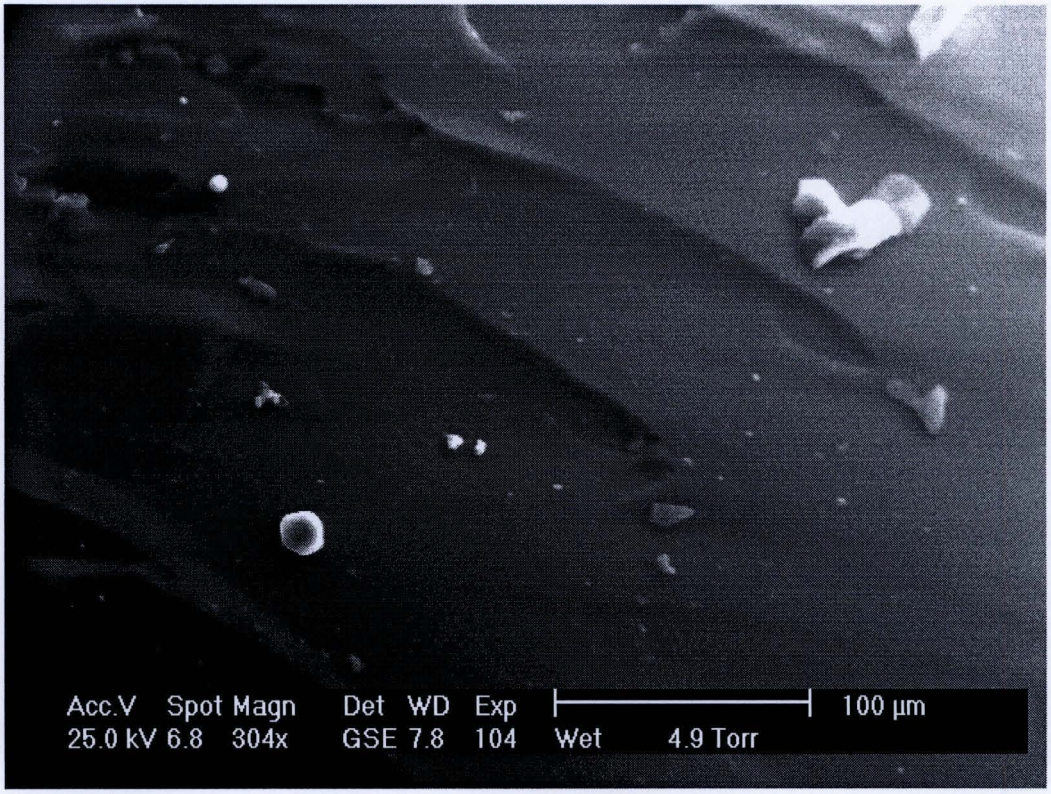

Figure 5.38 Cross-section of unloaded hydrogel in the hydrated state.

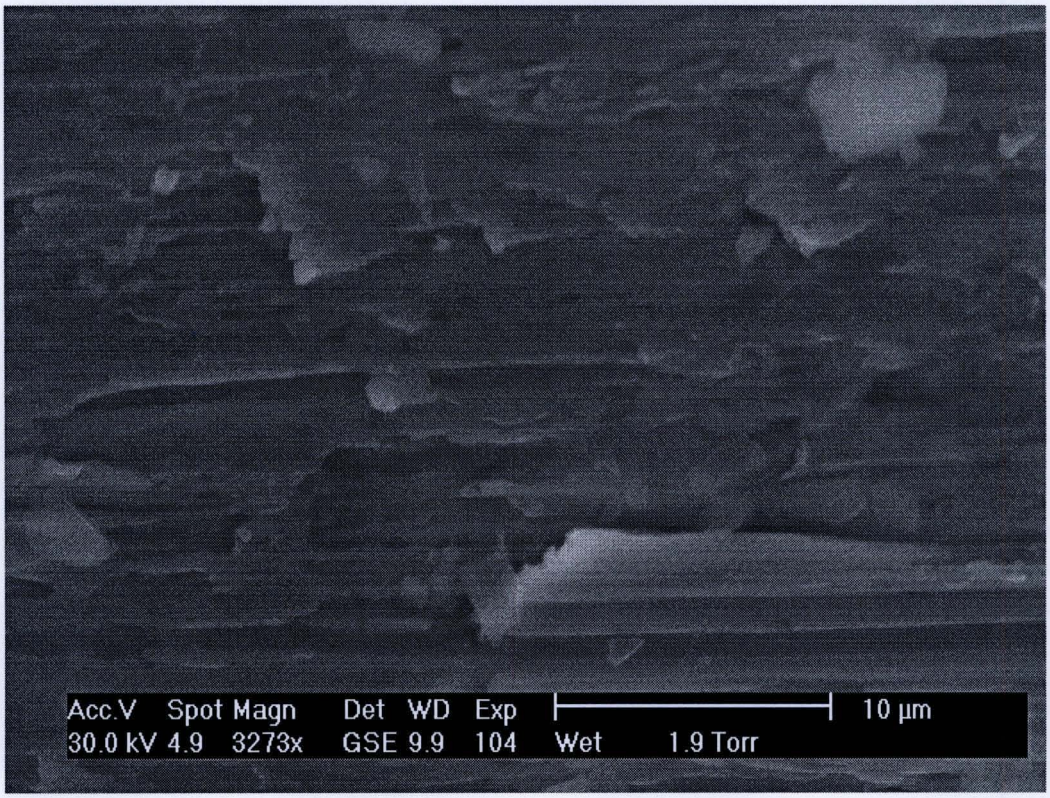

Figure 5.39 Freeze dried cross-section of unloaded hydrogel.

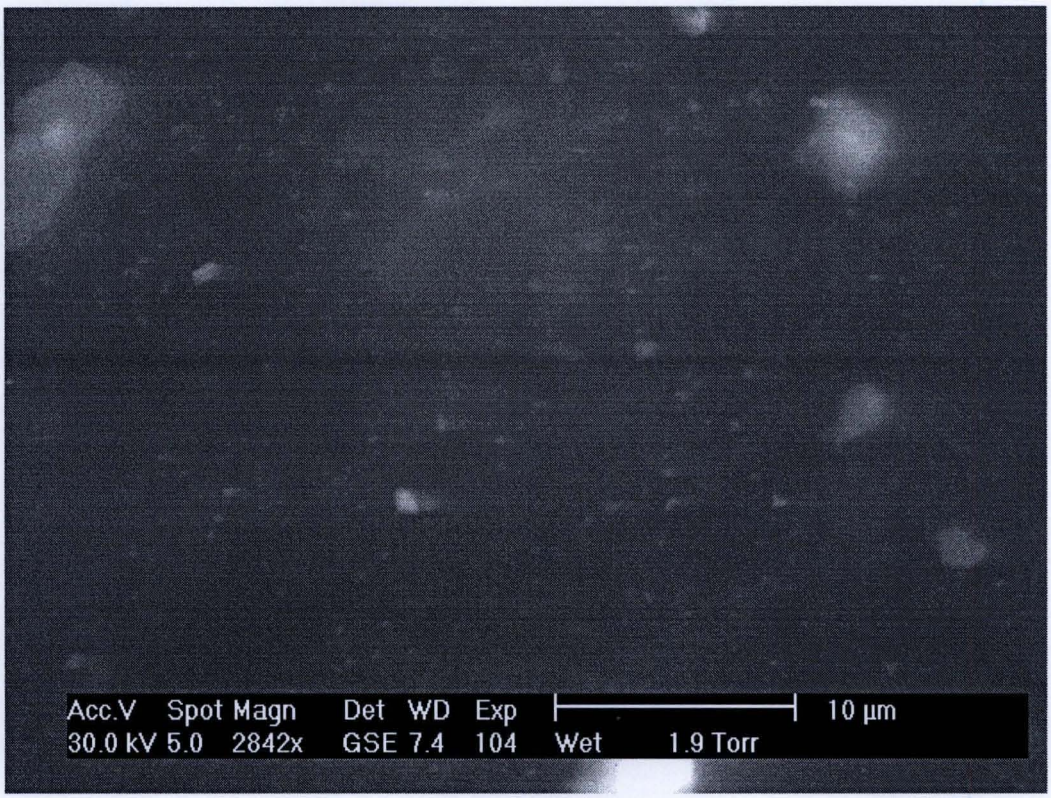

Figure 5.40 Hydrogel loaded with benzalkonium chloride, viewed in the hydrated state.

Hitachi S4 1000 Field Emission Microscope –

These samples were all dehydrated for viewing. Figure 5.41 shows an unloaded hydrogel surface. This image shows a pore type structure with some larger elongated pores visible. However, this structure could be a result of dehydrating the hydrogel. Figure 5.42 shows hydrated hydrogel which was soaked in seawater prior to drying and figure 5.43 shows it cut in cross-section. In conclusion, little detail of the hydrogel structure can be seen using this method.

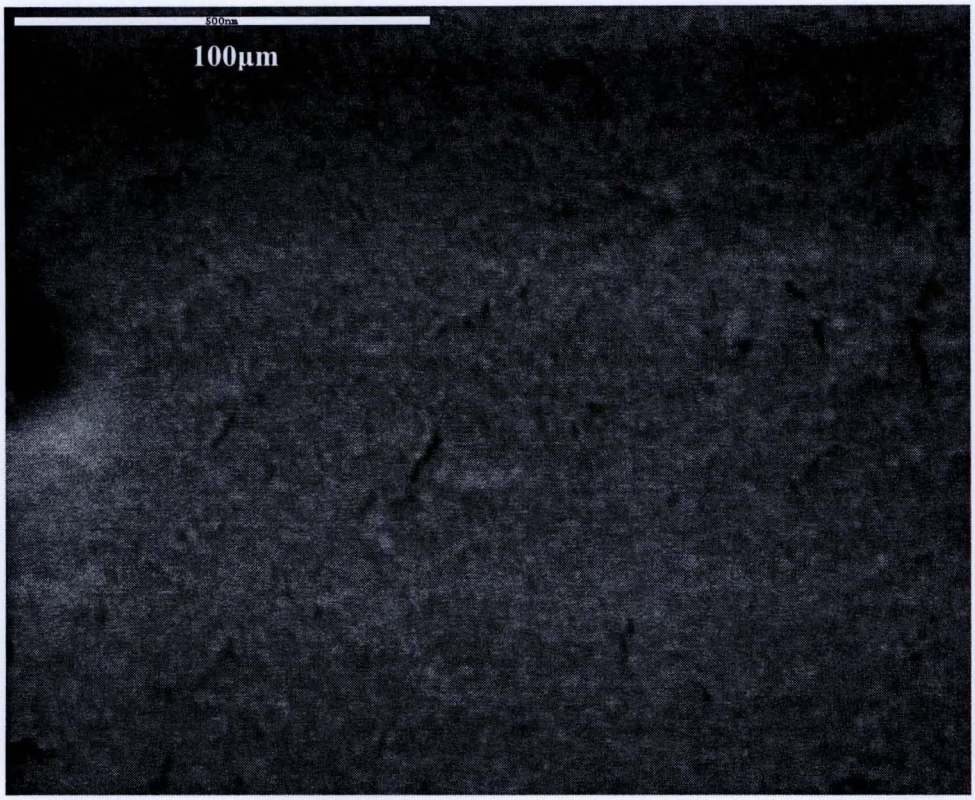

Figure 5.41 Dehydrated unloaded hydrogel surface.

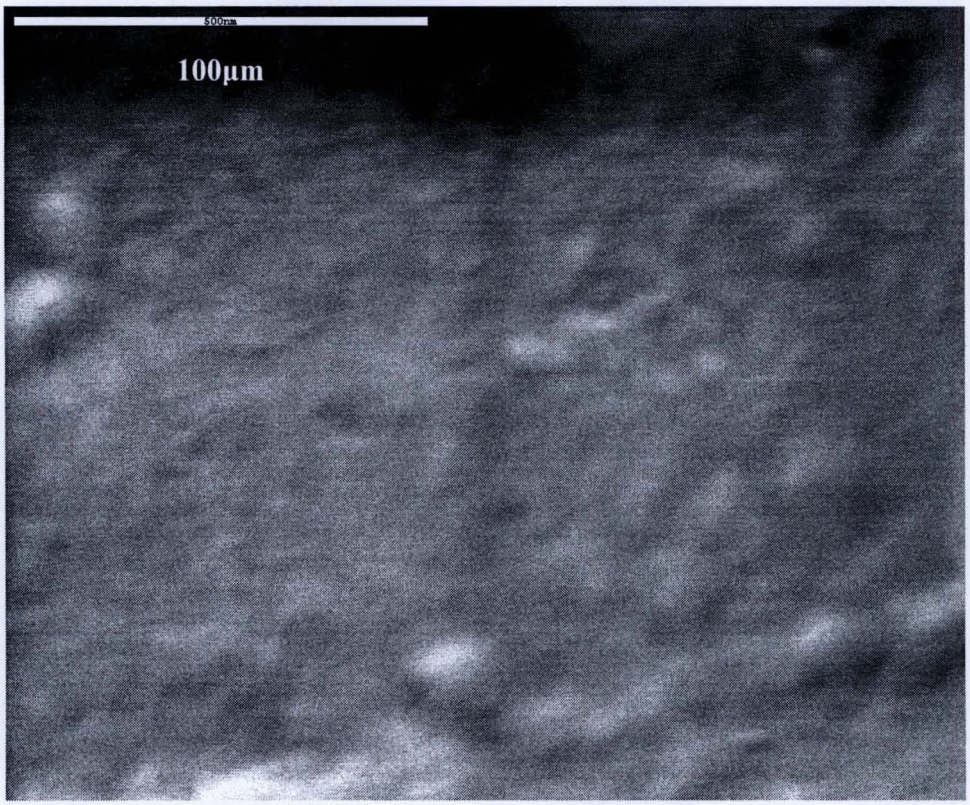

Figure 5.42 Dehydrated unloaded hydrogel that had been soaked in seawater prior to drying.

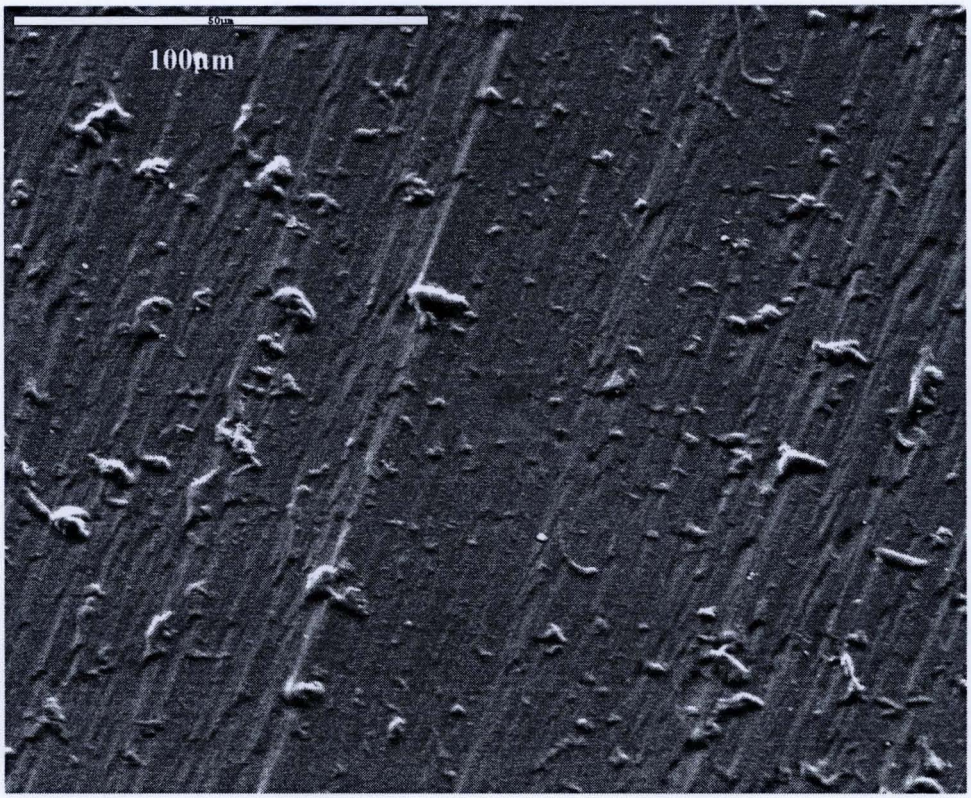

Figure 5.43 Dehydrated unloaded hydrogel cut in cross-section that had been soaked in seawater prior to drying. The lines visible are likely to have been caused by the scalpel blade when cutting the cross-section.

FE1 200F Environmental Scanning Electron Microscope (ESEM)-

The hydrogels were viewed in their wet state.

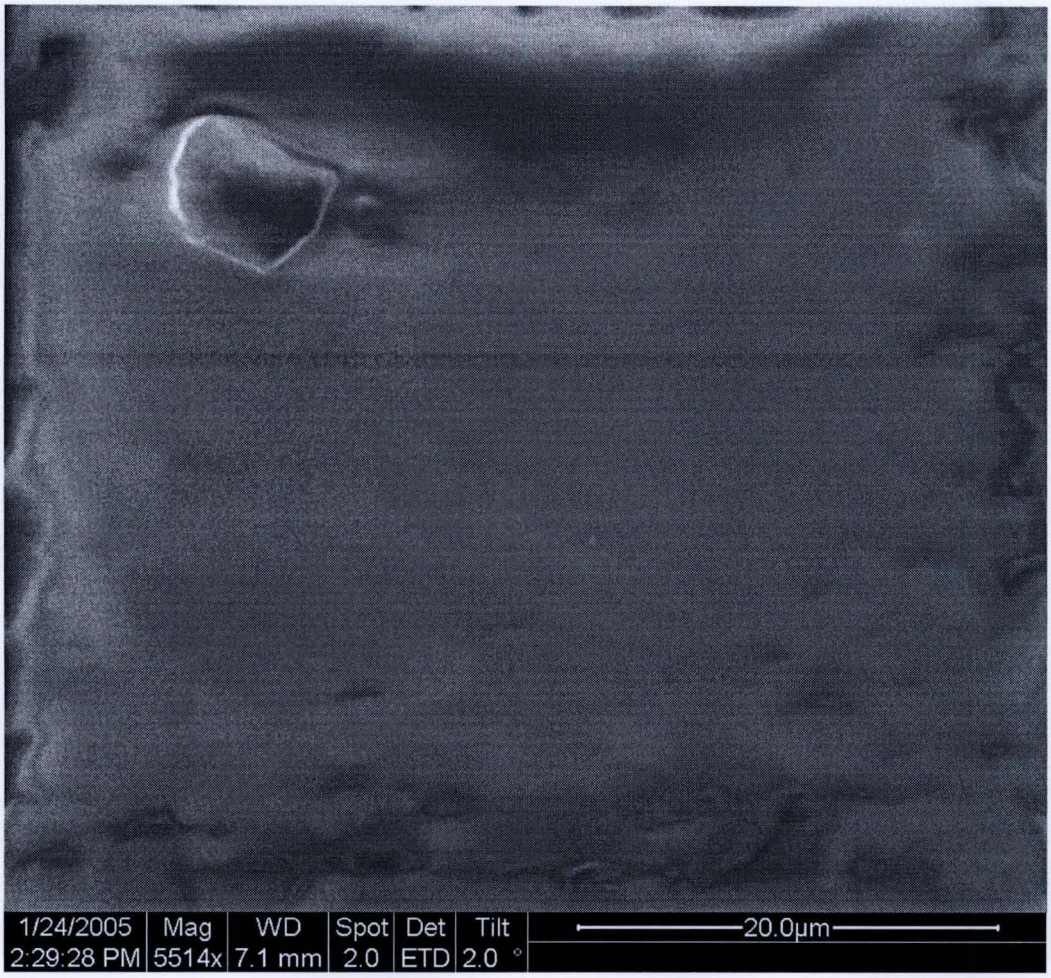

Figure 3.44 ESEM image of a hydrated unloaded hydrogel using a magnification of x 5514 at a low kV setting.

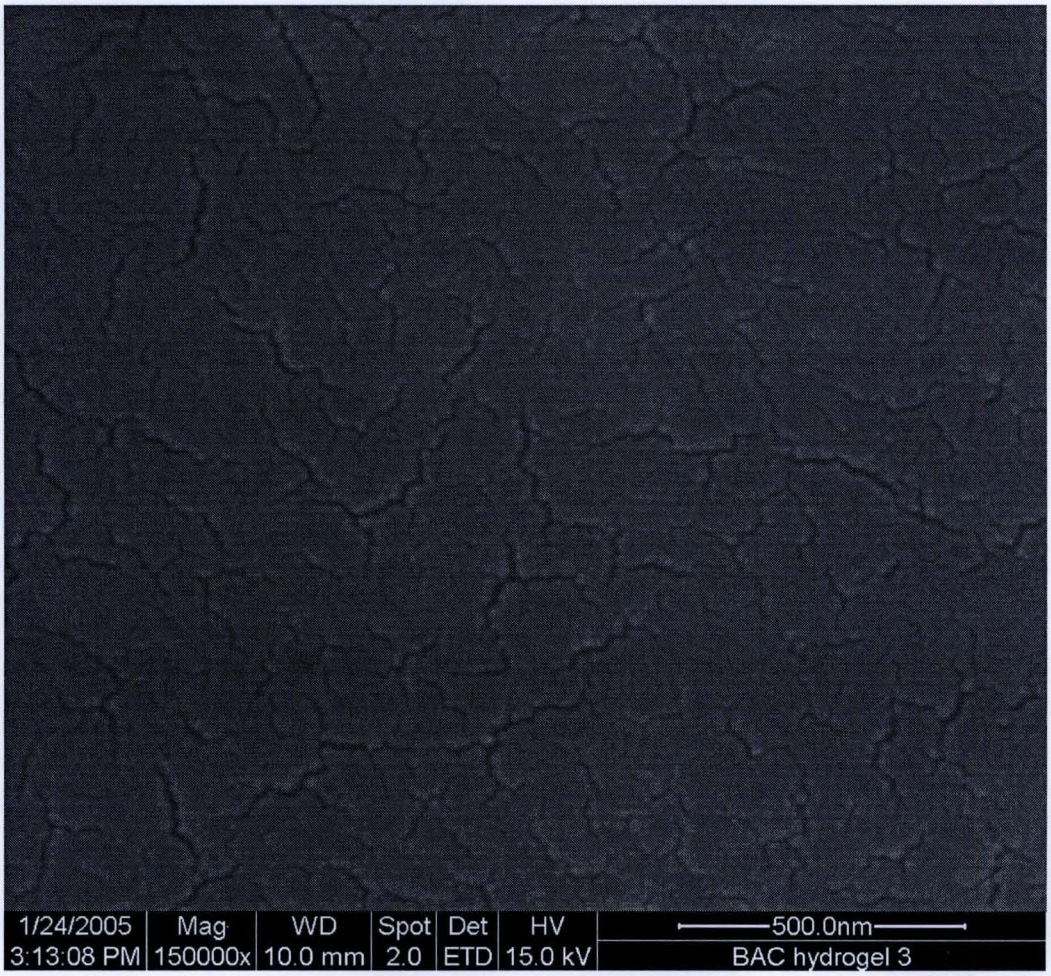

Figure 5.45 Hydrated hydrogel loaded with benzalkonium chloride, showing surface cracking as the hydrogel dries out.

The image shown in figure 5.44 was taken using the Environmental Scanning Electron Microscope (ESEM), low kV setting, and shows the surface of the hydrogel to be featureless. Figure 5.45 shows benzalkonium chloride loaded hydrogel image taken in a hydrated state using a higher kV setting. It shows how quickly the hydrogel's surface begins to dry out as cracking is visible after only a few minutes imaging

It was extremely difficult to achieve good quality images of either dehydrated or hydrated hydrogel material. This is due to the lack of surface features or irregularities. In the literature there was very little evidence of SEM imaging of hydrogels apart from to study bacterial growth on contact lens material (Kaplan and Gundel, 1996).

5.7.2.2 Atomic Force Microscopy

The images shown in figures 5.46 and 5.47 demonstrate that there is little surface structure other than the imprint of the poly (methylmethacrylate) mould in which the hydrogel was made. The hydrogels have extremely smooth surfaces. This is less evident on the blank hydrogel than on the hydrogel containing Arquad 2C-75. This could be due to slight swelling on the surface, due to the surfactant, which has reduced the lines created by the mould. The RMS surface roughness of areas was found to be 26nm for the blank hydrogel and around 7nm for the hydrogel containing Arquad 2C-75. The 3-dimensional images shown in figures 5.48 and 5.49 show that the surface is even; again the imprint of the mould is visible as lines.

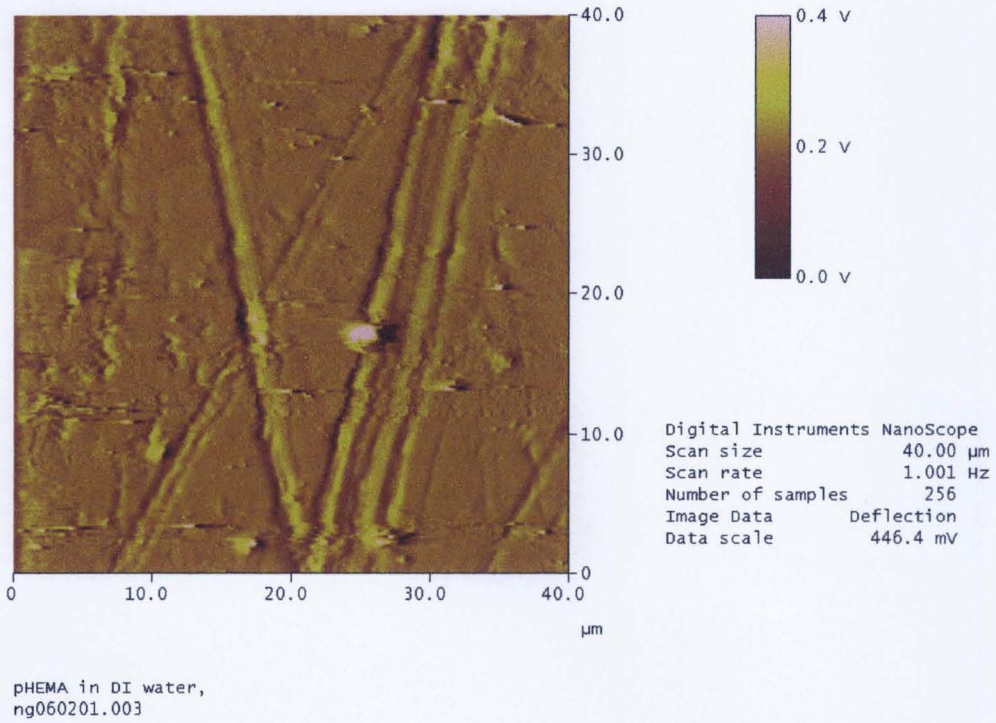

Figure 5.46 AFM image of the blank hydrogel. 40µm scan.

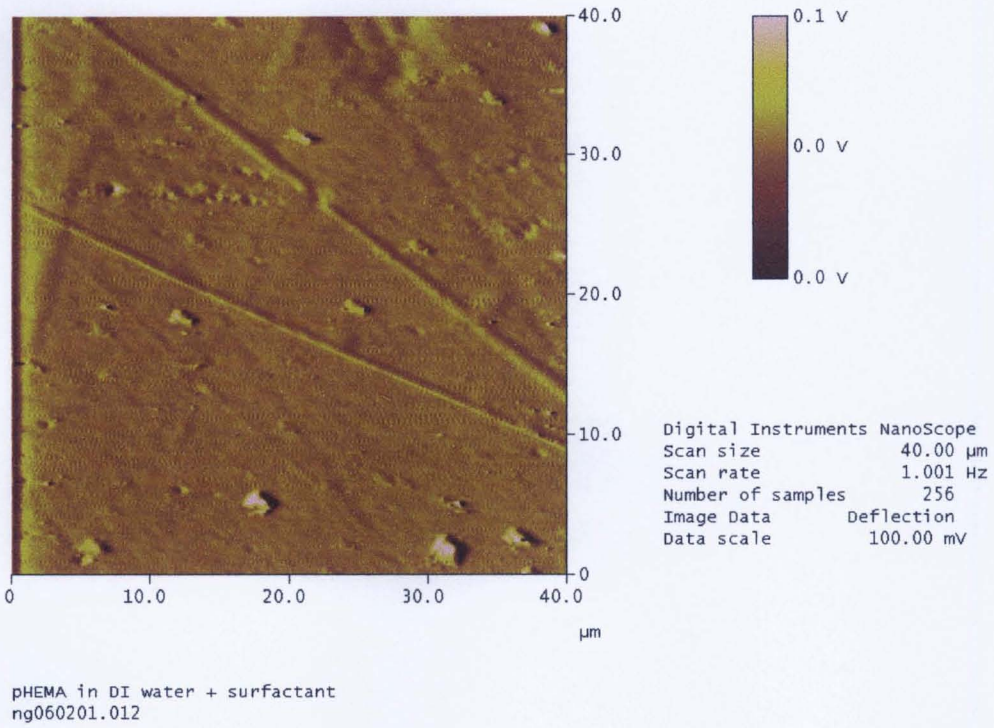

Figure 5.47 AFM image of hydrogel containing surfactant. 40µm scan.

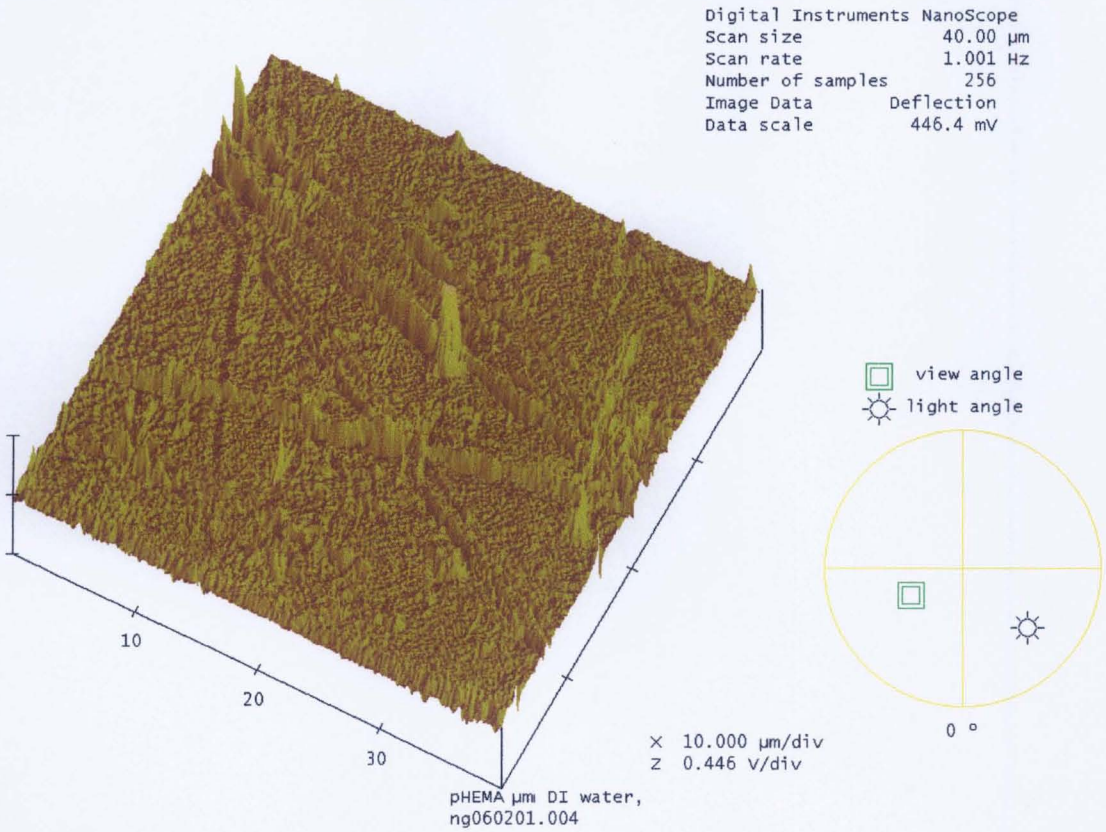

Figure 5.48 3-D AFM image of the blank hydrogel. 40µm scan.

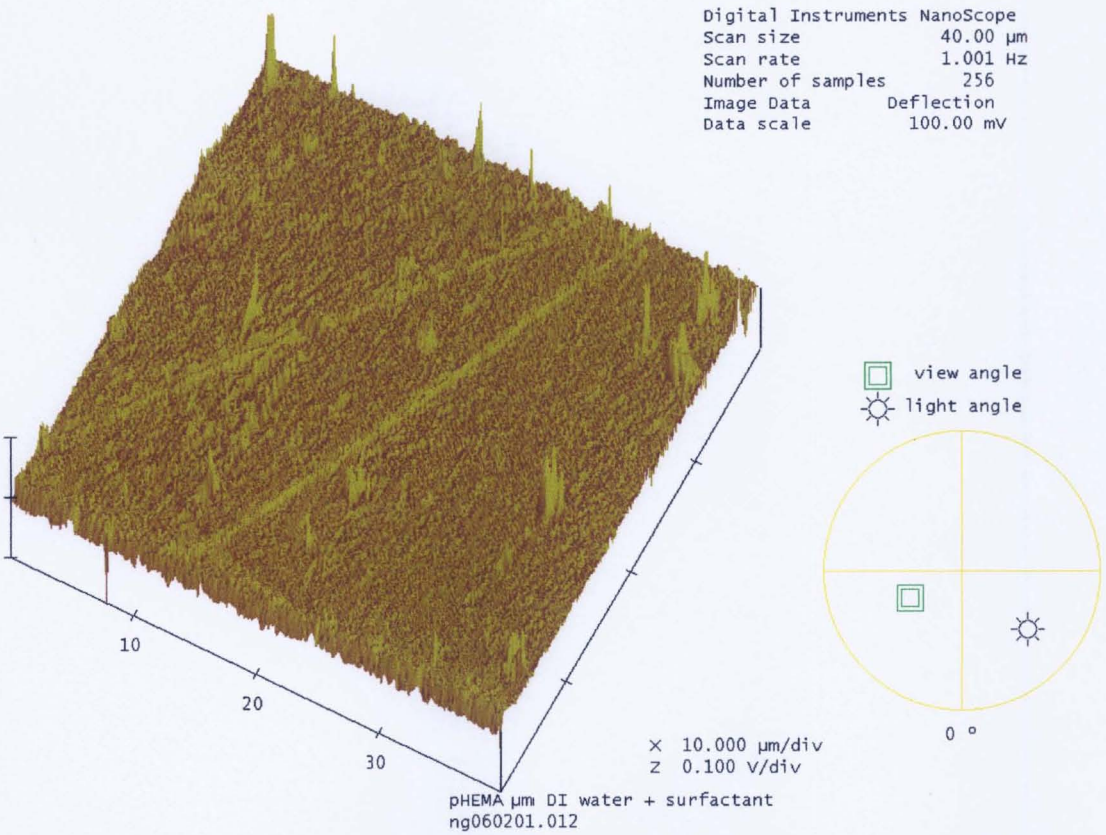

Figure 5.49 3-D AFM image of hydrogel containing surfactant. 40µm scan.

Grobe et al. (1996) investigated the effect of the lens manufacturing processes in the fabrication of hydrogel contact lens; cast-moulded and lathed. There was little evidence of surface morphology on the lens apart from the grooves which would have been characterised from the original polishing process after lathing and the cast – moulded lens appeared smooth and uniform apart from some slight defects such as directional flow lines which may be the result of the replication of the moulding polymer originating. They found that lathed lens had a RMS surface roughness ranging from 22.3-25.2nm and the cast-moulded lens 5.0-9.2nm over an area of 50 x 50 µm). Maldonado-Codina and Efron (2005) considered surface morphology of contact lens manufactured is three ways, lathed, spun-cast and cast moulded. They found that the cast-moulded PHEMA hydrogel had the smoothest surface with a RMS roughness of around 5nm.

Blank hydrogel and hydrogel loaded with Arquad 2C-75 were soaked in artificial seawater (Instant Ocean, Aquarium Systems, Sarrebourg, France) for 14 days and again looked at using AFM. Figures 5.50 and 5.51 show that the surface has become

rougher after being in seawater, with measurements of 66 and 77nm respectively. This could be due to the abrasive action of the seawater.

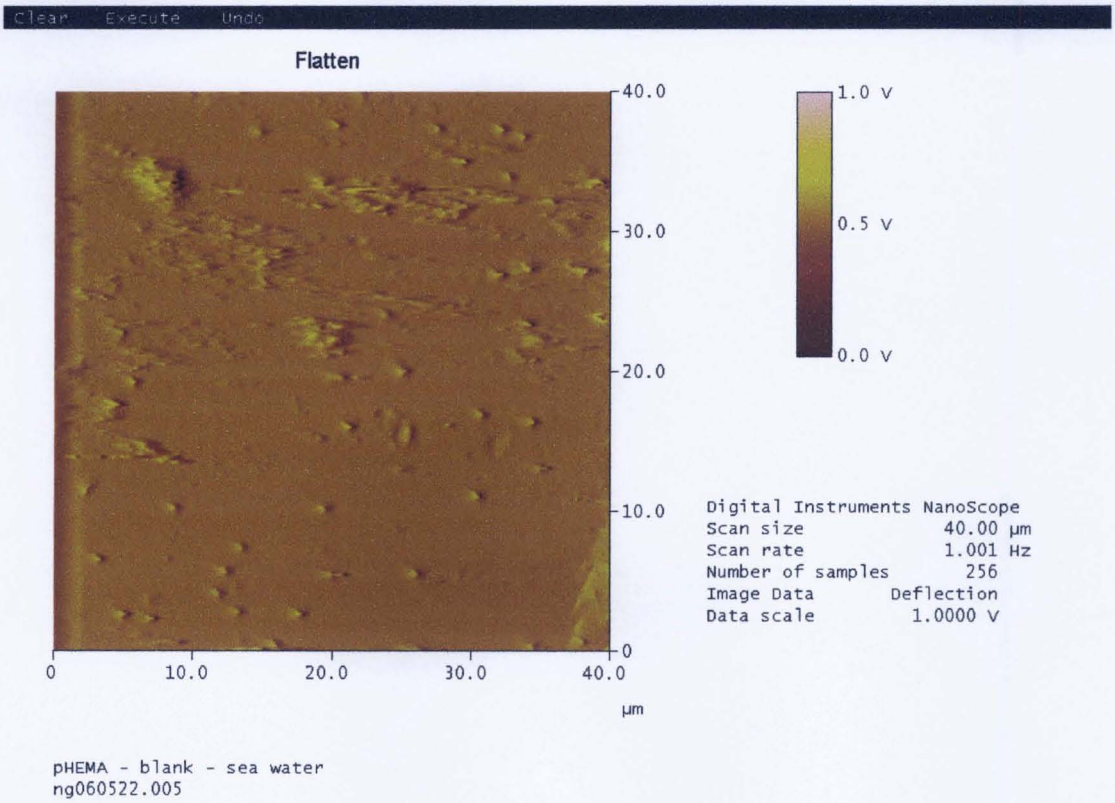

Figure 5.50 Blank hydrogel after being soaked in seawater. 40µm scan

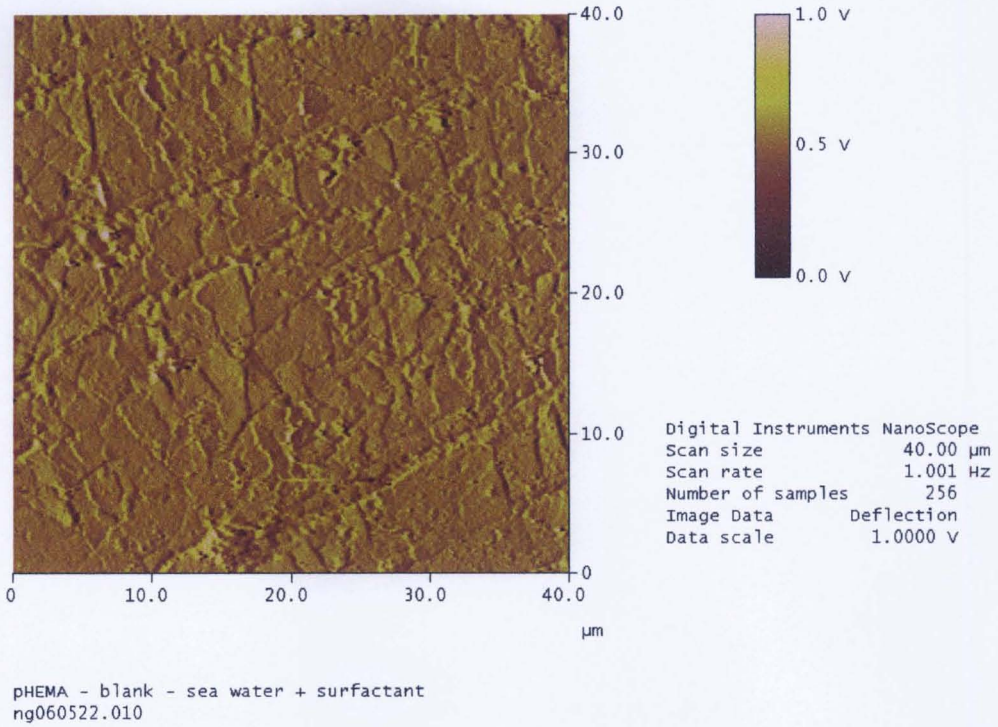

Figure 5.51 Hydrogel containing Arquad 2C-75 after being soaked in sweater. 40µm scan.

5.8 Hydrogels – Contact Angle Measurements

The adhering gas bubble was measured using the dynamic captive bubble technique (Zhang & Hallström, 1990). It was chosen, as it was desirable to keep the membrane wet throughout the test, as this method would prevent drying of the surface leading to anomalous results. The wet state of the samples provides better initial conditions and ensures more stable results (Hermitte et al., 2004).

5.8.1 Method

The work was carried out in an optically clear glass box (55 x 55 x 55mm), which was filled with synthetic seawater (3.5%) (Instant Ocean, Aquarium Systems, Sarrebourg, France). All the work was carried out at ambient temperature which was 22±2°C for the duration of the tests. The hydrogel and poly- (methylmethacrylate) (PMMA) pieces were held in place using a holder made of PMMA, which allowed the test piece

to be exposed to the water in the tank. The surfaces tested were soaked in seawater for 48 hours prior to testing to allow them to acclimatise to the polar environment. Polymer surfaces are particularly mobile and the molecular orientation of the surface at any point in time may be modified in response to the surrounding environment (Tonge et al., 2001). The surfaces were also tested after 10 weeks of soaking in seawater to determine changes to the angles over time. The bubble was supplied to the surface via a 1ml syringe with a 25-gauge needle to allow control of the volume. The bubbles were generated in the liquid and captured on the test surface as a result of buoyant transport and attachment. The bubbles were all between 2-3 mm in diameter. `It had been observed that no change in angle size was found on a homogeneous surface for bubbles raging from 1-7mm (Drelich et al., 1996). The hydrogels investigated had a smooth surface and appeared glossy and so surface roughness would not be detrimental to the measurements. The measurements were carried out in triplicate on each sample piece and three pieces of each material were tested.
The bubbles were photographed using a JVC video camera fitted with a Viviter 55mm F2.8 macro lens. Figure 5.52 shows the experimental set up. A computer program was written to measure the angles in order to prevent the errors encountered when measuring these angles manually. The image is selected and displayed in its frame. The user then draws, using the mouse, the incident angle of the bubble. The mouse positions in x and y are stored in a matrix. A curve-fitting algorithm is used to determine the mathematical function of the curve from this function is differentiated to get the angle. Figure 5.53 shows a typical image of a bubble.

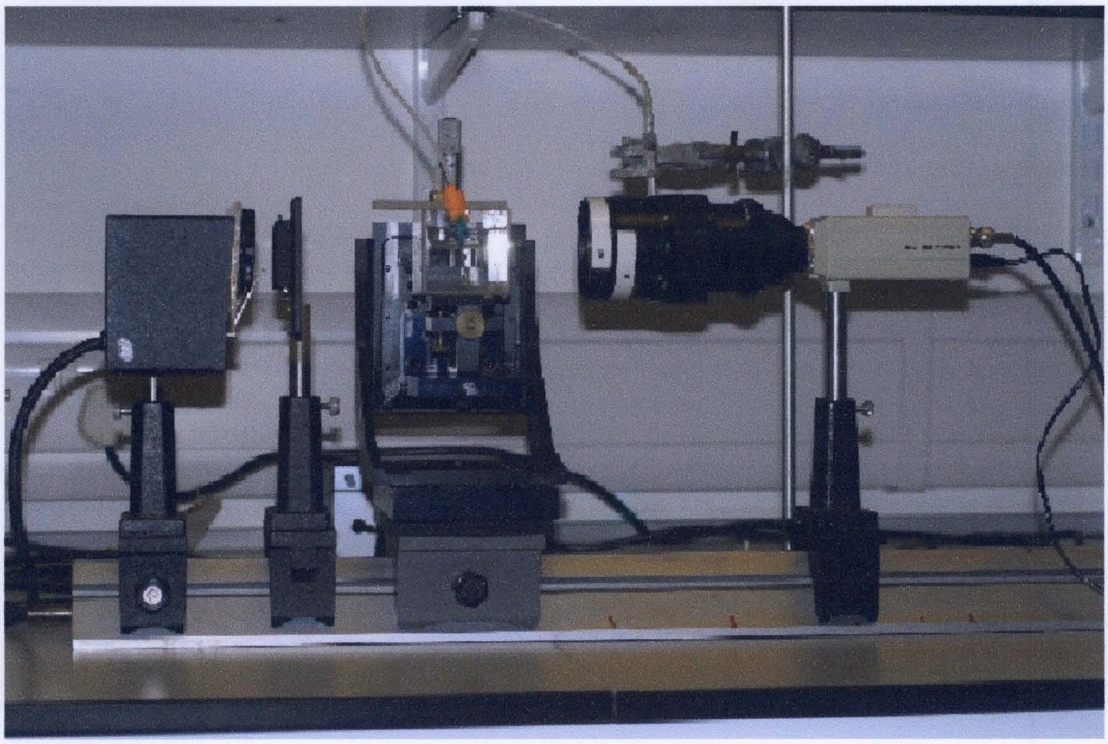

Figure 5.52 The set up with light, tank and camera to record dynamic captive bubbles.

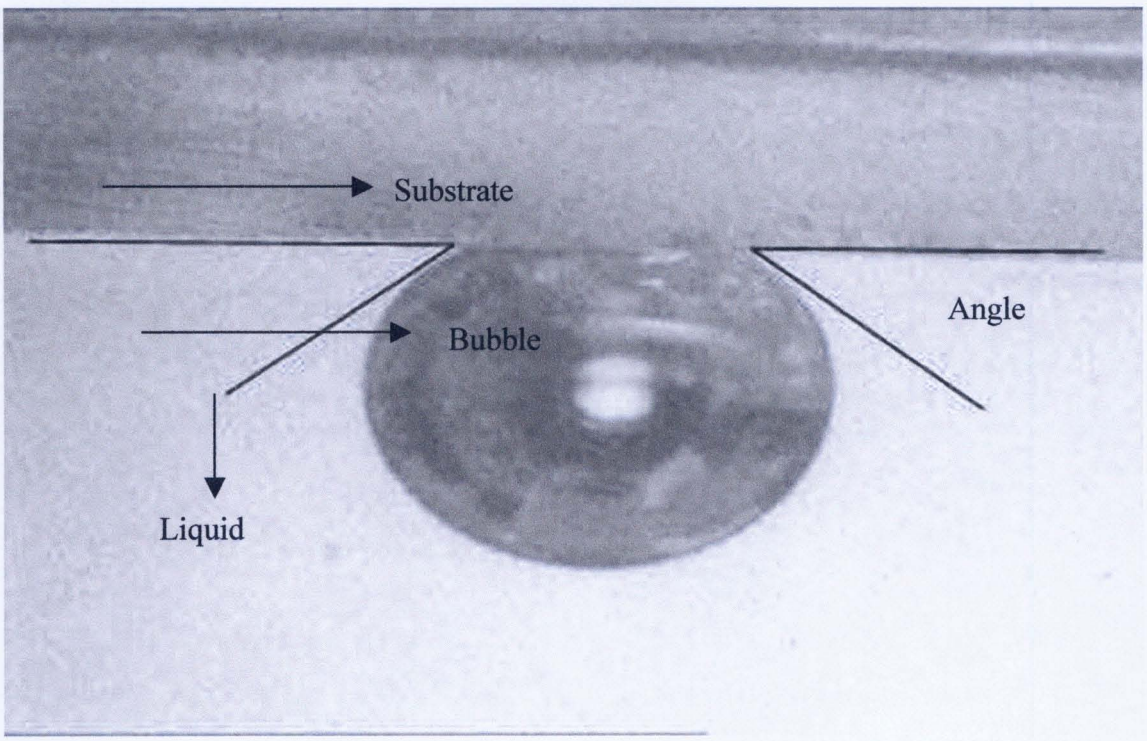

Figure 5.53 Typical image of an air bubble in water.

5.8.2 Results and Discussion

Figure 5.54 shows the angles measured on the 3 types of hydrogel and PMMA after 3 days and 10 weeks soaking in seawater.

At the day 3 time-point the PMMA had a much higher angle value than the hydrogel samples. Within the hydrogels tested there was no significant difference between the untreated hydrogel and the hydrogel containing benzalkonium chloride (BAC). The value found for the untreated hydrogel was similar to that found by Hermitte at al. (2004). Holly and Refojo (1975) found PHEMA hydrogel containing 40% water to have critical surface tension values of 36 and 36.9 when measured by Ziemen and Wolfram plots respectively. Grobe et al. (1996) found hydrogel contact lens (Etafilon-A, Johnson & Johnson) to have a contact angle of 34°. However, the hydrogel containing the Arquad 2C-75 (twin-chained surfactant) had a much lower angle at around 16°, making it a more hydrophilic material than the other hydrogel materials tested. In marine fouling trials the hydrogel containing Arquad 2C-75 demonstrated superior fouling resistance when compared with the other hydrogels tested. The similarity of angle size between the untreated hydrogel and the hydrogel containing BAC was not reflected in resistance to fouling as the hydrogel containing the BAC showed much better resistance to fouling than the untreated hydrogel.

After 10 weeks soaking in seawater the sample pieces were retreated to determine if there was any change in their surface properties. It was found that all four materials showed an increase in angle size after the 10 weeks. The percentage increases were PMMA 11.4%; Hydrogel 42.3%; BAC/hydrogel 42.3% and Arquad 2C-75/hydrogel 121.7%. The PMMA still had a higher angle than the all of the hydrogels and there now was no significant difference between the 3 hydrogel materials. The increase in angle size is indicative of changes to the materials over time in the marine environment. These could be increase in surface roughness, a reorientation of the polymer and also due to the release of the surfactant in the case of the 2 treated hydrogels.

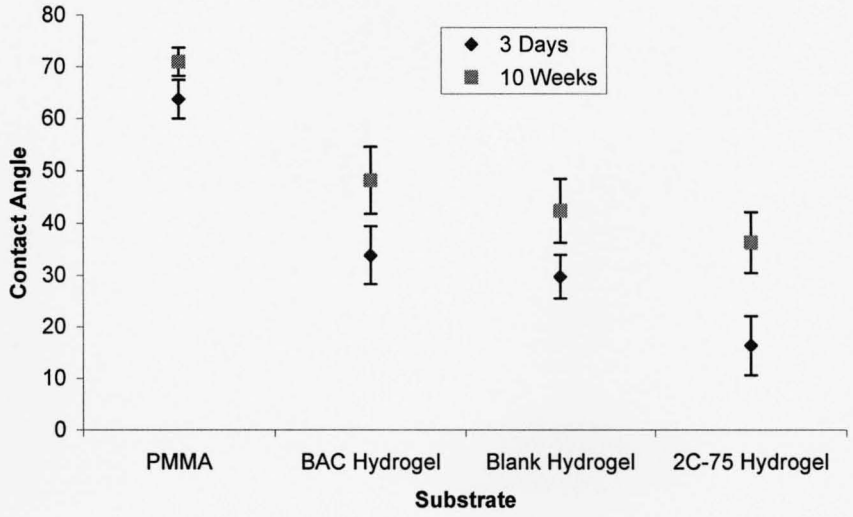

Figure 5.54 Contact angles on hydrogel substrates after 3 days and 10 weeks in seawater.

The low contact angle of the hydrogel containing the Arquad 2C-75 demonstrated that the surfactant did lower the surface tension of the surface of the hydrogel. The same could not be said for BAC. Kim et al. (1992) found that low interfacial tension between hydrogel surfaces and aqueous solution had been found to minimize protein and cell adhesion.

5.9 General Summary

A method was developed to produce a high quality, transparent hydrogel which was able to absorb surfactant uniformly resulting in a reproducible product. The BAC could easily be quantitatively analysed using HPLC/UV detection both at the beginning and throughout the marine deployment trials. A method was developed for the twin –chain surfactant, Arquad 2C-75. Using ion chromatography the amount could be quantified when there were no competing cations. However, due to ions in

the seawater it proved difficult to produce a robust technique for this compound during marine deployment trials. Thus only the amount present at the beginning of experiments could be quantified.

The diffusion of BAC in seawater was successfully measured as 2.44×10^{-6} cm^2 s^{-1} showing diffusion to be around a third of the rate of diffusion in distilled water, 7.78×10^{-7} cm^2 s^{-1}.

The weight and swelling studies added to the understanding of the nature of hydrogel behaviour when loaded with surfactant and also when these hydrogels were deployed in a variety of media. BAC caused the hydrogels to swell considerably; however, the Arquad 2C-75 did not cause this to happen. Seawater did not have any adverse effects on the hydrogels which has positive implications for marine deployment.

The mechanical studies of the hydrogels demonstrated the effects of both surfactants and seawater on the mechanical properties of the hydrogel coatings. The results showed that the hydrogel loaded with Arquad 2C-75 was not adversely affected as the strength, elongation or elastic modulus of the hydrogel was not significantly different to the unloaded hydrogel. The BAC loaded hydrogel demonstrated reduced strength, modulus and elongation. The elongation at failure increased after seawater exposure for all hydrogel specimens tested.
Detailed SEM work did not show any surface features on the hydrogel. However, AFM did show some features that were a result of the production process. AFM also demonstrated that the hydrogels were extremely smooth coatings and they became slightly rougher after seawater exposure. Visible microscopy showed the effects on hydrogel structure of BAC as it created a honeycomb pattern within the gel.

The reduction in the contact angle measurements of the hydrogel containing Arquad 2C-75 was an efficient method to show that the surfactant had the effect of increasing the hydrophilic nature of the hydrogel material.

Chapter 6

Gas Membranes - Experimental Methods, Results and Discussion

In this chapter the study of the materials used as gas membranes is split into four sections. Firstly the gas membranes used are detailed and the design and fabrication of pseudo sensors used to test the permeability of gases through these membranes is explained. The apparatus made for measuring gas membrane permeability is described and the analytical technique used to quantify gas permeability is detailed. The gas measured is ammonia as it proved to be easily measured and quantified. The second section describes the experiment carried out to measure the effect on permeability of using hydrogel overlays on the membranes. Thirdly the structures of the gas membranes are examined using scanning electron microscopy (SEM) and atomic force microscopy (AFM). Lastly, section 6.4 describes the contact angle measurements made on the gas membranes which is related to the surface energy of these materials and further elucidates their properties.

6.1 Gas Membranes

An experimental system to measure the diffusion of gaseous species through membranes commonly used on gaseous sensors was developed. This system could also be used to monitor the effects of biofouling on gaseous diffusion through the membranes as anything that raises or lowers gaseous diffusion will affect the sensors performance. Gaseous sensors are frequently used in environmental monitoring of both fresh and marine waters to measure such species as ammonia, carbon dioxide and oxygen; thus accuracy of measurements is essential. Ideally, such an experimental system would allow replicates to be tested and so prevent the requirement to use actual sensors in this experimental work, as this would be cost prohibitive.

A variety of poly tetrafluorethylene (PTFE) membranes were tested, these were: YSI standard membrane and YSI high sensitivity membrane (Fisher Scientific Ltd, UK); Rank Bros membrane (Polyflon Technology Ltd, UK); ABB membrane (Gore-Tex®)

(ABB Ltd, UK); PTFE tape (Gore-Tex®) (W &L Gore, Delaware, USA); TFE (made in the USA, a gift); PTFE wide tape (Fisher Scientific Ltd, UK)) and one high density polyethylene (HDPE) membrane were investigated in order to understand fully the diffusion of gas through them. Some were membranes supplied by manufacturers for their own gas sensors while others were cut from PTFE tape produced by various manufacturers. These tapes have been shown to be useful as sensor membranes (Tarsiche and Ciurchea, 1997; Watson et al. 2005). Table 6.1 lists each membrane tested with measurement of membrane thickness.

Membrane	Thickness (µm)
YSI standard membrane	30
YSI high sensitivity membrane	20
Rank membrane (Polyflon)	12
ABB membrane (Gore-Tex®)	70
PTFE tape (Gore-Tex®)	85
TFE (Made in the USA)	100
PTFE wide tape (Fisher)	190
HDPE	20

Table 6.1 The thickness of each membrane measured in micrometres.

6.1.1 Development of Pseudo Sensors for Membrane Testing

Ammonia, carbon dioxide and oxygen sensors all employ gas permeable membranes at their detection ports, which allow the gas of interest to pass through into the electrode. Pseudo sensors were developed to enable replicate gas diffusion studies to be carried out on the various membranes of interest. In order to construct these pseudo sensors, adaptation of tubes already available was investigated. Initially 100ml syringes were adapted by cutting the needle fitting off leaving a space that the membrane could be fitted to using an o-ring. It proved difficult to retain the o-ring in place and also the membrane appeared uneven with slight gathering at the edges. From this first design a more suitable tube was blown from glass (Figure 6.1). These

rounded end and a slight lip allowing the membrane to be attached and the o-ring was retained behind the lip. At the other end a glass flange was constructed to allow ease of use when stoppering the tube.

Initial tests to measure the diffusion of ammonia indicated that there was poor reproducibility between the replicates. It was thought that the o-ring/membrane fitting led to variations in the surface area of exposed membrane resulting in differing amounts of gas diffusion and also some leakage of liquid at the folds of the membrane.

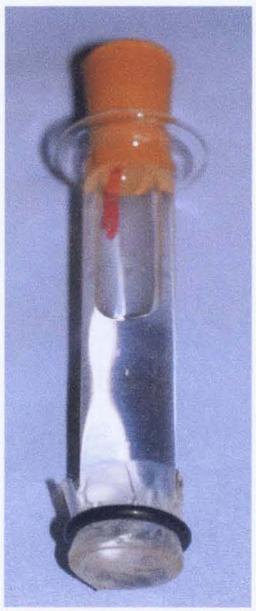

Figure 6.1 Glass pseudo sensor with membrane attached.

A more reproducible way of fitting the membranes was required. Pseudo sensors were constructed using poly-methylmethacrylate (PMMA) rod. The rod was drilled out making a tube with an inner diameter of 20mm with a screw cap, which screwed on to one end with a circular cut-out to expose the membrane (20mm diameter). A locking nut was also added to ensure the top did not become slack. Figure 6.2 shows the improved sensor.

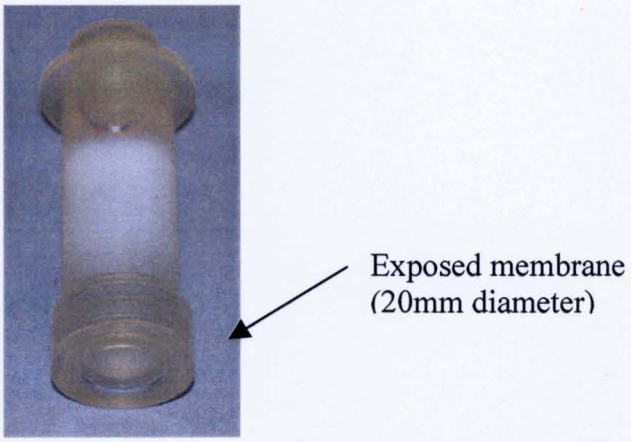

Figure 6.2 PMMA pseudo sensor with membrane attached.

This sensor ensured that a specific area of membrane was exposed as each sensor was constructed to a high tolerance. Silicone gaskets were used either side of the membrane and the screw top to create a good seal. Membrane discs with a diameter of 23mm were cut using a stainless steel cutter made for the purpose. The pseudo sensors were stoppered using silicone stoppers.

6.1.2 Test Method and Apparatus to Measure Gas Permeability

Ammonia was chosen to test diffusion rates through the membranes as it was both easier and more efficiently measured than carbon dioxide or oxygen. Diffusion through each membrane was measured. The measurement was performed by creating a source of ammonia which would diffuse through the membrane on test. A similar method was used successfully by Tarsiche and Ciurchea (1997). The test vessel was filled with 500ml of 0.1M sodium hydroxide (NaOH) which had 0.1M ammonium salt (NH^{+}_{4}) added to liberate ammonia (Figure 6.3).

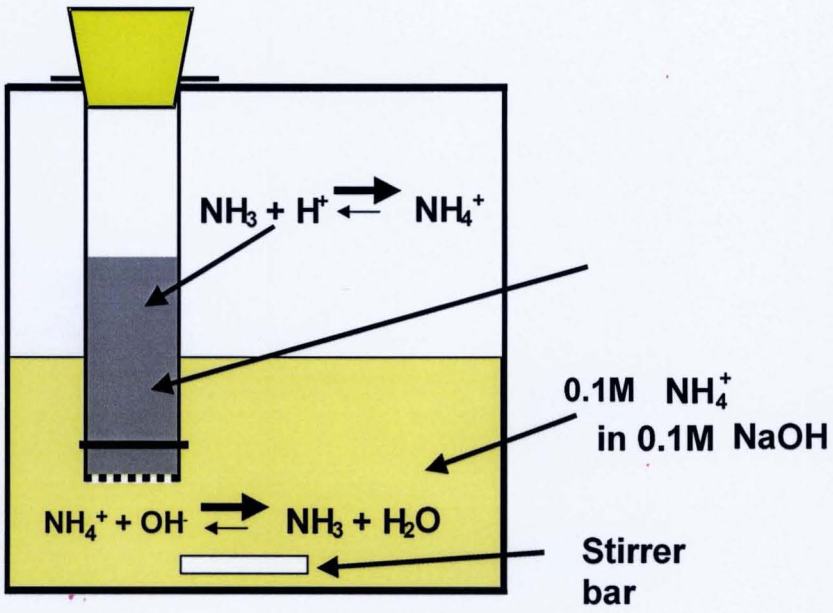

Figure 6.3 Diagram of liberation of ammonia.

The ammonium salt was added just as the test was about to begin. The solution was mixed using a magnetic stirrer to ensure even release of ammonia. The pseudo sensors were held in a PMMA lid with holes drilled to hold them securely in place. The lid was a tight fit ensuring that there would be little escape of ammonia gas. Each sensor was stoppered using a silicone stopper and a ring of PMMA held these stoppers evenly in place. Each sensor was filled with 5ml 0.1M hydrochloric acid (HCl). The vessel was placed in a temperature control cabinet, at 25°C. Figure 6.4 shows the vessel containing the pseudo sensors. Each vessel held 5 sensors. The diffusion experiments were run for fixed periods of time, 5 and 25 hours. A time series was also run for some of the membranes.

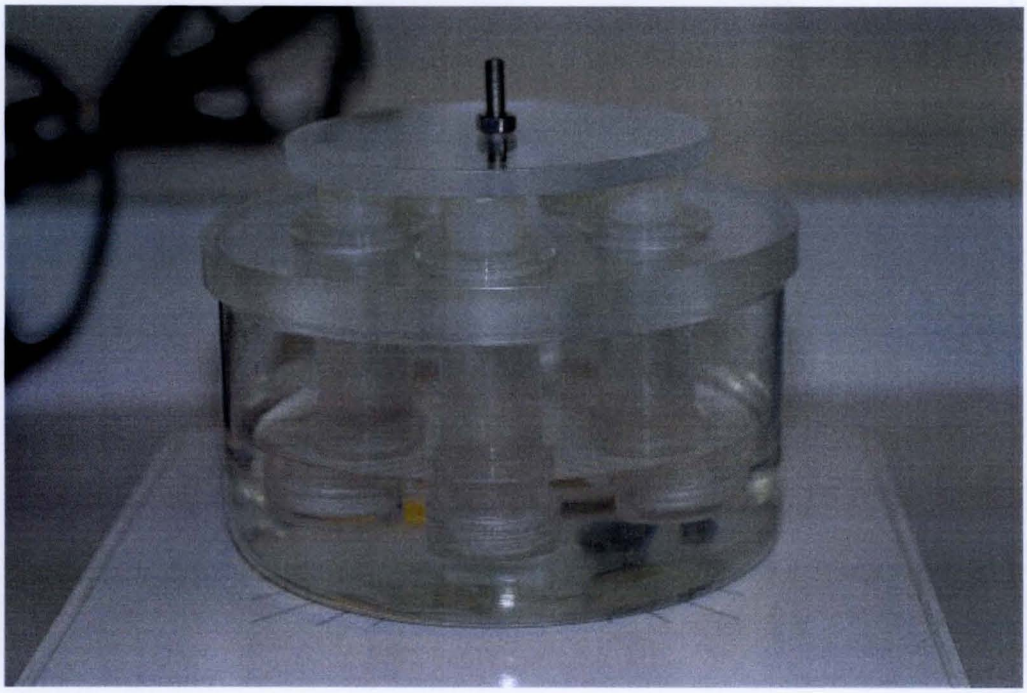

Figure 6.4 Vessel containing pseudo sensors in a solution rich in ammonia, continually stirred.

At the conclusion of each run the vessel was removed from the stirrer and the contents of each sensor transferred by pipette to 25ml volumetric flasks. Each flask was made up to the mark using 0.1M HCl.

6.1.3 Analysis of Ammonia

Ammonia was determined by modification of the indophenol green method using a complexing reagent to prevent interferences due to the precipitation of hydroxides in the reagent system. Measurement was made using a Technicon auto analyser that consisted of a continuous flow system leading to a colourimeter that detects the sample of interest at a wavelength of 650nm and is linear in the range 1-5 mg l^{-1}. The instrument was fitted with an auto sampler and was capable of running 50 samples per hour.

Gas membrane samples were initially tested on the o-ring pseudo sensor system described in section 6.2. The experiments were repeated using the PMMA pseudo sensor system.

6.1.4 Results and Discussion

Table 6.2 shows the results obtained from the glass pseudo sensors where there membrane was fitted using an o-ring. It can be seen that these are variable between 5 replicates. Despite these variations between replicates the results indicated a wide range of diffusion rates between the various PTFE membranes.

	PTFE tape(wide)	YSI(SM)	Rank	PTFE tape(GT)
	Flux (ug cm^{-2} h^{-1})			
	349	37.3	1.83	1770
	270	8.4	0.62	1619
	354	8.8	1.73	1668
	334	21.6	0.74	1691
	236	8.8	0.52	1310
Mean	308.6	16.9	1.09	1612
SD	52.6	12.6	0.64	177

Table 6.2 Flux measurements of ammonia through membranes fitted by o-rings to pseudo sensors after 5 hours diffusion.

Further diffusion experiments were run using the improved pseudo sensor. Tables 6.3 and 6.4 show the flux of ammonia gas through the membrane when fitted to the PMMA pseudo sensors with screw fit caps after 5 and 25 hour runs, respectively. The membranes made from PTFE tape, TFE tape and that supplied by ABB (Gore-Tex®) for the Kent ammonia probe all showed high rates of flux at 5 hours, all around 1000 μg cm^{-2} h^{-1} whereas both the YSI standard and high sensitivity membranes and the Rank membrane showed low rates of diffusion, 0.05, 0.12 and 0.58 μg cm^{-2} h^{-1} respectively.

The reduction in flux of ammonia after 25 hours when compared with the 5 hour result can be explained that a build up of ammonium in the HCl immediately above the membrane causing this area to become 'stagnant' and preventing free diffusion of

ammonia ions. This could be rectified by including a stirring bar in each pseudo sensor which would prevent the build up of ammonia.

PTFE tape (GT)	ABB membrane	TFE tape	YSI (HS)	YSI (SM)	Rank Bros
		Flux (μg cm^{-2} h^{-1})			
948.48	1133.31	917.40	0.10	0.05	0.44
958.01	1149.94	929.95	0.11	0.06	0.57
953.99	1123.80	891.15	0.13	0.04	0.66
949.92	1104.80	926.53	0.15	0.05	0.58
917.38	1147.56	867.19	0.13	0.04	0.63
Mean 945.56	1131.88	906.44	0.12	0.05	0.58
SD 16.18	18.53	26.69	0.02	0.01	0.08

Table 6.3 Flux measurements of ammonia through membranes after 5 hours diffusion.

PTFE tape (GT)	ABB membrane	TFE tape	YSI (HS)	YSI (SM)	Rank Bros
		Flux (μg cm^{-2} h^{-1})			
205.92	190.55	220.99	8.06	0.05	0.41
188.18	191.50	221.42	9.84	0.05	0.39
210.96	239.49	221.42	9.79	0.05	0.43
200.66	192.45	226.58		0.10	0.57
203.14	242.34	211.11		0.05	0.37
Mean 201.78	211.27	220.31	9.23	0.06	0.43
SD 8.51	27.09	5.64	1.01	0.02	0.08

Table 6.4 Flux measurements of ammonia through membranes after 25 hours diffusion.

The time series test was carried out over 25 hours on the YSI standard membrane. The amount of ammonia diffusing through the membrane was measured hourly from 1 to 9 hours and at 25 hours. The amount of ammonia diffusing through the membrane becomes reduced indicating the problem of a build up in ammonium in the initial part of the HCl solution preventing free diffusion. Figure 6.5 shows the flux measured through YSI standard membrane.

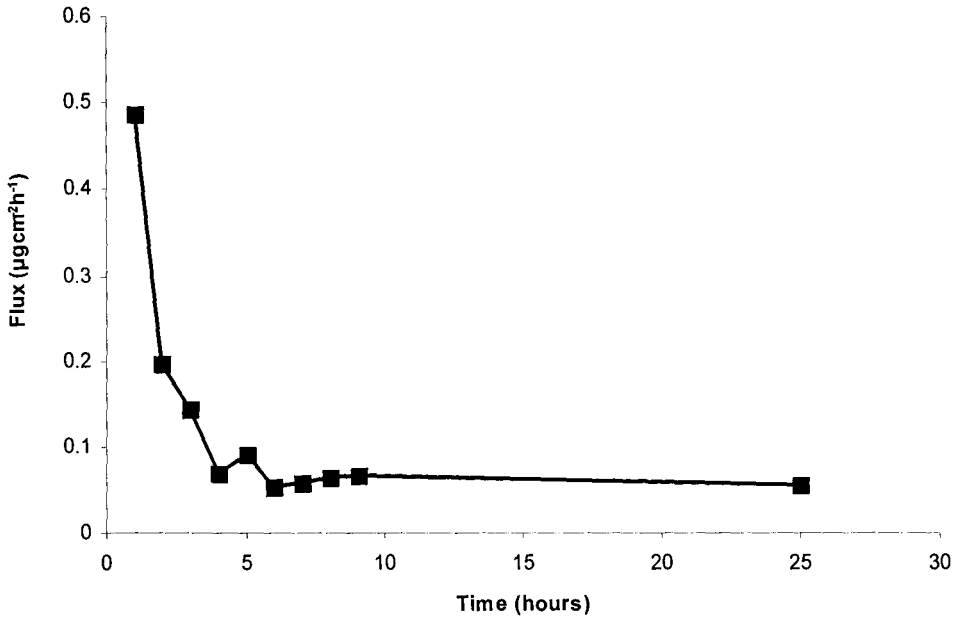

Figure 6.5 Flux measurements of ammonia through YSI standard membrane during 25 hours diffusion.

This method demonstrated the variation in flux of ammonia and therefore gaseous species through a variety of commonly used membranes. The problem of ammonium build up in the sensors can be rectified by modification of the method to include separate stirrers in each sensor. Depending on the application of the sensor, careful consideration should be taken when choosing which membrane to use. In waters with low ammonium concentrations the membranes with high diffusion rates, such as the ABB membrane, would be suitable as the fast diffusion through these would result in a fast response, even if the levels were low.

6.2 Ammonia Diffusion using Hydrogel Overlays

6.2.1 Method

The experiment described in section 6.1 was repeated to include hydrogel overlays to determine what effects the hydrogel had on ammonia gas diffusion. Discs of hydrogel were cut to fit into the pseudo sensors as shown in figure 6.6.

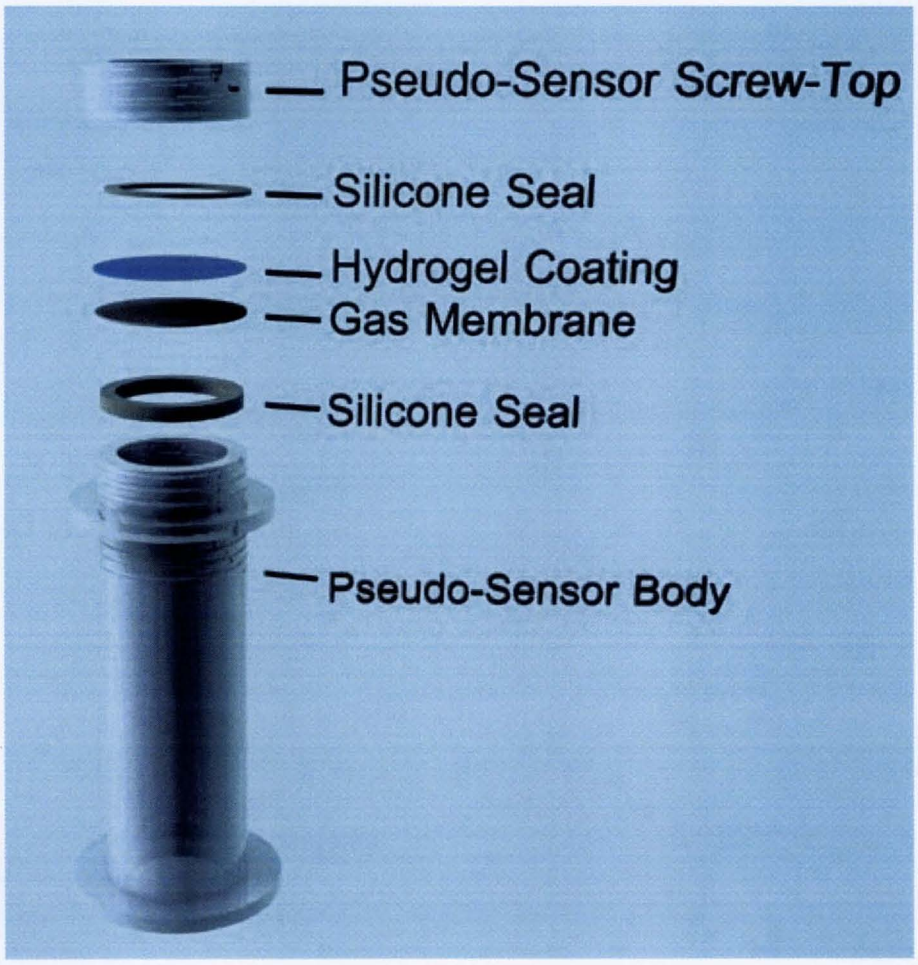

Figure 6.6 Pseudo sensor with hydrogel overlay

Gore-Tex® tape was used as the gas membrane and experiments were run for 5 and 25 hours.

6.2.2 Results and Discussion

As expected, the presence of the hydrogel overlay caused ammonia to diffuse at a lower rate than when the sensors were fitted with the PTFE membrane alone (details in section 6.1.4).

Table 6.5 shows the flux through the Gore-Tex® tape with hydrogel overlays.

Gore-Tex® tape with hydrogel overlays		
	(Flux μg $h^{-1}cm^{-2}$)	
	5 hours	**25 hours**
	68.57	93.61
	85.71	95.33
	70.71	94.04
	68.57	104.39
	68.57	84.55
Mean	72.42	94.38
SD	7.48	7.04

Table 6.5 Flux of ammonia through Gore-Tex® membrane with hydrogel overlays.

The hydrogels do allow gaseous diffusion to occur and can therefore be used as overlays on membranes to extend their fouling free lifetime. Espada-Torre and Meyerhoff (1995) suggested that hydrogel overlays would be useful as antifouling protection on the membranes of intra-arterial ion-selective electrodes. Wisniewski and Reichert (2000) suggested that they were an attractive option for biosensor membrane protection due to their biocompatibility. The response time is slowed down and this could be accounted for as the instrument could be calibrated to account for this.

6.3 Microscopic Study of Gas Membranes

6.3.1 Methods

Scanning electron microscopy (SEM) and atomic force microscopy (AFM) were used to study the morphology of each of the membranes used in the gas diffusion experiments. These techniques offer different ways of examining the physical structure of the membranes and are able to show detail at micro and nanometer levels. The instruments used were a Cambridge S360 analytical SEM (Cambridge Instruments, Cambridge, UK) and a Veeco Explorer Atomic Force Microscope (Topometrix). For the SEM the membranes were prepared with vacuum deposition of a thin layer of gold. The membrane samples required no preparation for the AFM where a 100micron scanning head and silicon nitride contact scanning probes were used.

6.3.2 Results and Discussion

SEM

The SEM images of the 3 PTFE tapes and ABB membrane showed their pore structure very clearly. Figures 6.7 to 6.14 shows these four membranes.
The image of each pair at two magnifications 1.27 and 7.28K respectively. The second shows the detail of the pore structure. The ABB membrane (made by Gore-Tex®) has a different structure to the PTFE tape (Gore-Tex®), as the pores are not predominately extended in one direction i.e. long thin ladder like pores. The SEM images of the YSI membranes and the Rank membrane did not show any visible structure and for this reason they are not shown. Variations in the structure are a result of the manufacturing process. Expanded PTFE is a result of thin sheets of PTFE being stretched while warm and this causes a break up on the micro-scale while remaining coherent on the macro-scale. As a result the amount of stretching causes the variations in structure.

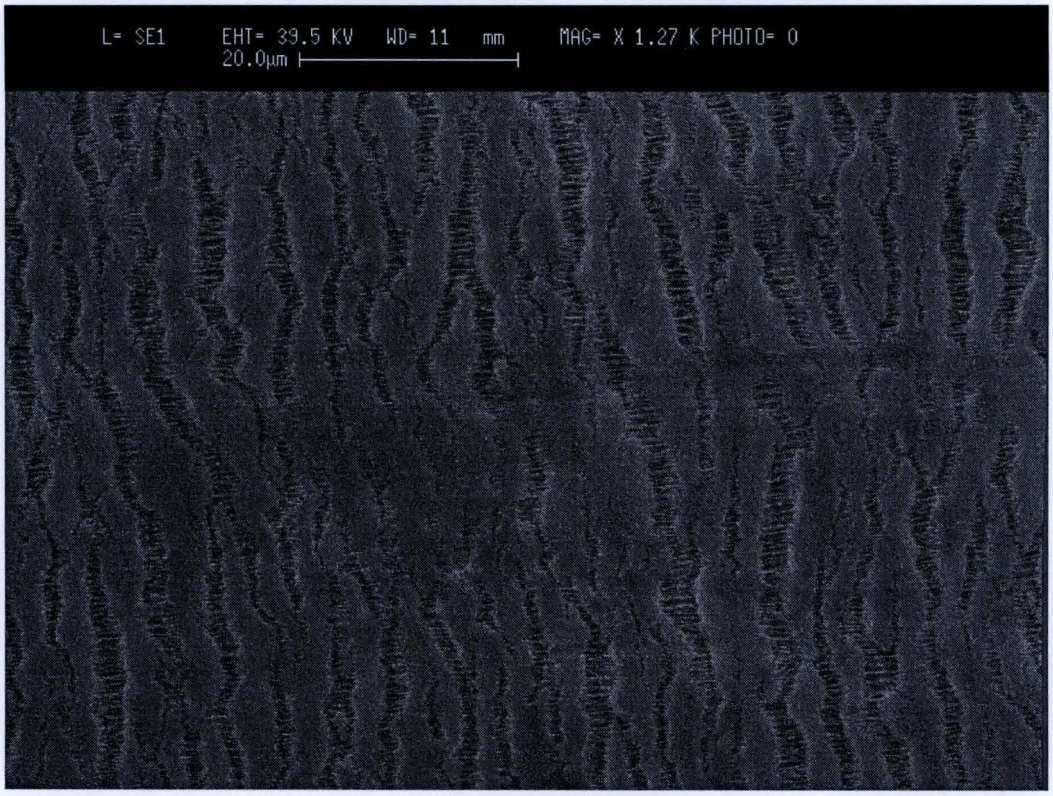

Figure 6.7 SEM image of PTFE tape (Gore-Tex®) showing the pore structure.

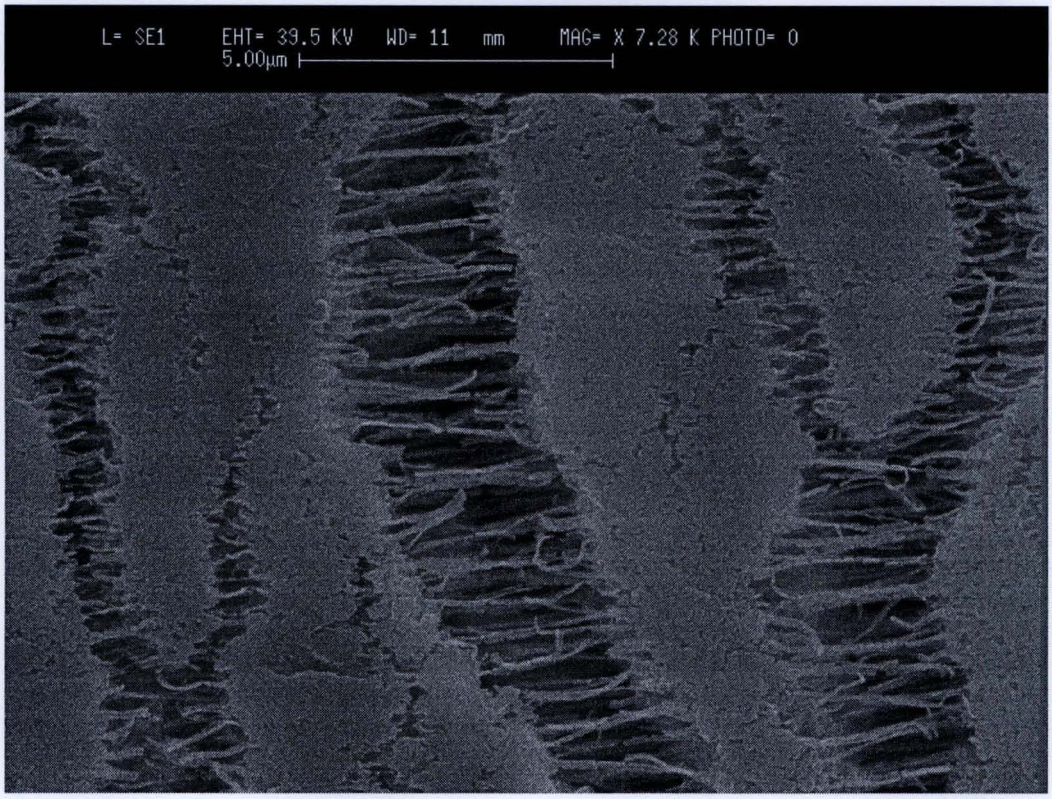

Figure 6.8 SEM image of PTFE tape (Gore-Tex®) showing the structure within the pores.

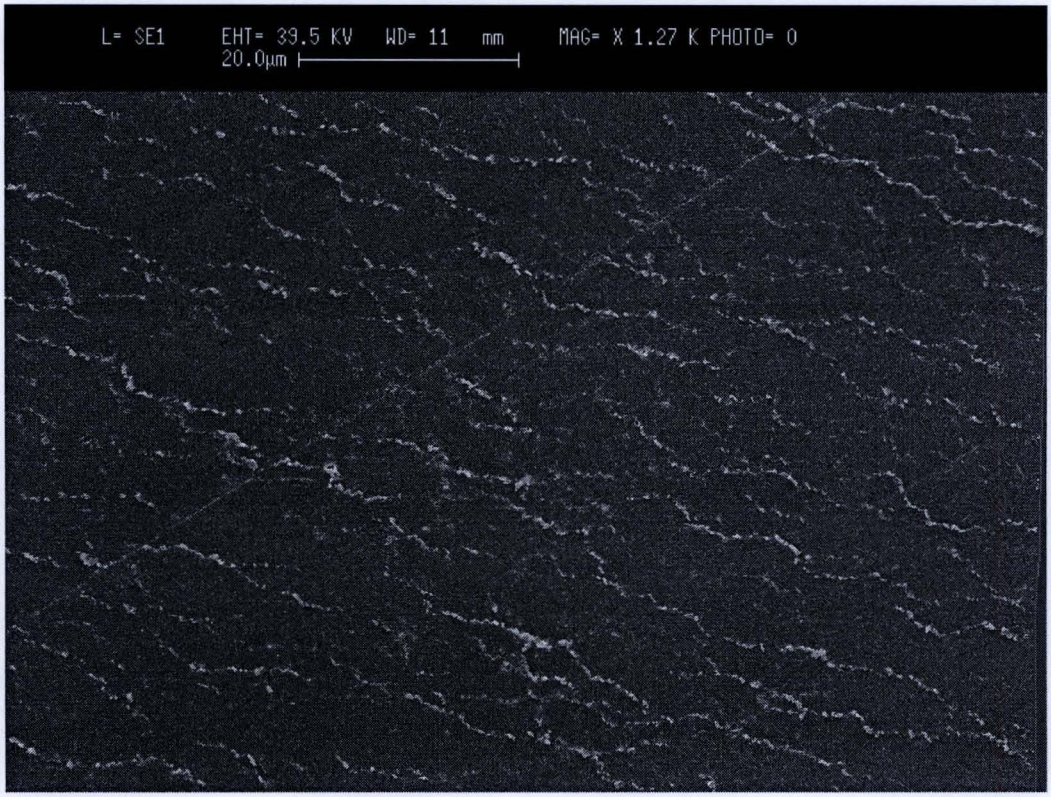

Figure 6.9 SEM image of PTFE tape (Fisher);

Figure 6.10 SEM image of PTFE tape (Fisher) showing detail

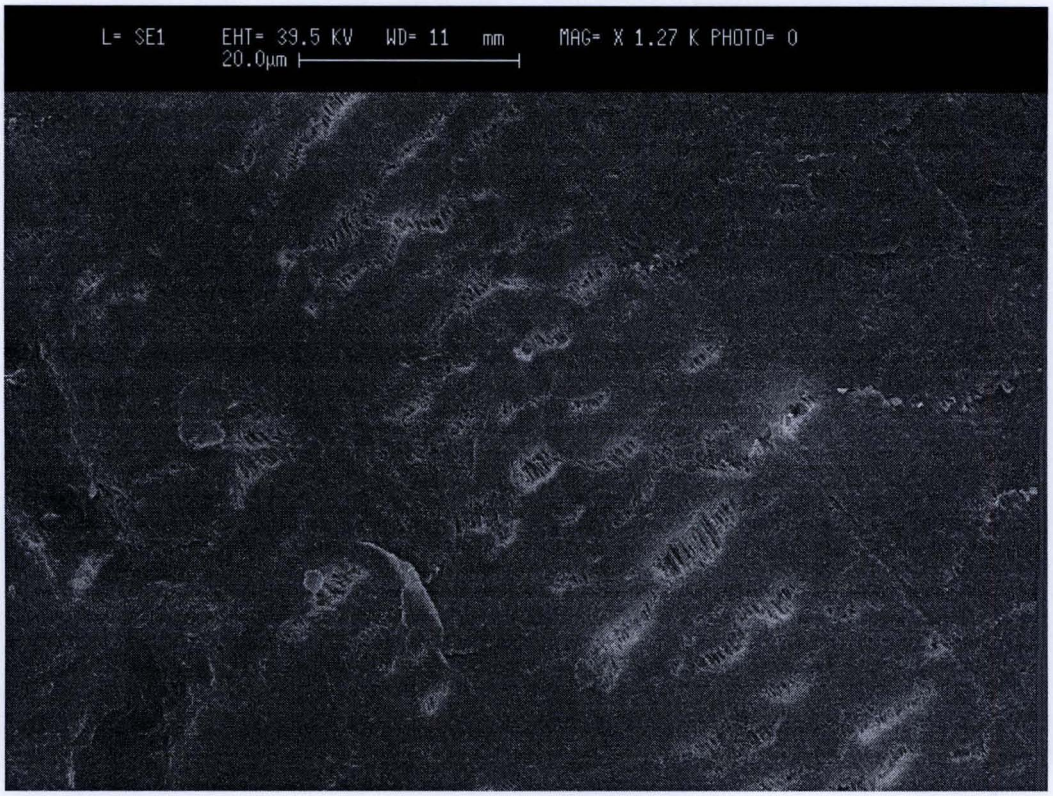

Figure 6.11 SEM image of TFE1 tape

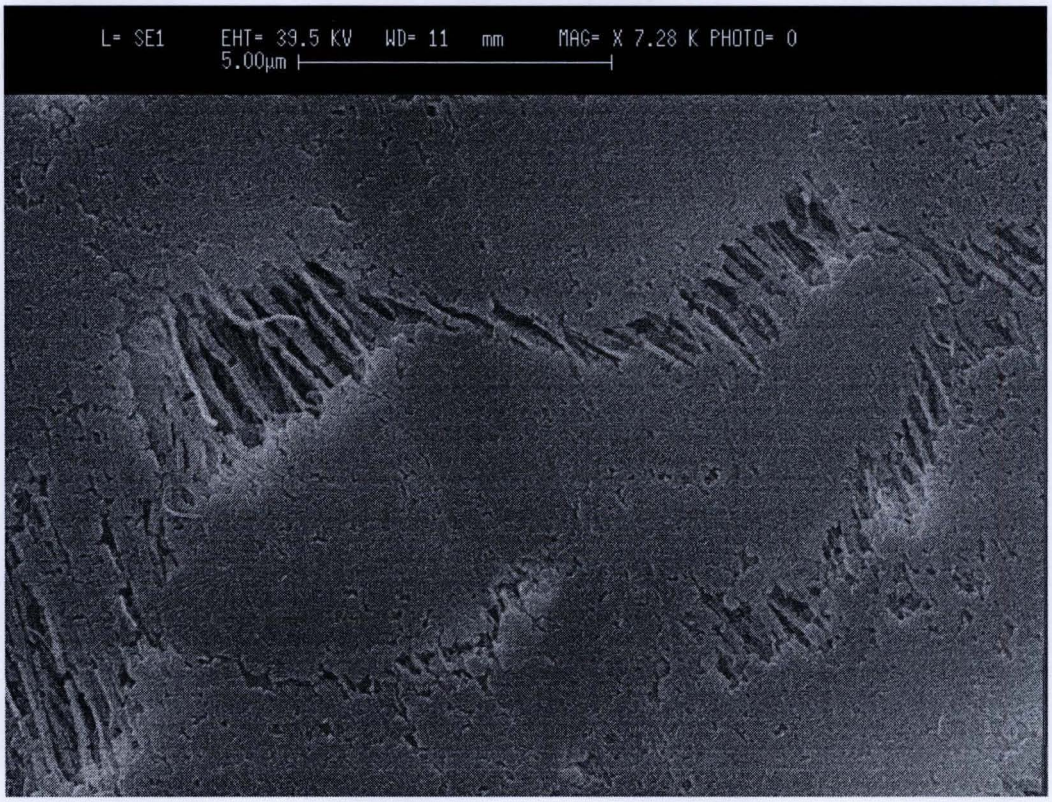

Figure 6.12 SEM images of TFE1 tape showing the structure within the pores.

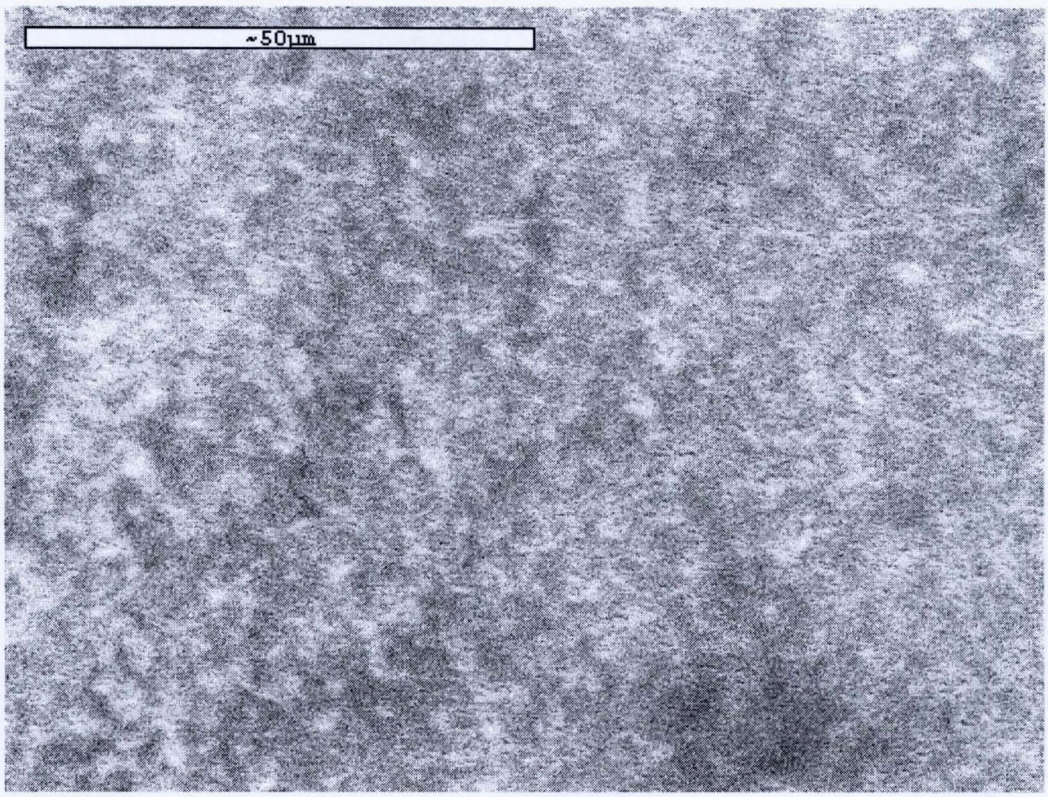

Figure 6.13 SEM image of ABB membrane

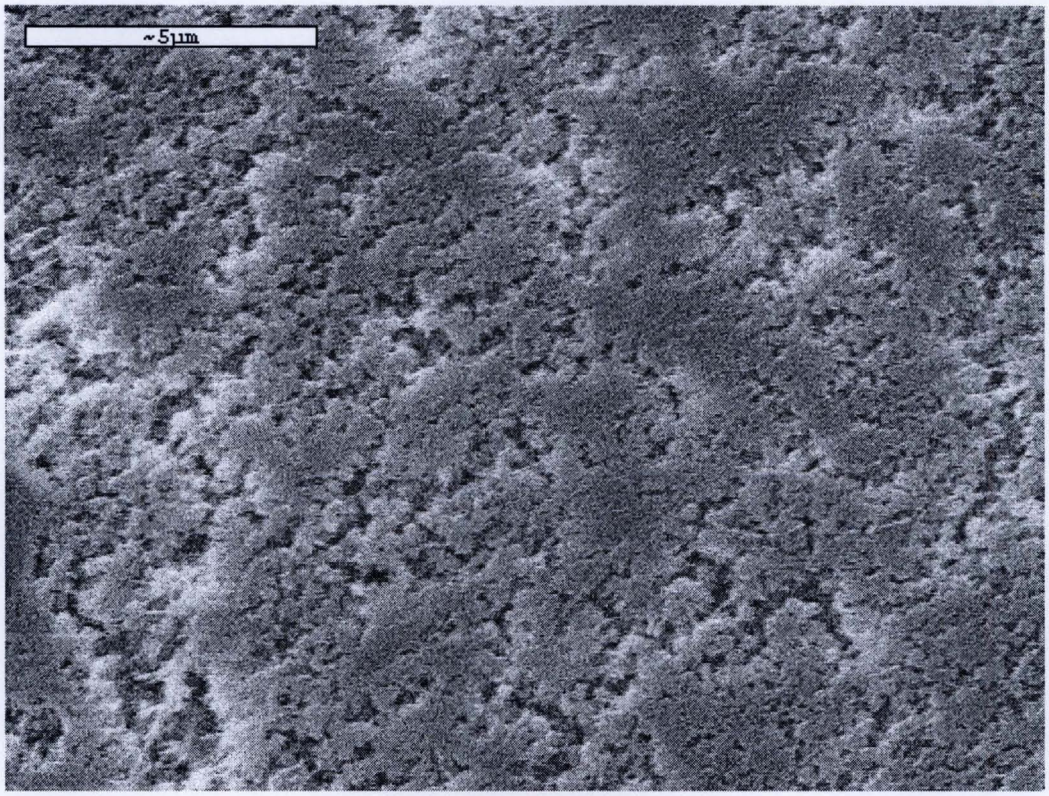

Figure 6.14 SEM image of ABB membrane showing the pore structure

AFM

The AFM images showed structure in all of the membranes examined. Both the YSI high sensitivity and the Rank membrane images showed very clear pore definition. The images of the YSI standard membrane were slightly less clear but the presence of pores can be seen. Figure 6.15 shows the pore arrangement of YSI high sensitivity. The pores are even in arrangement. Figures 6.16 and 6.17 show the Rank membrane, again the arrangement is reproduced across the membrane. Figures 6.18-6.19 show the YSI standard membrane which has a fairly even pore distribution. Figures 6.20-6.21 show the HDPE membrane; it appears to have a 'stringy' structure. Figures 6.22-6.23 show the ABB membrane.

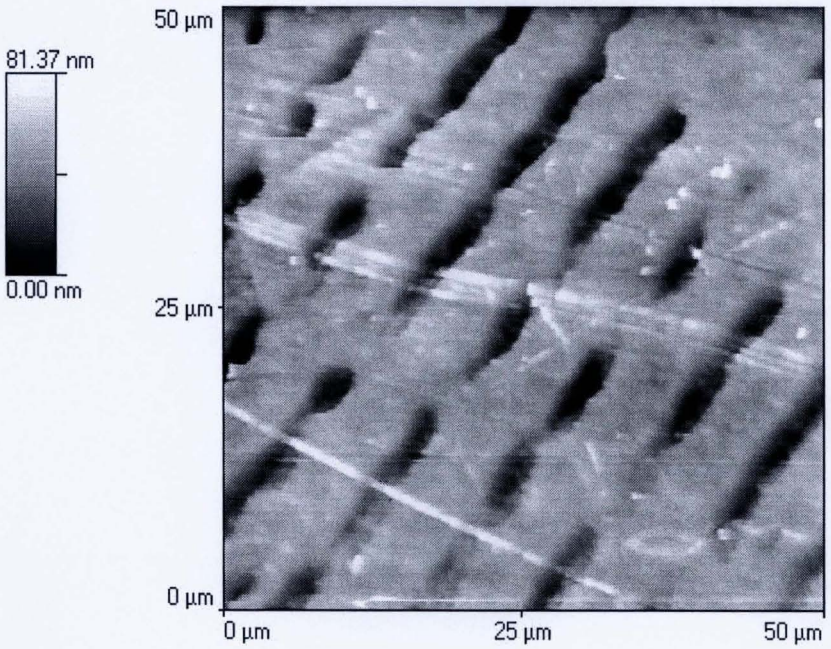

Figure 6.15 AFM image of the YSI high sensitivity membrane showing the pore arrangement.

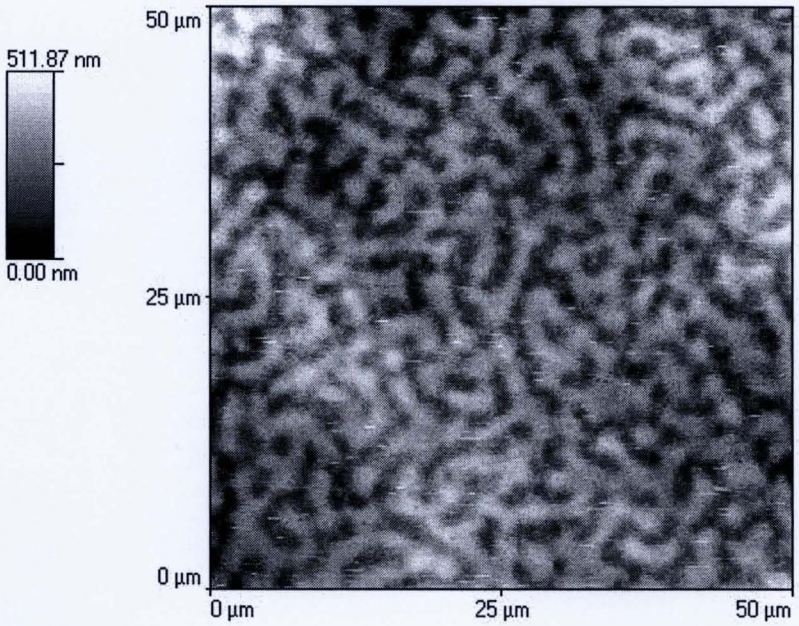

Figure 6.16 AFM image of the Rank membrane showing the pore arrangement over an area of 50 x 50µm.

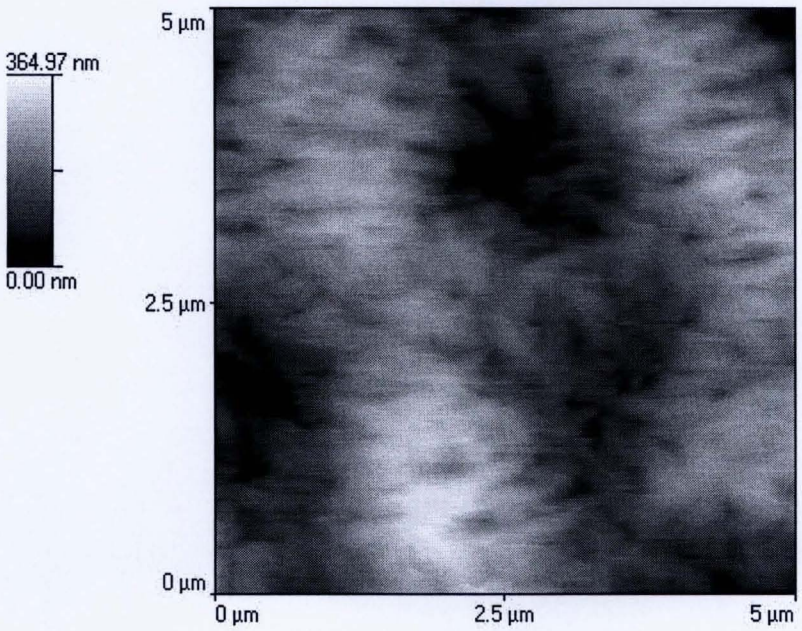

Figure 6.17 AFM image of the Rank membrane showing the in detail pores over an area of 5 x 5µm.

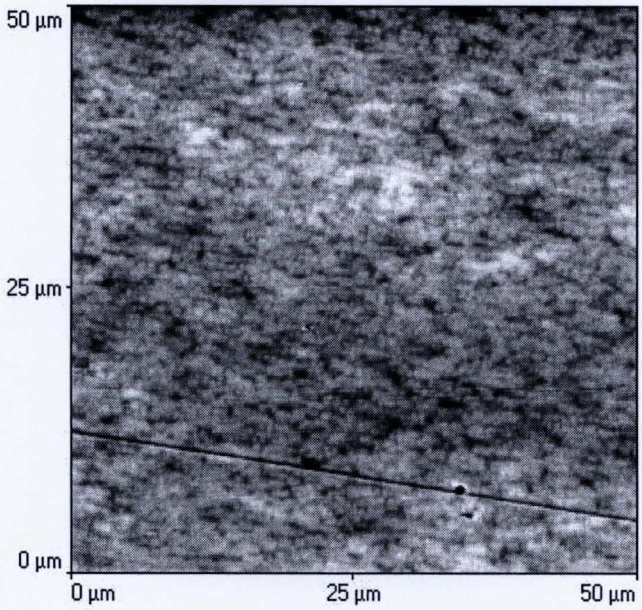

Figure 6.18 AFM image of the YSI standard membrane where the darker area indicates the pores.

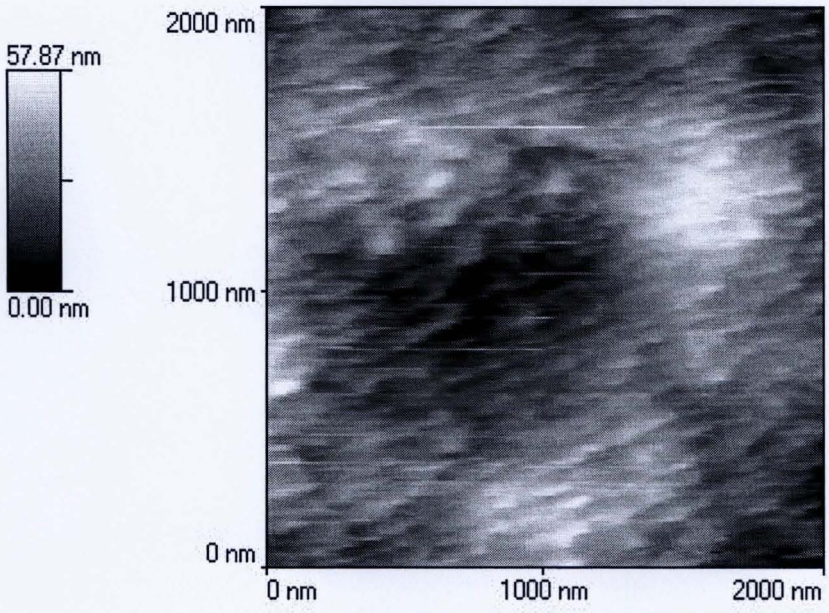

Figure 6.19 AFM image of the YSI standard membrane showing detail of a pore.

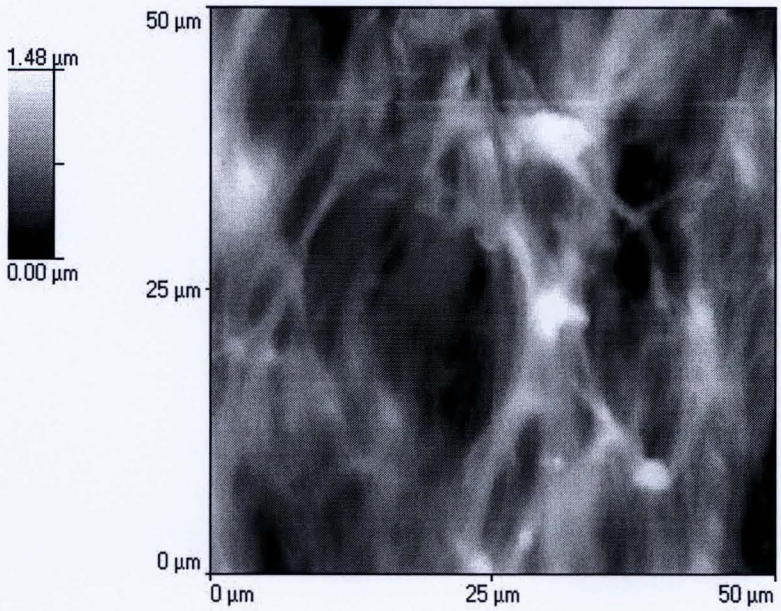

Figure 6.20 AFM image of the HDPE membrane showing the pore arrangement.

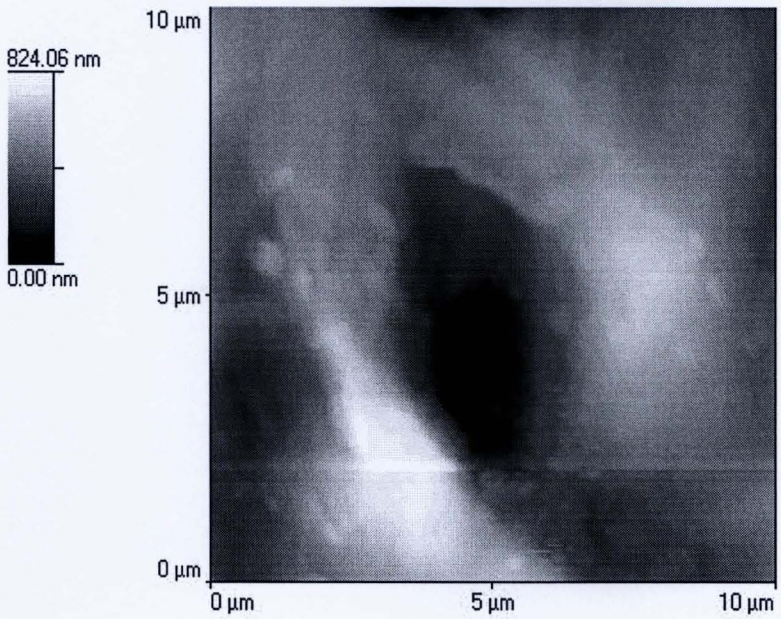

Figure 6.21 AFM image of the HDPE membrane showing a pore.

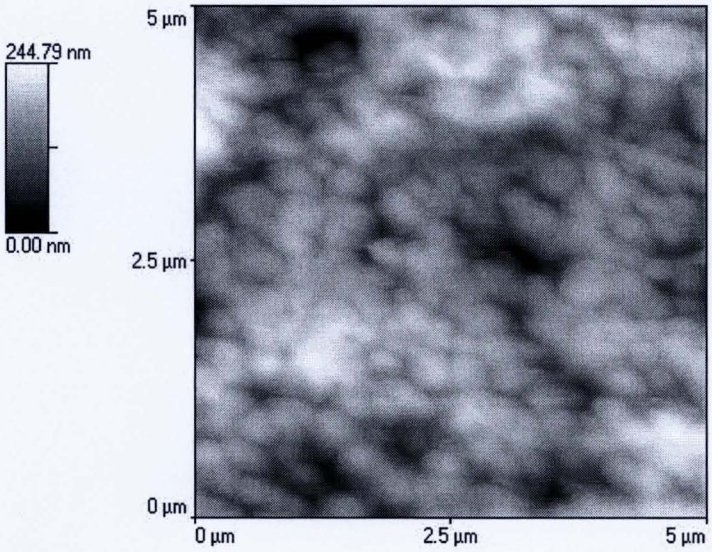

File: 6bptfe
2nd location PTFE
25/11/04

Figure 6.22 AFM image of the ABB membrane showing the pore arrangement.

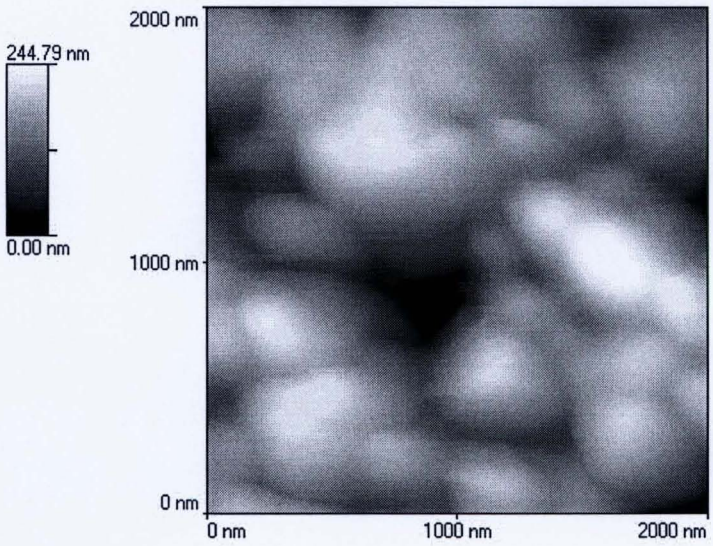

File: a12ptfe
as a11ptfe,
diff settings

Figure 6.23 AFM image of the ABB membrane showing a pore

Table 6.6 shows the pore size and shape found in the membranes.

Membrane	Pore size	Comments
Gore-Tex® tape	Width 1-3μm; length up to 20μm	Elongated pores
PTFE tape	Width 100nm; length 0.5-1μm	Elongated pores
TFE tape	Width 1-2μm; length up to 10μm	Elongated pores
ABB membrane	Width about 500nm	Circular pores
YSI standard	Width 0.5-1μm	Circular pores
YSI high sensitivity	Width 1-2μm; length up to 20μm	Elongated pores
Rank membrane	Width 0.5-1μm; length 1-20μm	Elongated pores
HDPE	Width 4-5μm	Circular pores

Table 6.6 The pore sizes measured from the AFM and SEM images.

The Gore-Tex® tape showed fairly uniform pore formation, the pores having a high aspect ratio, 1:20. Within each pore there were lateral threads giving the pores a ladder-like appearance. The TFE tape had long elongated pores that were about 10μm in length. The PTFE tape also had elongated pores but these pores were much smaller than the previous two materials at around 100nm in width and 0.5-1μm. The ABB membrane had more circular pores that were relatively small at around 500nm. Tarsiche at al. (1997) found that the PTFE tapes they examined to have sparse pores with diameters of 2-8μm. The YSI Standard membrane had pores that were circular in shape whereas the YSI High Sensitivity pores were elongated and were sometimes up

to 20μm in length. The Rank membrane had elongated pores that appeared to be interconnected. The HDPE membrane pores were circular in shape and around 4-5μm in size. This membrane had a stringy appearance.

Some of the AFM images showed very clearly defined pores and it was possible using software to calculate pore areas. The pore area is highlighted in blue. The pore area for the YSI high sensitivity membrane (figure 6.24) had a pore area of 8% while the Gore-Tex® tape had an area of 13% (figure 6.25). As it was not possible to apply the software to all of the images (due to lack of a clear pore boundary) it is not possible to make direct comparisons of pore area between all of the membranes tested.

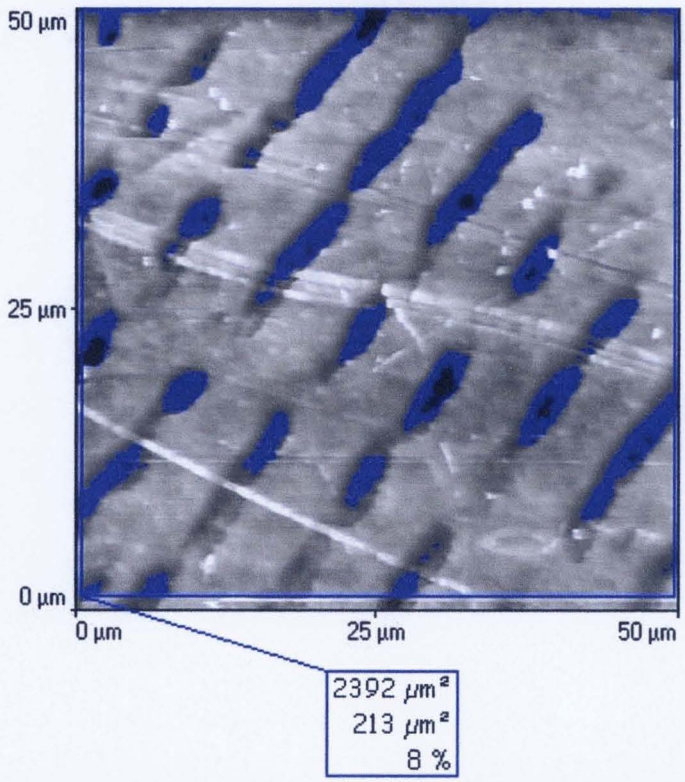

Figure 6.24 YSI high sensitivity membrane. The pore area is highlighted in blue. The percentage of pores is 8%

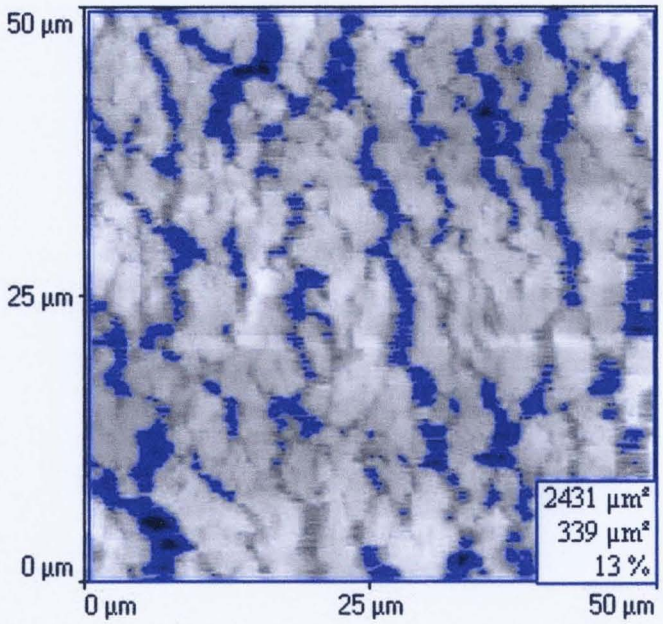

Figure 6.25 PTFE tape (Gore-Tex®) the pore area is highlighted in blue. The percentage of pores is 13%.

Three dimensional images of the membranes were also taken using AFM. These show how the surface of each membrane is arranged. Figure 6.26-6.33 shows the variation between the membranes when viewed in this manner. All are shown as 50 x 50µm areas.

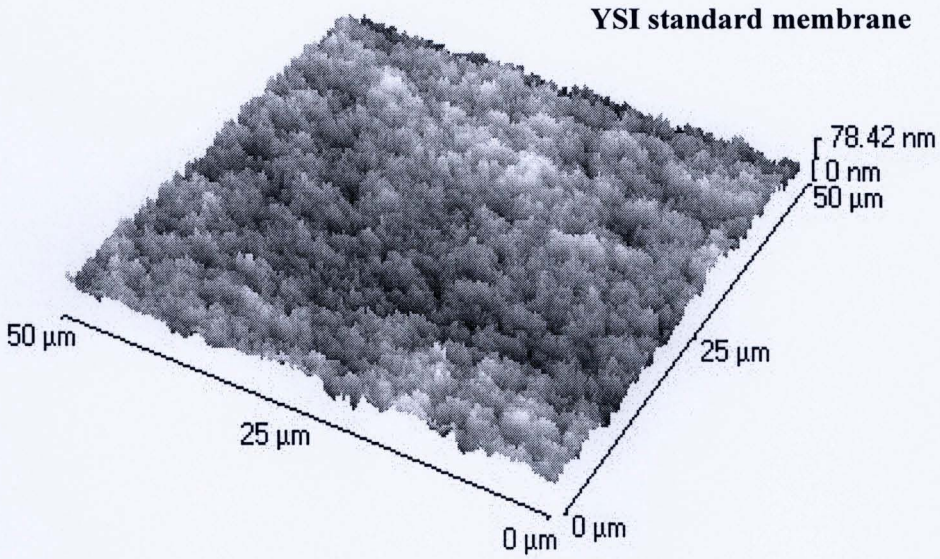

Figure 6.26 Three-dimensional AFM image of YSI standard membrane.

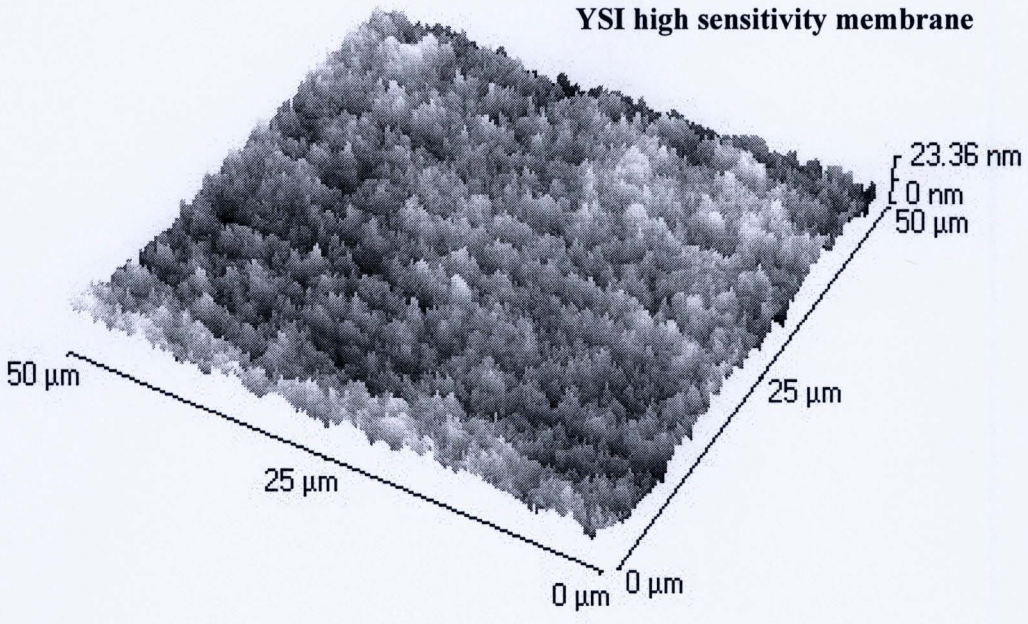

Figure 6.27 Three-dimensional AFM image of YSI high sensitivity membrane.

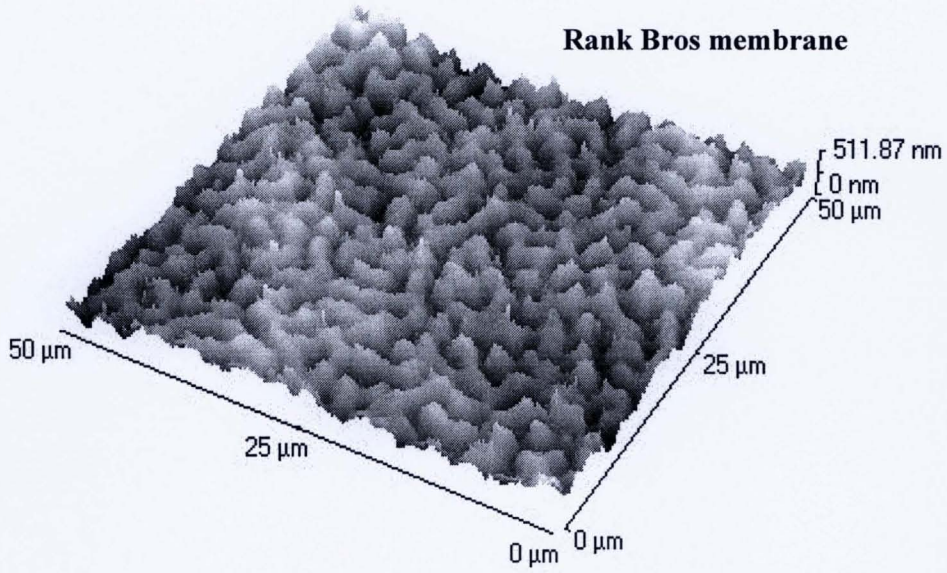

Figure 6.28 Three-dimensional AFM image of Rank Bros. membrane.

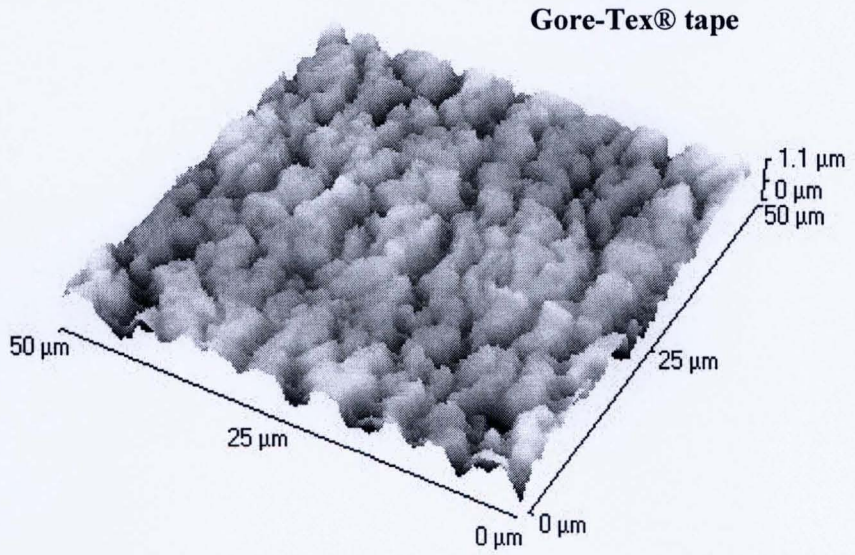

Figure 6.29 Three-dimensional AFM image of Gore-Tex® tape.

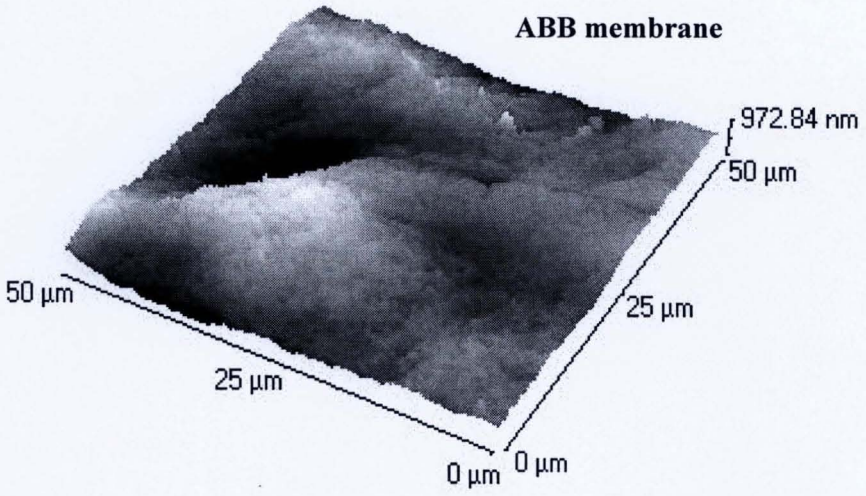

Figure 6.30 Three-dimensional AFM image of ABB membrane (Gore-Tex®).

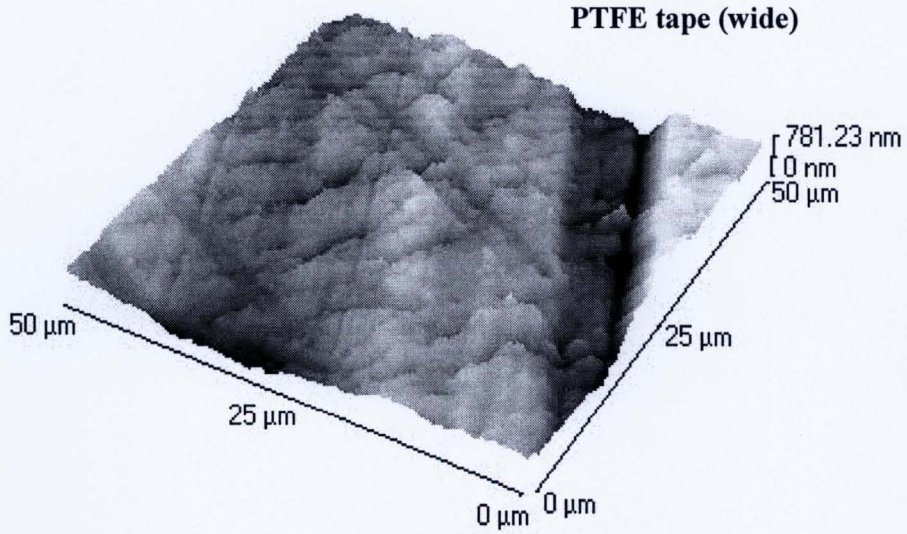

Figure 6.31 Three-dimensional AFM image of PTFE tape (wide).

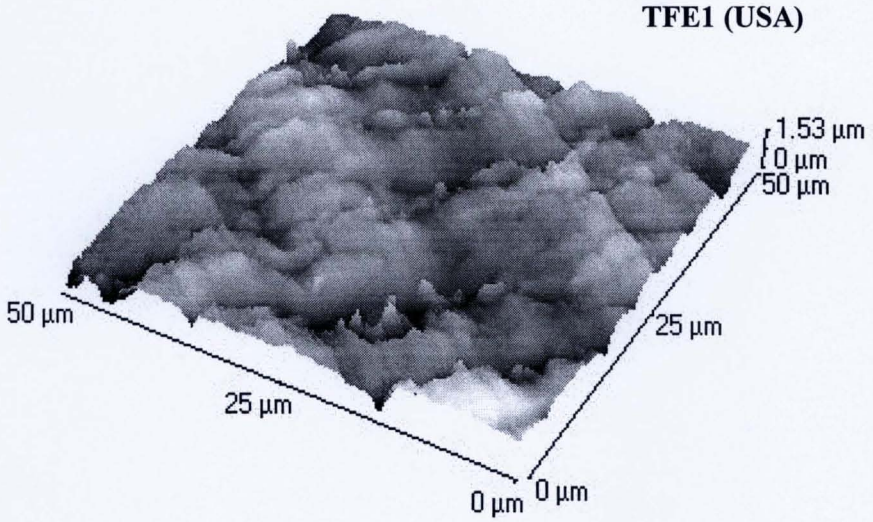

Figure 6.32 Three-dimensional AFM image of TFE1 (USA) tape.

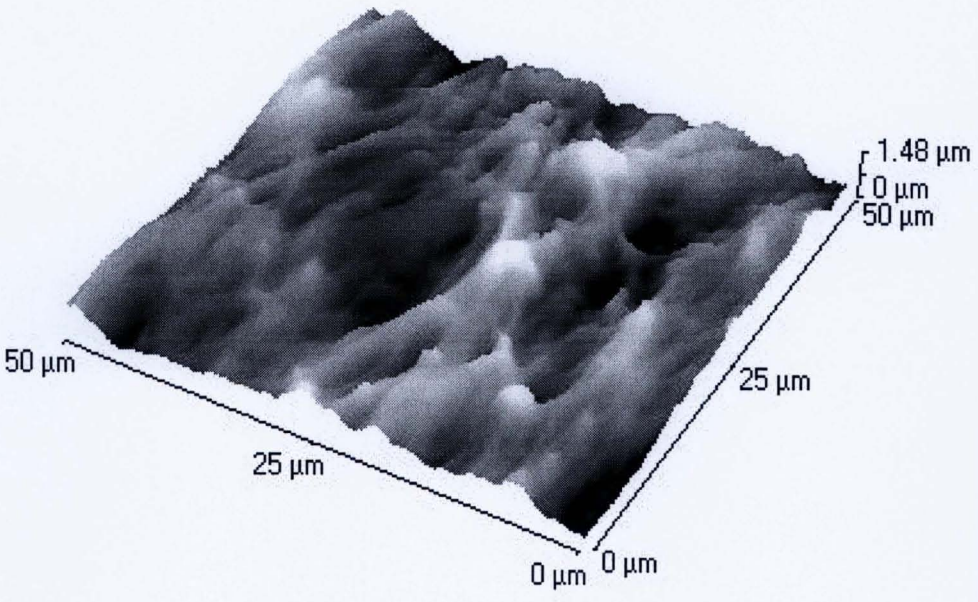

Figure 6.33 Three-dimensional AFM image of high density polyethylene.

When viewing the three-dimensional images showing an area of 50 x 50μm (figures 6.26-6.33) the maximum surface roughness is given. These are listed in table 6.7, as well as the maximum roughness measured at 20 x20μm and 100 x 100μm. The larger the area viewed the greater the variation in roughness, demonstrating that it is crucial to quote the area viewed in any comparative studies. The membrane with the lowest surface roughness was the YSI high sensitivity closely followed by the YSI standard membrane. The PTFE tapes and ABB membrane were much rougher than the YSI and Rank Bros membranes. When viewing a 50 x 50μm area the sequence of membranes in order of increasing roughness is YSI high sensitivity < YSI standard membrane < Rank Bros < PTFE wide tape < ABB membrane < PTFE tape < HDPE < TFE 1.

Membrane	**20 x 20μm**	**50 x 50μm**	**100 x100μm**
	Area Roughness (measurements in nm)		
YSI standard membrane	69.82	78.42	353.7
YSI high sensitivity	20.95	23.36	283.9
Rank membrane	370.5	511.8	558.6
ABB membrane	513.07	972.8	1670
PTFE tape	1008	1100	1480
TFE1	947.3	1530	1980
PTFE wide tape	466.1	781.2	802.2
HDPE	951.9	1480	1520

Table 6.7 Maximum roughness of each membrane. Measurements taken within areas of 20 x 20, 50 x 50 and 100x 100μm.

Each of the PTFE membranes exhibited different structures when studied microscopically. Although the tapes had similar structures the pore size and regularity varied. This was also found by Tarsiche and Ciurchea (1997) who used SEM to study the structure of a variety of PTFE tapes. They found a structure very similar to the Gore-Tex tape in Nemous tape made by Du Pont. Huang et al. (2004) looked at the effects of stretching PTFE sheeting made by a process of extrusion, rolling and stretching. As the material was stretched the fibrils became longer and thus the pore size increased. The ABB membrane (Gore-Tex®) had a very different structure to the Gore-Tex® tape despite appearing visually very similar. This can be attributed to the amount of stretching that was carried out in the manufacturing process. From the SEM images the pore size is smaller than in the PTFE tapes indicating that less stretching has taken place (Huang et al. 2004). The YSI standard and YSI high sensitivity membranes were very different from each other and as the high sensitivity membrane was designed to be used in areas where there are low levels of dissolved gases it was expected that its pore size would be larger and it would be thinner. The Rank membrane was similar in pore size to the YSI high sensitivity membrane, but exhibited more variation in pore length. The Rank membrane was the thinnest of the membranes tested at 0.02mm.

6.4 Gas Membranes - Surface Energy

6.4.1 Methods

Contact Angle Measurements on Gas Membranes

The adhering gas bubble was measured using the dynamic bubble technique as described in chapter 5, section 5.8.1. The gas membranes were held in place by attaching each one to a glass slide that was held in a PMMA holder made for the purpose. The membranes were soaked for three days in artificial seawater (Instant Ocean) at ambient temperature prior to testing.

Measurement of Surface Tension

A small study was undertaken using the Cam200 (KSV Instruments Ltd, Helsinki, Finland). Using a series of homologous liquids of known differing surface tensions, a graph was produced of cos θ versus γ (surface tension). The data forms a line which approaches cos θ=1 at a given value of γ, i.e. 0° perfect wetting. This is the maximum surface tension of a liquid which may completely wet a solid. The plot obtained is known as a Zisman plot.

Gore-Tex® tape and YSI standard membrane were tested 'as is' (air) and after 3 days soaking in synthetic seawater (Instant Ocean).

6.4.2 Results and Discussion

Figure 6.34 shows the contact angles of the gas membranes tested. Both the YSI standard and high sensitivity membranes gave contact angles of 70.2°±1.08 and 71.7°±0.6 and were the lowest of the materials measured. Interestingly the PTFE wide tape had a lower angle than all of the other similar tapes measured, with a value of 72. 2°±0.2. The remainder of the membranes gave contact angles ranging from 77.8° (Rank Bros membrane) to 82.4° (HDPE). There was no significant difference in the contact angle measured between TFE1and Gore-Tex® tapes or the ABB membrane.

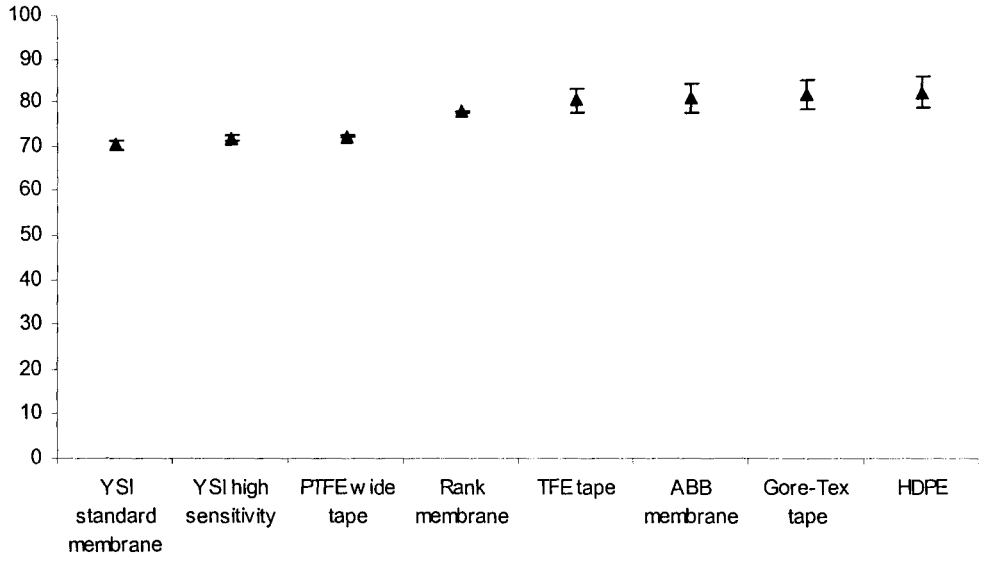

Figure 6.34 Contact angles measured on gas membranes after 3 days soaking in seawater.

This result shows that all of the membranes tested were hydrophobic in character.

The surface tension increased for both membranes tested after they had been soaked in the synthetic seawater. Table 6.8 show the values obtained for each membrane.

Membrane	**Air (mNm^{-1})**	**Seawater (mNm^{-1})**
Gore-Tex® tape	20.83	37.76
YSI standard membrane	18.89	34.96

Table 6.8 Surface tension of membranes.

From these results it is obvious that both of the polymer materials tested reorganised their surface chemistry when they are moved from air into a polar medium such as seawater. This was only a small study, as access to the instrument was limited, but it illustrated the dramatic effect the medium to which a membrane is subject can alter

its'surface properties. Silver et al. (1999) stated that multiphase materials such as polyurethanes may show surface reorientation between the dry and hydrated states making it difficult to evaluate the surface composition using methods in which the polymer surface is analysed in air or in vacuo. It would therefore be necessary to measure surface tension of gas membranes after exposure to fresh or seawater to correctly determine its surface energy properties.

6.5 General Summary

The variations of properties of PTFE membranes have a significant effect on the diffusion of gases through them. These differences can be attributed to the physical properties of each membrane; these being thickness; pore size and quantity of pores. In general those with larger pores have a higher surface roughness value and faster diffusion of gases as is the case for membranes with a high percentage of pores relative to the material. The membrane thickness affects the diffusion of gases as the path length will increase resulting in the time taken for the gas to reach the sensor being increased. However, these factors would have a constant time response and this could be accounted for at the initial stages of calibration of the sensor.

Chapter 7

Biofouling Resistant Coatings and Gas Membranes - Field Trials

In this chapter the results of field trials of potentially biofouling resistant hydrogels containing surfactant are reported. The release of surfactant is monitored and the samples visually inspected and photographed throughout the trials. At the conclusion of the trials the biofouling is quantified using fluorescein diacetate (3′ 6′ -diacetyl-fluorescein) hydrolysis. The application of hydrogel coatings to instrument ports is reported and the pros and cons of a variety of fixing methods used are discussed. Finally a biofouling field trial of a variety of gas membrane materials is reported. This was carried out to determine if there were any differences between the gas membranes in resisting biofouling.

7.1 Hydrogel Coatings

To assess the biofouling resistance of the hydrogel coatings field trials were carried out by deploying the test coatings in a marine environment. These deployment trials of the hydrogel coatings were carried out in the Firth of Clyde, Scotland. PMMA racks were suspended, containing the hydrogel coatings, from Keppel Pier at the University Marine Biological Station, Millport, Isle of Cumbrae, Scotland. The racks were always below the low water mark and were suspended to depths from 1-4m depending on tides. The testing took place around 30-40 m from the shoreline.

7.1.1 Methods

Preparation of Hydrogels

The hydrogel sheets were prepared as described in chapter five, section 5.1.1. They were prepared in batches of three each measuring 250 x 250 x 1mm. They were rinsed in distilled water and soaked for 2-3 days in order to remove unreacted monomer and

exchange ethylene glycol for water. They were then soaked in either 5%w/v BAC, 5%w/v Arquad 2C-75 or distilled water for three weeks prior to deployment in order to load them with each test solution.

BAC and Arquad 2C-75 Content

At the beginning of the marine deployment trials the BAC and Arquad 2C-75 contents were measured using HPLC/UV and flow injection IC detection respectively, as described in chapter five. The Arquad 2C-75 was analysed by a method developed using a flow injection system with suppressed ion-conductivity detection also described in chapter five, section 5.3.2. The Arquad 2C-75 can be quantified when it is dissolved in a solution of extremely low ion content and so quantitative analysis of hydrogels before marine exposure can be carried out and a zero time value obtained. This method involves injection of the test solution straight into a flow of solvent. At the end of the marine trials the BAC content was quantified. It was not possible to quantify Arquad 2C-75 after marine deployment as no method was found to do this effectively, due to interfering cations.

Marine Deployment Trials using Hydrogel Coatings

In order to compare the fouling resistance of hydrogels with and without active ingredients blank hydrogel, hydrogels containing BAC and Arquad 2C-75 and poly-(methylmethacrylate) PMMA coupons, for control, were exposed from the pier at UMBS Millport. From each hydrogel sheet, three rectangular test pieces were cut. The test pieces were held in place using PMMA frames with rubber spacers used to prevent the hydrogel coating from excessive pressure. They were arranged on the rack in a pseudo Latin-square formation. The exposed area of each hydrogel sample was 60mm x 80mm, sample thickness 1mm. The rack was suspended from Keppel Pier in a vertical orientation to a depth of 3 metres in the sea.
The three test racks were put out on consecutive dates (March-May 2004) in order to ensure that they were subjected to maximum fouling pressure over the high fouling spring period. The test racks were laid out randomly ensuring each test coating appeared on each row to take in to account any depth effects. At the conclusion of the trial all the racks were removed and taken to the laboratory for analysis. This resulted

in racks 1-3 being deployed for 14 weeks, 12 weeks and 11 weeks respectively. Figure 7.1 shows a typical layout.

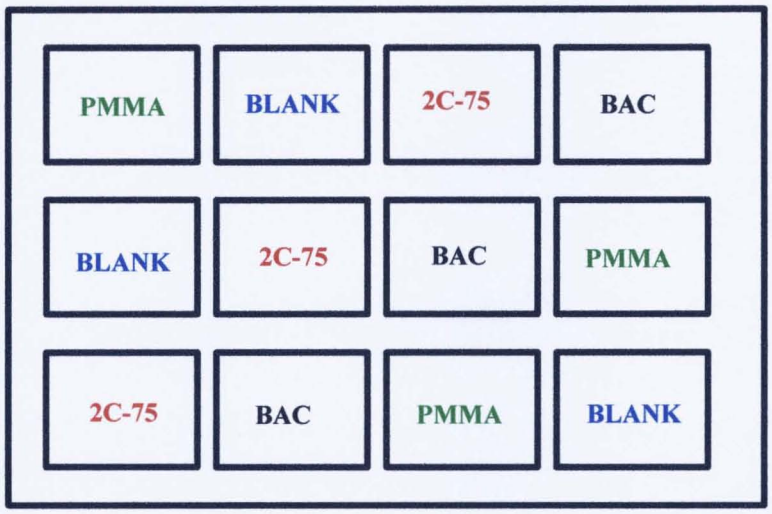

Figure 7.1 Typical rack layout of hydrogel coatings

Marine Biofilm Activity using Fluorescein Diacetate (FDA)

Fluorescein diacetate (3′ 6′ -diacetyl-fluorescein) hydrolysis was used to quantify biofilm formation. This colourless compound is hydrolysed by both free and membrane bound enzymes (Stubberfield & Shaw, 1990) releasing a coloured end product, fluorescein, which can be measured by spectrophotometry. Fluorescein diacetate (FDA) hydrolysis has been used to assess microbial activity in marine (Gumprecht et al; 1995 Poremba, 1995) and freshwater sediments (Battin, 1997), activated sludge (Fontvielle et al., 1992) as well as in pure cultures of bacteria (Schnürer & Rosswall, 1982) and algae (Gilbert et al., 1992). Only recently has this method been applied to biofilm estimation on surfaces (De Rosa et al., 1998). This work follows the development of marine biofilms on submerged, surfactant treated hydrogels using FDA hydrolysis. The advantages of the FDA method are the whole sample can be measured, the biofilm remains attached to its substrate, it can be used on opaque samples where light transmission microscopy is not useful and it measures over a wide range of biofilm thickness. The method provides a more accurate and sensitive estimation of biofilm activity and is easy and rapid to perform.

Estimation of marine biofilm activity was carried out using a modified method based on the Adam and Duncan (2000) method. Cores (25mm diameter) were cut from each hydrogel section (60 x 80 mm) and placed into individual 60 ml glass powder jars. 15 ml of 60 mM potassium phosphate buffer pH 7.6 (8.7 g K_2HPO_4 : 1.3 g KH_2PO_4 made up to 1 litre in deionised water) was added to each jar and 0.2 ml of 1000 μg fluorescein diacetate (3′6′ - diacetyl-fluorescein, Sigma-Aldrich Co. Ltd) ml^{-1} acetone solution added to start the reaction. One jar from each treatment was retained as a blank without the addition of the FDA substrate. The lids were replaced on the jars and the jars then placed in an orbital incubator (Gallenkamp orbital incubator, 100 rev min^{-1}) at 10 °C ± 1 °C for 1 hour. The following steps involving chloroform/methanol were carried out in a fume cupboard. Once removed from the incubator, the 25 mm diameter cores were taken out of the buffer/FDA solution and 15 ml of chloroform/methanol (2:1 v/v) added immediately to the buffer/FDA to terminate the hydrolysis reaction. The lids were replaced on the jars and the contents shaken thoroughly by hand. The contents of each jar were filtered (Whatman, No. 2) into 100 ml conical flasks and the filtrates measured at 490 nm on a spectrophotometer (Shimadzu UV-2101PC). The blank from each treatment was used to zero the spectrophotometer before reading the sample absorbance.
The concentration of fluorescein released during the assay was calculated using the calibration graph produced from 0-5 μg fluorescein ml^{-1} standards which were prepared from a 20 μg fluorescein (fluorescein sodium salt, Merck-BDH, Analar) ml^{-1} standard solution by appropriate dilution in 60 mM potassium phosphate buffer pH 7.6.

7.1.2 Results and Discussion

Surfactant Content in Hydrogels

Figures 7.2 shows the values of surfactant found for each hydrogel at the beginning of each marine deployment trial. There was no significant difference between the values found in each of the hydrogels. The zero time content of BAC was approximately 5%w/w (4.67 ± 0.24) and the Arquad 2C-75 approximately 1% (0.87 ± 0.20). Hence

the Arquad 2C-75 content was approximately 20% of the BAC content at the beginning of the deployment trials.

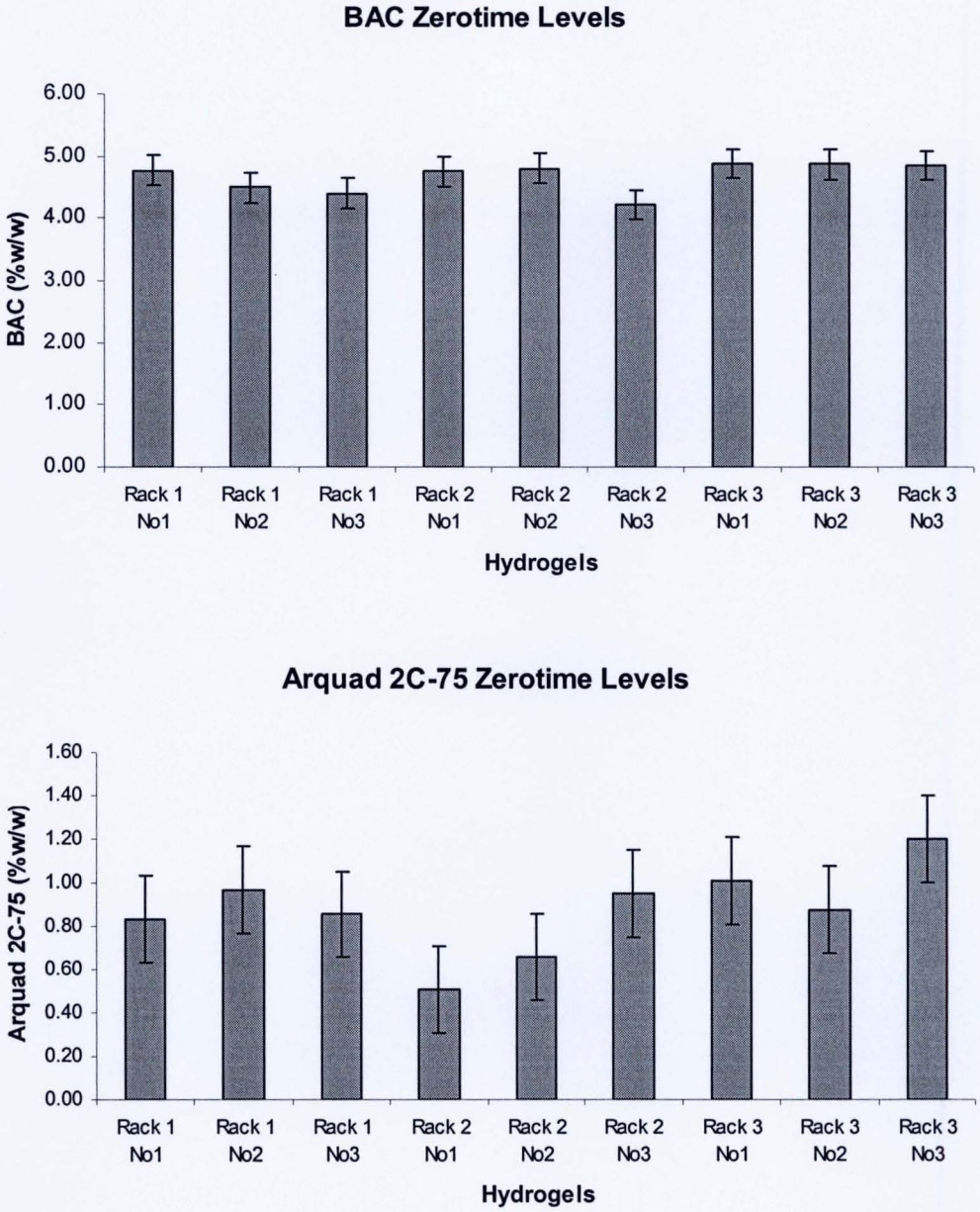

Figure 7.2 Zerotime content of BAC and Arquad 2C-75 in each of the hydrogels used for racks 1-3.

Benzalkonium Chloride Release

At the conclusion of the trials the hydrogel samples containing BAC were analysed.

Figure 7.3 shows that the BAC levels in the coatings had dropped to around 2%w/w for both racks 1 and 2 with no significant difference between them. Rack 3 had dropped to 2.7%w/w BAC and was significantly higher than that found in racks 1 and 2. Previous work had shown that BAC released from the hydrogel resulting in the eventual fouling of the coating (Smith et al. 2002).

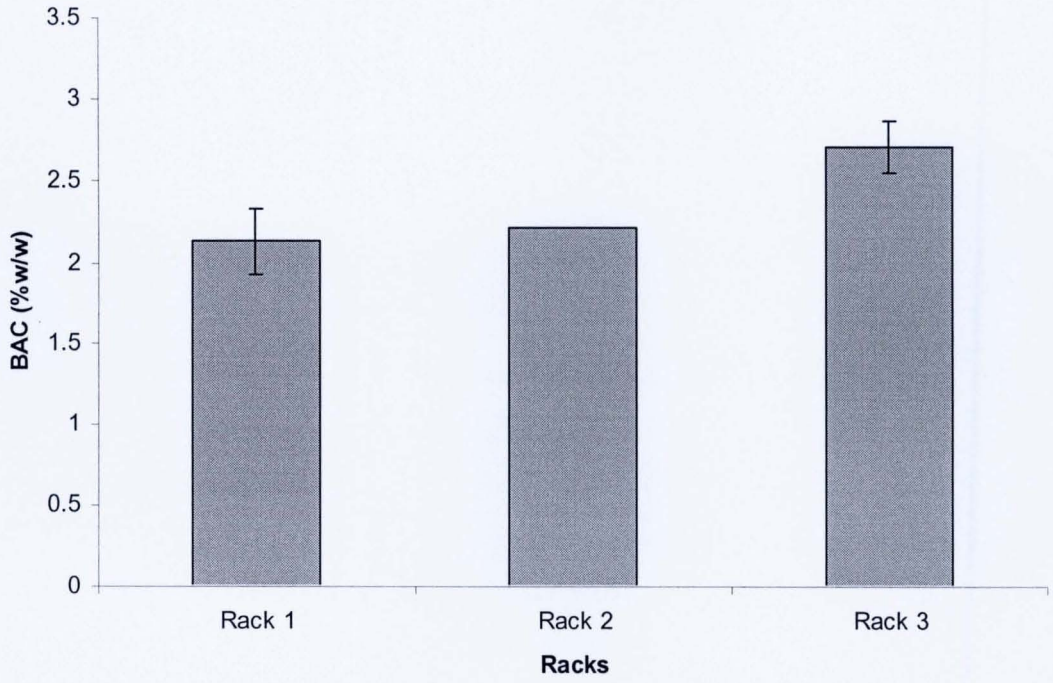

Figure 7.3 BAC content in coatings after 14, 12 and 11 weeks marine deployment respectively.

Marine Deployment Trials

Figure 7.4 shows the precise layout of each rack to make it clear which coating was in each position. The racks were visually inspected and photographed at various time points through out the deployment period.

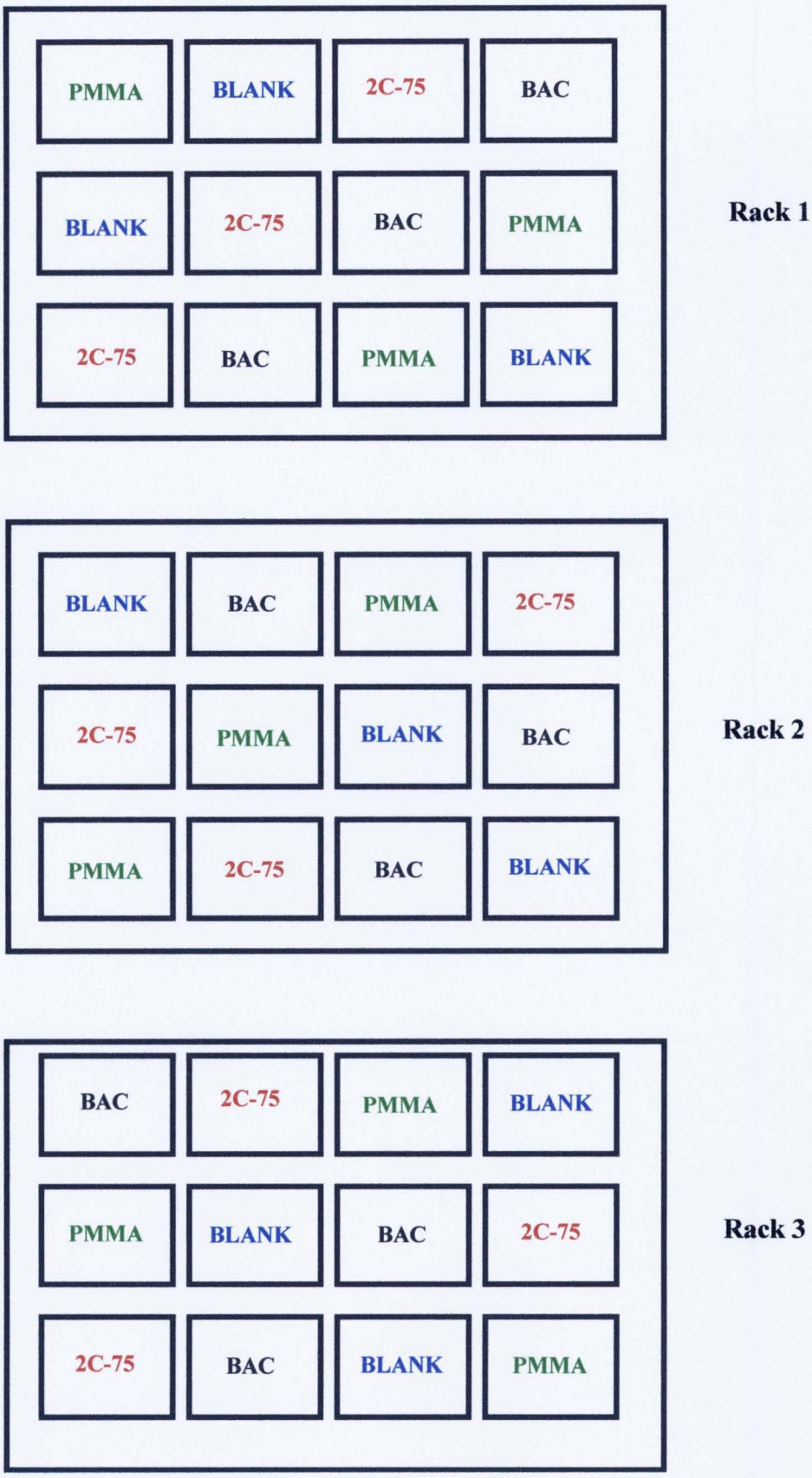

Figure 7.4 The layout of racks 1-3.

Figures 7.5 and 7.6 shows rack 1 at 10 weeks and then at 14 weeks at the end of the marine deployment trial. At 10 weeks both the blank hydrogel and the PMMA coupons are heavily fouled. The rack itself is fouled with brown algae and barnacles. The hydrogels containing the BAC look fairly clean. However, when viewed closely there is evidence of a biofilm on them and the beginning of algal growth. Figure 7.7 shows the hydrogel/BAC and hydrogel/Arquad 2C-75 samples in close up at 10 weeks. The hydrogel/Arquad 2C-75 sample is visibly clean and transparent while the edges of the frame are heavily fouled there is no real fouling encroachment onto the sample. The hydrogel/BAC sample has some evidence of algal fouling although it is still very light relative to the fouling on the blank and PMMA samples. At 14 weeks (figure 7.8) the same two samples show that the hydrogel/BAC is now fouled with brown algae whereas the hydrogel/Arquad 2C-75 sample is still clean despite the fact that the edges of the frames are now heavily fouled and the fouling is trying to encroach onto the sample. A white background is placed behind each rack in order to show any fouling on the samples more clearly. The sample labelling (placed behind the rack) helps show the level of transparency still exhibited by the hydrogel/Arquad 2C-75 at 14 weeks.

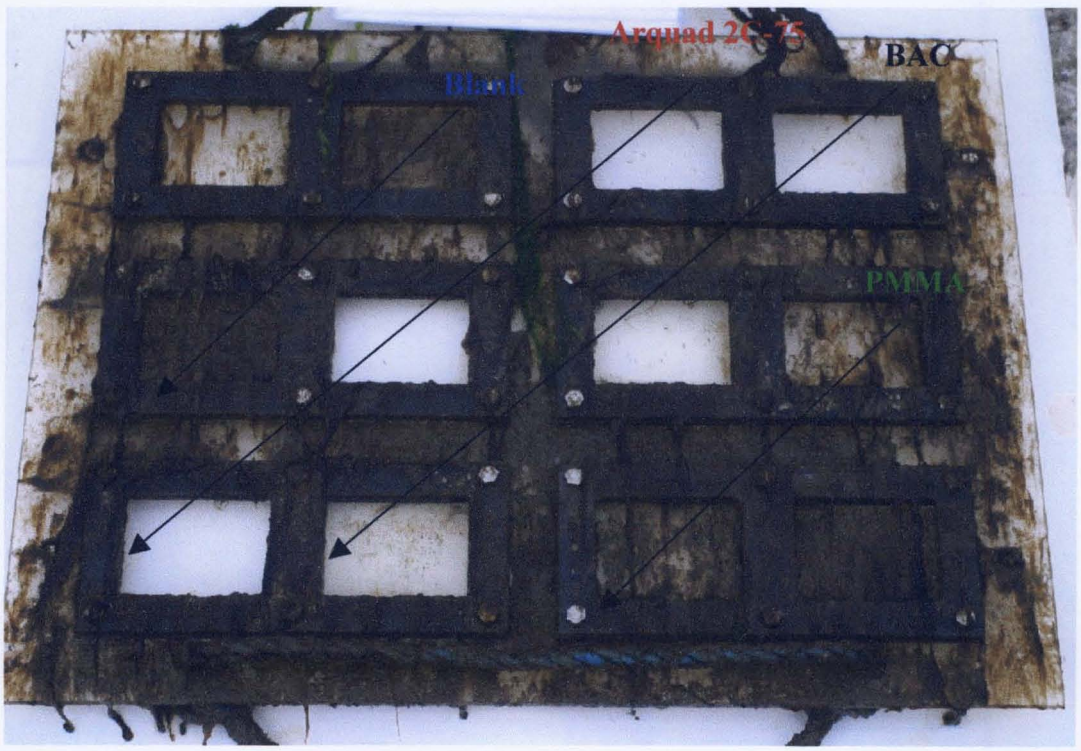

Figure 7.5 Rack 1 at 10 weeks marine deployment.

Figure 7.6 Rack 1 at 14 weeks marine deployment.

Figure 7.7 The hydrogel/Arquad 2C-75 and hydrogel/BAC coatings after 10 weeks marine deployment.

Figure 7.8 The hydrogel/Arquad 2C-75 and hydrogel/BAC coatings after 14 weeks marine deployment.

Figures 7.9 and 7.10 show rack 2 at the 8 and 12 week time points. Again the blank hydrogel and PMMA samples are heavily fouled with brown algae and some barnacles. At 8 weeks the hydrogel/BAC and the hydrogel/Arqaud 2C-75 samples are visibly clean. At 12 weeks there is more evidence of fouling on the hydrogel/BAC samples than on the hydrogel/Arquad 2C-75 samples. From the 8 to 12 week time point it is evident from looking at the fouling on the rack that there has been considerable fouling growth over the 4 week period from 8 weeks.

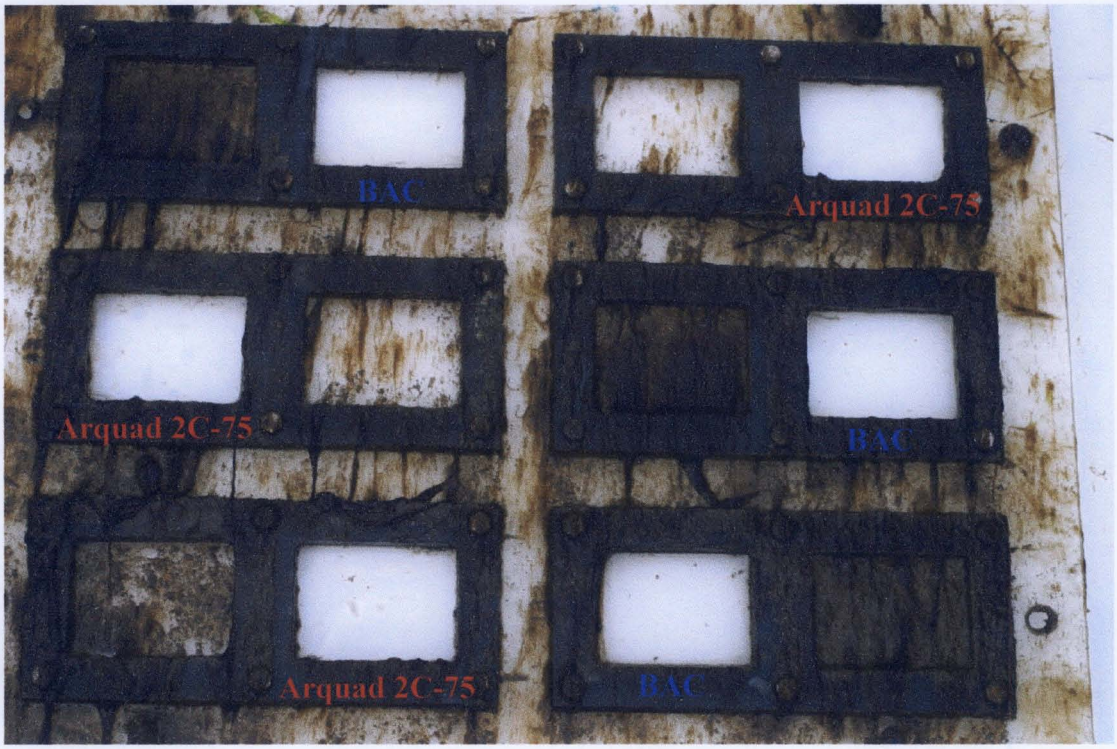

Figure 7.9 Rack 2 after 8 weeks marine deployment.

Figure 7.10 Rack 2 after 12 weeks marine deployment.

Figure 7.11 shows rack 3 at the 11 weeks marine deployment. Again the blank hydrogel and the PMMA samples are heavily fouled while the hydrogel/BAC has less fouling, although biofilms and algae are evident on the samples. The hydrogel/Arquad 2C-75 samples are relatively free of fouling. Figure 7.12 shows a biofilm sloughing off a hydrogel/BAC sample.

Figure 7.11 Rack 3 at the 11 weeks marine deployment.

Figure 7.12 Hydrogel/BAC sample at 11 weeks marine deployment. The biofilm is sloughing off.

From the photographs it is evident that the hydrogel/2C-75 coating offers the superior fouling resistance as even at 14 weeks in the marine environment there is very little fouling. The blank hydrogel showed no intrinsic antifouling as it fouled more than the PMMA control samples. The hydrogel/BAC sample did resist fouling up to around 10 weeks making it a good coating for its purpose although the use of Arquad 2C-75 gives superior performance. The success of the hydrogel containing the surfactant Arquad 2C-75 may be due to a variety of the properties which the coating possesses. Brady and Singer (2000) stated that polymer surfaces that fail to accumulate marine organisms may do so in one of two ways. They may resist the formation of strong bonds to marine adhesives or they may be mechanically designed to favour failure of any adhesive joint that forms.

Figure 7.13 shows the calibration graph obtained for the FDA analysis.

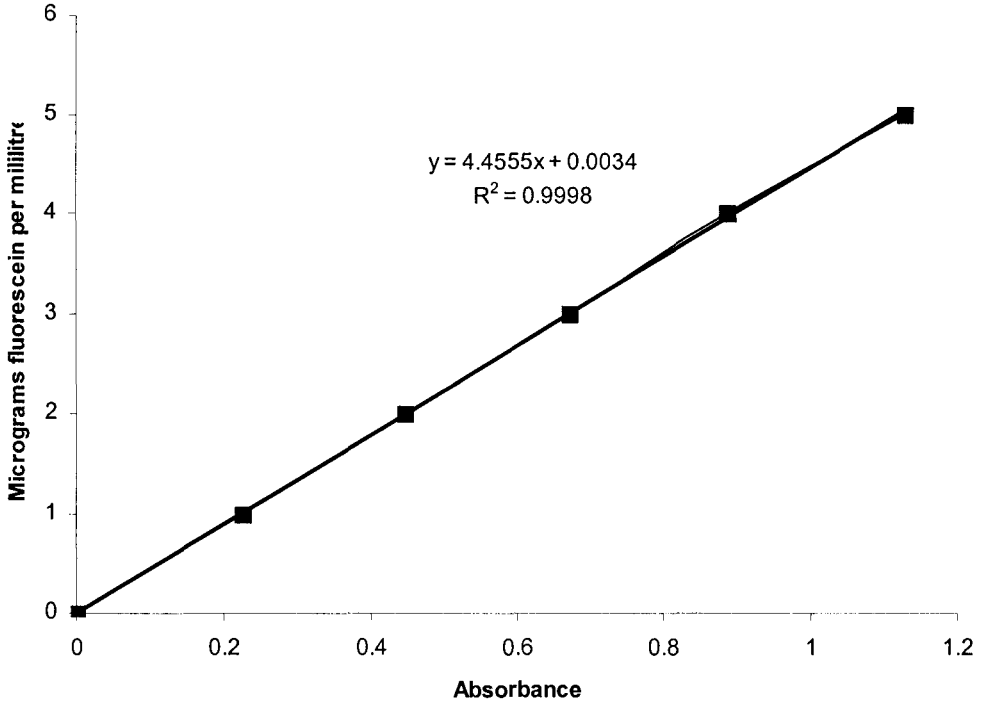

Figure 7.13 A typical calibration graph obtained for quantification of FDA.

Figure 7.14 shows the amount of fluorescein released per hour for each rack. The y-axis scale varies for each rack to reflect the FDA values obtained. The FDA analysis showed the blank hydrogel to be the most heavily fouled on all of the racks. From the variation in the results it can be seen that the fouling is relatively patchy, although it should be noted that the blank hydrogels were completely covered with algae and other organisms. There was no pattern over the 11, 12 and 14 weeks; values of 1.49, 1.47 and 1.96 mg fluorescein h^{-1} $core^{-1}$ were recorded.

The PMMA coupons were the next heavily fouled material, again there are variations in the amounts, but at the end of the trial the PMMA samples were covered with fouling. The BAC/hydrogel coatings at 14 weeks had some fouling on them but very little when compared to either the blank hydrogel or the PMMA samples.

At 12 weeks the BAC samples are visibly fouled and around half the FDA value that was detected at 14 weeks, although comparing values at this point is not particularly useful as it would be unlikely that fouling would be repeated precisely in the marine environment. At 10 weeks the BAC results vary as on two of the three samples no fouling is detected by the FDA method. At 14 weeks the Arquad 2C-75/hydrogel coating had practically no fouling although values of 0.013, 0.058, and 0.076 mg fluorescein h^{-1} were recorded. At 12 weeks the values were 0.015, 0.017 and 0.016 mg fluorescein h^{-1}. The FDA method of fouling quantification mirrored that of the visible appearances of the 3 racks at the end of the trial.

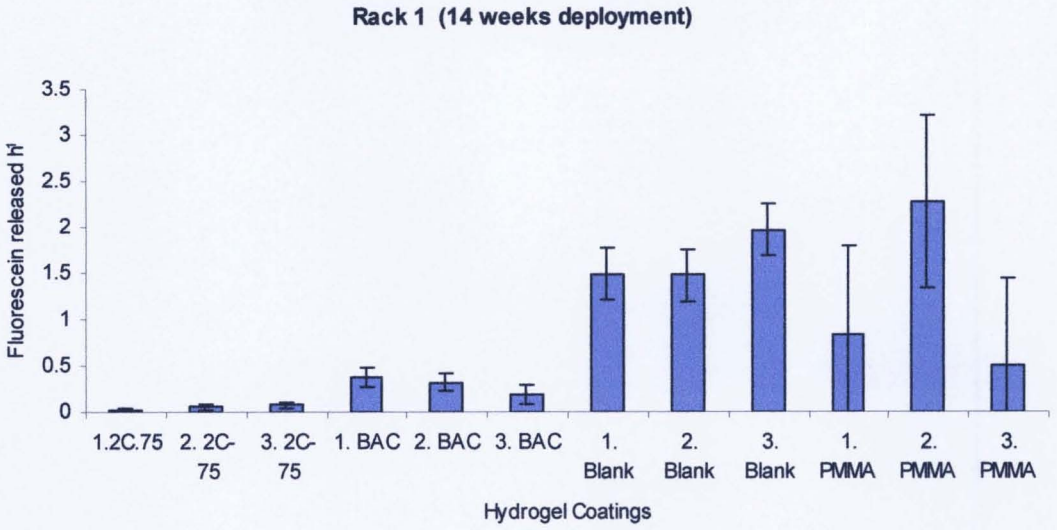

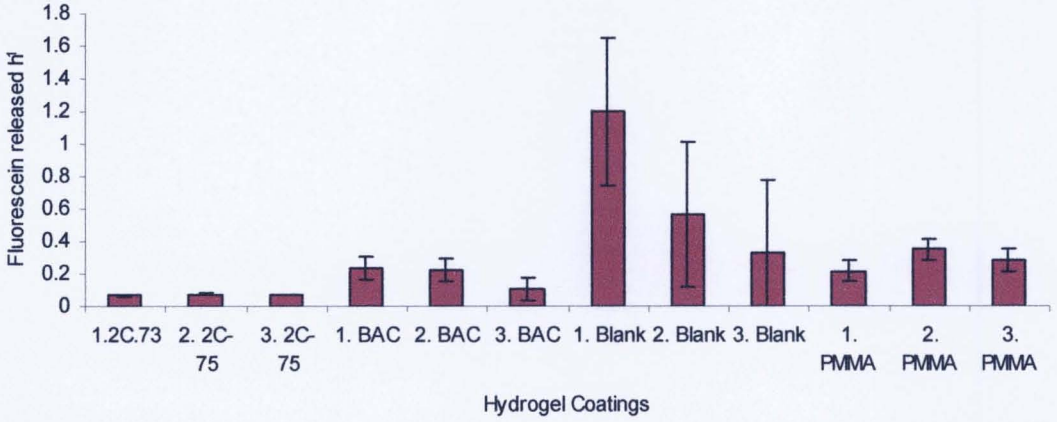

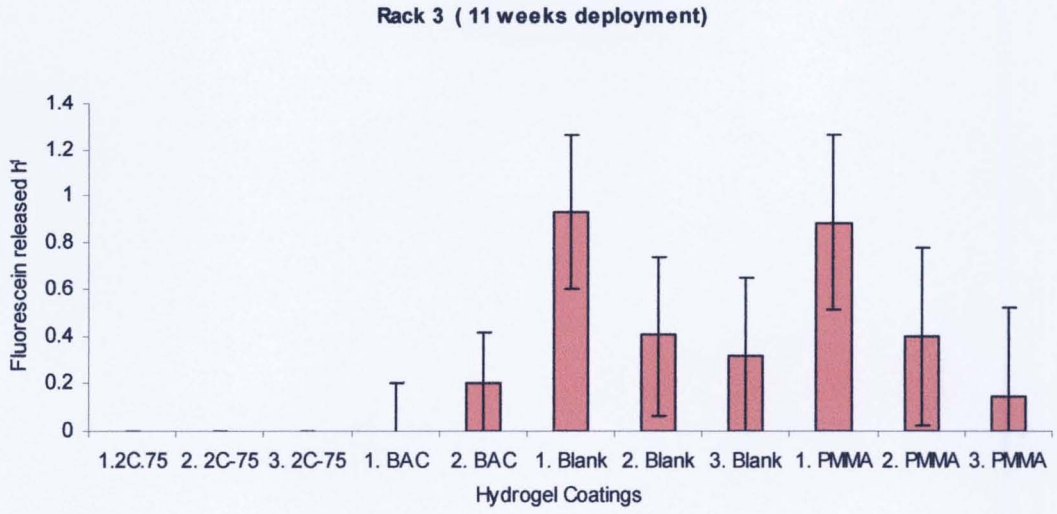

Figure 7.14 FDA levels recorded from each of the surfaces of the coatings tested.

Hydrogel coatings containing either of the cationic surfactants BAC or Arquad 2C-75 prevented biofouling growth for 10 and 14 weeks respectively. The trials were concluded at 14 weeks, in order to make useful comparisons between the coatings tested; therefore the ultimate duration of the fouling free life of the hydrogel/Arquad 2C-75 coating was not established in this experiment. At this time point, although fouling was not visible, a small amount of microbial activity was detected by FDA on the hydrogel/Arquad 2C-75. The FDA method was a good quantitative measurement of fouling as it is easily performed and robust for its purpose.

7.1.3 Freshwater Trials using Hydrogel Coatings

This work was carried out by Institute of Applied Freshwater Ecology, Seddin, Germany. Two spectrophotometers were deployed in a freshwater lake one had its optical port coated with hydrogel loaded with 1% Arquad 2C-75 and the other was uncoated. They were deployed for 45 days. After this times it ws found that there was patchy fouling on the hydrogel whereas the uncoated sensor was completely covered with fouling. The algae on the uncoated sensor were identified as *Scenedemus ecornis* and *Mycrocystis wesenbergie*. On the hydrogel coated sensor *Scenedemus ecornis* and only a sparse presence of Mycrocystis *wesenbergie*. From this result the lifetime of the surfactant/hydrogel coating is reduced in the freshwater environment. However, it still offered some extended deployment.

7.2 Application of Hydrogels to Instruments

The application of the hydrogel coating to an instrument's optical port is extremely important to the overall success of the prevention of biofouling on optical windows. Various ways of fixing the hydrogel coatings were considered and then tested on instruments or 'pseudo' instruments.

Hydrogels were fitted to instruments using different fixings. Those fixings included 'push-fit' holders, screw on bezels and holders which were bolted down.

7.2.1 Hydrogel Fixings and Bezels

In order to find a successful method of fixing the hydrogel to instruments a variety of techniques were tested.

The criteria required for successfully fixing the hydrogel to optical ports includes the following:

- The hydrogel is 1-2mm in thickness and is very pliable therefore requires to be held in place with a bezel or holder
- The bezel chosen to hold it securely must not leach into the hydrogel e.g. corrode
- The bezel should not damage the hydrogel
- However, it must be secure enough to prevent the hydrogel slipping

The bezels and holders were tested as follows:

- Push fit holders (as used on the Optisens transmissometers in Trondheim, Norway)
- The bezel is bolted on (as on the Chelsea Technologies Group transmissometers and fluorimeters). These were tested in the Firth of Clyde, Scotland and also in laboratory trials
- The screw-on fittings, in laboratory trials

A variety of instrument trials were carried out using the hydrogel as a biofouling resistant coating.

- Three trials using the Optisens transmissometers at Trondheim Norway
- A trial on the Scufa fluorimeter at UMBS, Millport
- A trial on the Chelsea Technologies transmissometers and fluorimeters

7.2.2 Method - Push-fit Holders

Instrument Trials

Three marine trials were carried out, the first beginning March 2004 and subsequent trials begun in June and September 2004.
Push-fit holders held hydrogel discs in place on the Optisens. Figure 7.15 shows an Optisens transmissometer with a hydrogel coating held in place in front of the optical port using a push-fit bezel.

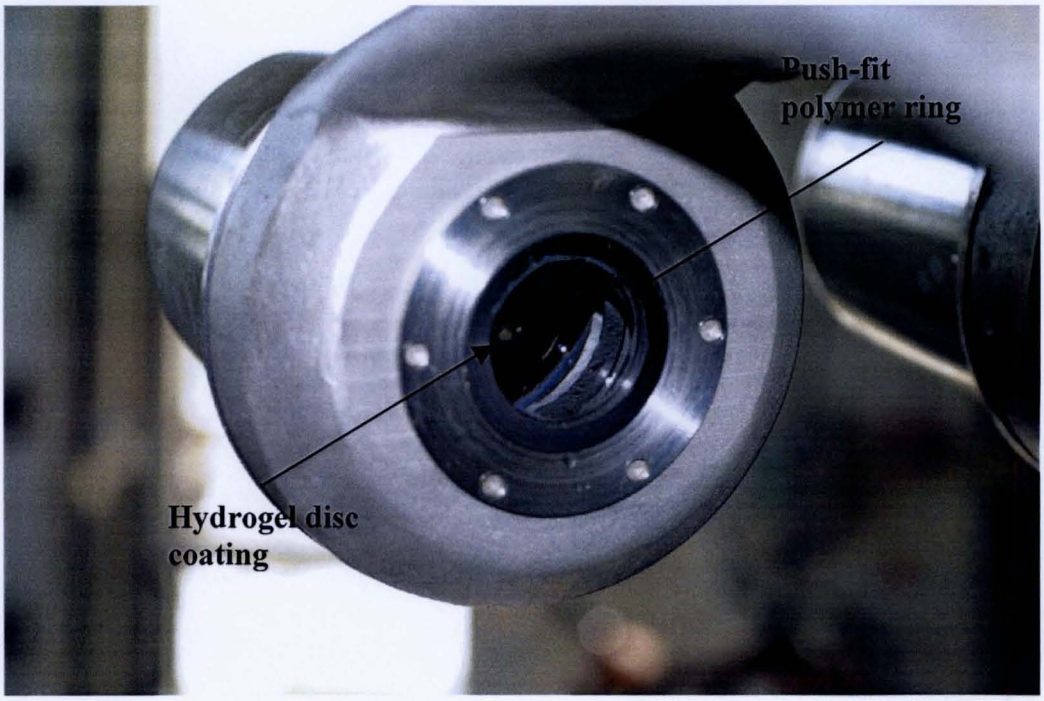

Figure 7.15 A transmissometer with a hydrogel held in place using a push-fit ring made from a hard polymer.

During the setting up of the trial the transmissometers were held for 24 hours in a seawater tank. This prevented the hydrogel disc drying out and also allowed readings to be taken to assess the effects of the coating on transmission prior to deployment. It also meant that the hydrogel could be refitted to account for any initial swelling. The hydrogel discs were soaked in seawater for 4 hours prior to fitting thus allowing them to adjust to the new environment. Figure 7.16 shows a pair of transmissometers being lowered into a tank containing seawater.

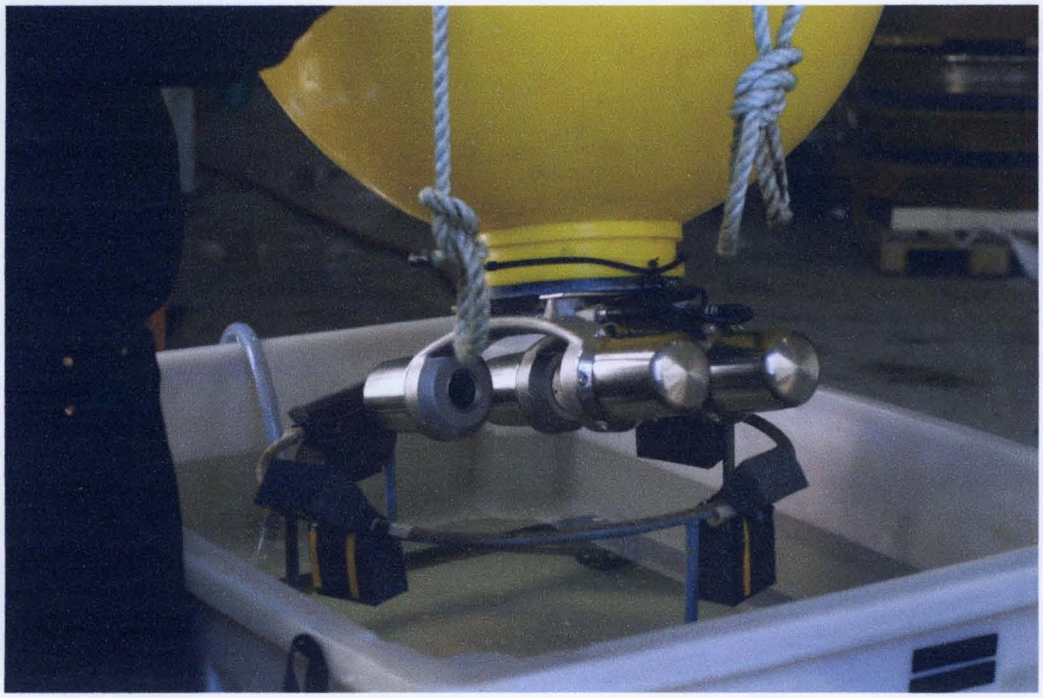

Figure 7.16 The transmissometers attached to a buoy being lowered into a tank of seawater to test transmission through hydrogels.

Laboratory and Field Assessment of Push-fit Bezels

In order to assess the fixing method a rack containing discs of hydrogel was set-up in the laboratory and tested in a seawater tank. Subsequently a field trial of the rack was carried out. Four hydrogel discs with 50mm diameters were placed in metal rings attached to a PMMA backing plate. The hydrogel discs were held in place using push-fit rings. As the fitment was tight they were put in place using a metal tube pusher. The laboratory trial was carried out at ambient temperature. The hydrogels were inspected and photographed at regular intervals.

7.2.3 Results and Discussion - Push-fit Holders

Instrument Trials

The first trial proved successful extending the useful output from the transmissometer by 100% i.e. from typically four weeks to eight weeks.

The subsequent two trials using this system proved to be less successful. It was believed that the push-fit holder allowed the hydrogel to slip and 'bubble out' from the surface of the lens, distorting the light path. To test this theory, laboratory and field trials were carried out. The tendency for the hydrogel to 'bubble out' had been noted in the 24 hour period the transmissometers were held in the seawater tank prior to deployment and rectified at this stage.

Transmission readings were then taken in a seawater tank, comparing the uncoated and the hydrogel coated lens. Table 7.1 shows the difference in transmission from the two instruments.

Light Type (%)	**Time (Minutes)**		
	0	10	20
	Light Transmission (%)		
Blue 1	68	68	68
Blue 2 (gel)	59	59	59
Green 1	76	75	75
Green 2 (gel)	65	65	65
Red 1	78	78	78
Red 2 (gel)	65	65	66

Table 7.1 Transmission readings taken from the coated and uncoated lenses over time

Transmission in seawater for the unprotected instrument was reduced from the calibration 100% value to Blue 68%, Green 76% and Red 78%. The additional reduction due to the two hydrogel coatings on the protected instrument was Blue 9%, Green 9% and Red 13%. These additional reductions in transmission are unlikely to

have any significant effect on the usefulness of the Optisens instruments in monitoring changes in the water quality, advent of algal blooms, etc.

Laboratory and Field Assessment of Push-fit Bezels

The rack was inspected after 24 hours and it was found that already one of the hydrogel discs had sagged and water had accumulated behind it. By the six week time point three of the discs had sagged.
Figure 7.17 shows the rack at six weeks and figure 7.18 shows a close-up of one of the hydrogel discs bubbling out from its' fitting.

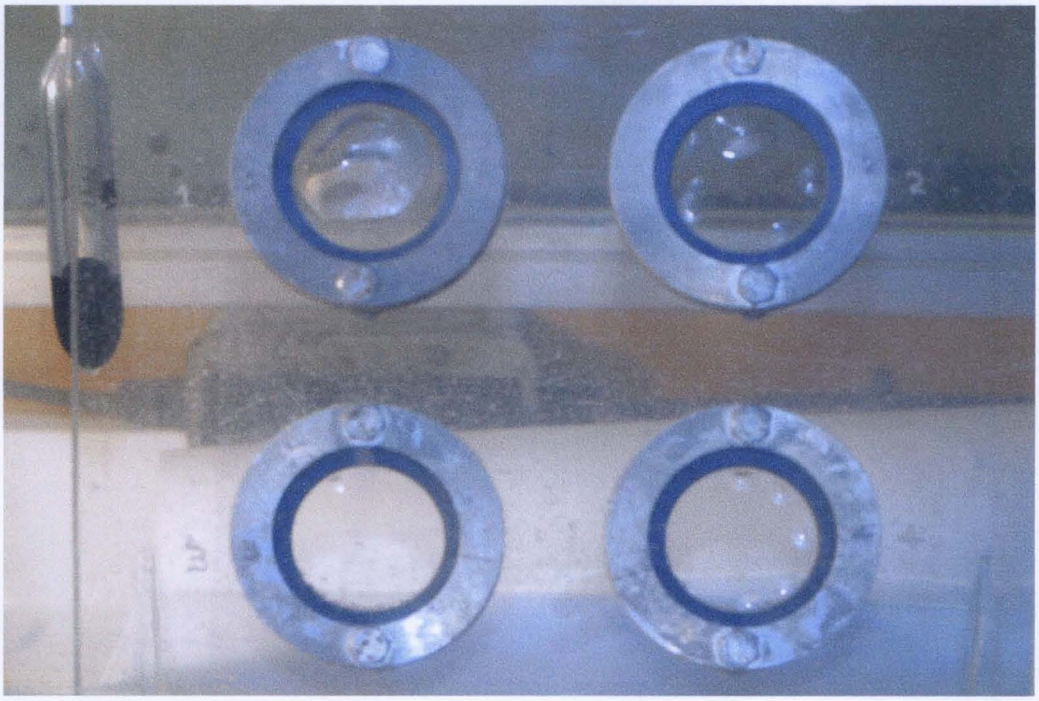

Figure 7.17 The test rack after 6 weeks immersion in a tank containing seawater.

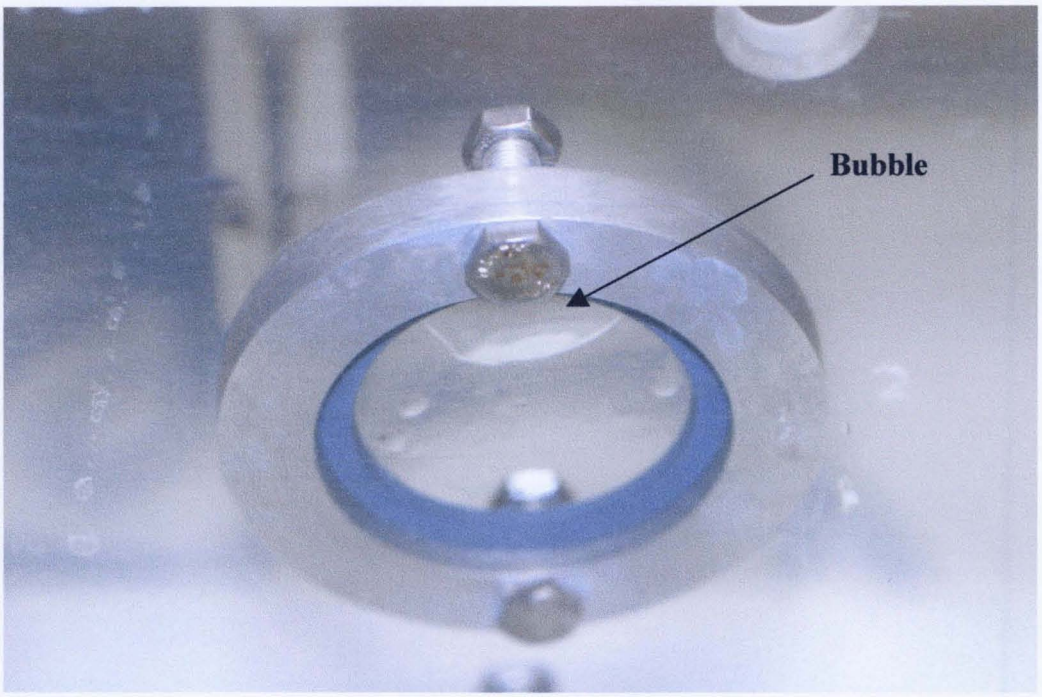

Figure 7.18 Rack with hydrogel 'bubbled out' at the 6 week time point.

A field trial of this fixing method was carried out in the Firth of Clyde, Scotland. Figure 7.19 shows the rack after 12 weeks marine deployment and again three out of the four test discs had bubbles behind them. However, it should be noted that the hydrogel discs have remained free of biofouling despite the heavy fouling on the rack. Therefore the problems associated with trials 2 and 3 of the Optisens transmissometer were not due to fouling, but to fixing problems.

Figure 7.19 The push-fit rack after 12 weeks marine deployment

These subsequent trials have confirmed that the 'failure' of the Optisens transmissometers in the Trondheim trials were due to hydrogel fixing issues.

7.2.4 Method-Bolted Down Bezel Fittings

The hydrogel was fixed to these transmissometers using acrylic holders bolted down. Figure 7.20 shows the set-up.

Figure 7.20 Shows the hydrogel laid on the optical port and the acrylic holder fixed on to it and secured down by bolts.

7.2.5 Results and Discussion -Bolted Down Bezel Fittings

This method of securing the hydrogel was very successful as no bubbling occurred and it also resulted in the prevention of biofouling on the transmissometer optical port. Trials of the unprotected and protected were carried out in a seawater tank at University Marine Biological Station Millport (UMBS), Isle of Cumbrae, Scotland. The tank used was 20m x 10m x 2m, constructed from concrete and refilled from the Firth of Clyde over a four-hour period during local high tides. Figure 7.21 shows the output from transmissometers, one of which was cleaned daily and another which was unprotected. The optical lens which was not cleaned became considerably fouled reducing the transmission to around 20% after 40 days. The cleaned lens shows the fluctuation of transmitted light as the natural environment changes over time. Figure 7.22 shows two transmissometers, one with the optical port protected with hydrogel/Arquad 2C-75 coating and another unprotected lens. After 40 days deployment the hydrogel protected lens was still transmitting light at around 75 % (both began at 80%). This demonstrates the success of the coating on optical ports.

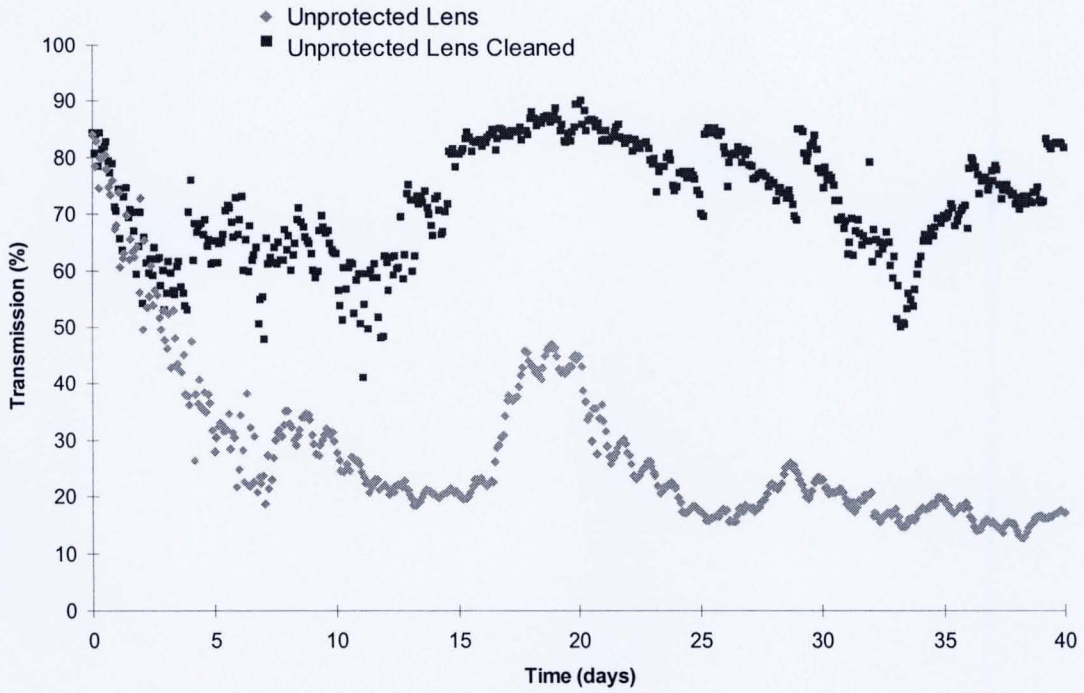

Figure 7.21 The output from two transmissometers one with an optical window which was not cleaned and one which was cleaned. (Courtesy of the BRIMOM Project)

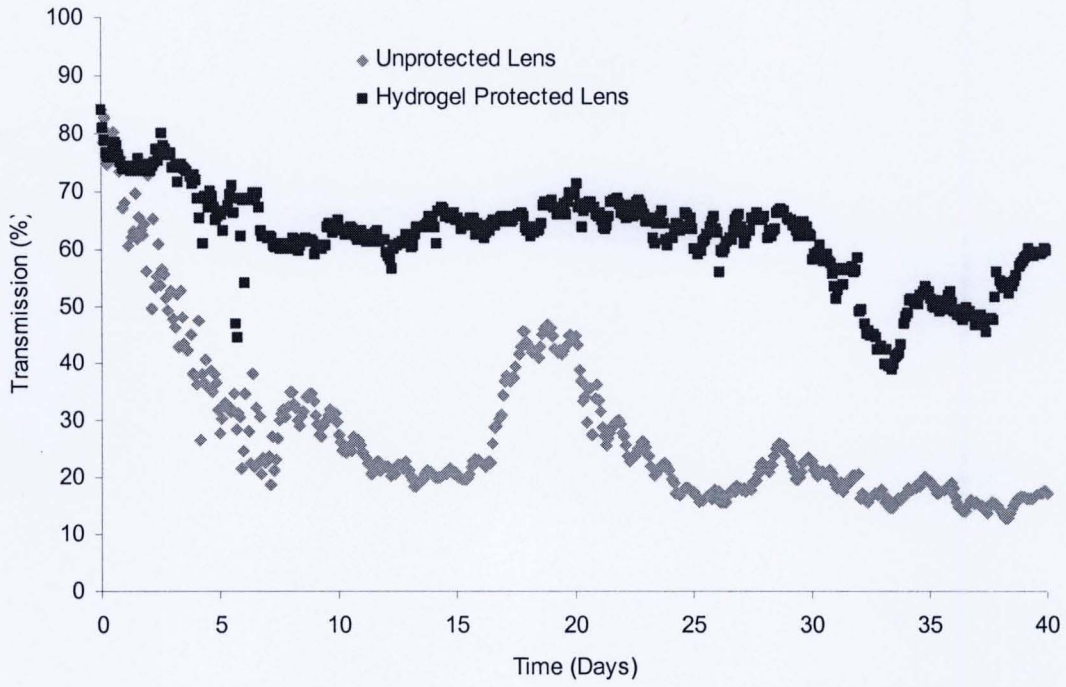

Figure 7.22 The output from two transmissometers one which had a protective hydrogel/Arquad 2C-75 on the optical and one which did not. (Courtesy of the BRIMOM Project)

7.2.6 Method - Screw-Fit Holders

Screw-fit holders were designed to hold the hydrogel in place in front of the optical window. PMMA pseudo sensors were prepared to test the suitability of this system. Hydrogel discs were cut to fit on the top of the PMMA rod and these were held in place by a screw-fit top, figure 7.23 shows such a pseudo sensor. These systems were tested in a seawater tank in the laboratory. Figure 7.24 shows the setup.

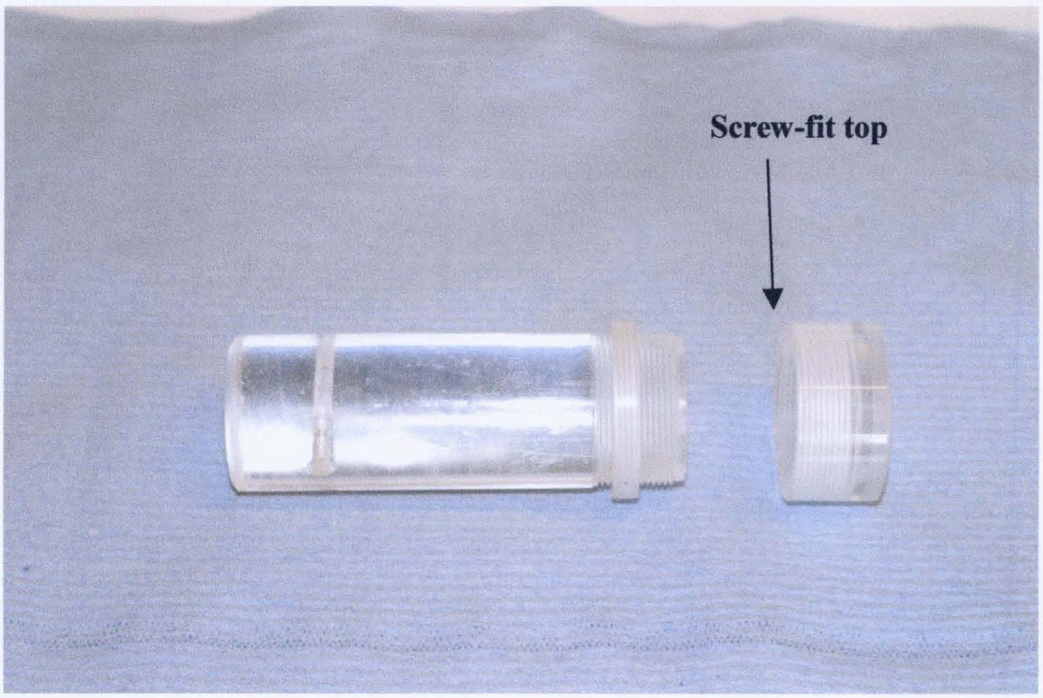

Figure 7.23 A PMMA pseudo sensor with screw-fit top to hold the hydrogel coating in place.

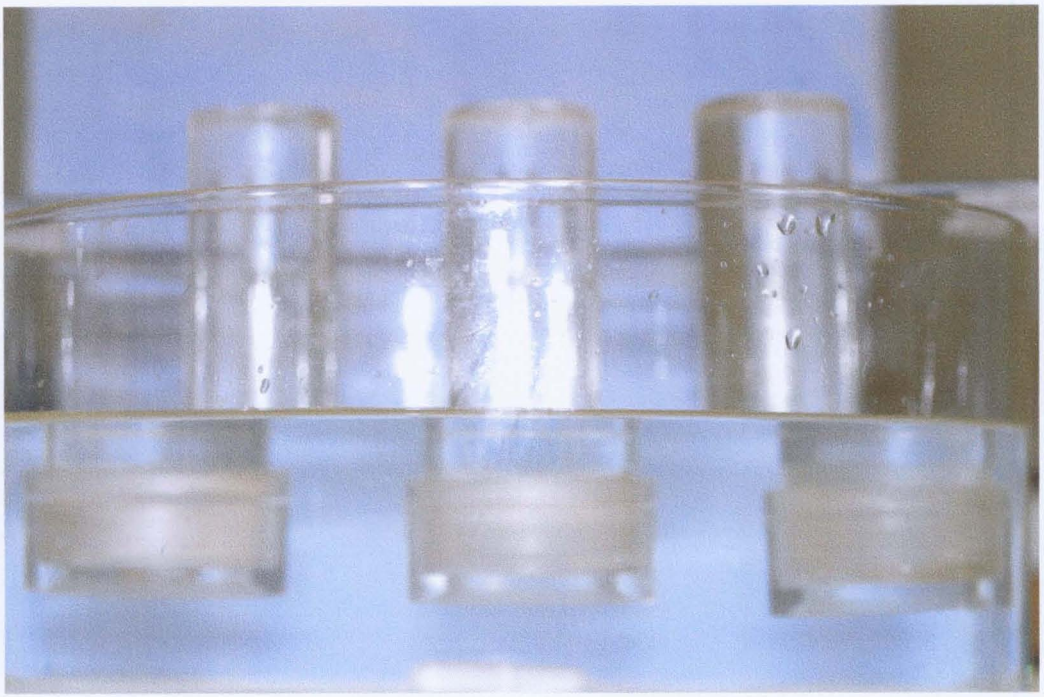

Figure 7.24 Screw-fit pseudo sensors with hydrogel discs in place in a tank of seawater.

7.2.7 Result - Screw-Fit Holders

This manner of fixing the hydrogel was successful and in a 10 week tank test the hydrogels stayed fixed in the screw-fit holders with no bubbling out. This was attributed to the fact that hydrogel discs were held in securely due to ring being wide enough to prevent slippage.

7.2.8 Method - Screw-down Bezel Fittings

These fittings were tested on the Chelsea Technologies Group Minitrackas. The exposed optical windows were 6mm and 10mm.
Recessed bezels were prepared and these were 11mm and 15mm in diameter and hydrogel discs were cut to size, 10.3mm and 14.3mm respectively, using cork borers. Figure 7.25 shows the hydrogel in place on the windows. The Minitracka was held in a seawater tank (Instant Ocean) and monitored at regular time intervals.

7.2.9 Result- Screw-down Bezel Fittings

After 12 weeks the hydrogels were still in place, providing a clear optical coating for the light path to travel through.

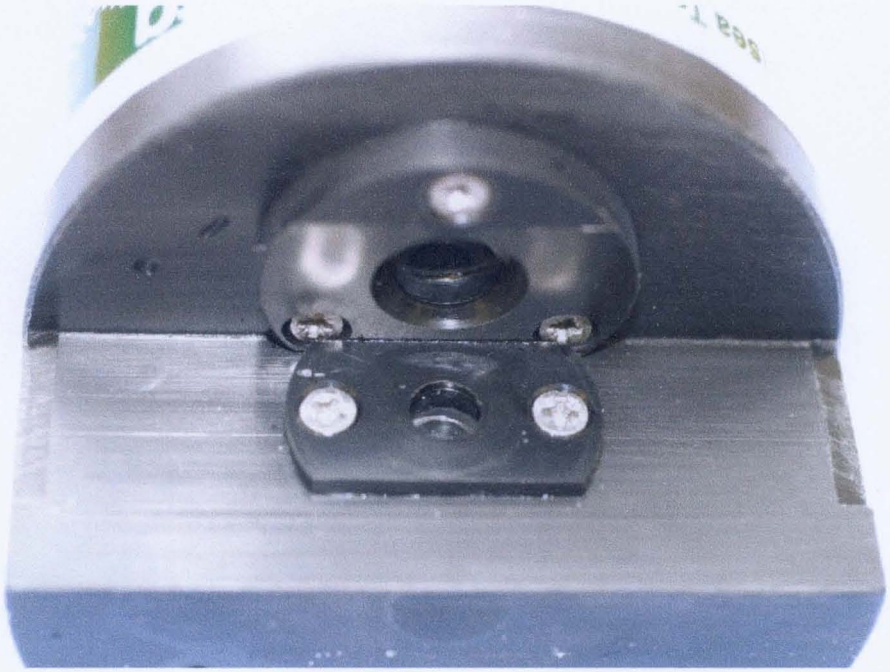

Figure 7.25 The optical ports of the Minitracka with hydrogel coatings held in place using a screw on bezel.

7.2.10 Recommended Criteria for Fixing Hydrogel Coatings to Optical Ports

- The hydrogel should be held in place using a bezel which secured by bolts or a screw-fit bezel
- It is preferred that the bezel is fabricated from a polymer as metal bezels may corrode and leach into the hydrogel
- Push-fit holders are not successful as water is able to ingress causing the hydrogel coating to 'bubble out' from the surface
- Hydrogels containing Arquad 2C-75 are successful biofouling resistant coatings. The success of the bezel is crucial to the optical performance of hydrogel coatings on optical sensors

7.2.11 Suitability of Hydrogel Coatings

The most successful fouling resistant coating was the hydrogel containing Arquad 2C-75 (details in section 7.1.3.1). Therefore on all the instrument trials this material was used. From the physical tests on this material it proved to be an ideal choice as it did not swell or shrink in seawater conditions; it had a low contact angle; it remained transparent; it had a very smooth surface and had a low modulus of elasticity. All properties postulated to produce a successful antifouling coating.

Any coating used to prevent biofouling must have its environmental impact assessed, as any detrimental action on the environment would make it unacceptable.

There are many sources of surfactants that result in discharges into natural waters from industrial, domestic and from agricultural applications (UK Marine SACs Project). Fernández et al. (1996) stated that in 1987 consumption of cationic surfactants from laundry detergents were approximately 80,000 tons in the USA and 72,000 tons in Europe. Wee (1984) found that 22.7 x 10^6 kg yr^{-1} surfactants typically enter the environment via wastewater treatment plants in the USA. Boethling and Lynch (1992) stated that the average concentration of cationic surfactants in domestic sewage should be around 1mg l^{-1}. They also said that biodegradation was the ultimate fate of cationic surfactants released to wastewater treatment and the environment. Ginkel et al. (2003) tested the biodegradation of 2mg l^{-1}didecyldimethylammonium chloride by adding bacteria in a Closed Bottle test. They found that after 3 days the value had dropped to less than 0.6 and complete biodegradation was as achieved within 10 days. This result permits classification of didecyldimethylammonium chloride as readily biodegradable.

The hydrogels at zerotime, i.e. at time of deployment, contained 50mg g^{-1} and 10mg $g^{-1}$of hydrogel for the BAC and Arquad 2C-75 respectively. At the end of 14 weeks the amount of BAC had reduced to around 20mg g^{-1} of hydrogel. It was not possible to quantitatively analysis Arquad 2C-75 at the conclusion of the deployment trials. However, it would appear that it is likely that the relatively small surfactant release from the hydrogels would be readily biodegraded.

7.2.12 Preparation and Fitting of Dome Shaped Hydrogel to Underwater Cameras

To fabricate a hydrogel coating for an underwater camera with a domed head required a mould to be produced to the exact size of the dome; all previous coatings were cut to size from a sheet of hydrogel. The size of the dome was also fairly large as it had a diameter of 195mm.

Figure 7.26 shows a drawing of the camera that the hydrogel coating was to protect.

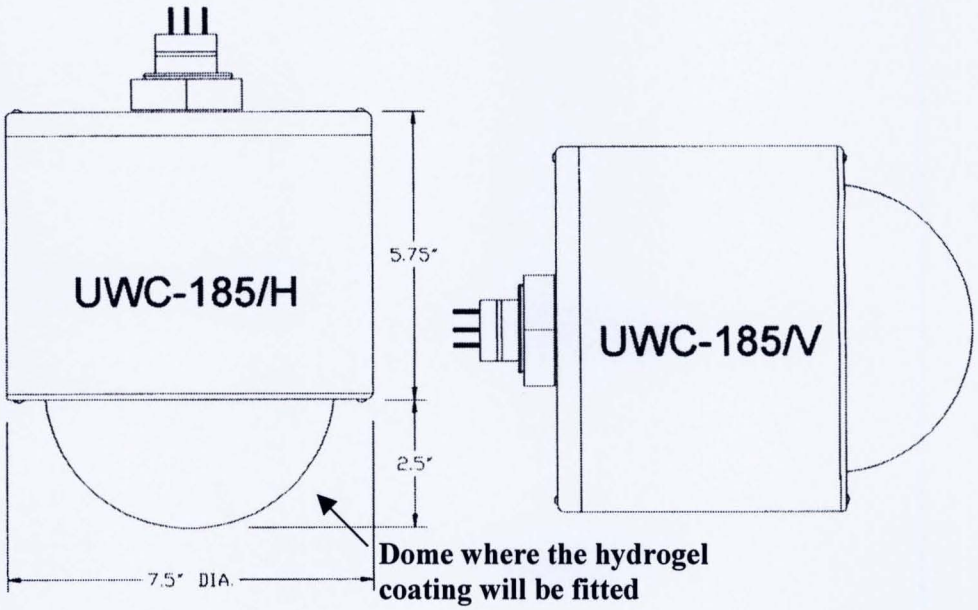

Figure 7.26 Diagrammatical representation of the pan/tilt camera supplied by the manufacturer (measurements are shown in inches)

The moulds were prepared from two doomed wooden formers, the inner one 2mm smaller then the outer. They were formed from styrene using a hot pressing technique. The hydrogel were prepared as previously described (Chapter 5, section 5.1.1). The hydrogel was cured overnight in an oven at 60°C. It was removed from the oven and allowed to reach room-temperature; it was then soaked in a container of distilled water and left for 24 hours. This soaking allowed the water to creep in at the edges and eased the removal of the hydrogel. The hydrogel was then cleaned up by

successive washing in distilled water and stored in water until required. Figure 7.27 shows the mould. The mould produced a hydrogel which was slightly larger than the dome to account for polymer shrinkage.

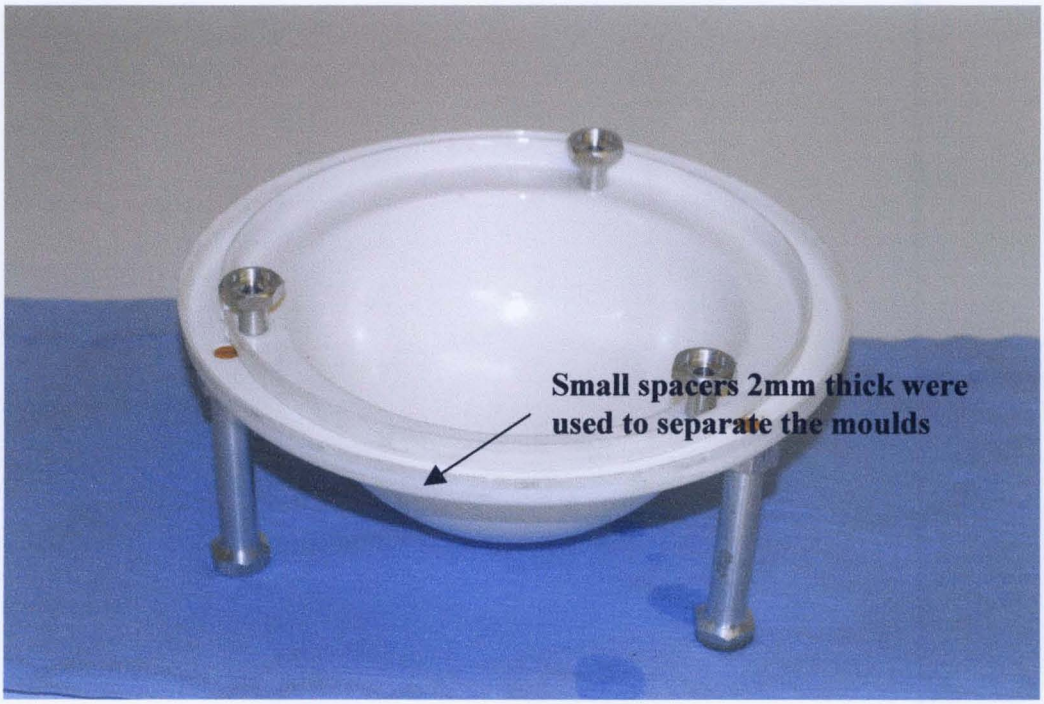

Figure 7.27 The mould used to prepare the domed shaped hydrogel.

Testing of this hydrogel is currently being carried out by the University of Wisconsin, Milwaukee, Great Lakes Water Institute, USA.

7.3 Gas Membranes-Biofouling Studies

In order to determine if any of the commonly used gas membranes had any intrinsic biofouling resistance a variety of field trials were carried out. Such trials would also determine if membranes produced by different manufacturers varied in their fouling resistance. Both preliminary fresh and marine trials were carried out.

7.3.1 Methods

Freshwater Biofouling Studies

Initial Field Trials- An initial freshwater trial was carried out in Bardowie Loch which is situated to the north of Glasgow, Scotland. A rack containing 14 replicates with YSI membranes held on place with o-rings on pseudo sensors was exposed during July 2003. At the time of exposure the loch was exhibiting an algal bloom.

Marine Biofouling Studies

To determine whether there were differences in the rate at which gas membranes fouled in the marine environment a variety of commonly used membranes were tested, figure 7.28 shows the layout.

- BDH Super Premium Microscope Slides (Glass) - acting as a control material
- Polyethylene, High Density Film (HDPE), 20μm thick, Goodfellow Cambridge Ltd.) - O_2 membrane
- Rank membrane – Polytetrafluoroethylene (PTFE), 12μm thick, Rank Brothers Ltd) - O_2 membrane
- YSI standard membranes- 30μm thick - O_2 membrane
- Gore-Tex PTFE tape-70μm thick (used for ammonia determination)

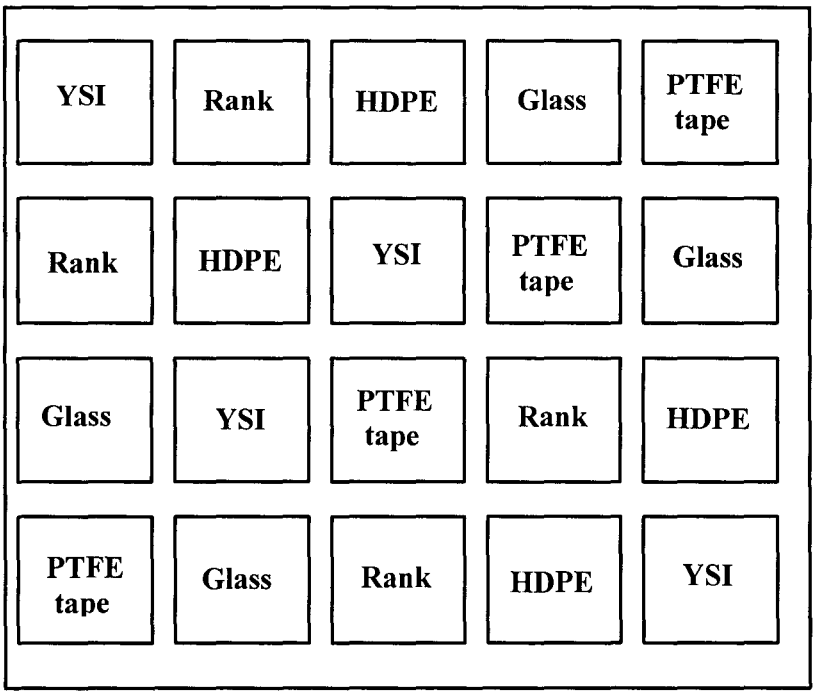

Figure 7.28 Membrane rack layout.

Membranes were attached to glass slides in a manner designed to prevent flexing of the material and possible biofilm removal. Templates were cut out of black rubber and a central portion of the rubber was removed leaving a rectangle of 4.2 cm^2. Membranes were then attached to the glass slides and the rubber template placed over the top and clipped into place. Templates were also attached to glass-slides acting as controls. This system was designed to mimic the exposure of relatively small membrane surface areas as commonly found in instruments used in detection ports of membrane sensors. Glass slides and membranes were cleaned with 60% ethanol (to remove manufacturing and handling residues) and left to dry. Materials were then 'dip-rinsed' in sterile filtered seawater to remove any possible traces of ethanol and placed in fresh sterile filtered seawater for 3 days to 'age'. Aged materials were attached to a PMMA rack in a 5 x 4 random block design.

7.3.2 Results and Discussion

Freshwater

The membranes were examined at three weeks later and no biofouling was visible on either the rack or the membranes; figure 7.29 shows the rack at this time point. At six weeks this was still the case. The heavy algal bloom had utilised all the nutrients and therefore the bacterial population had been depleted. Thus the initial fouling organisms were not available to foul the membranes. Some of membranes detached from the top of the sensors as the O-rings were not sufficiently strong to hold them in place. This method of testing was therefore not useful to determine fouling.

Figure 7.29 Rack containing the pseudo sensors with YSI gas membrane attached using O-rings. After 3 weeks some of the membranes had detached.

Marine

Figure 7.30 shows the rack after 6 weeks marine deployment. The samples were fouled with a variety of organisms and from the photograph mainly algae are visible. At this point all of the membranes tested were significantly fouled. Figure 7.31 shows the YSI standard membrane with Figure 7.32 shows a close-up photograph of the Gore-Tex tape where patchy fouling can be observed. Figure 7.33 shows the rack at 13 weeks. At this time point there is extensive macrofouling on all of the membranes and the glass control. This was composed of barnacles, spirobid polychaetes and most prominently, large tunicates. The most heavily fouled membrane was the PTFE tape (Gore-Tex). This can be explained by the large pore size of this material which is known to cause fouling to be more severe than on membranes with smaller sized pores (Brauker et al. (1995). This Gore-Tex material also had the roughest surface of those tested.

Becker (1996) looked at the retention of bacteria on a variety of hydrophobic membranes and found that all fouled, although the attachment to those with a surface tension between 20-25 mN m^{-1} was weaker; attachment strength was not tested on the fouled membranes. However, these surface measurements were carried out on samples which were in air and were in agreement with the value of around 20 mN m^{-1} found for PTFE tape. This value for PTFE increased to around 38 mNm^{-1} when the membrane was immersed in seawater (Chapter 6, section 6.6.2).

In conclusion the membranes tested do not prevent biofouling for extended periods of time, although there could be slight advantages of choosing a membrane with a smooth surface and a small pore size. At 6 weeks all were fouled and this would have reduced the diffusion rate of gases through them.

Figure 7.30 Rack containing gas membranes after 6 weeks marine deployment.

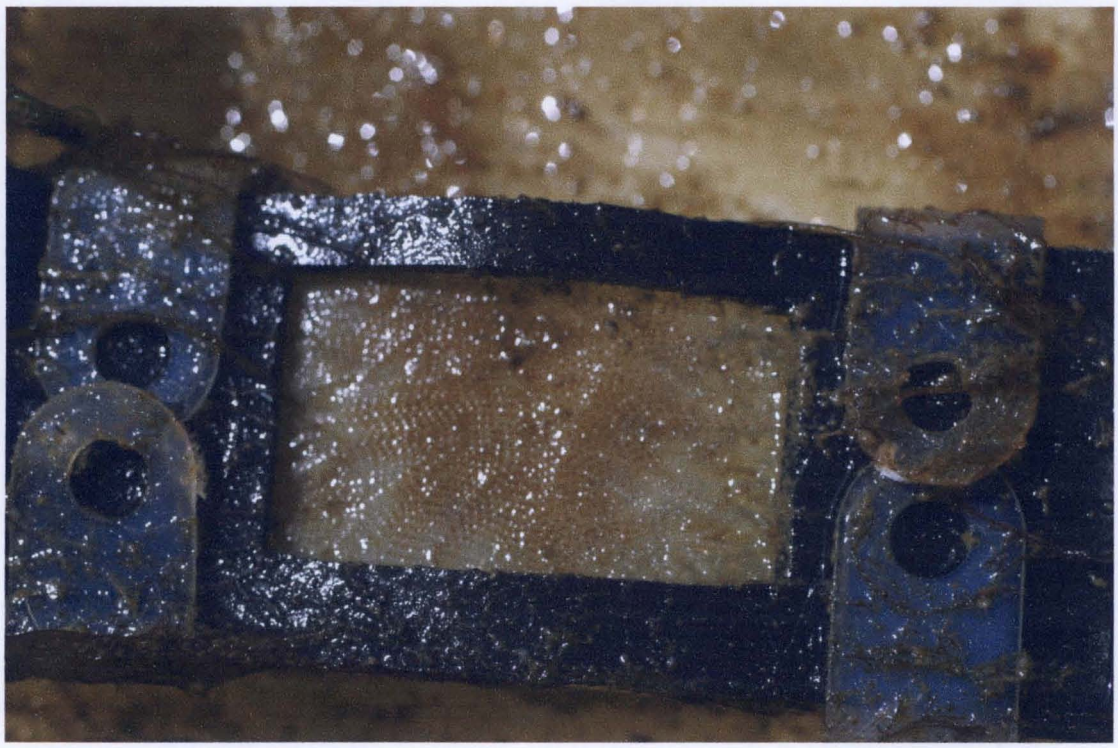

Figure 7.31 YSI standard membrane tape has fouling after 6 weeks marine deployment.

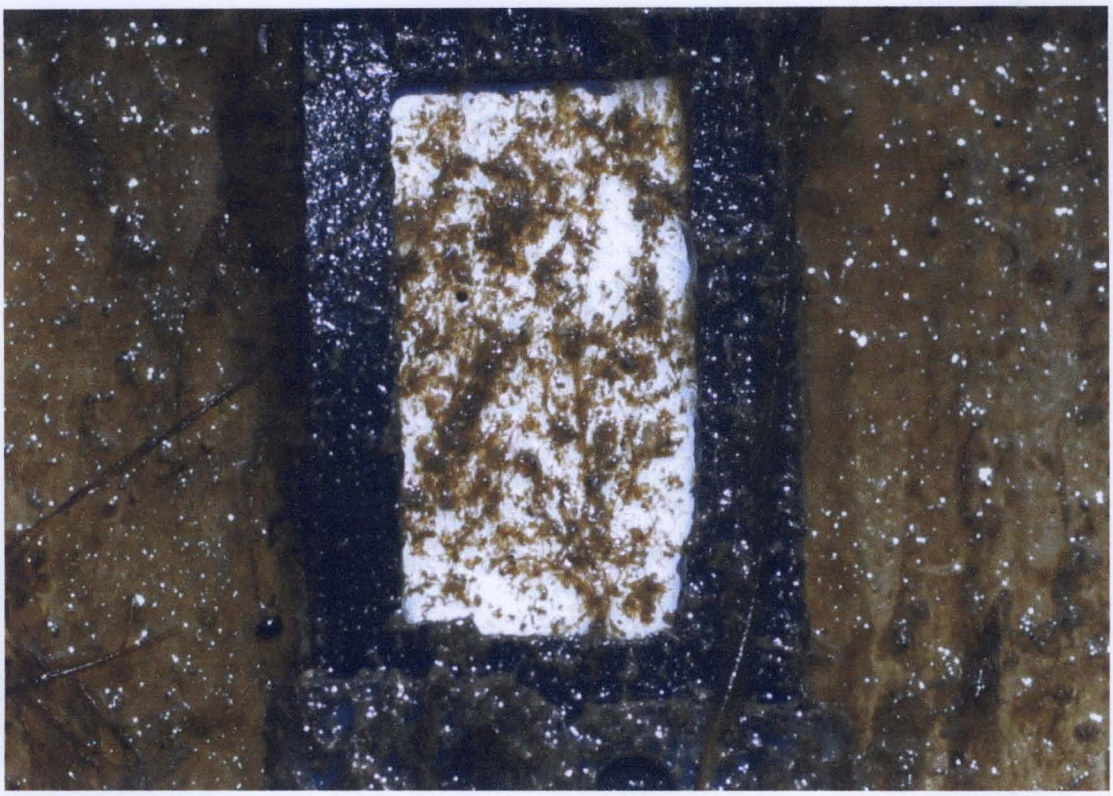

Figure 7.32 Gore-Tex tape has patchy fouling after 6 weeks marine deployment.

Figure 7.33 The gas membrane rack after 13 weeks marine deployment (Courtesy of the BRIMOM Project).

7.4 General Conclusions

The hydrophilic hydrogel coatings containing the surfactants benzalkonium chloride or Arquad 2C-75 offer extended fouling free surfaces for 10-14 weeks. The hydrogel containing the BAC releases the surfactant over time resulting in localised chemical, which prevents biofouling. The release of the Arquad 2C-75 appears to occur much more slowly if it reflects the absorption rate and it is therefore likely that the Arquad 2C-75/hydrogel coating is able to prevent fouling by modification of the hydrogel surface resulting in it becoming inhospitable to fouling organisms. Despite the theories that conclude that bacteria adhere less to hydrophobic substrata, opposite conclusions are also drawn. The diversity in the bacterial world is a factor contributing to the confusion, particularly since bacterial cell surfaces can be as hydrophilic as glasses while other strains can have cell surfaces as hydrophobic as wax. When comparing the performance of the hydrogels to reported work on hydrophobic surfaces, the absence of any fouling makes the hydrogel superior. Hydrophobic surfaces may, however, be ideal as wipe-off surfaces as the retention to hydrophobic surfaces appears to be less than to hydrophilic surfaces (Bos et al. 2000). Manov et al. (2003) reviewed a variety of biofouling resistant strategies for optical sensors including an automatic scrubbing device which cleaned the optical window of a fluorimeter once per day; the optical port of a transmissometer was surrounded with a ring coated with the optically clear paint (Aquatek); bronze rings impregnated with TBT and used to protect transmissometer; optical lenses of several transmissometer were coated with OMP-8 but when they were recovered it was found that flaking of the coating had occurred. All of the methods reviewed did delay fouling but not substantially. Given the extended period that the hydrogel/Arquad 2C-75 coating offered it would be an excellent choice for optical sensor window protection.

The in-depth study of gas membranes has shown that the choice of membrane should be determined depending on the application of the sensors as diffusion rates vary depending on the manufacture of the PTFE membrane. The gas membranes did become fouled at varying rates; although at six weeks fouling was visible on all membranes it was patchy in appearance. It was found that the YSI standard membrane was the least fouled and this result backed up the theories that small pore size and a

smooth surface are two of the properties crucial to fouling resistant coatings. The patchy appearance is common to hydrophobic materials.

Chapter 8

Overall Conclusions

8.1 Summary Conclusions

The overall conclusions from this thesis fall into seven specific areas:

1. Since (marine) biofouling develops rapidly on underwater sensor surfaces and effects the measuring performance there is a need to develop biofouling resistant technologies to protect the ports of underwater instruments from biofouling and thus prolong the useful data collection lifetime and measurement accuracy.

2. There are many biofouling resistant technologies on the market and in the literature but few are applicable for the protection of optical or gaseous ports. However, there are some, which do offer some useful lifetime extension, but these are mechanical in nature, such as wipers and brushes, and require power input.

3. Hydrogel coatings containing cationic surfactants, specifically benzalkonium chloride and Arquad 2C-75, prolong the fouling free period of optical ports for periods of 10 to 14 weeks. This effectively allows useful data to be collected and reduces maintenance costs significantly.

4. Hydrogel can be successfully retro-fitted to optical sensors using a bezel which secured by bolts or a screw-fit bezel. Such arrangements would also permit in field replacement of the coating.
5. The choice of gas permeable membrane used on gaseous sensors can affect the fouling-free time period of sensors. Some PTFE membranes with a smooth surface and small pores can, to a small extent, extend the lifetime of a sensor relative to other commercially available membranes.

6. Hydrogels allow the diffusion of gases through them and therefore they can be applied to the membranes of gas sensors to extend their fouling free lifetime, but with some effect on sensor response times.

7. Therefore, from the findings here, there is a requirement for instrument manufacturers to adapt and more importantly to manufacture instruments to include emerging biofouling resistant technologies.

8.2 Methods

Within this thesis a variety of experimental methods have been developed, these are:

Hydrogel Production

A successful method was developed for the production of a very smooth hydrogel sheet. Careful attention is required in production as inclusion of air results in poor quality coatings being produced. It is best to produce the hydrogel as a thin sheet which can easily have discs cut from it as opposed to a thick block to be sectioned. When produced as a block the hydrogel would not polymerise successfully and thus a heterogeneous product would be produced. Such sheet gels have adequate optical properties for high performance optical instruments, such as transmissometers and fluorimeters, as well as underwater cameras.

Loading of hydrogel with surfactant

Two methods were investigated; the first involved soaking the hydrated hydrogel in a surfactant solution for specific time periods. The second method involved soaking the dehydrated hydrogel in the surfactant. Less surfactant was absorbed using the first method but the coating produced was robust and known to be successful in application (Parr et al. 1998; [a]Smith et al. 2002). Further development of the second method is advisable as it may offer a coating with a longer biofouling resistant lifetime.

Analysis of cationic surfactants

Benzalkonium chloride was analysed using a robust method which had been developed previously (Smith, 1997; Guilfoyle, 1990). Extensive method development was carried out to quantitatively analyse the twin-chained surfactant Arquad 2C-75. A successful method using an ion chromatography was chosen as the most robust of those tested. However, this method was only applicable when there were no competing ions i.e. when the surfactant was in distilled water. It was therefore not applicable to extractions from coatings which had been in the marine environment.

Biofouling Prevention and Application of Coatings

Successful methods of fitting the hydrogel coatings to instruments were developed. These allowed instruments ports to remain free of fouling for 10-14 weeks in temperate waters. Bezels which held the hydrogel in place were either lightly bolted or screwed down and must be used to achieve this lifetime.

Gas Membranes

A method was developed which allowed the measurement of gas diffusion through replicate membranes. This enabled the comparison of diffusion rates through a variety of membranes to be carried out.

8.3 Findings

Hydrogel

Hydrogel coatings successfully prevent fouling in temperature marine waters for 10-14 weeks in the face of significant fouling pressure. The properties of these hydrogels are transparent in the required wavelength range; they are hydrophilic; they have a low elastic modulus; they can imbibe biofouling resistant chemicals such as the cationic surfactants as used here; their release rate is easily controlled by the crosslinking in the hydrogel and they are tolerant to a wide range of temperatures.

These coatings are a passive technology not requiring an external power source. They also meet the majority of properties that a coating should possess to resist adhesion of microorganisms.

Gaseous Membranes

Gaseous membranes made from PTFE have considerably different structures and surface properties. Careful selection of such membranes can ensure optimum detection of gaseous species and the biofouling-free lifetime of the membrane. The rate of gaseous diffusion through these membranes various between manufacturers; this is likely to be due to the production process. Expanded PTFE is a result of thin sheets of PTFE being stretched while warm and this causes a break up on the micro-scale while remaining coherent on the macro-scale. As a result, the amount of stretching causes the variations in structure.

Hydrogel overlays can be fitted to gaseous sensors to extend their biofouling resistant lifetime. The extended response time due to these overlays can be accounted for by initial recalibration of the sensor.

8.4 Reflections on the Literature

Whelen and Regan (2006) said that the ideal antifouling strategy for sensors would provide a low cost, easily implemented, environmentally benign solution to fouling which would allow sensors to operate unattended for more than a year. At the time of writing a variety of mechanical and passive technologies for the prevention of fouling on detection ports have been suggested and developed. However, few of these have reached the commercial stage. This may be because, as yet, the demand is largely limited to research and monitoring activity. In the future the market will expand as new environmental policies evolve and the requirement to record data becomes mandatory. The negative aspects of using certain types of coatings are detailed by Manov et al. (2004). The use of coatings has mainly been of fluorosilicones, the so called fouling release coatings. There has been application of hydrogels in biomedical sensor ports (Wisniewski and Reichert, 2000; Parr et al., 1998) and also in marine

applications. The adaptation of sensors for coatings to be successfully fitted is a crucial part of effective biofouling prevention. The hydrogels can be fitted with only small alterations to sensors. As there is increasing prevalence of environmental legislation, many industries and agencies are now required to monitor the effect they have on the surrounding environment (Fraher and Clarke, 1998) the need for antifouling protection for sensors will therefore increase.

Literature from thesis

Most of the work has been communicated to the project partners and the scientific community via conferences, posters and publications.

One journal paper has been published in the journal Biofouling, another has been accepted by the Journal of Environmental Monitoring and the other has been submitted to the journal Estuarine, Coastal and Shelf Science. All three papers are attached in the appendix.

References

Aanderaa Data Instruments AS, Bergen, Norway.

Adam, G. and Duncan, H. J. (2001). "Development of a More Sensitive and Rapid Method for the Measurement of Total Microbial Activity using Fluorescein Diacetate (FDA) in a Range of Soils." Soil Biology and Biochemistry, **33** (7-8): 943-951.

Anderson, C., Atlar, M., Callow, M., Candries, M., Milne, A. and Townsin, R.L. (2003). "The Development of Foul-Release Coatings for Seagoing Vessels". Journal of Marine Design and Operations **B4**: 11-23.

Anseth, K., Bowman, C.N. and BrannonPeppas, L. (1996). "Mechanical Properties of Hydrogels and their Experimental Determination." Biomaterials **17**(17): 1647-1657.

Aquatic Biome, www.ucmp.berkeley.edu

Atkinson, B. (1964). Biochemical Reactors. Pion Press, London.Atkinson, B.,

Barbu, E. P.R., Graham, P., Eaton, P., Ewen, J, Smart, J. D., Nevell, G. and Tsibouklis J (2002). "Poly(Di-1H,1H,2H,2H-Perfluoroalkylitaconate) Films: Surface Organisation Phenomena, Surface Energy Determinations and Force of Adhesion Measurements." Polymer **43**(6): 1727-1734.

Barnes, R.S.K. and Hughes, R.N. (2002). An Introduction to Marine Ecology. Oxford, Blackwell Scientific Ltd.

Battin, T. J. (1997). "Assessment of Fluorescein Diacetate Hydrolysis as a Measure of Total Esterase Activity in Natural Stream Sediment Biofilms." The Science of the Total Environment **198**: 51 – 60.

Becker, K. (1996). "Exopolysaccharide Production and Attachment Strength of Bacteria and Diatoms on Substrates with Different Surface Tensions." Microbial Ecology **32** (1): 23-33.

Berglin, M., Wynne, K.J. and Gatenholm, P.(2003). "Fouling-Release Coatings Prepared From Alpha,Omega-Dihydroxypoly(Dimethylsiloxane) Cross-Linked With (Heptadecafluoro-1,1,2,2-Tetrahydrodecyl)Triethoxysilane." Journal of Colloid and Interface Science **257** (2): 383-391.

Beveridge, C.M., Parr, A.C.S., Smith, M.J., Kerr, A., Cowling, M.J. and Hodgkiess, T. (1998). "The Effect of Benzalkonium Chloride Concentration on Nine Species of Marine Diatom." Environmental Pollution **103 (1)**: 31-36.

Biofouling Prevention Technologies for Coastal Sensor/ Sensor Platforms (2003) Alliance for Coastal Technologies. UMCES Technical Report Series: TS-426-04-CBL/ Ref No. [UMCES] CBL 04-016.

Biofouling Resistant Infrastructure for Measuring, Observing and Monitoring (2006) FP5 Contract EVR1-CT-2002-40023 BRIMOM.

Blurton, K.F. and Ridderford A.C. (1967). A Modification of the Diaphragm Cell Technique for Measurement of The Diffusion Coefficient of an Electroactive Species in the Presence of Supporting Electrolyte. Journal of the Chemical Society (A). 1076-1079.

Boethling, R.S. and Lynch, D.G. (1992). Quaternary Ammonium Surfacatnts. The Handbook of Environmental Chemistry, Part F. Ed. O.Hutzinger. Springer-Verlag, Berlin and Heidelberg. **3**: 145-177.

Bos, R., Mei, H.C. van der, Gold, J. and Busscher, H.J. (2000)."Retention of Bacteria on a Substratum Surface with Micro-Patterned Hydrophobicity." FEMS Microbiology Letters **189** (2): 311-315.

Bott, T. and Miller, P.C. (1983). "Mechanisms of Biofilm Formation on Aluminum Tubes." Journal of Chemical Technology and Biotechnology B-Biotechnology **33** (3): 177-184.

Bott, T.R., Miller, P.C. and Patel, T.D. (1983). "Biofouling in an Industrial Cooling Water-System." Process Biochemistry 18 (1): 10&

Brady, R. and Singer, I.L. (2000). "Mechanical Factors Favoring Release from Fouling Release Coatings." Biofouling **15**(1-3): 73-81.

Brauker, J .H., Carr-Brendel, V.E, Martinson, L.A, Crudele, J., Johnston, W.D. and Johnson, R.C. (1995). "Neovascularization of Synthetic Membranes Directed by Membrane Microarchitecture." Journal of Biomedical Materials Research **29**: 1517-1524.

Brönmark, C. and Hansson, L-A. (1999). The Biology of Lakes and Ponds. Oxford, Oxford University Press: 7-52.

BROS Project (1998). EU MAST III contact number MAS3-CT95-0028.

Bryers, J.D. (2000). Biofilms II: Process Analysis and applications. A. John Wiley & Sons, New York and Chichester.

Callow, M. (1990). "Ship Fouling Problems and Solutions". Chemistry and Industry: May, 123-127.

Callow, M.E. and Clare, A.S. (2003). "Some New Insights into Marine Biofouling." Paints and Coatings **1**: 34-39.

Capurro, L.R.A. and Griffith, D.E. (1970). Oceanography for Practising Engineers. Barnes & Noble, New York.

Cauich-Rodriquez, J.V., Deb, S. and Smith, R. (1996). "Effect of Cross-linking on the Dynamic Mechanical Properties of Hydrogel Blends of Poly (acrylic acid)-poly(vinyl alcohol-vinyl acetate)." Biomaterials **17**: 2259-2264.

Characklis, W.G., Marshall and Kevin, C. (1990). Biofilms - Industrial Applications. A. John Wiley & Sons, New York; Chichester.

Choi, P., Criddle, W.J. and Thomas J (1979). "Determination of Cetrimide in Typical Pharmaceutical Preparations Using Pyrolysis-Gas Chromatography." Analyst **104**: 451-455.

Clark, R.B. (2002). Oxygen-demanding Wastes. Marine Pollution. Oxford, Oxford University Press: 35-63.

Clarkson, N.E. and Evans L V, (1993). "Evaluation of a Potential Non-Leaching Biocide Using the Marine Fouling Diatom Amphora-Coffeaeformis." Biofouling **7**: 187-195.

Clint, J. (1992). Surfactant Aggregation. Blackie, Glasgow, 82-129.

Cloete, T.H. (2005). "Alternative and conventional anti-fouling strategies." International Biodeterioration and Biodegradation **56**: 121-134.

Compañ, V., Garrido, J., Manzanares, J.A., Andres, J., Esteve, J.S. and Lopez, M. (1992). "True and Apparent Oxygen Permeabilities of Contact-Lenses." Optometry and Vision Science **69**(9): 685-690.

Compañ, V., Lopez, M.L., Andrio, A., Lopez-Alemany, A. and Refojo, M.F. (1999). "Determination of the Oxygen Transmissibility and Permeability of Hydrogel Contact Lenses." Journal of Applied Polymer Science **72**(3): 321-327.

Costerton, J.W., Irvin, R T. and Cheng, K.J. (1981). "The Bacterial Glycocalyx in Nature and Disease." Annual Review of Microbiology **35**: 299-324.

Costerton, J.W., Lewandowski, Z., Caldwell, D.E., Korber, D.R. and Lappin-Scott, H.M. (1995). "Microbial Biofilms." Annual Review of Microbiology **49**: 711-745.

Cowling, M.J., Hodgkiess, T., Kerr, A., Parr, A.C.S., Smith, M.J. and Beveridge, C.M., 'Biofouling of Oceanographic Sensors – Is there a Solution?', Proceedings OI '98, Brighton, March 1998.

Cowling, M.J., Hodgkiess, T., Parr, A.C.S., Smith, M.J. and Marrs, S.J. (2000). "An Alternative Approach to Antifouling based on Analogues of Natural Processes." The Science of the Total Environment **258**:129-137.

Crank, J. and Park, G.S. (1968). Methods of Measurements. Ed. Crank J. Academic Press London and New York, 1-39.

CRC handbook of Chemistry and Physics, Volume 86 :(2005). Ed. Lide, D.R.Taylor and Francis, London.

Cunningham, R.E. and Williams, R.J.J. (1980). Diffusion in Gases and Porous Media. Plenum, New York.

Delauney, L. (2005). "A promising and adaptable biofouling prevention method for marine environmental sensors". Abstracted in: Cloete, T.H. "Alternative and conventional anti-fouling strategies." International Biodeterioration and Biodegradation **56**, 121-134.

De Rosa, S., Sconza, F. and Volterra, L. (1998). "Biofilm Amount Estimation by Fluorescein Diacetate." Water Research, **32** (9): 2621 – 2626.

Drelich, J., Miller, J.D. and Good, R.J. (1996). "The Effect of Drop (Bubble) Size on Advancing and Receding Contact Angles for Heterogeneous and Rough Solid Surfaces as Observed with Sessile-Drop and Captive-Bubble Techniques." Journal of Colloid and Interface Science **179**(1): 37-50.

Espadas-Torre, C. and Meyerhoff, M.E. (1995). "Thrombogenic Properties of Untreated and Poly(Ethylene Oxide)-Modified Polymeric Matrices Useful for Preparing Intraarterial Ion-Selective Electrodes." Analytical Chemistry **67**(18): 3108-3114.

Estarlich, F.F., Nevell, T.G., Thorpe, A.A., Tsibouklis, J. and Upton, A.C. (2000). "The Surface Properties of Some Silicone and Fluorosilicone Coating Materials Immersed In Seawater." Biofouling **16**(2-4): 263-275.

Faille, C., Dennin, L., Bellon-Fontaine, M.N. and Benezech, T. (1999). "Cleanability of Stainless Steel Surfaces Soiled by *Bacillus thuringiensis* Spores Under Various Flow Conditions." Biofouling **14**(2): 143-151.

Faimali, M.S.K., Turk, T. and Geraci, S. (2003). "Non-Toxic Antifouling Activity of Polymeric 3-Alkylpyridinium Salts From the Mediterranean Sponge Reniera Sarai (Pulitzer-Finali)." Biofouling **19**(1): 47-56.

Fernàndez, P., Alder, A.C., Suter, M, J-F. and Giger, W. (1996). "Determination of the Quaternary Ammonium Surfactant Ditallowdimethylammonium in Digested Sludges by Supercritical Fluid Extraction and HPLC with Postcoulum Ion-Pair Formation." Fourth World Surfactants Congress. Dübendorf, Switzerland. **4**: 102-109.

Fletcher, R., Lupelli, L. and Rossi, A. (1994). Contact Lens Practice. A Clinical Guide. Blackwell Scientific Publications, Oxford.

Flory, P.J., Rehner, J. (1943). "Statistical Mechanics of Cross-Linked Polymer Networks I Rubberlike Elasticity." Journal of Chemical Physics **11**(11): 512-520.

Fontvieille, D.A., Outagueroine, A. and Thevenot, D.R. (1992). "Fluorescein Diacetate Hydrolysis as a Measure of Microbial Activity in Acquatic Systems: Application to Activated Sludges." Environmental Technology **13**: 531-540.

Fraher, P.M.A., and Clarke, D.W. (1998). "Fouling Detection and Compensation in Clark-Type Dox Sensors." IEEE Transactions On Instrumentation And Measurement **47**(3): 686-691.

Fredell, D. (1994). Biological Properties and Applications of Cationic Surfactants. Cationic Surfactants Analytical and Biological Evaluation. J. Cross, Singer, EJ, Marcel Dekker Inc. **53:** 32-59.

Gehrke S, Biren, D, Hopkins, JJ (1994). "Evidence for fickian water transport in initially glassy poly(2-hydroxyethyl methacrylate)". Journal of Biomaterials Science-Polymer Edition **6**: 375-390.

Gehrke, S.H. and Lee, P.I. (1990). Hydrogels for Drug Delivery Systems, ,Vol 41. Specialized Drug Delivery Systems: Manufacturing and Production Technology. Ed. T. Praveen. Marcel Dekker Inc., New York and Basel: 333-393.

Gilbert, F., Galgani, F. and Cadiou, Y. (1992). "Rapid Assessment of Metabolic Activity in Marine Microalgae:Application in Ecotoxicological Tests and Evaluation of Water Quality." Marine Biology **112**: 199 - 205.

Ginkel, C.G. van, Hoenderboom, A., Haperen, A.M. van and Guerts, M.G.J.(2003). "Assessmnet of the Biodegradability of Dialkyldimethylammonium salts in Flow through Systems". Journal of Environmental Science and Health- Part A Toxic/Hazardous Substances and Environmental Engineering **38** (9):1825-1835.

Glasspool, W.V., and Atkinson, J. (2003). "An Evaluation of the Characteristics of Membrane Materials Suitable for the Batch Fabrication of Dissolved Oxygen Sensors." Microelectronics International **20**(2): 32-40.

Greenberg, A.E., Clesceri, L.S. and Eaton A.D. (1992) Standard methods for the examination of water and wastewater. 18th edn. American Public Health Association, Washington, DC.

Grobe, G., Valint, P.L. and Ammon, D.M. (1996). "Surface Chemical Structure for Soft Contact Lenses as a Function of Polymer Processing." Journal of Biomedical Materials Research **32**(1): 45-54.

Guilfoyle, D., Roos, R. and Carito, S.L. (1990). "An Evaluation of Preservative Adsorption onto Nylon Membrane Filters." Journal of Parenteral Science and Technology **44**(6): 314-319.

Gumprecht, G., Gerlach, H. and Nehrkorn, A. (1995). "FDA Hydrolysis and Resazurin Reduction as a Measure of Microbial Activity in Sediments from the South-East Atlantic." Helogoländer Meeresuntersuchungen **49**: 189-199.

Helboe, P. (1983). "Separation and Quantitative-Determination of Long-Chain Alkyltrimethylammonium Ions By Reversed-Phase Ion-Pair Liquid-Chromatography Using Ultraviolet-Absorbing Counter Ions." Journal of Chromatography **261**(1): 117-122.

Hermitte, L., Thomas, F., Bougaran, R. and Martelet, C. (2004). Contribution of the Comonomers to the Bulk and Surface Properties of Methacrylate Copolymers. Journal of Colloid and Interface Science, **272**, (1), 82-89.

Hoch, G., Chauhan, A, Radke, C.J. (2003). "Permeability and diffusivity for water transport through hydrogel membranes." Journal of Membrane Science **214** (2): 199-209.

Hoffman, A. (2002). "Hydrogels for Biomedical Applications." Advanced Drug Delivery Reviews **54**(1): 3-12.

Holly, F.J. and Refojo, M.F. (1975). "Wettability of Hydrogels I. Poly(2-Hydroxyethyl Methacrylate)." Journal of Biomedical Research **9**: 315-326.

Howell, J.A. and Atkinson, B. (1976). "Sloughing of Microbial Film in Trickling Filters." Water Research **10**: 307-315.

Howell, J.A., Chi, C.T. and Pawlowsky, U. (1972). "Effect of Wall Growth on Scale–up Problems and Dynamic Operating Characteristics of Biological Reactor". Biotechnology and Bioengineering **36**:810-816.

Huang, H., Zhang, J., Hao, X and Guo, Y. (2004). "Study of a New Process for Preparing and Co-Stretching PTFE Membrane and its Properties". European Polymer Journal **20**:667-671.

Huglin, M., and Rego, J.M. (1991). "Influence of a salt on Some Properties of Hydrophilic Methacrylate Hydrogels." Macromolecules **24**(9): 2556-2563.

Hugo, W.B. (1965). Surface Active Agents in Microbiology, SCI Monograph 19, Society of the Chemical Industry, London: 67-82.

Ilavsky, M. (1982). "Phase Transition in swollen Gels. 2. Effect of Change Concentration on the Collapse and Mechanical Behaviour of Polyacrylamide Networks." Macromolecules **15**: 782-788.

Ista, L., Callow, M.E., Finlay, J.A., Coleman, S.E., Nolasco, A.C., Simons, R.H., Callow, J.A. and Lopez, G.P. (2004). "Effect of Substratum Surface Chemistry and Surface Energy on Attachment of Marine Bacteria and Algal Spores." Applied and Environmental Microbiology , **70**, (7), 4151-4157.

Kaplan, E. and Gundel, R.E. (1996). "Anterior Hydrogel Lens Deposits: Polished Vs Unpolished Surfaces." Optometry And Vision Science **73**(3): 201-203.

Keevil, C.W., West, A.A., Walker, J.T., Lee, J.V., Dennis, P.J.L. and Colbourne, J.S. (1989). Biofilms: Detection, Implications and Solutions. Permagon Press, Oxford.

Kerr, A, Smith, M.J. and Cowling, M.J. (2003) "Optimising Optical Port Size on Underwater Marine Instruments to Maximise Biofouling Resistance." Materials and Design **24**: 247-253.

Kerr, A., Head, R M., Cowling, M J., Davenport, J., Beveridge, C M., Smith, M J., Parr, A C S. and Hodgkiess, T (1998).'The Early Stages of Marine Biofouling and its Effect on Two Types of Optical Sensors', Environment International **24**: (3), 331-343.

Kim, S.W., Bae, Y.H. and Okano T (1992). "Hydrogels - Swelling, Drug Loading, and Release." Pharmaceutical Research **9**(3): 283-290.

Kiremitci-Gumusderelioglu, M. and Pesmen, A. (1996). "Microbial Adhesion to Ionogenic PHEMA, PU and PP implants." Biomaterials **17**(4): 443-449.

Kodjikian, L, B.C., Chanloy, C., Bostvironnois, V., Pellon, G., Mari, E., Freney, J. and Roger T (2002). "In Vivo Study of Bacterial Adhesion to Five Types of Intraocular Lenses." Investigative Ophthalmology & Visual Science **43**(12): 3717-3721.

Kyritis, A., Pissi, P., Gómez Ribelles, J.L and Monleón Pradas (1995). "Polymer-water Interactions in Poly(hydroxyethylacrylate) Hydrogels Studies by Dielectric, Calorimetric and Sorption Isotherm Measurements." Polymer Gels and Networks **3**:445-469.

Larson, J.R. and Pfeiffer, C.D. (1983). "Determination of Alkyl Quaternary Ammonium-Compounds by Liquid-Chromatography with Indirect Photometric Detection." Analytical Chemistry **55**(2): 393-396.

Lee, S. and Laibinis, P.E. (1998). "Protein-Resistant Coatings for Glass and Metal Oxide Surfaces Derived from Oligo(Ethylene Glycol)-Terminated Alkyltrichlorosilanes." Biomaterials **19**(19): 1669-1675.

Lemoine, L (1993) "Experimental Assessment of the Effect of Marine Fouling on Sensors". IRFEMER Report DITI/GO/MM-93-07.

Lindman, B., Wennerstöm, H. and Eicke, H.F. (1980)."Introduction and Phenomenological Description of Amphiphile Solutions." Micelles, Topics in Current Chemistry **87**: Springer-Verlag, Berlin, Heidelberg and New York.

Mack, E. J., Okano, T., and Kim, S.W. (1987). Biomedical Applications of Poly (2-Hydroxyethyl Methacrylate) and its Copolymers. Hydrogels in Medicaine and Pharmacy. Ed. Peppas, N. A. Florida, CRC Press Inc. Boca Raton. **2**.65-93.

Maldonado-Codina, C. and Efron, N. (2005). "Impact of Manufacturing Technology and Material Composition on the Surface Characteristics of Hydrogel Contact Lenses." Clinical and Experimental Optometry **86**(6): 396-404.

Maldonado-Codina, C. and Efron, .N. (2004). "Impact of Manufacturing Technology and Material Composition On The Mechanical Properties Of Hydrogel Contact Lenses." Ophthalmic and Physiological Optics **24**(6): 551-561.

Manov, D.V., Chang, G.C. and Dickey, T.D. (2003). "Methods for Reducing Biofouling of Moored Optical Sensors." Journal of Atmospheric and Oceanic Technology 21:958-968.

Marshall, K.C., Stout, R. and Mitchell, R. (1971). "Mechanism of the initial Events in the Sorption of Marine Bacteria to Surfaces." Journal of General Microbiology **68**:337-348.

Marshallsay, D. (1989). A Review of Sensor Fouling within Water Treatment Processes. Water Research Centre Report No. 365E, 9-10, Swindon.

Masilamoni, G., Jesudoss, K.S, Nandakumar, K., Satapathy, K.K., Azariah, J. and Nair, K V.K. (2002). "Lethal and Sub-Lethal Effects of Chlorination on Green Mussel Perna Viridis in the Context of Biofouling Control in a Power Plant Cooling Water System." Marine Environmental Research **53**(1): 65-76.

McNeill, M.E. and Graham, N.B. (1992). "Properties Controlling The Diffusion and Release of Water-Soluble Solutes from Poly(Ethylene Oxide) Hydrogels 1. Polymer Composition." Journal of Biomaterials Science, Polymer Edition **4**(3): 305-322.

Meakin J.R, Hukins, D.W.L., Imrie, C.T., Aspden, R.M. (2003). "Theraml Analysis of Poly(2-Hydroxyethyl Methacrylate) (pHEMA) Hydrogels." Journal of Materials Science: Materials in Medicine **14**: 9-15.

Merianos, J. (2001). Surface-Active Agents. In Disinfection, Sterilization and Preservation. S. Block, Lippincott, Williams & Wilkins: 283-320.

Metcalfe, L. (1963). "Direct Gas Chromatographic Analysis of Long Chain Quaternary Ammonium Compounds." Journal of the American Oil Chemists Society **40**: 25-27.

Mirtaheri, P., Grimnes, S., Martisen, Ø G., and Tønnessen, T. I. (2004). "A New Biomedical Sensor for Measuring pCO_2." Physiological Measurement **25**:421-436.

Moroi Y., (1992). Micelles: Theoretical and Applied Aspects New York: Plenum Press, New York; London.

Morton, L.H.G., Gaylarde, C.C. and Surman, S.B. (1998). "Consideration of Some Implications of the Resistance of Biofilms to Biocides." International Biodeterioration & Biodegradation **41**((3-4)): 247-259.

Munro, W., Thomas, C.L.P., Simpson, I, Shaw, J. and Dodgson, J. (1996). "Deterioration of pH Electrode Response due to Biofilm Formation on the Glass Membrane." Sensors and Actuators B-Chemical **37**(3): 181-194.

Nakamura, A.K. and Morikawa, Y. (1982). "Separation of Surfactant Mixtures and Their Homologs by High-Performance Liquid-Chromatography." Journal of the American Oil Chemists Society **59 (1)**: 64-68.

Naldrett, M. J. (1993). "The Importance of Sulphur Crosslinks and Hydrophobic Interactions in the Polymerization of Barnacle Cement". Journal of the Marine Biological Association, UK 73:689-702.

Neu, T. R., Eitner, A. and Luz Paje, M. (2003).Development and Architecture of Complex Environmental Biofilms. Fossil and Recent Biofilms. A Natural History of Life on Earth. Eds. Krumbein, W.E., Paterson, D.M. and Zavarin, G.A.Kluwer Academic Publishers Dordrecht. 29-45.

Ng, C.O. and Tighe, B.J. (1976). Polymers in contact lens applications. VI. The 'dissolved' oxygen permeability of hydrogels and the design of materials for use in continuous-wear lenses. British Polymer. Journal **8**,118–123.

Opdahl, A.K.S. Kim, S.H., Koffas, T.S., Marmo, C. and Somorjai, G.A. (2003). "Surface mechanical properties of pHEMA contact lenses: Viscoelastic and adhesive property changes on exposure to controlled humidity." Journal of Biomedical Materials Research Part A **67A**(1): 350-356.

Parr, A.C.S., Smith, M.J., Beveridge, C.M., Kerr, A., M., Cowling, M. J. and Hodgkiess, T. (1998). "Optical Assessment of a Fouling-Resistant Surface (PHEMA Benzalkonium Chloride after Exposure to a Marine Environment." Advanced Materials for Optics and Electronics **8 (4)**: 187-193.

Peppas, N., and Reinhart, C.T. (1983). "Solute Diffusion in Swollen Membranes.Part 1. A New Theory." Journal of Membrane Science **15**(3): 275-287.

Peppas, N., Bures, P, Leobandung, W. and Ichikawa, H. (2000). "Hydrogels in Pharmaceutical Formulations." European Journal Of Pharmaceutics And Biopharmaceutics **50**(1): 27-46.

Peppas, N.A. and Moynihan, H.J. (1987). Structure and Phsical Properties of Poly (2-Hydroxyethyl Methacrylate) Hydrogels. Hydrogels in Medicine and Pharmacy. Ed. N. A. Peppas. Florida, CRC Press Inc. Boca Raton. **2**:49-64.

Pickard, G.L. and Emery, W.J. (1982). Descriptive Physical Oceanography. An Introduction. Oxford, Pergamon Press.

Poremba, K. (1995). "Hydrolytic Enzymatic Activity in Deep Sea Sediments. FEMS Micrbial Ecology." **16:** 213-222.

Quinn, C. P.,Pathak C.P., Heller, A.and Hubbell, J.A. (1995). "Photo-Cross-Linked Copolymers of 2-Hydroxyethyl Methacrylate, Poly(Ethylene Glycol) Tetra-Acrylate

Ratner, B.D. (1995). "Surface Modification of Polymers:Chemcial,Biological and Surface Analytical Challenges." Biosensors and Bioelectronics **10**: 797-804.

Refojo, M., and Yasuda, H. (1965). "Hydrogels from 2-Hydroxyethyl Methacrylate and Propylene Glycol Monoacrylate." Journal of Applied Polymer Science **9**: 2425-2435.

Refojo, M.F. (1965 [a]). "Glyceryl Methacrylate Hydrogels." Journal of Applied Polymer Science **9**: 3161-3170.

Refojo, M.F. (1965 [b]). "Permeation of water through some hydrogels." Journal of Applied Polymer Science **9**:3417-3426.

Refojo, M.F. (1976). Vapour Pressure and Swelling Pressure of Hydrogels. Hydrogels for Medical and Related Applications. ACS Symoposium Series.Ed. Andrade, J.D. Washington D C, American Chemical Society. **31**: 37-51.

Ricka, J and Tanaka, T. (1984). "Swelling of Ionic Gels: Quantitative Performance of the Donnan Theory." Macromolecules **17**: 2916-2921.

Robinson R.A. and Stokes R.H. (1968). The Measurement of Diffusion Coefficients. In Electrolyte Solutions, Butterworths Publications, London: 45-48.

Rooda, W.E., Bouwstra, J.A., De Vries, M.A., Kosho, C. and Junginger, H.E. (1987). "Changes in the Internal Structure of Hydrogels." Thermochemica Acta **112**: 111-116.

Rosso, F., Barbarisi, A., Barbarisi, M., Petillo, O., Margarucci, S., Calarco, A. and Peluso G (2003). "New Polyelectrolyte Hydrogels for Biomedical Applications." Materials Science & Engineering C-Biomimetic and Supramolecular SYSTEMS **23**(3): 371-376.

Saltzman, W.M. and Tena, L.B. (1991). "Spermicide Permeation through Biocompatible Polymers." Contraception **43** (50): 497-505.

Sawada, H.T.K., Tomita, T., Kawase, T., Baba, M., and Ide, T. (1997). "Antibacterial Activity of Fluoroalkylated Allyl- and Diallyl-Ammonium Chloride Oligomers." Journal of Fluorine Chemistry **84**: 141-144.

Schmidt, D.L., Lam, K., Schmidt, D.C. and Chaudhury, M.K. (2004). "Contact Angle Hysteresis, Adhesion, and Marine Biofouling." Langmuir **20**(7): 2830-2836.

Schnürer, J. and Rosswall, T. (1982). "Fluorescein diacetate hydrolysis as a measure of total microbial activity in soil and litter." Applied and Environmental Microbiology **43**: 1256-1261.

Silver, J.H., Lin, J.C., Lim, F., Tegoulia, V.A., Chaudhury, M.K. and Cooper, S.L. (1999). "Surface Properties and Hemocompatibility of Alkyl-Siloxane Monolayers Supported on Silicone Rubber: Effect of Alkyl Chain Length and Ionic Functionality." Biomaterials **20**(17): 1533-1543.

Smith, M. J., Adam, G., Duncan, H. J. and Cowling, M. J. (2002[a]). "The Effects of Cationic Surfactants on Marine Biofilm Growth on Hydrogels." Estuarine, Coastal and Shelf Science. **55**: 361-367.

Smith, M.J. The Use of Cationic Surfactants in Marine Anti-fouling Applications. M.Sc. Thesis, 1997, University of Glasgow.

Smith, M.J., Flowers, T.H., Cowling, M.J. and Duncan, H.J. (2002[b]). Method for the measurement of the diffusion coefficient of benzalkonium chloride. Water Research **36**: 1423-1428.

Stanczak, M. (2004). "Biofouling: It's not just barnacles". Cambridge Scientific Abstracts.

Steinberg, P.D. (2005). "Natural anti-fouling stratrgies". Abstracted in :Cloete, T.H.. "Alternative and conventional anti-fouling strategies." International Biodeterioration and Biodegradation **56**, 121-134.

Steinberg, P.D. (2005). "Natural anti-fouling stratrgies". Abstracted in :Cloete, T.H.. "Alternative and conventional anti-fouling strategies." International Biodeterioration and Biodegradation **56**, 121-134.

Stewart, P.S. and Costerton, J.W. (2001). Antibiotic Resistance of Bacteria In Biofilms. The Lancet **358**: 135-138.

Stewart, P.S., McFeters, G.A. and Huang, C-H. (2000). Biofilms II: Process Analysis and Applications. A John Wiley & Sons, New York and Chichester: 373-405.

Stokes R.H. (1950) An Improved Diaphragm-Cell For Diffusion Studies, and some Tests of the Method. Journal of American Chemical .Society **72**: 763-767.

Stubberfeild, L.C.S. and Shaw, P.J.A. (1990) "A Comparison of Tetrazolium Reduction and FDA Hydrolysis with Other Measurements of Microbial Activity." Journal of Microbiological Methods **12**: 151-162.

Suortti, T. and Sirvio, H. (1990). "Determination of Fungistatic Quaternary Ammonium-Compounds in Beverages and Water Samples by High-Performance Liquid-Chromatography." Journal of Chromatography **507**: 421-425.

Swan, E.A. and Peppas, N.A. (1981). "Drug Release Kinetics from Hydrophobic Porous Monolithic Deivices." Controlled Release Bioactive Materials **8**: 18-23.
Tanaka, T. (1981). Gels. Scientific America **244**:110-123.

Swilley, E.L., Busch, A.W. and Williams, D.A. (1967). "Kinetics Mass Transfer and Organisms Growth in a Biological Film Reactor". Transactions in Instruments in Chemical Engineering **45** (6): T257-T264.

Tarsiche, I.H.E. and Ciurchea, D. (1997). "Least-Squares Analysis of Ammonia Diffusion through PTFE Membranes." Measurement Science & Technology". **8**(11): 1367-1371.

Taylor, R., Verran, J., Lees, G.C. and Ward, A. J. P. (1998). "The Influence of Substratum Topography on Bacterial Adhesion to Polymethyl Methacrylate." Journal of Materials Science-Materials in Medicine **9**(1): 17-22.

Tighe, B. (1992). "Eye Contact". Chemistry in Britain **March**: 241-244.

Tonge, S., Jones, L., Goodall, S. and Tighe, B (2001). "The Ex Vivo Wettability of Soft Contact Lenses." Current Eye Research **23**(1): 51-59.

Topiwala, H.H. and Hamer, G. (1971). "Effect of Wall Growth in Steady State Continuous Culture. Biotechnology and Bioengineering **8**: 919-922.

UK Marine SACS Project –Surfactants. www.ukmarinesac.org.uk.

Varade, D., Joshi, T., Aswal, V.K., Goyal, P.S., Hassan, P.A. and Bahadur, P. (2005). "Effect of Salt on the Micelles of Cetyl Pyridinium Chloride". Colliods and Surfaces A: Physiochemical Engineering Aspects **259**: 95-101.

Vaidyanathan, L.V. and Nye, P.H. (1966). "Measurement and Mechanism of Ion Diffusion in Soils 2. An Exchange Reisn Paper method for Measurement of Diffusive Flux and Diffusion Coefficient of Nutrient Ions in Soils." Journal of Soil Science **17** (2):175-183.

Waite, J. (1983). "Adhesion in Byssally Attached Bivalves." Biological Reviews of the Cambridge Philosophical Society **58**(2): 209-231.

Waite, J. (1983). "Evidence for a Repeating 3,4-Dihydroxyphenylalanine-Containing and Hydroxyproline-Containing Decapeptide in the Adhesive Protein of the Mussel, *Mytilus-Edulis*-L." Journal of Biological Chemistry **258**(5): 2911-2915.

Watson, R.J, Butler, E.C.V., Clementson, L.A. and Berry, K.M. (2005). "Flow-injection Analysis with Fluorescence Detection for the Determination of Trace Levels of Ammonium in Seawater." **7**: 37-42.

Wee, V. (1984). "Determination of Cationic Surfactants in Wastewater and River Water." Water Research **18**(2): 223-225.

Weissman, B.A. and Fatt, I. (1991.) "Contact lens wear and oxygen permeability measurements" Current Opinion in Ophthalmology **2**:88–94.

Whelan, A. and Regan, F. (2006). "Antifouling strategies for marine and riverine sensors." Journal of Environmental Monitoring **8**: 880-886.

White, D.C. (2005). "Fouling-control using novel non-toxic, biodedradable small molecules derived from combinatorial chemistry based on natural antifoulant" . Abstracted in: Cloete, T.H.. "Alternative and conventional anti-fouling strategies." International Biodeterioration and Biodegradation **56**, 121-134.

Wichterle, O., and Lim, D. (1960). "Hydrophilic Gels for Biological Use." Nature, **185**: 117-118.

Wichterlova, J., Wichterle, K. and Michalek, J. (2005). "Determination of Permeability and Diffusivity of Oxygen in Polymers by Polarographic Method with Inert Gas." Polymer **46**(23): 9974-9986.

Wilke, C.R. and Chang, P. (1955). "Correlation of Diffusion Coefficients in Dilute Solutions." Journal of the American Institute of Chemical Engineers **1**(2): 264-270.

Wimpenny, J. (1996). "Ecological Determinants of Biofilm Formation." Biofouling **10**: (1-3): 43-63.

Wisniewski, N. and Reichert, M. (2000). "Methods for Reducing Biosensor Membrane Biofouling." Colloids and Surfaces B-Biointerfaces **18**(3-4): 197-219.

Wisniewski, N., Moussy, F. and Reichert, W.M. (2000). "Characterization of Implantable Biosensor Membrane Biofouling." Fresenius Journal of Analytical Chemistry **366**(6-7): 611-621.

Wisniewski, S. J., Gregonis, D.E., Kim, S.W. and Andrade, J.D. (1976). Permeation of Water through Poly (2-Hydroxyethyl Methacrylate) and Related Polymers. Diffusion through Hydrogel Membranes: 80-87.

www.firsttenangstroms.com, Portsmouth, Virginia23704, USA.

Xiao, D, Mo, Y.Y. and Choi, M.M.F. (2003). "A Hand-Held Optical Sensor for Dissolved Oxygen Measurement." Measurement Science & Technology **14**(6): 862-867.

Yancy (2002). Deep-Sea Biology. SciLinks Program, National Science Teachers Association. www.whitman.edu/-yancy/deepsea.html.

Yasuda, H., Ikenberry, L.D. and Lamaze, C.E. (1969). "Permeability through Hydrated Polymer Membranes. Part II Permeability of Water Soluble Organic Solutes." Die Makromolekulare Chemie **125**: 108-118.

Yasuda, H., Lamaze, C.E. and Ikenberry, L.D. (1968). "Permeability through Hydrated Polymer Membranes. Part I Diffusion of Sodium Chloride". Die Makromolekulare Chemie **118**: 19-35.

Yebra, D., Kiil, S. and Dam-Johansen, K (2004). "Antifouling Technology - Past, Present and Future Steps Towards Efficient and Environmentally Friendly Antifouling Coatings." Progress in Organic Coatings **50**(2): 75-104.

YSI Corporation Literature, YSI Incorporated, 1725 Brannum Lane, Yellow Springs, OH 45387, USA.

Zhang, W and Hallstrom, B. (1990) Membrane Characterization Using the Contact-Angle Technique.1. Methodology of the Captive Bubble Technique. Desalination **79**: 1-12.

Ziegelaar, B, Fitton, J.H., Clayton, A.B., Platten, S.T., Maley, M.A.L. and Chirila, T. V. (1999). "The Modulation of Corneal Keratocyte and Epithelial Cell Responses to

Poly(2-Hydroxyethyl Methacrylate) Hydrogel Surfaces: Phosphorylation Decreases Collagenase Production in Vitro." Biomaterials **20**(21): 1979-1988.

Zobell, C. E. (1943). "The Effect of Solid Surfaces upon Bacterial Activity." Journal of Bacteriology **46**: 39-56.

Appendix

Biofouling, 2006; 22(3): 173–185

Taylor & Francis
Taylor & Francis Group

The prevention of microfouling and macrofouling on hydrogels impregnated with either Arquad 2C-75® or benzalkonium chloride

PHILLIP R. COWIE[1], MARGARET J. SMITH[2], FIONA HANNAH[1], MIKE J. COWLING[2] & TREVOR HODGKEISS[2]

[1]*University of London, Marine Biological Station Millport, Isle of Cumbrae, Scotland, and* [2]*Glasgow Marine Technology Centre, University of Glasgow, Glasgow, Scotland, UK*

(Received 2 December 2005; accepted 21 March 2006)

Abstract
Optically clear, surfactant loaded poly (2-hydroxyethyl methacrylate) (pHEMA) hydrogels can be used to prevent fouling on optical windows of marine underwater sensors. To act successfully in this capacity, hydrogels need to prevent both microfouling and macrofouling. Panel trials were conducted using four different materials: unloaded hydrogels, hydrogels containing either benzalkonium chloride (BAC) or dicocodimethylammonium chloride (Arquad 2C-75®) and PMMA coupons. Three panels were deployed at staggered intervals (2, 4 and 6 weeks) before the main settlement season of *Semibalanus balanoides* and *Mytilus edulis* in the Firth of Clyde, Scotland. Panels were left for a total period of 10, 12 and 14 weeks respectively. Results showed that no sample completely resisted fouling, but Arquad 2C-75® hydrogels were extremely effective at preventing both microfouling and macrofouling. The most heavily fouled materials were unloaded hydrogels and PMMA, despite differences in initial hydrophilicities. Arquad 2C-75® hydrogels were equally effective at preventing larval settlement, for up to 14 weeks.

Keywords: *Hydrogels, antifouling, barnacles, microfouling, optical sensors*

Introduction

The economic impact of marine biofouling on a range of commercial activities is well known. These range from the reduction of commercial ships' speed and manoeuvrability to negative impacts on heat exchanger systems found within desalination plants and power stations (Mussalli & Tsou, 1989). Biofouling has also been shown to cause considerable problems with more specialised scientific monitoring equipment placed into the sea (Kerr et al. 1998). Recent changes in the European Union Water Quality Directive (Commission of the European Communities, 1997/1998) and concerns about issues of global warming have resulted in increased usage of scientific equipment placed in the seas of the world to monitor a range of parameters including fluorescence and turbidity. The composition of the sensor arrays on these instruments varies according to the parameter being monitored and many of these sensors possess optical components. Studies have shown that even moderate microbial fouling can impair the ability of optical instruments to take accurate readings (Kerr et al. 1998). This, combined with the fact that modern technology allows uninterrupted data logging over long time periods, means that the need has arisen for optical sensor windows that will remain clean during extended deployments in the marine environment. Various methods of preventing fouling on optical sensors have been developed including wipers and shutters. These techniques are viewed as being 'active', utilising electrical energy for their operation. Novel, passive antifouling techniques also exist, including optically clear hydrogels poly-(hydroxyethyl methacrylate) (pHEMA) with microporous structures that allow the hydrogels to be easily loaded with water-soluble fouling-resistant chemicals. These antifouling polymer coatings have been developed at the Glasgow Marine Technology Centre (Cowling et al. 1998).

Previous trials in the Firth of Clyde showed that hydrogels containing either of the cationic surfactants benzalkonium chloride (BAC) or dicocodimethylammonium chloride (Arquad 2C-75®) are highly effective at preventing microfouling for up

Correspondence: Phillip Cowie, University of London, Marine Biological Station, Isle of Cumbrae, Scotland. Fax: + 01475 530601.
E-mail: pcowi001@udcf.gla.ac.uk

ISSN 0892-7014 print/ISSN 1029-2454 online
DOI: 10.1080/08927010600783296

to 3 months (Smith et al. 2002). However, in the Firth of Clyde, these trials mainly have been conducted during times of the year when the fouling pressure is not predominantly macrofaunal in nature. The development of bacterial and algal biofilms on optical sensors is initially important and may significantly impair instrument readings (Kerr et al. 1998). Subsequent macrofouling may completely obliterate the signals in some instrumentation. The panel trials conducted during the present study were specifically designed to test the antifouling properties of impregnated hydrogels against both microfouling and, more importantly, the major fouling organisms *Semibalanus balanoides* (Linnaeus) and *Mytilus edulis* (Linnaeus).

In the Firth of Clyde, *S. balanoides* has a typically well-defined settlement period from March to mid-April when high numbers of barnacle cyprids (from 2–10 cm^{-2}) can occur on various surfaces (Hills & Thomason, 1998; Hills et al. 1998). Trials were aimed at utilising this relatively predictable settlement season to answer three questions: i) do Arquad 2C-75® hydrogels prevent microfouling and the settlement of *S. balanoides* and *M. edulis*? ii) is there a difference in the abundance of *S. balanoides* and *M. edulis*, which settle on Arquad 2C-75® and BAC-impregnated hydrogels, unloaded (blank) gels and PMMA coupons? and iii) is prevention of barnacle and mussel settlement affected by the time hydrogels are exposed to the environment prior to the settlement season through the reduction of antifouling action over time?

Materials and methods

Hydrogel preparation

The hydrogels prepared for this trial were based on the monomer hydroxyethylmethacrylate (HEMA) and were crosslinked with tetraethylene glycol dimethacrylate, producing the polymer poly-hydroxyethylmethacrylate (pHEMA) which is a transparent lightly cross-linked material containing 40% water. The coating was fabricated in sheet form by solution polymerisation. Hydrogels, so prepared, contained either the cationic surfactants benzalkonium chloride (BAC) or dicocodimethylammonium chloride (Arquad 2C-75®) or remained as blank hydrogels (containing no antifoulant). Blank hydrogels used were transparent and contained 40% water. They were prepared in 250 × 200 mm poly-methyl methacrylate (PMMA) moulds to a thickness of 1–2 mm then stored in distilled water until required. The full details of their preparation can be found elsewhere (Refojo, 1966; Smith, 1997). For each of the three panels deployed, three hydrogel sheets were prepared and soaked in either BAC or Arquad 2C-75® (2C-75®) solution for 3 weeks prior to the marine exposure trial. Zero time analysis of the BAC levels in the hydrogels was carried out using high performance liquid chromatography (HPLC) ultra-violet detection at 214 nm (Guilfoyle et al. 1990). Arquad 2C-75® was analysed using a Dionex Ion Conductivity Detector ED-40 with a cation suppresser. The instrument was used as a flow injection system. Water was used as the eluent with a flow rate of 1 ml min^{-1}. Three replicate discs (25 mm diameter) of hydrogel were removed from each sheet and quantitatively analysed for BAC and 2C-75®. At zero time, the BAC content was 46.7 ± 2.41 mg g^{-1} of hydrogel and the 2C-75® content was 8.7 ± 2.0 mg g^{-1} of hydrogel.

Each hydrogel sheet was cut into smaller hydrogel coupons (60 × 80 × 1 mm) and three pieces of each differently treated hydrogel, along with three PMMA samples of the same size, were attached to a polymethylmethacrylate (PMMA) rack in a four by three arrangement. PMMA samples were incorporated into the trial to act as controls for optical windows constructed from PMMA. After deployment, the amount of BAC and 2C-75® remaining in the three replicates from each panel was determined using the techniques described above.

Marine deployment

There was a staggered deployment of panels, with 2-week intervals between each deployment. Each panel was prepared on the same day as it was deployed. The four materials used were arranged on the three panels in 'pseudo-latin squares' with three replicates of each material per panel. Table I shows a typical layout. Panels were deployed by suspending them 0.5 m below the sea surface at Keppel Pier, located in the Firth of Clyde. All panels were then removed on 21 June 2004 and taken to the laboratory for processing. This meant that panel 3 was deployed for a total of 14 weeks, panel 2 for 12 weeks and panel 1 for 10 weeks.

Laboratory techniques

The (48 cm^2) rectangular coupons were removed from the panels and the numbers of barnacles and mussels present on each coupon counted using a

Table I. Example of 'pseudo-latin square' arrangement of materials on Panel 3 deployed for a total of 14 weeks.

PMMA	BLANK	2C-75®	BAC
BLANK	2C-75®	BAC	PMMA
2C-75®	BAC	PMMA	BLANK

binocular microscope. Following macrofaunal counts, three 2.5 cm^2 sub-cores were taken from each coupon for use in subsequent BAC and Arquad 2C-75® quantification, fluorescein diacetate (FDA), and chlorophyll *a* analysis. It was impossible to core the PMMA coupons and, where appropriate, equivalent surface areas of PMMA were scraped for FDA analysis and chl *a* quantification.

FDA analysis

Estimation of marine biofilm activity was carried out using a modification of the Adam and Duncan (2001) method. One sub-core from each hydrogel coupon was placed into individual 60 ml glass powder jars. Fifteen millilitres of 60 mM potassium phosphate buffer, pH 7.6 (8.7 g K_2HPO_4 : 1.3 g KH_2 PO_4, made up to 1 l in deionised water) was added to each jar and 0.2 ml of 1000 μg fluorescein diacetate (FDA) (3′6′-diacetyl-fluorescein, Sigma-Aldrich Company Ltd) ml^{-1} acetone solution were added to start the reaction. Acetone-killed controls were also prepared as per Battin (1997), where subcores were prepared in 50% acetone v/v 30 min prior to the addition of buffer and FDA. All jars were then placed in an orbital incubator (Gallenkamp orbital incubator, 1000 rev min^{-1}) at 10°C ± 1°C for 1 h. Once removed from the incubator, the 25-mm diameter cores were taken out of the buffer/FDA solution and 15 ml of chloroform/methanol (2:1 v/v) were added immediately to terminate the hydrolysis reaction. Jars and their contents were then shaken thoroughly by hand and the contents of each jar were filtered (Whatman, No. 2) into 100 ml conical flasks. Filtrates were measured at 490 nm on a spectrophotometer (Schimazdu UV-visible 2101PC spectrophotometer). Blanks from each treatment were used to zero the spectrophotometer before reading sample absorbance. The concentration of fluorescein released during the assay was calculated using the calibration graph produced from 0–5 μg fluorescein ml^{-1} standards, which were prepared from a 20 μg fluorescein (sodium salt, Merck-BDH, Analar) ml^{-1} standard solution by appropriate dilution in 60 mM potassium phosphate buffer, pH 7.6.

Chlorophyll a quantification

Biofilms on sub-cores were scraped into acetone-resistant test tubes containing 10 ml of acetone. Subsequent chl *a* extraction and quantification followed the methods of Parsons et al. (1984) using an LKB Biochrom spectrophotometer (Model: Ultrospec 4050). The equations of Nusch (1980) were used to calculate the final concentrations of chl *a* in the sample, which gave an indication of the quantities of photosynthetically active organisms (macroalgae, microalgae and photosynthetic bacteria) that were present on the core samples.

Optical assessment using visible spectrophotometric analysis

Optical assessment was carried out using the methods described in Parr et al. (1998). Briefly, transmittance data were collected using a Shimadzu UV-2101PC UV-visible scanning spectrophotometer fitted with a LISR-2100 integrating sphere attachment. A wavelength range of 400–700 nm was selected (encompassing the wavelengths commonly used by optical instruments). Measurements were made with quartz cells (Hellma, internal dimensions 60 × 80 × 20 mm) using a seawater-filled cell as the reference. The coupon material remaining after subsampling for other techniques was cut into a rectangle (80 × 30 mm) and clamped between cut out PMMA templates. This enabled the samples to fit into the sample quartz cell without 'sagging'. Two scans of different areas on the coupons were taken to compensate for biofouling heterogeneity on the slides.

Captive bubble measurement

The wettability of the four test materials was determined using the captive bubble technique (Zhang & Hallström, 1990). This technique was chosen because it kept the hydrogels hydrated throughout the test, preventing drying of their surfaces and anomalous results (Hermitte et al. 2004). Captive bubble measurement was carried out in an optically clear glass box (55 × 55 × 55 mm), filled with sterile seawater (3.5%). Work was carried out at ambient temperature, which was 22 ± 2°C for the duration of the tests. The hydrogel and pMMA pieces were held in place using a holder made of PMMA, which allowed the test piece to be exposed to the water in the tank. The surfaces were soaked in sterile seawater for 72 h prior to testing to allow them to acclimate to the polar environment. Polymer surfaces are particularly mobile and the molecular orientation of the surface at any point in time may be modified in response to the surrounding environment (Tonge et al. 2001). The surfaces of test materials also were tested after 10 weeks soaking in sterile seawater to determine changes to contact angles over time. The bubble was supplied to the surface via a 1 ml syringe with a 25-gauge needle to allow control of the volume. The bubbles were generated in the liquid and captured on the test surface as a result of buoyant transport and attachment. All bubbles were 2–3 mm in diameter. It previously has been observed that no change in angle was found on a homogeneous surface for bubbles ranging from 1–7 mm (Drelich et al. 1996). Measurements were carried out in triplicate

on each sample piece and three pieces of each material were tested.

Captive bubbles were photographed using a JVC video camera fitted with a Viviter 55 mm F2.8 macro lens. The contact angles of captive bubbles were determined by image analysis of photographs using a computer program ('C' Builder program for Windows) written to measure contact angles. The image is selected and displayed in its frame. With the mouse, the user then draws the incident angle of the bubble. The mouse positions in x and y are stored in a matrix. A curve-fitting algorithm is used to determine the mathematical function of the curve which is differentiated to obtain the angle.

Results

BAC and Arquad 2C-75® quantification

As noted earlier, the zero time content of BAC in the hydrogels was 46.7 $\pm$ 2.41 mg g^{-1} of hydrogel. At the end of the 10, 12 and 14 weeks deployment, the BAC contents of the hydrogels were 27.1 $\pm$ 1.57 mg g^{-1} of hydrogel, 22.7 $\pm$ 1.00 mg g^{-1} of hydrogel, and 21.3 $\pm$ 1.97 mg g^{-1} of hydrogel, respectively. 2C-75® in the 14-week panels dropped to final levels of 5.82 $\pm$ 0.69 mg g^{-1} of hydrogel (zero time content was 8.7 $\pm$ 2.0 mg g^{-1} of hydrogel).

Fouling prevention efficacy of Arquad 2C-75® hydrogels

Macrofouling. Figure 1 shows the extent of fouling on the test pieces immersed for a total of 14 weeks. This photograph shows that there are marked visible differences in the extent of fouling on the different materials and that the hydrogels incorporating 2C-75® were the least fouled of those tested. Similar fouling patterns were observed on the panels exposed for 12 and 10 weeks. Enumeration of macrofouling organisms on the panels showed that barnacle settlement was less than expected. This was due to unseasonably strong storms, which occurred in March and early April and hindered barnacle settlement. Consequently, barnacle cyprids settled later (last week in April), in lower numbers, and over a much longer time period than typically occurs in this region (personal observations). This meant that, prior to the challenge of barnacle settlement, panel 3 had been deployed for 6 weeks, panel 2 for 4 weeks and panel 1 for 2 weeks. High numbers of mussels settled out on some of the materials during the exposure period.

On all three panels, the highest numbers of juvenile barnacles and mussels were found on the PMMA and blank hydrogels (Figure 2). On the 14-week panel, macrofouling organisms were present on the test coupons in the order of (from the highest to the lowest abundance) blank hydrogels → PMMA → BAC → 2C-75® hydrogels. The highest mean abundances of *S. balanoides* (18 $\pm$ 17 per 42 cm^2) and *M. edulis* (44 $\pm$ 4 per 42 cm^2) were found on the 14-week blank hydrogel samples. No barnacles or mussels were found attached to the 2C-75® hydrogel test-pieces on the 14-week panel and only one mussel was found attached to a BAC hydrogel via byssus threads in contact with the gel but not directly attached to the hydrogel surface.

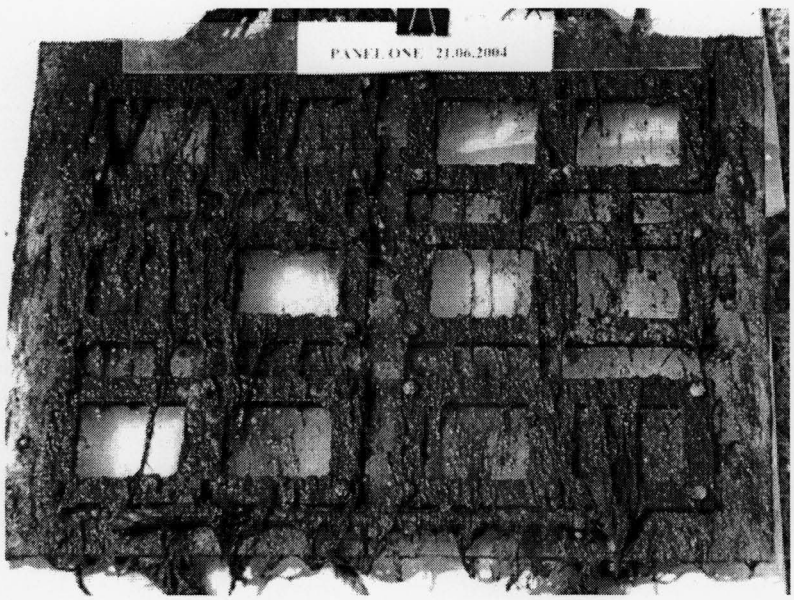

Figure 1. Extent of biofouling on hydrogel coupons and PMMA controls on a PMMA frame after 14 weeks' deployment. Top row (from left to right) = PMMA, unloaded hydrogel, Arquad 2C-75® and BAC.

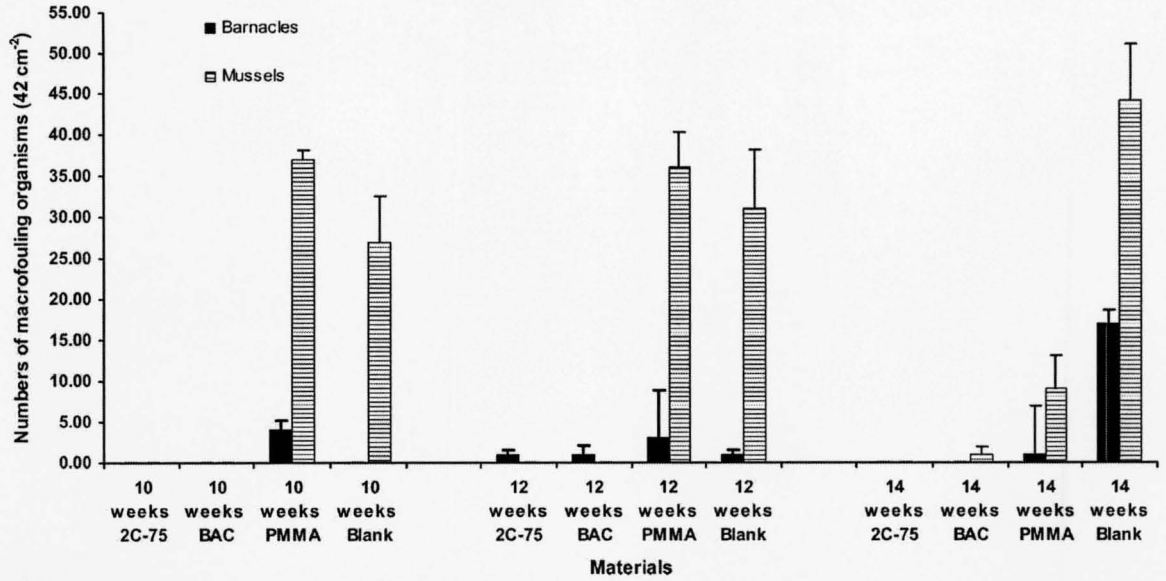

Figure 2. Mean abundance ($n = 3$) of macrofouling organisms (per 42 cm^2) found on test coupons after the removal of all racks on 21 June 2004. Periods of panel deployment are indicated on the graph. Error bars = upper SDs.

A similar pattern of fouling was observed on the panels deployed for 12 and 10 weeks (only). On these panels, there was less of a clear-cut distinction between the abundance of macrofouling organisms attached to the blank hydrogels and PMMA. On the 12-week panel, there were similar numbers of mussels on the blank hydrogels and PMMA (31 ± 4 per 42 cm^2 and 36 ± 7 per 42 cm^2, respectively). Only one barnacle was found attached to a 2C-75® hydrogel on the panel deployed for 12 weeks.

Chl a and FDA analysis. Chl *a* analysis (Table II) showed that the most heavily fouled substrata in terms of micro- and macroalgae, were the unloaded (blank) hydrogels. Blank gels on the panel that were deployed for only 10 weeks showed the highest levels of algal fouling, viz., 12.7 ± 1.8 $\mu g\ cm^{-2}$. PMMA coupons were the next most heavily fouled, with the PMMA coupons on the panel deployed for 14 weeks showing the highest mean levels of fouling (2.3 ± 2.0 $\mu g\ cm^{-2}$). Chl *a* levels extracted from the surfaces of the unloaded hydrogels and PMMA coupons were indicative of the presence of both microalgal and macroalgal biomass because multicellular algae were visible on both these substrata. Lower levels of algal fouling were found on BAC coupons and, similar to the fouling on PMMA and blank hydrogels, the lowest levels of chl *a* were extracted from 12-week hydrogels. Negligible amounts of chl *a* (0.1 ± 0.1 $\mu g\ cm^{-2}$) were extracted from 2C-75® cores on the panel deployed for 14 weeks. These values were indicative of the development of mixed bacterial/diatom biofilms on this substratum because multicellular algae were not visible on these hydrogels. No chl *a* was extracted from the 10- or 12-week 2C-75® coupons.

Table II. Mean levels ($n = 3$, $\pm$ 1 SD) of chl *a* ($\mu g\ cm^{-2}$) and results of FDA ($\mu g\ ml^{-1}\ h^{-1}$) analysis of coupons from the different panels.

	Material	Chl *a* ($\mu g\ cm^{-2}$)	FDA ($\mu g\ ml^{-1}\ h^{-1}$)
10 weeks	2C-75®	0.0 (±0)	0.0 (±0)
	BAC	1.1 (±0.8)	0.07 (±0.1)
	PMMA	1.5 (±0.6)	0.47 (±0.4)
	BLANK	12.7 (±1.8)	0.55 (±0.3)
12 weeks	2C-75®	0.0 (±0.0)	0.07 (±0.1)
	BAC	0.1 (±0.1)	0.19 (±0.1)
	PMMA	0.9 (±0.3)	0.28 (±0.1)
	BLANK	3.8 (±0.8)	0.69 (±0.5)
14 weeks	2C-75®	0.12 (±0.1)	0.05 (±0.1)
	BAC	0.7 (±0.6)	0.29 (±0.1)
	PMMA	2.3 (±2.0)	1.20 (±0.9)
	BLANK	5.5 (±1.2)	1.64 (±0.3)

Results of FDA analysis (an estimate of biofilm activity) indicated that the materials with the highest levels of algal fouling (PMMA and blank hydrogels) also had the highest levels of microbial fouling on all three panels. The highest levels of hydrolytic activity were found on blank hydrogel and PMMA coupons after 14 weeks deployment (1.64 ± 0.3 and 1.20 ± 0.9 μg FDA $ml^{-1}\ h^{-1}$ respectively). The lowest levels of microbial activity were found on 2C-75® coupons deployed for 10 weeks where no reduction of FDA was recorded.

Effect of prior exposure period on efficacy of antifouling action of Arquad 2C-75®

Macrofouling. Figure 2 shows that there was no obvious evidence of a temporal fouling pattern with the panel deployed the longest, showing a greater settlement of barnacles and mussels than panels deployed for shorter periods. There also was no apparent reduction in the ability of 2C-75® gels, which been deployed for 6 weeks prior to barnacle/mussel settlement, to deter settlement when compared with hydrogels that had been deployed for 4 and 2 weeks before settlement. All 2C-75® hydrogels were equally effective at preventing macrofouling over the period studied. Similarly, there was no evidence that the efficacy of BAC-impregnated hydrogels to prevent macrofouling decreased with increased time of deployment. No macrofoulers were found on BAC coupons deployed for 10 weeks, mean values of 1 ± 1 barnacles 42 cm^{-2} were found on the 12 weeks hydrogels, while 1 ± 1 mussels were found attached to the 14 week BAC hydrogels. With the blank hydrogels, there was evidence of increasing abundances of *M. edulis* with increased deployment time. Higher abundances (44 ± 7 per 42 cm^2) of *M. edulis* were found on blank hydrogels deployed for 14 weeks in comparison with abundances on 10-week hydrogels (27 ± 6 per 42 cm^2).

Chl a and FDA analysis. Table II indicates that, on the 2C-75® hydrogels, no recordable microbial activity was measured on panel 1 (10 weeks) and only low levels on subsequent panels, as indicated by the results of FDA analysis on samples deployed for 12 and 14 weeks (0.07 ± 0.1 $\mu g\ ml^{-1}\ h^{-1}$ and 0.05 ± 0.1 $\mu g\ ml^{-1}\ h^{-1}$ respectively). There was no obvious evidence of steadily increasing levels of pigmented cells occurring on the panels deployed over time. Low levels of microalgal fouling (0.12 ± 0.1 $\mu g\ cm^{-2}$ chl *a*) were found on the 14-week samples, only.

Optical assessment using visible spectrophotometric analysis

Examination of the transmission data for the materials removed from 10-, 12-, and 14-week panels (Figures 3, 4, and 5) showed that the level of transmission through these materials in order of greatest transmission to least was: 2C-75® hydrogels > BAC hydrogels > PMMA > blank hydrogel.

Transmission through all materials was reduced within the 400–450 nm range. Optical assessment showed that the poorest light transmission was through blank hydrogels, with negligible levels of transmittance occurring through 10-week blank hydrogels. Only slightly less impaired transmission (10–15%) occurred through the blank samples removed from the 12- and 14-week panels. Transmission through PMMA coupons was greater than through blank hydrogels, from 20–30%

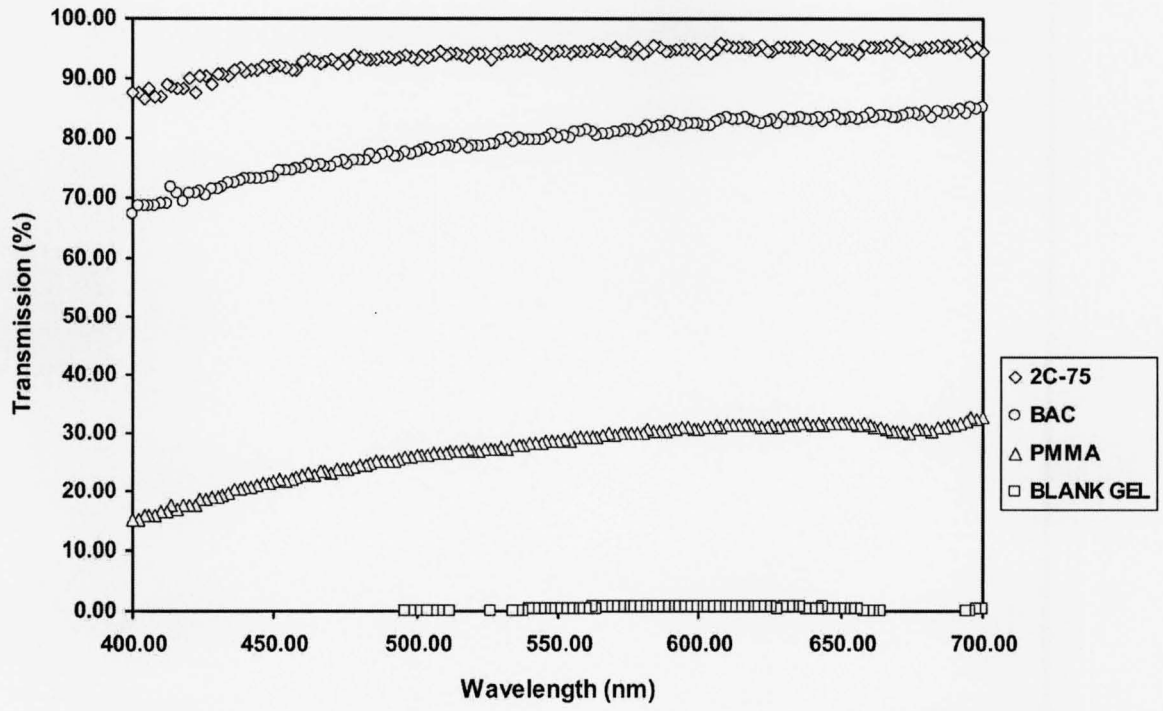

Figure 3. Mean transmission spectra ($n = 3$) obtained for materials removed from the rack immersed for 10 weeks.

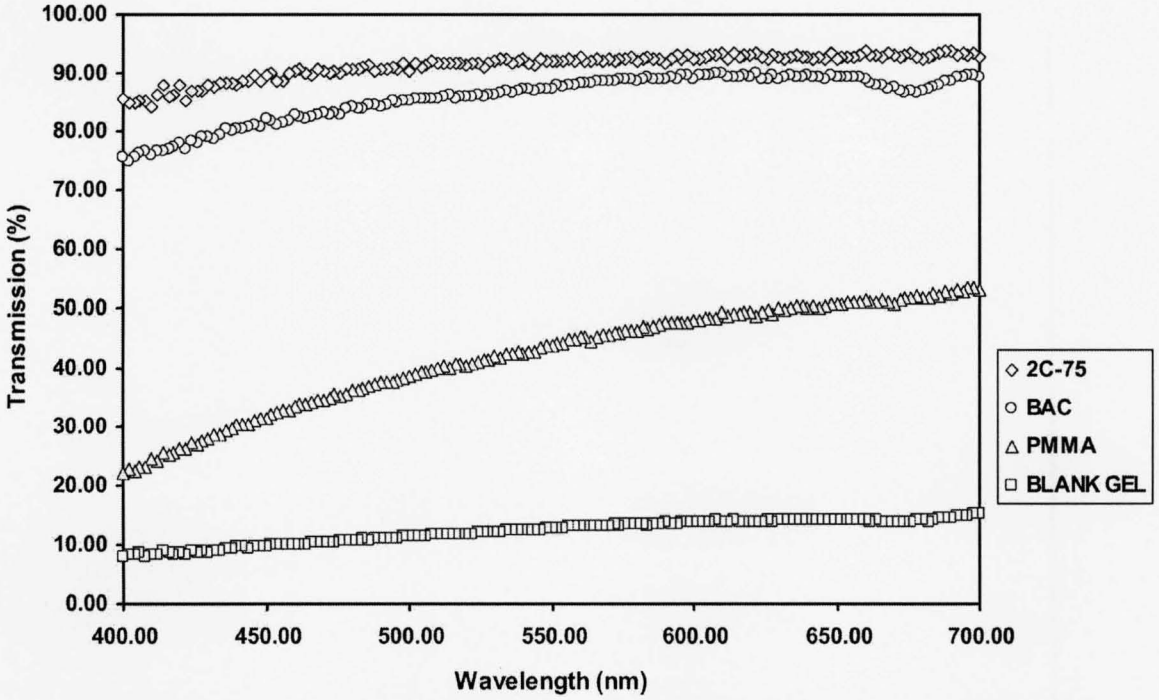

Figure 4. Mean transmission spectra ($n = 3$) obtained for materials removed from the rack immersed for 12 weeks.

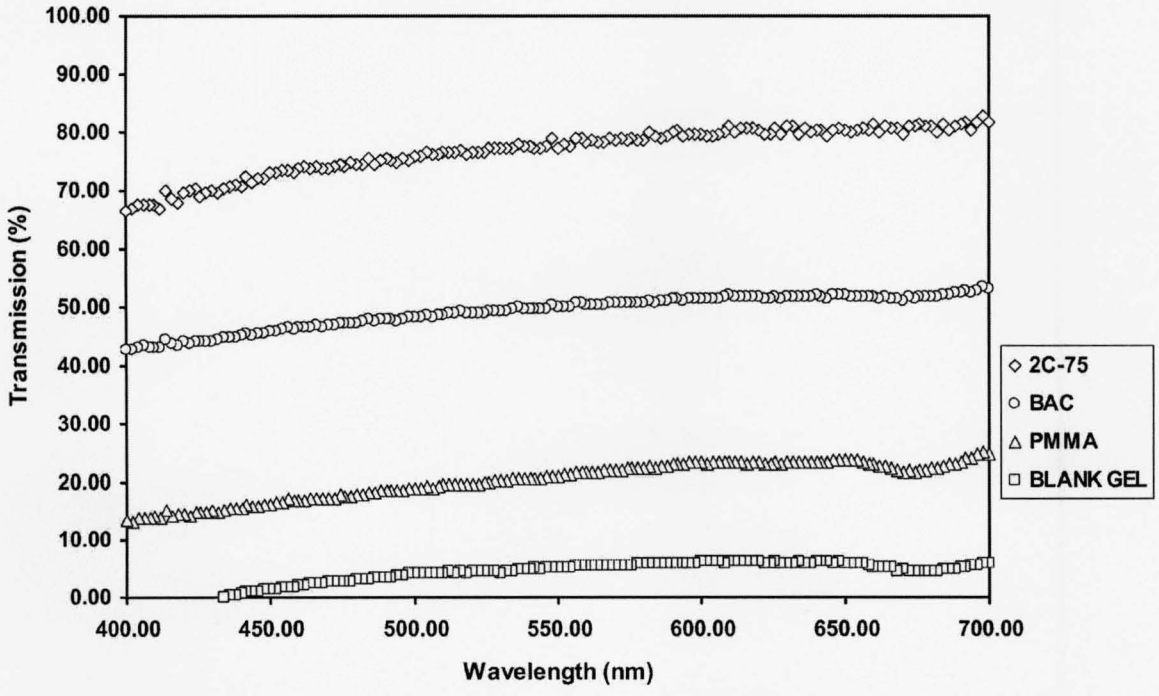

Figure 5. Mean transmission spectra ($n = 3$) obtained for materials removed from the rack immersed for 14 weeks.

transmission through the 10- and 14-week samples, increasing to *ca.* 50% transmission within the 650–700 nm range for 12-week samples.

Depending on the wavelengths being examined, transmission through 10-week BAC hydrogels was up to 50% higher than the transmission through the PMMA coupons. The difference in transmission between the two materials was reduced for the 12-week (BAC 10–25% higher) and 14-week (BAC 15–30% higher) coupons.

There was evidence of a slight temporal trend in the transmission data with successive decreases in transmission occurring with increased biofouling exposure periods. This trend was most consistently seen in transmission through 2C-75® hydrogels. Examination of two representative wavelengths (400 nm and 700 nm) shows that transmissions through the 10-week 2C-75® hydrogels were *ca.* 88% (400 nm) and 95% (700 nm), dropping to 67% (400 nm) and 82% (700 nm) for the 14-week samples.

Contact angle measurements

Figure 6 summarizes the underwater contact angles obtained after soaking the test materials in sterile seawater for 72 h and 10 weeks. The mean values obtained after 72 h show that 2C-75® hydrogels had the lowest contact angles ($16 \pm 5°$); i.e. a higher hydrophilicity than both the BAC ($33 \pm 6°$) and unloaded hydrogels ($30 \pm 4°$). The value found for the untreated hydrogel was similar to that found by Hermitte et al. (2004). PMMA control samples had the highest contact angles ($64 \pm 4°$), and this was the most hydrophobic of the materials tested. Following the 10-week soaking period, samples were retested to determine if there was any change in their hydrophilicities. It was found that contact angles on all four materials increased after the 10 weeks. The percentage increases were PMMA 11.4%; hydrogel 42.3%; BAC/hydrogel 42.3% and 2C-75®/hydrogel 121.7%. PMMA contact angles ($71 \pm 3°$) were still much greater than all of the hydrogels. By 10 weeks, there was no significant difference in contact angles among the three hydrogel materials.

Discussion

This trial showed that biocide-releasing Arquad 2C-75® hydrogels are extremely effective at preventing the development of biofilms and the settlement of barnacles and mussels for a period of up to 14 weeks under the conditions of this study. The results from the contact angle measurements indicate that the prevention of fouling is unlikely to be directly related to hydrophilicity changes of these hydrogels. Results showed that, after soaking for 3 d in seawater, BAC-impregnated hydrogels, which subsequently proved to have a considerable antifouling action, possessed similar contact angles ($33 \pm 6°$) to the unloaded blank hydrogels ($30 \pm 4°$), which fouled the most heavily of all the materials tested. 2C-75® hydrogels, with the most effective antifouling properties, had the lowest contact angles and, therefore, the highest water wettability. The ability of surfactants to associate at interfaces would enable them to alter the surface of the hydrogel and, therefore, influence its wetting characteristics (Tonge et al. 2001). The addition of BAC to the hydrogel, however, did not reduce the contact angle as it was found not to be significantly different from the contact angles of the untreated hydrogels. This may be explained by the fact that BAC is very water-soluble and, therefore, will be predominantly in the water portion of the hydrogel, enabling it to diffuse out (Smith et al. 2002). 2C-75® is less water soluble and possibly will attach to the more hydrophobic backbone of the polymer, allowing it to have more influence on the surface properties of the polymer. The contact angle measured on the PMMA was 64°; Hermitte et al. (2004) found it to be 65.8° when measured in

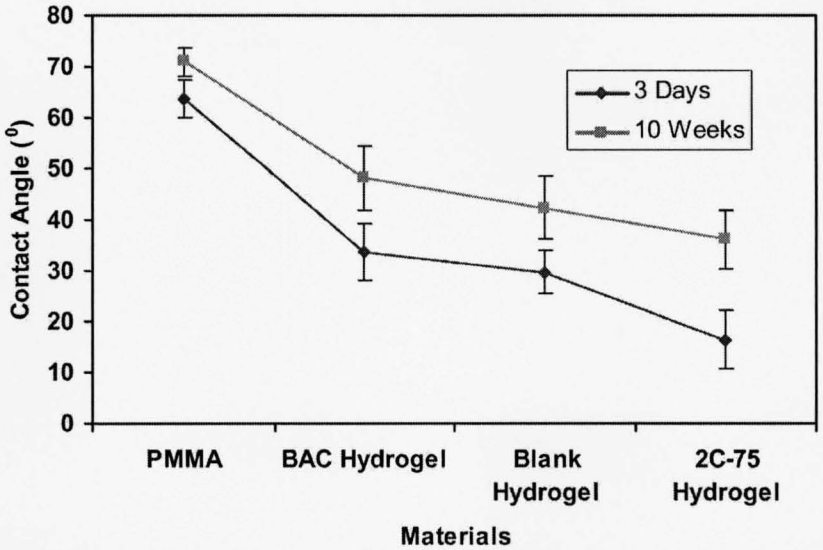

Figure 6. Contact angle (°) measurements obtained for the four materials after 3 d and 10 weeks' soaking in seawater.

distilled water. Over the 10-week period soaking in seawater, all the contact angles increased. The most marked increase was seen in the contact angles of the 2C-75® hydrogel coating. Increases in contact angles were indicative of changes occurring to the materials over time in the marine environment. These could be due to increases in surface roughness, a reorientation of polymers and surfactant release (in the case of the 2 treated hydrogels).

Over the past two decades, bacterial adhesion to and subsequent biofilm development on substratum surfaces with different hydrophobicities have been studied extensively. Some studies have shown that bacterial adhesion is less to hydrophobic substrata, whilst others have shown that the opposite is true (Bos et al. 2000). Despite this, it is unlikely that the 2C-75® and BAC hydrogels with initial contact angles of $16 \pm 6°$ and $33 \pm 6°$, respectively, represent extremes in hydrophobicities that would be enough to prevent initial bacterial adhesion and subsequent biofilm development.

The prevention of initial biofilm formation by BAC and 2C-75® is more likely to be related to the bactericidal and bacteriostatic nature of these cationic surfactants, which can reduce surface tension at interfaces upon absorption and, therefore, are attracted to biological surfaces possessing a negative charge (e.g. proteins, bacteria) (Merianos, 1991). These and other quaternary ammonium salts exhibit a wide-action spectrum because of their ability to interact with the phospholipids of bacterial cytoplasmic membranes (Franklin & Snow, 1981). Once in contact with cell membranes, the lipophilic regions of BAC or 2C-75® become inserted into membrane lipids, resulting in disorganisation of the cytoplasmic membrane, alteration in its semipermeable properties, and accompanying leakage of metabolites and coenzymes resulting in cytolysis (Armstrong, 1957; Merianos, 1991). In laboratory testing with nine diatom species, BAC also has been shown to have an algicidal and algistatic effect with a minimum effective concentration of $1\ mg\ l^{-1}$ (Beveridge et al. 1998).

The relative differences in the antifouling efficacy of the two different compounds are related to differences in their respective chemical structures and the way they interact with the cross-linked molecules of the hydrogel matrix. BAC is predominately composed of C_{12} and C_{14} chains and is water-soluble. It is, therefore, contained mainly in the pore water of the hydrogels with only a small amount becoming irreversibly bound to the hydrophobic parts of the hydrogel (Smith et al. 2002). Over time, the BAC diffuses out of the hydrogel through a diffusion gradient. 2C-75® also is composed mainly of C_{12} and C_{14} chains. However, it is twin-chained and has a more hydrophobic character than the single chained BAC. Thus, 2C-75® is able to attach by hydrophobic interaction to the non-water portions of the hydrogels.

Differences in the chemical interactions of the surfactants with the pHEMA substratum are reflected in their release rates. After 14 weeks, approximately 67% of the initial 2C-75® remained in the hydrogels. In contrast, after 14 weeks approximately 46% of the initial BAC remained in samples. The diffusion co-efficient of BAC at 5°C has been shown to be $1.13 \times 10^{-9}\ cm^2\ s^{-1}$ (Smith et al. 2000).

Quantitative analysis of the 2C-75® remaining after 14 weeks shows that 2C-75® was largely retained by the hydrogel, suggesting, despite its water solubility, that it is predominately held in the non-polar regions of the hydrogel and released only very slowly. Additionally, twin chain quaternary compounds such as 2C-75® were initially developed for their superior biocidal activity over the 'first-generation' benzalkonium chlorides (Merianos, 1991). The superior action of the 2C-75® ensured that, after 14 weeks deployment, only very low levels of chl *a* ($0.12 \pm 0.1\ \mu g$ chl *a* cm^{-2}) and enzymatic activity ($0.05 \pm 0.1\ \mu g$ FDA $ml^{-1}\ h^{-1}$) were recovered from the hydrogel surface.

The mode of action by which BAC and 2C-75® hydrogels prevented the settlement of macrofouling larvae is less clear than their antimicrobial properties and may have been due to a combination of mechanisms. Surfactants within hydrogels may be directly toxic to exploratory cyprids/pediveliger or interfere with the searching behaviour of the larvae by interacting with the proteinaceous secretions of pediveliger feet and the antennular discs of cyprids. To the authors' knowledge, no laboratory work has been conducted where the toxicity of BAC and 2C-75® released from pHEMA hydrogels has been tested against cultured barnacle cyprids or mussel pediveliger larvae. Rasmussen et al. (2002) tested the settlement of cultured *Balanus amphitrite* cyprid larvae and naupliar larvae of *Artemia salina* on gels consisting of alginate, chitosan, agarose and polyvinyl alcohol substituted with a light-sensitive stilbazolium group. However, the materials tested did not include pHEMA hydrogels and were not loaded with antifouling surfactants. In another study, the toxicity of alkyldimethylbenzylammonium chlorides (dissolved in seawater) to the larvae of *Balanus* sp. was tested; $2.5\ mg\ l^{-1}$ of alkyldimethylbenzylammonium chlorides were shown to have no effect, whereas $5\ mg\ l^{-1}$ caused 100% mortality within a limited period of time (Boethling & Lynch, 1992). Using the oyster embryo bioassay, His et al. (1996) showed that the 24 h EC_{50} for *Crassostrea gigas* embryos was 138 μg BAC l^{-1}, which is two orders of magnitude less toxic than TBT ($EC_{50} = 1.3\ \mu g\ l^{-1}$,

Roberts, 1987) and more than one order of magnitude less toxic than copper ($EC_{50} = 5.3\ \mu g\ l^{-1}$, Martin et al. 1981). In contrast to the apparent inhibitory effects on juveniles, His et al. (1996) studied the effects of BAC-pHEMA-coated cages on adult *C. gigas* and showed no impact on the size increase or viability of gametes and embryos in BAC-exposed adults compared with control specimens after seven months.

There are difficulties in using this information to establish the minimum concentrations of BAC and 2C-75® needed to inhibit the settlement of barnacles and mussels on pHEMA hydrogels. However, it is apparent that the concentrations of BAC (21.3 ± 1.97 mg g^{-1}) and 2C-75® (5.82 ± 0.69 mg g^{-1}) within the hydrogels and at the hydrogel/seawater interface were still high enough after 14 weeks to deter attachment of most barnacle and mussel larvae.

In addition to direct toxicity of the BAC and 2C-75® preventing settlement, the absence of a significant biofilm on the Arquad 2C-75® hydrogels (as indicated by chl *a* and FDA analysis) may have had a negative effect on the cyprids/pediveliger. Bacterial and algal biofilms have been shown to play an important role in providing settlement cues for many invertebrate larvae, including barnacle cyprids and mussel pediveliger, and the absence of these cues may prevent settlement (Kiseleva, 1966; Maki et al. 1990). Larval responses to biofilm cues in the field, however, can be highly species-specific and may be either facilitatory or inhibitory (Wieczorek & Todd, 1988).

It is unknown whether the BAC and 2C-75® hydrogels prevented initial cyprid/pediveliger settlement or whether settlement occurred, and subsequent metamorphosis from metamorphs to juveniles was inhibited. The presence of one fully developed barnacle on the 12-week 2C-75® hydrogel indicates that, for the barnacles at least, full metamorphosis on this substratum is possible. The development of this lone barnacle on a 2C-75® hydrogel may be related to the structure of the hydrogels. Hydrogels are constructed of cross-linked polymers and there is a possibility that the concentration of 2C-75® in one particular region of the gel is lower than in others, thus allowing settlement. If this barnacle originated from an older cyprid with declining energy reserves, it may have been more inclined to settle on an unfavourable substratum (Rittschof et al. 1984; Maki et al. 1990).

Previous work has investigated the modification of various polymers with cationic surfactants such as BAC (Gott et al. 1964). Clarkson and Evans (1995) modified silicone with BAC to prevent biofouling. These polymers, however, were not able to absorb the surfactant, but only adsorb it, resulting in the surfaces being modified and thus limiting the amount of effective biocide absorbed by the coating. Surfaces modified with tri-dodecylmethyl ammonium chloride-heparin were produced by Polysciences Inc. (1978). Their purpose was to slowly release heparin to prevent blood clotting during the procedure for resection of aneurysm rather than the surfactant having any direct action other than to create positive sites to which the heparin could bond. Kerr et al. (2001) reported the results of biofouling trials using six hard polymers modified with BAC and 2C-75® and found that there was a limited improvement in antifouling protection when compared with unmodified polymers. In contrast to hard polymers, hydrogels contain 40% water, which can act as a reservoir for water-soluble cationic surfactants, greatly increasing the amount of surfactant able to be imbibed by the coating. In addition to their abilities to act as reservoirs, pHEMA-based hydrogels have good light transmission properties and were initially developed for use in biomedical applications including soft contact lens manufacture (Tighe, 1986). Due to environmental concerns, recent antifouling research has focused on the development of non-toxic fouling-release polymers (Truby et al. 2000). These coatings typically require water to flow over the protective coating at a high velocity to keep the surface fouling free (Brady & Singer, 2000). Oceanographic equipment with optical windows are deployed in a variety of habitats that experience different current flows, ranging from areas with high flow velocities to the relatively static conditions within some ports and harbours. Under these conditions, it is unlikely that the current generation of non-toxic fouling release coatings (even if optically clear) would be suitable for protecting instruments deployed in this wide range of fouling conditions. Coatings are being developed with dual antifouling/fouling release properties, where biocides such as Triclosan are bonded to silicone coatings in a non-leachable manner (Thomas et al. 2004). Future developments in antifouling/fouling release coatings may provide a non-leachable alternative to the coatings described here, but the optical properties of such coatings will have to equal or better the optical transmission through pHEMA hydrogels.

This trial showed that the ability of 2C-75® hydrogels to deter barnacle and mussel settlement was not affected by the length of time they were deployed before the macrofouling challenge occurred. There was no apparent reduction in the ability of 2C-75® gels, which been deployed for 6 weeks prior to barnacle/mussel settlement, to deter settlement when compared with hydrogels which had been deployed for only 4 and 2 weeks before the settlement peak. All 2C-75® hydrogels were equally effective at preventing macrofouling over the

14-week period studied. This information is important for users of oceanographic equipment. Periods of high bivalve and crustacean settlement are frequently of interest to marine biologists who, typically, monitor the biological and physical conditions before and after such settlements, using equipment such as fluorimeters and turbidometers. The optical windows of these instruments are vulnerable to fouling, which can reduce the reliability of readings. However, instruments with optical windows protected by 2C-75® hydrogels could be deployed for at least 6 weeks before the main settlement season and still be effective.

In contrast to the surfactant-loaded hydrogels, unloaded (blank) hydrogels became extensively fouled with micro- and macroorganisms on all of the three panels deployed. Surprisingly, the highest levels of chl *a* (12.7 ± 1.8 μg cm^{-2}) were recorded on the unloaded hydrogel panel that was deployed for only 10 weeks and were due to the high levels of filamentous algae attached to the substratum surface. The extensive fouling of the unloaded hydrogels by filamentous algae was possibly a reflection of the macroporous structure of hydrogels that would enable the rhizoids of algal zoospores to penetrate into the substratum and provide a perfect attachment surface. This is in contrast to the solid PMMA substratum that would not enable rhizoid penetration. Other researchers (Hardy, 1979; Hardy & Moss, 1979; Fletcher et al. 1985) have highlighted the importance that different substrata have on rhizoid penetration and subsequent sporeling development. The high numbers of *M. edulis* found associated with the blank hydrogels also may have been related to the high density of filamentous algae. De Block and Geelen (1958) and Bayne (1964) showed that *M. edulis* pediveliger and plantigrades attach most readily to various filamentous substrata (Seed, 1976).

PMMA samples with the greatest hydrophobicity of the materials tested had a higher mean abundance of *M. edulis* and *S. balanoides* on the 10- and 12-week panels than the unloaded hydrogels. On all three panels, however, the mean level of chl *a* was higher on the unloaded hydrogels than on the PMMA. As discussed, this is possibly a result of reduced rhizoid penetration into the solid PMMA substratum. This suggests that factors such as surface texture (not just density of filamentous algae) play a significant role in the settlement of *M. edulis* pediveliger and plantigrades. Algal fouling of PMMA samples was not as extensive as on the unloaded hydrogels, but these levels still had a significant impact on the optical transmission through the PMMA as discussed below.

The suitability of using 2C-75® hydrogels to protect the optical windows of oceanographic instruments is further appreciated when the transmission data are examined. The poorest transmission of light was through samples of the blank hydrogel, which was related to the extensive fouling of this material as already discussed. Light transmission of all wavelengths also was poor through PMMA samples, with only 20–30% transmission occurring through samples that had been deployed for 10 weeks. This is important because PMMA (along with Spectrosil® and sapphire) is frequently used in the design of optical windows within instruments such as fluorimeters and transmissometers (personal communication, Chelsea Instruments). An 80% reduction in either the light transmitted from the excitation source within the instrument or in the light going to the instrument detector, as a consequence of fouling of the PMMA, has serious implications for instrument accuracy and sensitivity (Kerr et al. 1998). Transmission through BAC and 2C-75® hydrogels was far greater than the transmission through PMMA. Transmission levels as high as *ca* 88% (400 nm) and 95% (700 nm) were recorded through the 10-week C-75® hydrogels. Eventually, low levels of fouling recorded on these hydrogels after 14 weeks deployment did cause a drop in transmission to *ca.* 67% (400 nm) and 82% (700 nm) However, these levels were still much higher than the levels recorded through the PMMA samples (20–30% transmission) at the same time period. The trends of decreases in transmission with increased exposure of loaded hydrogels are consistent with reagent-induced organism death in-place after settlement and the accumulation of non-living inorganic material on the hydrogel surface.

Oceanographic instruments with optical windows constructed from PMMA and protected by 2C-75® hydrogels can be expected to have their effective working deployment extended by many weeks, as supported by instrument field trials (Kerr et al. 1998).

Conclusions

Arquad 2C-75® hydrogels are effective at preventing hard- and soft-fouling and are able to prevent the majority of settlement during the intensive barnacle and mussel settlement seasons under the conditions studied here. The length of time that hydrogel-protected instruments are deployed before the settlement season would not affect their macro-antifouling ability, as long as deployment prior to settlement did not exceed the working life of the hydrogels (*ca* 3 months).

Acknowledgements

This work was grant-aided by the European Commission through contract EVRI-CT-2002-40023 BRIMOM. This support is gratefully acknowledged.

The authors wish to thank Mr Ian Peden for the writing of the program to measure and calculate the contact angles.

References

Adam G, Duncan H. 2001. Development of a more sensitive and rapid method for the measurement of total microbial activity using flourescein diacetate (FDA) in a range of soils. Soil Biol Biochem 33:943–951.

Armstrong W. 1957. Surface active agents and cellular metabolism. I. The effects of cationic detergents on the production of acid and of carbon dioxide by bakers yeast. Arch Biochem 71:137–148.

Battin TJ. 1997. Assessment of flourescein diacetate hydrolysis as a measure of total esterase activity in natural stream sediment biofilms. Sci Total Environ 198:51–60.

Bayne BL. 1964. Primary and secondary settlement in *Mytilus edulis* L. J Anim Ecol 33:513–523.

Beveridge CM, Parr ACS, Smith MJ, Kerr A, Cowling MJ, Hodgkiess T. 1998. The effect of benzalkonium chloride concentration on nine species of marine diatom. Environ Pollut 103:31–36.

Boethling RS, Lynch DG. 1992. Quaternary ammonium surfactants. In: Hutzinger O, editor. The handbook of environmental chemistry: Vol. 3. Berlin: Springer-Verlag. pp 146–178.

Bos R, van der Mei HC, Gold J, Busscher HJ. 2000. Retention of bacteria on a substratum surface with micro-patterned hydrophobicity. FEMS Microbiol Lett 189:311–315.

Brady JR, Singer IL. 2000. Mechanical factors favouring release from fouling release coatings. Biofouling 15:73–81.

Clarkson N, Evans LV. 1995. Further studies investigating a potential non-leaching biocide using the marine fouling diatom *Amphora coffeaformis*. Biofouling 9:17–30.

Commission of the European Communities. 1997/1998. Proposal for a Council Directive establishing a framework for community action in the field of water policy. Brussels. Report No. 97/0049/COM, 97/0614/COM, 98/0076/COM.

Cowling MJ, Hodgkiess T, Parr ACS, Smith MJ, Kerr A, Beveridge CM, Clegg M, Menlove R. 1998. The effects of biofouling on imaging underwater, including possible remedies. Proc Underwater Optics III, Applied Optics & Optoelectronics. Brighton. Bristol Institute of Physics Publishing. pp 245–254.

De Block JW, Geelen HJ. 1958. The substratum required for the settling of mussels (*Mytilus edulis* L.). Arch Neerl Zool Jubilee Volume. pp 446–460.

Drelich J, Miller JD, Good RJ. 1996. The effect of drop (bubble) size on advancing and receding contact angles for heterogeneous and rough solid surfaces as observed with sessile-drop and captive-bubble techniques. J Colloid Interface Sci 179: 37–50.

Fletcher RL, Baier RE, Fornalik MS. 1985. The effects of surface energy on germling development of some marine macroalgae. Br Phycol J 20:184–185.

Franklin TJ, Snow GA. 1981. Antiseptics, antibiotics and the cell membrane. In: Franklin TJ, Snow GA, editor. Biochemistry of antimicrobial action. London: Chapman & Hall. pp 58–78.

Gott VL, Daggett RL, Whiffen JD, Young WP, Boake WC, Koepke DE. 1964. Techniques of applying graphite-benzalkonium-heparin coating to various plastic and metals. Trans Am Soc Art Int Org 10:213–224.

Guilfoyle DE, Roos R, Carito SL. 1990. An evaluation of preservative adsorption onto nylon. J Parenter Sci Technol 44:314–319.

Hardy FG. 1979. The effects of the substratum on the morphology of the rhizoids of *Fucus* germlings. Br Phycol J 14:124–129.

Hardy FD, Moss BL. 1979. Attachment and development of the zygotes of *Pelvetia canaliculata* (L.) Dcne. et Thur (Phaeophyceae, Fucales). Phycologia 18:203–212.

Hermitte L, Thomas F, Bougaran R, Martelet C. 2004. Contribution of the comonomers to the bulk and surface properties of methacrylate copolymers. J Colloid Interface Sci 272:82–89.

Hills JM, Thomason JC. 1998. The effect of scales of surface roughness on the settlement of barnacles (*Semibalanus balanoides*) cyprids. Biofouling 12:57–69.

Hills JM, Thomason JC, Milligan JL, Richardson M. 1998. Do barnacle larvae respond to multiple settlement cues over a range of spatial scales? Hydrobiologia 375/376:101–111.

His E, Beiras R, Quinou F, Parr ACS, Smith MJ, Cowling MJ, Hodgkiess T. 1996. The non-toxic effects of a novel antifouling material on oyster culture. Water Res 30:2822–2825.

Kerr A, Smith MJ, Cowling MJ, Hodgkiess T. 2001. The biofouling resistant properties of six transparent polymers with and without pre-treatment by two anti-microbial solutions. Mater Des 22:383–392.

Kerr A, Head RM, Cowling MJ, Davenport J, Beveridge CM, Smith MJ, Parr ACS, Hodgkiess T. 1998. The early stages of marine biofouling and its effect on two types of optical sensors. Environ Int 24:331–343.

Kiseleva GA. 1966. Factors stimulating larval metamophosis of the lamellibranch *Brachyodontes lineatus* (Gmelin). Zool Zh 45:1571–1573.

Maki JS, Rittschof D, Costlow JD, Mitchell R. 1990. Effect of marine bacteria and their exopolymers on the attachment of barnacle cypris larvae. Bull Mar Sci 46:499–511.

Martin M, Osborn KE, Billig P, Glickstein N. 1981. Toxicities of ten metals to *Crassostrea gigas* and *Mytilus edulis* embryos and *Cancer magister* larvae. Mar Pollut Bull 12:305–308.

Merianos JJ. 1991. Quaternary ammonium antimicrobial compounds. In: Block SS, editor. Disinfection, sterilization and preservation. Philadelphia: Lea & Febiger. pp 225–273.

Mussalli YG, Tsou J. 1989. Advances in biofouling control technologies: US and Japanese perspective. Proc 51st American Power Conference, Chicago, 1989. Illinois Institute of Technology. pp 1094–1099.

Nusch EA. 1980. Comparison of different methods for chlorophyll and phaeopigment determination. Arch Hydrobiol Beih 14:14–36.

Parr ACS, Smith MJ, Beveridge CM, Kerr A, Cowling MJ, Hodgkiess T. 1998. Optical assessment of a fouling-resistant surface (PHEMA/benzalkonium chloride) after exposure to a marine environment. Adv Mater Opt Electron 8:187–193.

Parsons RT, Maita Y, Lalli CM. 1984. A manual of chemical and biological methods for seawater analysis. New York: Pergamon Press Ltd.

Polysciences Inc. 1978. TDMAC-heparin complex coatings. Warrington, Pennsylvania USA. Data Sheet No. 172.

Rasmussen K, Willemsen PR, Østgaard K. 2002. Barnacle settlement on hydrogels. Biofouling 18:177–191.

Refojo MF. 1966. Perparation of water through some heterogeneous hydrophilic membranes. J Appl Poly Sci 10:185–190.

Rittschof D, Branscomb ES, Costlow J. 1984. Settlement and behaviour in relation to flow and surface in larval barnacles, *Balanus amphitrite* Darwin. J Exp Mar Biol Ecol 82:131–146.

Roberts MH. 1987. Acute toxicity of tributyltin chloride to embryos and larvae of two bivalve mollusks *Crassostrea virginica* and *Mercenaria mercenaria*. Bull Environ Contam Toxicol 39:1012–1019.

Seed R. 1976. Ecology. In: Bayne BL, editor. Marine mussels: their ecology and physiology. Cambridge: Cambridge University Press. pp 13–65.

Smith MJ. 1997. The use of cationic surfactants in marine antifouling applications MSc dissertation. Glasgow: University of Glasgow. 120 p.

Smith MJ, Adam G, Duncan HJ, Cowling MJ. 2002. The effects of cationic surfactants on marine biofilm growth on hydrogels. Est Coastal Shelf Sci 55:361–367.

Smith MJ, Flowers TH, Parr ACS, Cowling MJ, Hodgkiess T. 2000. Salinity and temperature effects on the release of benzalkonium chloride from hydrogel material. Polym Polym Compos 8:101–105.

Thomas J, Choi S-B, Fjeldheim R, Boudjouk P. 2004. Silicones containing pendant biocides for antifouling coatings. Biofouling 20:227–236.

Tighe BJ. 1986. Hydrogels as contact lens materials. In: Peppas NA, editor. Hydrogels in medicine and pharmacy. Vol. III, Properties and applications. Boca Raton, Florida: CRC Press. pp 53–82.

Tonge S, Jones L, Goodall S, Tighe B. 2001. The *ex vivo* wettability of soft contact lenses. Curr Eye Res 23:51–59.

Truby K, Wood C, Stein J, Cella J, Carpenter J, Kavanagh C, Swain G, Wiebe D, Lapoite D, Meyer A, Holm E, Wendt D, Smith C, Montemarono J. 2000. Evaluation of the performance enhancement of silicone biofouling-release coatings by oil incorporation. Biofouling 15:141–150.

Wieczorek SK, Todd CD. 1988. Inhibition and facilitation of settlement of epifaunal marine invertebrate larvae by microbial biofilm cues. Biofouling 12:81–118.

Zhang W, Hallström BD. 1990. Membrane characterization using the contact-angle technique.1. Methodology of the captive bubble technique. Desalination 79:1–12.

Effects of marine biofouling on gas sensor membrane materials.

M.J. Smith*, A. Kerr and M.J Cowling

Glasgow Marine Technology Centre, University of Glasgow, Glasgow, G12 8QQ UK.

*Corresponding author. E-mail: m.smith@mech.gla.ac.uk

Tel +44 (0) 141 330 4336 Fax +44 (0) 141 330 4343

Keywords: gas membranes; biofouling; pore-size; sensors; surface roughness

Abstract

The use of underwater gaseous sensors has increased rapidly in the last 10 years. The majority of such sensors employ a thin membrane through which the gas diffuses. These sensors are potentiometric gas-sensing probes and essentially they are ion-selective electrodes. The deployment time of these membranes is curtailed by the formation of biofouling on the membrane leading to erroneous results. The physical properties of a variety of commonly used membranes were investigated using SEM and AFM. This showed that there were differences in topography between the PTFE membranes, such as pore sizes and surface roughness, which may be attributed to the manner in which they are manufactured. The pore size of the PTFE membranes varied greatly ranging from circular pores with a diameter of 500nm to elongated pores measuring 1 x 22µm. The contact angle of each membrane showed that they were all hydrophobic. The amount of fouling on each was also observed and its affect on oxygen diffusion was monitored. Fouling slowed down the response of the instrument and caused reduced diffusion through the membranes. The amount of fouling varied between the membranes with the YSI membrane fouling least. Some of the membranes tested did foul less than others and there could be lifetime advantages of choosing a membrane with a smoother surface and a small pore size.

Introduction

Underwater sensors used to monitor gaseous species such as ammonia, carbon dioxide and oxygen are frequently used in rivers, estuaries, coastal areas and oceans. The increased interest in this area of monitoring has been driven by the need to measure climate change, environmental hazards and the oceanic environment. This has led to a plethora of models and types of sensors that the analyst can choose from. Improvements in electronic data collection can allow the long-term deployment of sensors, some for months at a time. As study regions have encompassed both open-ocean and coastal settings and have ranged from the equatorial Pacific to high-latitude areas off Iceland and the southern Ocean, these sensors are subject to a huge variety of climatic conditions. Despite these major accomplishments, biofouling of sensors still limits data quality and effective deployment periods of instrumentation on autonomous sampling platforms [1]. So despite rapid technological advances, the actual time of deployment is still restricted due to the age-old problem of biofouling.

Gas sensing probes have found widespread use in the determination of dissolved gases in water systems. These sensors are used for both discrete monitoring and continuous monitoring. They can be deployed singularly or as part of sensor pack. The manner in which they are employed in the oceans varies from floating buoys to towed vehicles.

Sensors are potentiometric gas-sensing probes and essentially they are ion-selective electrodes. They are generally constructed within a tube that contains a reference electrode, an ion selective electrode and an electrolyte solution. A thin, replaceable gas-permeable membrane is attached to the end of the tube and this serves two purposes; to provide a barrier between the internal and analyte solution and to allow the flow of gases species through from the measuring medium. The gas permeable membrane is fabricated from a hydrophobic polymer and is highly porous with a pore size in the region of 1μm and a thickness of about 0.1mm. Figure 1 shows a typical gas sensor. The diffusion coefficients of ammonia, carbon dioxide and oxygen at 20°C in water are 1.5×10^{-5} cm^2 s^{-1}, 1.67 10^{-5} cm^2 s^{-1} and 2.01×10^{-5} cm^2 s^{-1} respectively. Tarsiche et al. (1997)[2] found that the diffusion coefficient of ammonia through PTFE membranes was reduced two-fold compared with diffusion in water and that the concentration had an effect on diffusion, increasing as concentration increased. The diffusion of oxygen across a PTFE membrane was found to be 2.8×10^{-7} cm^2 s^{-1}. Thus the diffusion through PTFE gas membranes is reduced compared with in-water as would be expected.

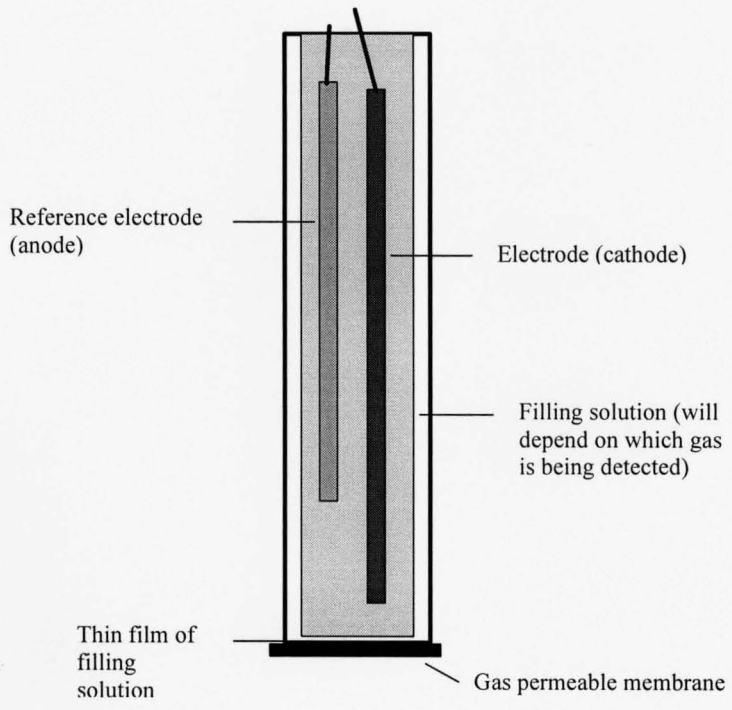

Fig.1. Schematic of gas sensor electrode

The formation of biofilms on objects immersed in a marine environment begins immediately upon immersion. Initially a conditioning layer of extracellular polymeric

substances EPS forms; bacteria, fungi and diatoms follow this and the resulting structure of biofilms is heterogeneous and highly dynamic[3] . Microorganisms inhabiting solid-water interfaces possess hydrophobic characteristics which are important for adhesion to surfaces and these enable the cells to benefit from advantages that might be derived from the association with surfaces while immersed in water [4].
The deleterious effect that biofouling has on sensor stability is a serious impediment to the development of long-term deployment of underwater instruments. Fouling can affect a sensor in a variety of ways such as component-based failures, electrical shorts, membrane degradation, and membrane biofouling [5]. However, it is the effects of membrane biofouling that will be studied here and, to a lesser extent, membrane degradation. In order to be detected by a sensor, the gas of interest must be able to freely diffuse through the membrane. Therefore any fouling on the membrane will reduce diffusion. Biofilms are dynamic and heterogeneous and will affect the diffusion of gases in a number of ways. Firstly a biofilm will increase the thickness and thus increase the diffusion path length for the species; it will also present a higher resistance to the species of interest and thus increase the response time of the sensor. The solution contained within the biofilm will create a buffering capacity, which will further increase the response time [6]. The reaction of the gaseous species within the biofilm may also cause an erroneous result. Fraher and Clarke (1998)[7] found that fouling on the membrane of an oxygen sensor caused the "gain" to be reduced and the resultant measured dissolved oxygen was lower than the actual level. Marshallsay (1989)[8] reported that biofilms on pH electrodes increased the response time from 14 seconds to nearly 3 minutes for a step change of 8 to 9.5 pH units after 3 weeks in situ at a water treatment plant. Munro et al. (1996) found that fouling on a pH electrode caused the response time to increase in a linear manner with increasing attached biomass and biofilm optical absorbance. Wisniewski et al. (2000)[5] and Wisniewski and Reichart (2000)[9] have published extensively on the affects of membrane fouling on implantable biosensors and reviewed various methods to prevent it.

When considering how to prevent fouling on gas sensor membranes it is important firstly to look at the available membranes, their structure and properties as often these membranes are chosen through habit or ease of access. More careful consideration of what material it had been made from or how it has been manufactured may help to reduce the fouling to a more acceptable level. Yebra et al. (2004)[10] suggested a list of properties which create an ideal biofouling resistant surface. This list included:

- A flexible, linear backbone which introduces no undesirable interactions
- A sufficient number of surface–active groups which are free to move to the surface and impact a surface energy in the desired range
- Low elastic modulus
- A surface which is smooth at the molecular level to avoid infiltration of a biological adhesive leading to mechanical interlocking
- High molecular mobility in the backbone and surface–active chains
- A thickness which can control the fracture mechanics of the interface
- Molecules which combine all the above factors and are physically and chemically stable for prolonged periods in the marine environment

Kiremitci-Gumusderelioglu and Pesmen, (1996)[11] stated that substrate surface properties which can influence adhesion are, surface tension, surface free energy, hydrophilicity-hydrophobicity and texture.

Most membranes for gas sensor membranes are made from polytetrafluoroethylene (PTFE) and some from high-density polyethylene (HDPE). A variety of poly tetrafluorethylene (PTFE) membranes and one high-density polyethylene (HDPE) membrane were investigated. Some were membranes supplied by manufacturers for their own gas sensors while others were cut from PTFE tape produced by various manufacturers. The structures of the membranes were studied using AFM and SEM. The surfaces were characterised using contact angle measurements. The effect of bacterial membrane fouling on oxygen diffusion was measured.

Materials and methods

Membranes

The membranes were investigated were: poly tetrafluorethylene (PTFE) membranes, YSI standard membrane; YSI high sensitivity membrane (YSI Incorporated Yellow Springs, Ohio, USA); Rank membrane (Polyflon); ABB membrane (Gore-Tex®); PTFE tape (Gore-Tex®); TFE (Fisher,Made in the USA); PTFE wide tape (Fisher) and one high density polyethylene (HDPE) (Goodfellows, Cambridge, UK). Table 1 shows each membrane tested and also a measurement of thickness.

Membrane	Material	Thickness (μm)
YSI standard membrane	PTFE	30
YSI high sensitivity membrane	PTFE	20
Rank membrane (Polyflon)	PTFE	12
ABB membrane	PTFE	70
PTFE tape (Gore-Tex®)	PTFE	85
TFE (Made in the USA)	PTFE	100
PTFE wide tape (Fisher)	PTFE	190
HDPE	HDPE	20

Table 1. The membranes and their thickness (PTFE-poly tetrafluroethylene; HDPE-high density polyethylene).

SEM and AFM microscopy

Scanning electron microscopy (SEM) and atomic force microscopy (AFM) and were used to study the morphology of each of the membranes. These techniques offer different ways of visualising the physical structure of the membranes and are able to show detail at micro and nanometre level.

The instruments used were a Cambridge S360 analytical SEM (Cambridge Instruments, Cambridge, UK) and a Veeco (Topometrix) Explorer Atomic Force Microscope (Vecco, USA). For use on the SEM the membranes were prepared with vacuum deposition of a thin layer of gold. The membrane samples required no preparation for the AFM where a 100micron scanning head and silicon nitride contact scanning probe was used

Contact angle measurements

Measurements of contact angles using the sessile-drop and captive-bubble techniques are among the most popular methods used in surface chemistry laboratories for this purpose, especially due to their simplicity and small amount of liquid and solid sample required [12]. The measurement of contact angles yield data which reflect the thermodynamics of a liquid/solid interaction. To characterise the wetting behaviour of a particular liquid/solid pair it is only necessary to report the contact angle[13]. Contact angles are determined by the upper two or three monolayers of molecules. This thin layer only 5 to 10 Angstroms (Å) thick is what determines adhesion, electrical properties, etc[14].

The adhering gas bubble was measured using the dynamic bubble technique. The work was carried out in an optically clear glass box (55 x 55 x 55mm), which was filled with synthetic seawater (3.5%) (Instant Ocean, Aquarium Systems, Sarrebourg, France). All the work was carried out at ambient temperature which was 22±2°C for the duration of the tests. The gas membranes were held in place by attaching each one to a glass slide that was held in a PMMA holder made for the purpose, which allowed the test piece to be exposed to the water in the tank. The membranes were soaked for three days in synthetic seawater (Instant Ocean) at ambient temperature prior to testing to allow them to acclimatise to the polar environment. Polymer surfaces are particularly mobile and the molecular orientation of the surface at any point in time may be modified in response to the surrounding environment [15]. The bubble was supplied to the surface via a 1ml syringe with a 25-gauge needle to allow control of the volume. The bubbles were generated in the liquid and captured on the test surface as a result of buoyant transport and attachment. The bubbles were all between 2-3 mm in diameter. It had been observed that no change in angle size was found on a homogeneous surface for bubbles raging from 1-7mm [12]. The measurements were carried out in triplicate on each sample piece and three pieces of each material were tested.
The bubbles were photographed using a JVC video camera fitted with a Viviter 55mm F2.8 macro lens. A computer program was written to measure the angles in order to prevent the errors encountered when measuring these angles manually. The image is selected and displayed in its frame. The user then draws, using the mouse, the incident angle of the bubble. The mouse positions in x and y are stored in a matrix. A curve-fitting algorithm is used to determine the mathematical function of the curve from this function is differentiated to obtain the angle.

Instrument testing

The Dissolved Oxygen Meters used were Rank Brothers Laboratory meters (Rank Bros., Cambridgeshire, U.K.). These operate on the Clark Cell system of oxygen detection. It has two main components, which are held together by a threaded collar when in use. The first component is a base unit, which houses the central Pt working electrode and the surrounding silver/silver chloride reference electrode. A thin layer of 3 molar potassium chloride ensures conduction between these two electrodes. The semi-permeable membrane separates the electrodes from the sample solution. The manufacturer supplies PTFE membrane material. The second component, the analysis chamber, is a PMMA vessel within a water jacket through which water, externally maintained at the chosen reaction temperature, can flow. The meters are designed to

monitor the consumption or production of dissolved oxygen during cell development in a fixed volume of solution. All results from the dissolved oxygen meters quoted here were carried out at 28°C ± 2°C, since this was the lowest temperature the water bath would maintain regardless of the ambient temperature.

Fouling environment

The natural fouling environment changes throughout the year with variations in temperature and variations in chemical composition due to changes in run-off from coastal regions. These add unnecessary additional variables to the experiment. To avoid this, the decision was taken to use a synthetic composition of seawater using fresh water and Instant Ocean aquarium mix (Aquarium Systems, France), that exactly mirrors the general chemical composition of seawater. To allow the creation of a realistic community of fouling bacteria, the initial mix was 45 litres of seawater (collected from the Firth of Clyde and used the same day) made up to 280 litres with the synthetic seawater. The volume was topped up almost daily with fresh water to keep the salinity constant. Every week a feed of glucose, dihydrogen phosphate and ammonium chloride was added that was carbon and nitrogen sufficient [16]. This allowed the support of the bacterial community. Every four weeks 100 litres of solution were removed from the tank and replaced with 100 litres of fresh synthetic seawater. In addition an unconnected immersion pump was mounted vertically to ensure mixing and adequate oxygenation of the seawater.
This provided a fouling community composed almost entirely of marine bacteria. Earlier work[17] has shown that reducing the bacterial load adhering to a surface is the crucial factor in prolonging the deployment of optical marine sensors and it was believed that the same would be true for the detection of dissolved gases. This also simplified the experimental design since it was proved using samples exposed to the natural marine environment that the presence of barnacles and other hard fouling obstructed the screw thread when combining the two components of the meter. The presence of algae would often cause leaks at the thread. These obstacles prevented any useful results being achieved using samples fouled in the natural environment.
The maintenance regime described above resulted in a bacterial community density that altered in a cyclic manner. The average bacterial density in the test environment was of the order of 10^7 bacteria per millilitre, this is five orders of magnitude greater than that reported for open ocean waters [18] although greater densities are likely in polluted coastal areas.
Since the exact fouling density of any one exposure could not be exactly duplicated, the materials were exposed in parallel. The need for prompt analysis of a fouled sample limited the number of samples that could be dealt with at any one time. Eight samples were removed at each sample point, two of each material tested. Sixteen samples were introduced at the start of each cycle, eight samples were removed and analysed after four days and the other eight were removed and analysed after ten days. Multiple cycles were run to provide adequate repetition.

Oxygen diffusion – method

In use the membrane material was recovered from the fouling chamber and halved using a sharp knife blade. Before the material was divided, it was placed in clean seawater for ten seconds and then removed. This ensured the removal of bacteria that were not fully adhered to the surface under examination. One piece was placed over

the electrodes, taking care to ensure that no air bubbles were trapped beneath the membrane, and the analysis volume filled with fully oxygenated water. After the temperature had stabilized oxygen free helium was bubbled through the analysis volume at a fixed rate, removing the oxygen. With an unfouled PTFE membrane it took 30 seconds for the meter to detect the total removal of the dissolved oxygen from the 50ml analysis volume. The results record the length of time, in minutes, for the meters to read zero with various membrane materials after various exposure times to the fouling environment. The other half of the membrane material was used to measure the percentage area fouled and was stained with Methylene Blue. The area fouled was measured using Image Analysis at a magnification of x500 (over 3 areas). This measured the percentage area fouled, this was considered a more reliable measurement than estimations of the numbers of bacteria adhering to the surface. Bacteria frequently attach to other bacteria already attached to the surface and these second tier bacteria do not add significantly to the area fouled or to the decline in diffusion resistance. Inevitably, many bacteria partially overlap other bacteria and therefore add a partial contribution to the resistance.

Results and Discussion

SEM and AFM

The SEM images of the YSI membranes, YSI high sensitivity membranes, HDPE and the Rank Bros membrane did not show any visible structure and for this reason they are not shown. The SEM images of the 3 PTFE tapes and ABB membrane exhibited their pore structure. Figure 2 shows these four membranes.
The Gore-Tex® tape had a fairly uniform pore formation, the pores having a high aspect ratio, 1:20. Within each pore there were lateral threads giving the pores a ladder like appearance (fibrils). The TFE tape had long elongated type pores that were approximately 10μm in length. The wide PTFE tape also had elongated pores but these pores were much smaller than the previous two materials at around 100nm in width and 0.5-1μm in length. The ABB membrane had more circular pores that were relatively small at around 500nm. Tarsiche at al. (1997)[2] found PTFE tapes to have sparse pores with diameters of 2-8μm. The variation in microstructure can be attributed to the production process. Expanded PTFE membranes are produced by means of extrusion, rolling and stretching. It is composed of tiny interconnected continuous fibrils[17]. The degree of stretching increases the fibril length and also the size of the resultant pores. The SEM images of the HDPE membrane showed the pores were circular in shape.

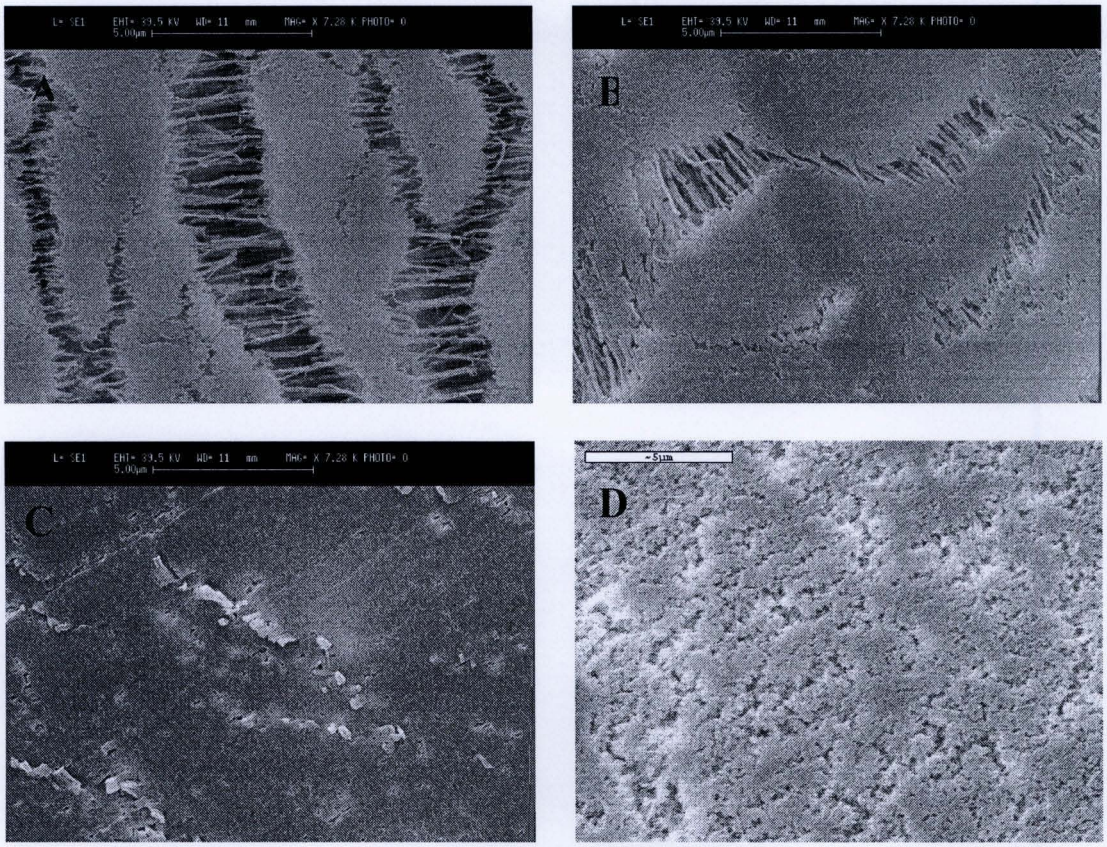

Fig. 2. SEM images showing the pore structure of A-PTFE tape (Gore-Tex®); B-TFE; C-PTFE wide tape and D-ABB membrane (Gore-Tex®).

The AFM images of all the membranes showed their structure clearly and these can be seen in figure 3. The YSI Standard membrane had pores that were circular in shape whereas the YSI High Sensitivity pores were elongated and were sometimes up to 20µm in length. The Rank membrane had elongated pores that appeared to be interconnected..

Expanded PTFE is a result of thin sheets of PTFE being stretched while warm and this causes a break up on the micro-scale while remaining coherent on the macro-scale. As a result the amount of stretching causes the variations in structure. The HDPE membrane was circular in shape and around 4-5µm in size. This membrane had a 'stringy' appearance

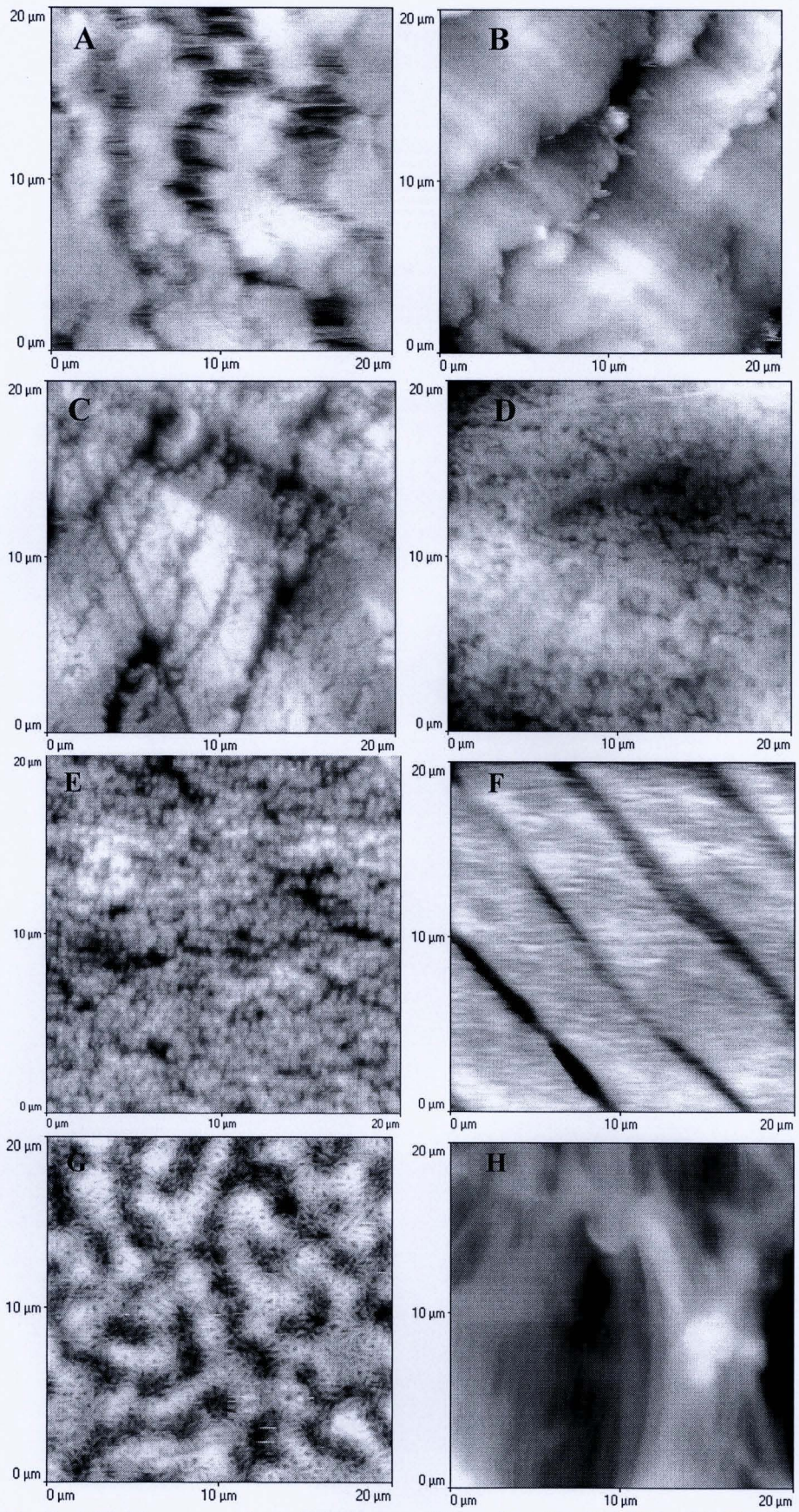

Fig.3. AFM images of A-PTFE tape (Gore-Tex®); B-TFE; C-PTFE wide tape; D-ABB membrane (Gore-Tex®); E-YSI standard membrane; F-YSI high sensitivity membrane; G- (Rank membrane (Polyflon) and H- High density polyethylene (HDPE) membrane, (20 x 20µm area).

The images show that the pore size between the membranes varies. Table 2 shows the pore sizes and shape, the YSI membranes have the smallest pores.

Membrane	Pore size	Pore Shape
Gore-Tex® tape	Width 1-3μm; length up to 20μm	Elongated pores
PTFE tape wide	Width 100nm; length 0.5-1μm	Elongated pores
TFE tape	Width 1-2μm; length up to 10μm	Elongated pores
ABB membrane	Width about 500nm	Circular pores
YSI standard	Width 0.5-1μm	Circular pores
YSI high sensitivity	Width 1-2μm; length up to 20μm	Elongated pores
Rank membrane	Width 0.5-1μm; length 1-20μm	Elongated pores
HDPE	Width 4-5μm	Circular pores

Table 2. The pore size and shape found in the membranes.

The 3D images (Figures 4) show the surface profile and also give a maximum roughness. All are shown as 20 x 20μm areas. Table 3 lists the maximum roughness measured at 20, 50 and 100μm. The larger the area viewed the greater the variation in roughness, demonstrating that it is crucial to quote the area viewed in any comparative studies. The membrane with the lowest surface roughness was the YSI high sensitivity, closely followed by the YSI standard membrane. The PTFE tapes and ABB membrane were much rougher than the YSI and Rank Bros membranes. The sequence of membrane increasing roughness is YSI high sensitivity < YSI standard membrane < Rank Bros < PTFE wide tape < PTFE tape < HDPE < ABB membrane < TFE 1. Morton et al (1998)[3] stated that rougher surfaces are preferentially colonised and the niches can even protect the bacteria from biocide activity. Brauker et al. (1995)[18] showed that implanted 5μm pore-size PTFE membranes had 80-100 fold more vascular structures in close proximity to the membrane than did implanted 0.02μm PTFE membranes. The contribution of surface topography to attachment is believed to be greater than physio-chemical interactions such as surface free energy and hydrophobicity (Taylor et al. 1998)[20]. In the natural world the self-cleaning of the skin of the pilot whale is attributed to the microtopography of its surface; specifically the small size of its pores. This small size reduces the surface area available for attachment of fouling organism (Whelan and Regan, 2006)[21]. Therefore the membrane pore size should influence the amount of fouling and so membranes with smaller pore size would be preferential in order to extend the fouling free lifetime.

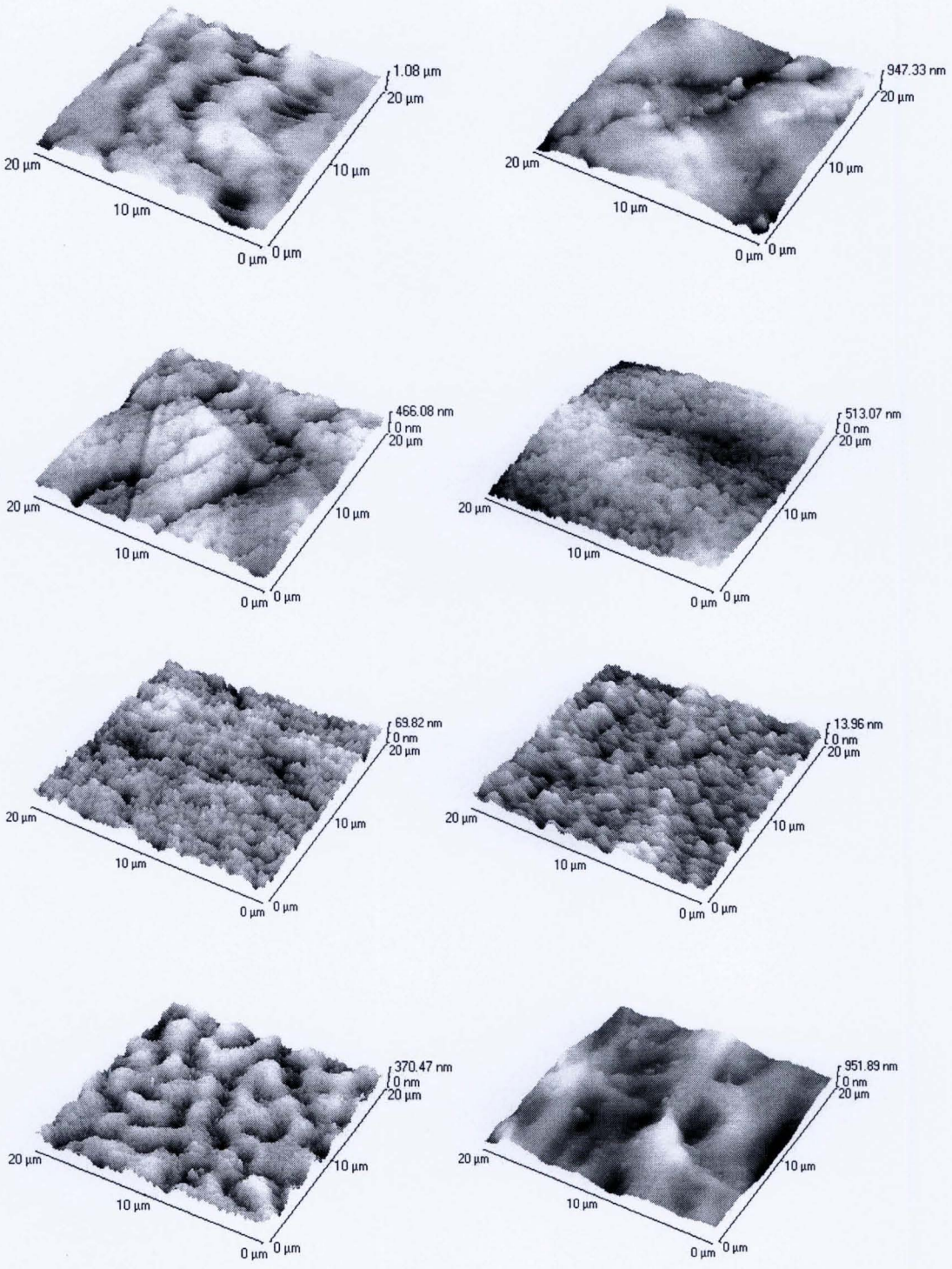

Fig. 4. 3D AFM images of PTFE tape (Gore-Tex®); TFE; PTFE wide tape; ABB membrane (Gore-Tex®); YSI standard membrane; YSI high sensitivity membrane (Rank membrane (Polyflon) and high density polyethylene (HDPE) membrane.

Membrane	20x20μm	50x50μm	100x100μm
	(Measurements in nm)		
YSI standard membrane	69.82	78.42	353.7
YSI high sensitivity	20.95	23.36	283.9
Rank membrane	370.5	511.8	558.6
ABB membrane	513.07	972.8	1670
PTFE tape	1008	1100	1480
TFE1	947.3	1530	1980
PTFE wide tape	466.1	781.2	802.2
HDPE	951.9	1480	1520

Table 3. Maximum roughness of each membrane. Measurements taken within areas of 20, 50 100μm^2.

Contact angles

Figure 5 shows the contact angles of the gas membranes tested. The YSI standard and high sensitivity membranes gave contact angles of 70.2°±1.08 and 71.7°±0.6 respectively and were the lowest values measured. Interestingly, the PTFE wide tape had a lower angle than all of the other similar tapes measured, with a value of 72.2°±0.2. These 3 membranes had significantly lower contact angles than the other 5 membranes tested ($P<0.05$) but were not significantly different from each other. The remainder of the membranes gave contact angles ranging from 77.8° (Rank Bros membrane) to 82.4° (HDPE). There was no significant difference between TFE1and Gore-Tex® tapes or the ABB membrane, which were all similar in appearance neither were they different from the Rank or the HDPE.

Much research has been carried out on the understanding of hydrophobicity and biofouling resistance [23,23]. Marmur [22] stated that super-hydrophobicity had implications in fouling prevention, i.e. (>150°) and concluded that such surfaces with the correct roughness value would create an air film, which would reduce fouling. Carmen [23] looked at microscale topography and concluded that by mimicking the skin of fast moving sharks that 85% zoospores settled on ridges of 2μm than on higher values. However Brady and Singer[24], (2000) stated that although the surface properties most frequently correlated with bioadhesion is its surface tension, resistance to fouling is also influenced by other bulk and surface properties of a polymer.

From this work it can be concluded that within the narrow contact angle range associated with these gaseous membranes no real relationship of surface tension and fouling can be drawn.

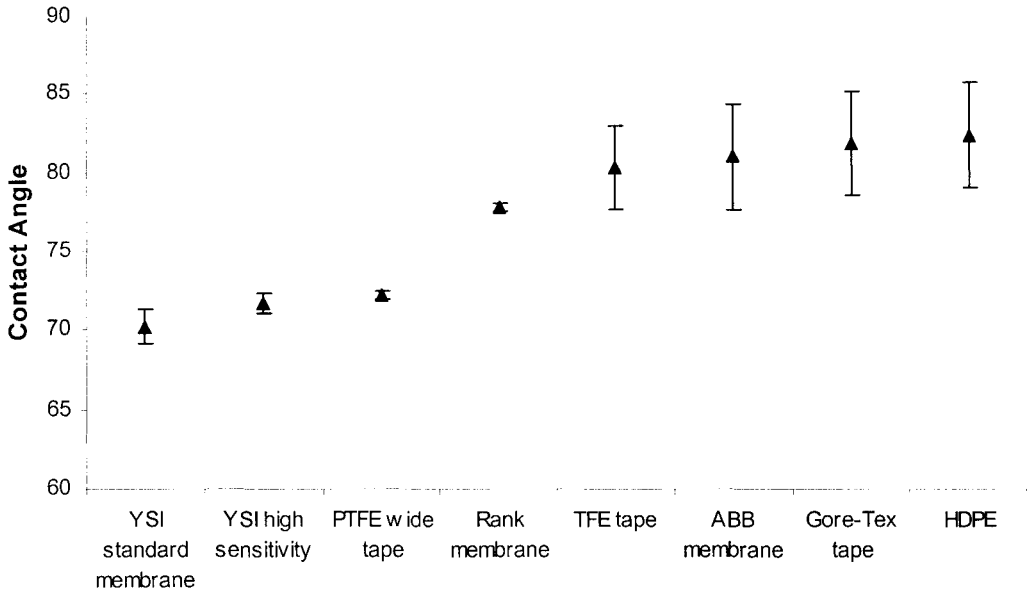

Fig. 5. Contact angles measured on gas membranes after 3 days soaking in seawater.

Oxygen diffusion vs fouling

The results recorded for the oxygen diffusion experiments on fouled membrane materials show extensive scatter for each material. This is indicative of the heterogeneous nature of the biofouling.

Only four of the materials examined Rank Bros. PTFE, YSI standard, YSI high sensitivity and the HDPE were tested on the dissolved oxygen meters. The other materials were not suitable for use on the Rank Bros. instruments. Since table 1 shows the other materials were substantially thicker. The inability to achieve acceptable readings from the instruments was due largely to the material thickness preventing an equilibrium concentration being achieved. It is worth noting, however, that the four materials suitable for use on the instruments were the four materials that did not show any visible features on the SEM.

When the helium gas was introduced to the measurement chamber of the dissolved oxygen meter, the dissolved oxygen concentration did not decrease in a linear manner. As Figure 6 shows, the oxygen concentration initially falls quite rapidly and as the concentration falls, so to does the rate of de-oxygenation.

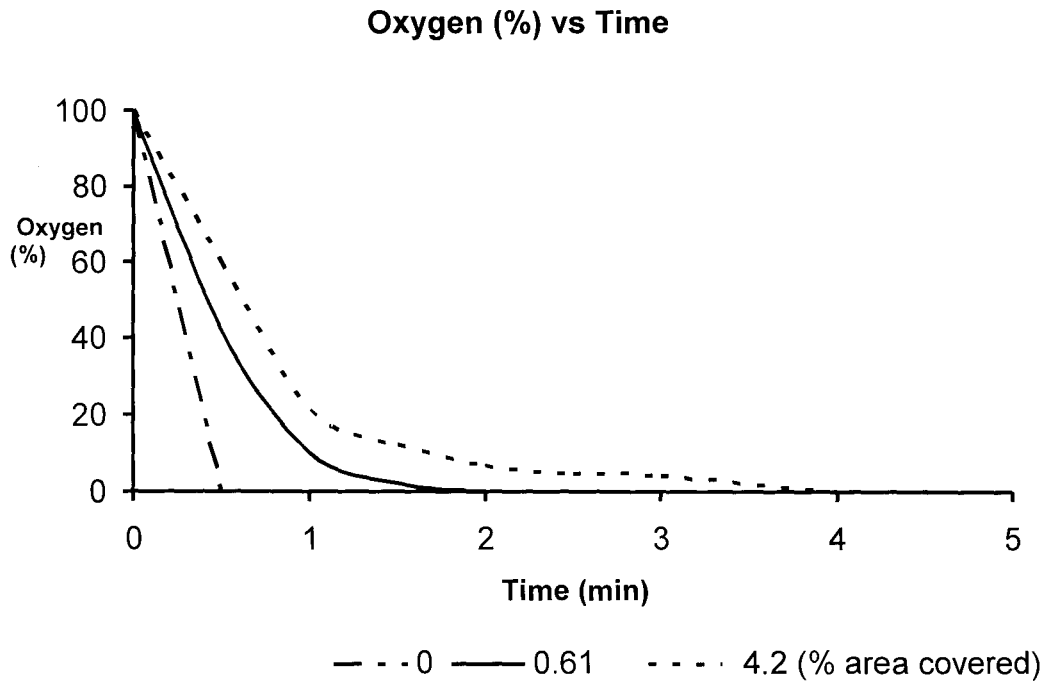

Fig 6. Reading of % oxygen against time since helium gas applied, for three samples of YSI standard PTFE, with different levels of biofouling on the surface.

Figure 6 also includes the different curves recorded from the same material (YSI standard thickness PTFE) with different levels of surface biofouling. As can be seen all samples gave curves of a similar general shape. However, it can also be seen that the increased response time, caused by greater levels of fouling, is present throughout the concentration range. Clearly, the difference becomes even more pronounced at low concentrations of dissolved oxygen. Figure 7 shows that all four materials exhibit an increasing response time for increasing fouling. For the Rank PTFE the time to zero increases to 11 minutes as the area fouled increases to 14.5% of the surface. The YSI standard membrane increases the time to zero to nine minutes as the fouling reaches 6% of the surface while the YSI high sensitivity membrane shows an increase in time to zero of 11½ minutes for a surface fouling of 10.5%. The HDPE has a time to zero of nine minutes for 6.5% surface fouling. The graphs in figure 7 shows that the relation between time to zero and area fouled corresponds approximately to a straight line for HDPE while the results for the Rank PTFE is definitely not a straight line. The Rank PTFE shows a more rapid increase in time to zero for the first 5% of surface fouling, subsequent fouling build-up has a less dramatic effect. The two YSI membranes do not show a clear pattern with the results presented here.

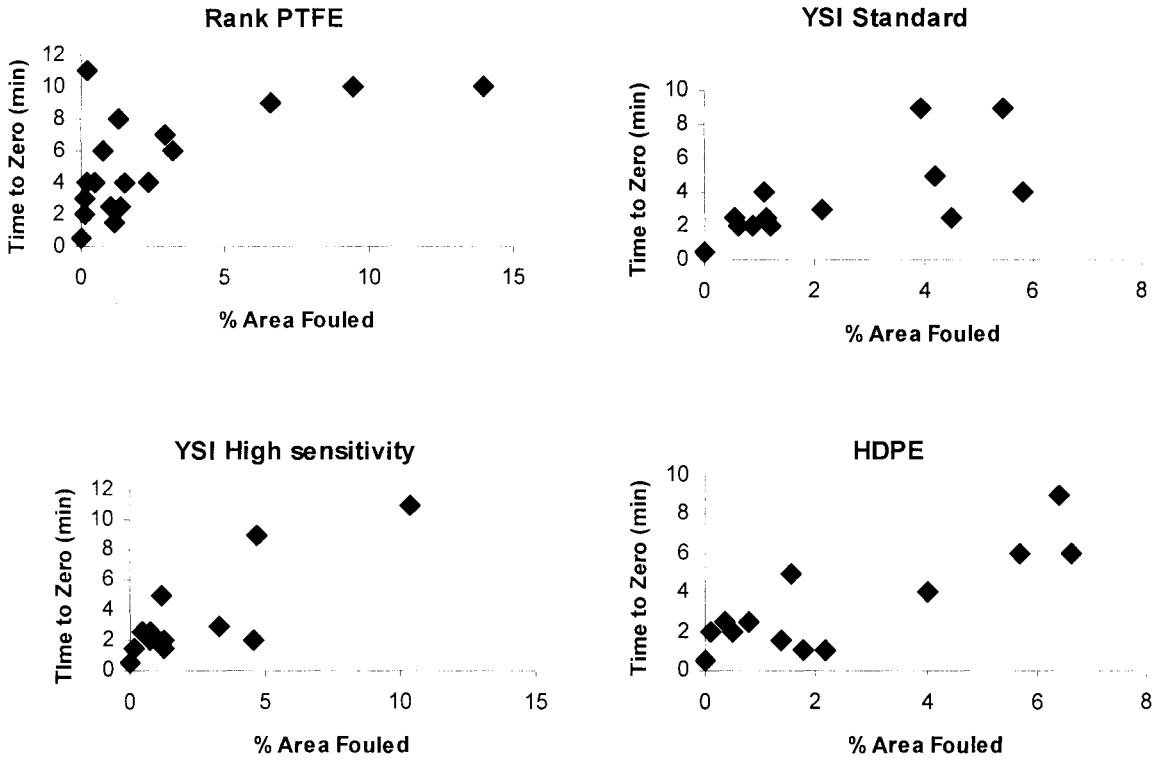

Fig. 7 Graphs for all four materials, of "Time to zero" for the dissolved oxygen meter against percentage surface fouling for each membrane sample.

One might expect that the initial attachment would have a disproportionate effect on the response time of the membrane. After fouling levels build up upon the surface, subsequent additional fouling would have a reduced effect on the response time. This expectation is due, at least in part, to the presence of extracellular polymeric substances (EPS) that are secreted by the bacteria and diatoms to aid their adhesion to the membrane (or any other surface). This EPS is not measured by the percentage area fouled results in Figure 7 since the EPS is not coloured by the Methelyne Blue stain. It could be expected that a considerable amount of EPS could adhere to the membrane, and disrupt the diffusion of oxygen, before any measurable biological fouling takes place. Furthermore subsequent EPS and biological fouling will not show any preference for the unfouled surface and so should, in part, become adhered to already contaminated areas of the surface. Fouling added to contaminated areas of the membrane would not contribute significantly to any further increase in response time. At first inspection, some results, especially the Rank Bros. PTFE appear to support this hypothesis. However some results do not. Figure 8 shows the results from all PTFE samples on the same graph (HDPE was not included since the different chemical combination would affect the fouling in unpredictable ways). Figure 9 shows the time to read zero plotted against the average percent surface fouling, for every time duration that had four or more results recorded from the three PTFE materials. This graph clearly shows that the increased response time appears to be

directly proportional to the amount of biological fouling measured on the material surface.

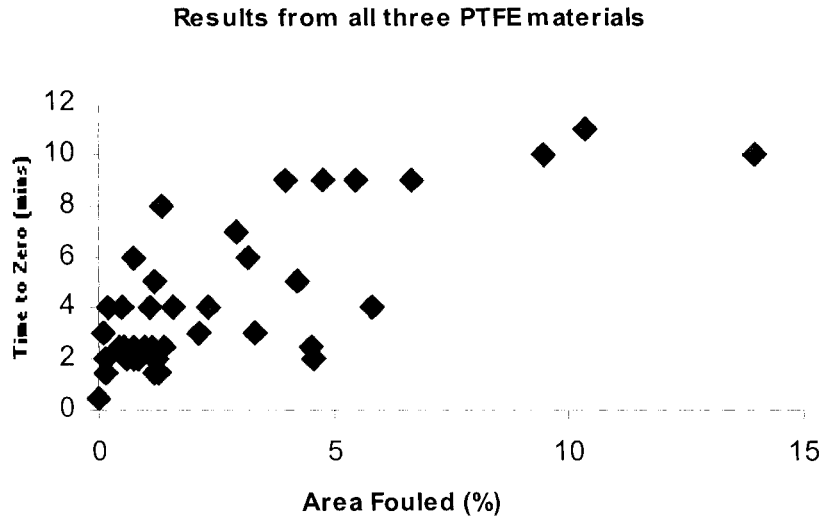

Fig 8. Combined "Time to Zero" against percentage area fouled for all three PTFE materials studied on the dissolved oxygen meter.

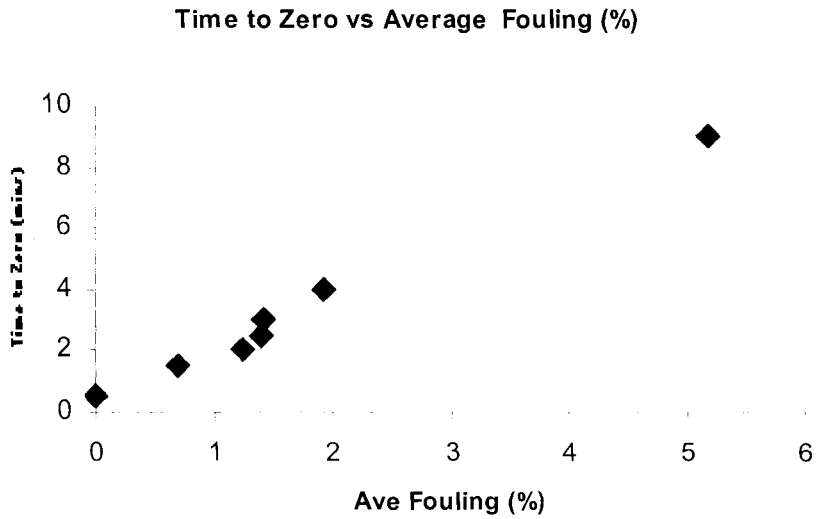

Fig.9 Time to zero values against average percentage fouling for all time to zero values for which four or more results were achieved using the PTFE materials.

The direct relationship between biological fouling and increased response time only holds at these low levels of surface fouling. It is probable that at higher levels of surface fouling the above hypothesis would hold. That is, once appreciable fouling has built up on the surface, subsequent fouling will have a reduced effect on the responsiveness of the sensor. The gradient of the best-fit line through the points in figure 9 is 1.63. This means that for every 1% surface covered by biological fouling

there is a 1.63 minute increase in the response time for a change from a fully saturated solution to an oxygen free solution.

Although the impact of surface roughness on fouling levels recorded here was less than might have been expected, it is still the case that the materials with the lowest surface roughness in table 3 – i.e. the two YSI materials – both recorded the lowest average fouling values of the materials tested. YSI standard thickness supported an average fouling level, as measured over all exposure time intervals, of 2.38% and the YSI high sensitivity material supported 2.41%. Both the other materials tested gave average fouling values of 2.61%. That the distinction was not greater for an order of magnitude change in surface roughness indicates that surface chemical properties of the materials are competent at resisting biofouling. However, it is to be expected that this is again only true at low fouling levels. Once more of the surface has become contaminated with EPS, the rougher surfaces will begin to support a greater mass of biofouling. The materials with a higher surface roughness can absorb a layer of EPS and remain rough enough to protect bacteria from the effects of flow across the membrane surface. The materials with lower surface roughness may find the EPS "fills" the surface imperfections leading to a surface that is "stickier" yet smoother and so is not as attractive to the micro-organisms.

Conclusions

The membranes tested did not prevent biofouling for extended periods of time, although there could be some advantages of choosing a membrane with a smoother surface and a small pore size such as the YSI membrane. It fouled to a lesser extent and thus the response time was less affected. The study demonstrated the physical differences in structure of PTFE membranes.

Acknowledgements

This work was grant aided by the European Commission through contract EVRI-CT-2002-40023 BRIMOM. This support is gratefully acknowledged. The authors would also like to thank Mr Ian Pedan for his help in the construction of the instrumentation used to measure contact angle. The AFM work was carried out by Marian Millar at Heriot-Watt University, Riccarton, Edinburgh, the authors wish to thank her.

References

1. D.V. Manov, G.C.Chang and T.D. Dickey, 2003, *J. Atmos. Ocean. Tech.*, 2003, **21**,958-968.

2. I. Tarsiche, E.Hopirtean and D. Ciurchea, *Meas. Sci. Tech.*, 1997, **8**, 1367-1371.

3. L.H.G. Morton, C.C. Gaylarde and S.B. Surman, *Int. Biodeterior. Biodegrad.*, 1998, **41**((3-4)), 247-259.

4. R.J. Doyle and M.Rosenburg, in *Microbial Cell Surface Hydrophobicity*, ed. J. Doyle and M.Rosenburg, American Society for Microbiology, Washington, 1990,ch.1, pp1-37.

5. N. Wisniewski and M. Reichert, *Colloids Surf., B* 2000, **18**, 197-219.

6. W. Munro, Thomas, C.L.P., Simpson, I., Shaw, J. J, Dodgson, *Sens. Actuators, B.*, 1996, **37**, 181-194.

7. P.M.A. Fraher and D.W. Clarke, *IEEE Trans. Instrum. Meas.* 1998, **47**, 686-691.

8. D. Marshallsay, *A Review of Sensor Fouling within Water Treatment Processes.* Water Research Centre Report No. 365E, 9-10, Swindon, 1989.

9. N. Wisniewski, F. Moussy, and W.M. Reichert, *Fresenius' J. Anal. Chem.*, 2000, **366**, 611-621.

10. D.Yebra, S. Kiil, and K. Dam-Johansen, *Prog. Organ. Coat.*, 2004, **50**(2), 75-104.

11. M. Kiremitci-Gumusderelioglu and A.Pesmen, *Biomaterials* 1996, **17**(4): 443-449.

12. J. Drelich, J.D. Miller and R.J. Good, *J. Colloid Interface Sci.*, 1996, **179**(1), 37-50

13. R. Fletcher, L.Lupelli, and A. Rossi, *Contact Lens Practice. A Clinical Guide.* Blackwell Scientific Publications, Oxford, 1994, ch. 3, pp17-32.

14. www.firsttenangstroms.com, Porstmouth, Virginia 23704, USA.

15. S. Tonge, L Jones, S.Goodall and B.Tighe, *Curr. Eye Res.*, 2001, **23**(1), 51-59.

16. S. McEldowey and M. Fletcher, *J. Gen. Microbio.*, 1986, **132**, 513-523.

17. A.Kerr, M.J. Cowling, C.M. Beveridge, M.J. Smith, A.C.S. Parr, R.M. Head, J. Davenport, T. Hodgkiess, *Environ. Internat.* 1998, **24**(3), 331-343.

18. G. F McEwen and C. E. Zobell, *Biol. Bull.,* 1935, **68**, 93-106.

19. J .H. Brauker, V.E Carr-Brendel, L.A Martinson, J.Crudele, W.D. Johnston, and R.C Johnson, *J. Biomed. Mater. Res.* 1995,**29**,1517-1524.

20. H. Huang, J. Zhang, X. Hao and Y. Guo, *Eur. Polym. J.,* 2004, **20**, 667-671.

21. R. Taylor, J. Verran, G.C. Lees, and A. J. P. Ward, *J. Mater. Sci. Mater. Med.* 1998, **9**(1): 17-22.

22. A. Whelan and F. Regan, *J. Environ. Monit*, 2006, **8**, 880-886.

23. A. Marmur, *Biofouling*, 2006, **22**,107-115.

24. M.L. Carman, T.G. Estes, A.W. Feinberg, J.F.Chumacher, W.Wilkerson, L.H.Wilson, M.E.Callow, J.A.Callow and A.B Brennan, *Biofouling.* 2006, **22,** 11-21.

25. R. Brady and I.L Singer, *Biofouling,* 2000,**15**(1-3), 73-81.

A Comparison of Methods used to quantify Marine Biofilms on Biofouling Resistant Hydrogel Coatings

M. J. Smith [a*], P. Cowie [b], F. Hannah [b], M. J. Cowling [a] and T. Hodgkiess [a].

[a] Glasgow Marine Technology Centre, University of Glasgow, Glasgow, G12 8QQ, UK.

[b]University of London, Marine Biological Station Millport, Isle of Cumbrae, Scotland, KA28 OEG, UK.

*Corresponding author. E-mail: m.smith@mech.gla.ac.uk Tel +44 (0) 141 330 4336 Fax +44 (0) 141 330 4343

Abstract

This study details the outcome of using five biofouling quantifying techniques on novel hydrogel coatings. Hydrogel coatings are used as biofouling resistant coatings to protect optical ports of underwater instruments and cameras in the marine environment and extend the useful deployment lifetime of these instruments by 12-16 weeks in temperate waters. In order to determine how these coatings eventually fail to prevent biofouling growth, it is important to be able to quantify biofouling accurately at its various stages. The techniques used were fluorescein diacetate hydrolysis, chlorophyll *a* analysis, micro-Lowry protein quantification, INT-Formazan staining of bacteria and diatom counts. The advantages and disadvantages of using these techniques are discussed. This work demonstrates that marine biofouling on hydrogel surfaces is patchy with variable community composition. Therefore no single method of quantifying biofouling will be conclusive. To obtain the maximum amount of information about the biofouling on hydrogel coatings it is necessary to use a range of quantitative techniques.

Keywords: Marine biofilm; hydrogel; cationic surfactant; quantitative methods; coating materials; biofouling.

1. Introduction

The increased use of marine underwater sensors and cameras in the latter decade of the twentieth century has led to improved and robust instruments, which can be deployed in coastal areas, from remote buoys and from ocean going research vessels. The data from these instruments is used in operational forecasting, environmental monitoring and to investigate climatic change. Scientific data need to be sampled at relatively high frequencies and accuracies for long periods of time, with minimal drift from predeployment calibrations (Manov et al., 2004). Instruments such as transmissometers, turbidity meters, fluorimeters and cameras collect data using optical windows. These windows are subject to biofouling, which limits the maintenance-free periods of data collection. This paper addresses the application of quantitative biofouling techniques to a novel coating that acts as a reservoir for antifouling chemicals - the coating is a hydrogel, poly–(hydroxyethyl methacrylate), pHEMA, with an equilibrium water content of 40%. This polymer coating has been developed at the Glasgow Marine Technology Centre (Cowling et al., 1998). It is a transparent polymer, which transmits light above 270nm and is therefore applicable to the majority of optical instruments. The hydrogel material has a macroporous structure allowing it to be easily loaded with water-soluble fouling resistant chemicals and, consequently, these pores allow the active chemicals to diffuse to the coating surface preventing biofilm formation (Wisniewski and Reichert, 2000). The hydrogels used here are loaded with the cationic surfactant benzalkonium chloride (BAC).

One application of such hydrogel polymers is in the protection of optical instruments. Marine underwater sensors and cameras are used to measure light transmission, turbidity, fluorescence and for imaging (Cowling et al., 1998). However, due to biofouling of the optical ports of these instruments and consequent signal degradation, they are typically deployed for limited periods only. It has been demonstrated that relatively low levels of fouling can have serious consequences, in terms of signal reduction (Kerr et al., 1998).

Hydrogels were originally developed for use in medical applications (Rejofo, 1966). They are widely used in soft contact lens manufacture, medical implants and as drug reservoirs and are therefore subject to a range of biofouling environments. Due to their extensive use in the biomedical field, many methods of quantifying biofilms have been used such as direct bacterial counts, indirect counts, and assessment of biofilm metabolic or physiological activities (Smith et al., 2002). *In vivo* medical biofilms may frequently occur as bacterial monocultures or be dominated by one species. However, in the marine environment biofilms are typically composed of many diverse species representing not only bacteria but also algae and protozoa (Brown and Gilbert, 1993). Thus the problem facing researchers in quantifying marine biofilms on antifouling hydrogels, especially in terms of bacteria, is different from that faced by researchers in other fields of biofilm detection.

Great advances have been made in the last decade in developing techniques for the quantification of biofilms in industrial, medical and ecological applications (Bakke et al., 2001). These include techniques used for the determination of the structure of biofilms (Paulsen et al., 1997; Khoury et al., 1992), and the composition of extracellular polymer secretions (EPS) (Neu et al., 2001; Strathmann et al., 2002). Additionally, molecular techniques have been developed which enable the characterisation of bacteria within certain biofilms (Dang and Lovell, 2000;

Thurnheer et al., 2004). Despite these advances, in routine trials determining the marine antifouling properties of paints, coatings or surfaces, researchers may not have access to the complex instrumentation required for some of these methods. Consequently, relatively basic techniques are still used to quantify the microfouling organisms present on these materials. This is because of their ease of use, low cost and the ability to process large numbers of test coupons quickly.

Using these basic techniques to quantify microfouling on any new antifouling substance requires an assessment of the efficacy of these techniques for the new application. It also serves as a revaluation of the usefulness of these basic techniques when used for biofilm assessment.

The aim of this study was to assess the usefulness of different techniques commonly used to quantify marine biofilm components when applied to biofouling resistant hydrogels. Assessment of biofilms on these hydrogels is difficult because the hydrated nature of their structure means that it is preferential to measure biofilm formation on hydrated hydrogels to avoid artefacts that may result from the drying process. The techniques chosen for this particular application were aimed at quantifying microfouling (bacteria, diatoms and associated products). They included direct (Int-formazan staining of bacteria and diatom counts) and indirect techniques (fluorescein diacetate (FDA) hydrolysis, chlorophyll *a* analysis and micro-Lowry protein quantification) and were chosen for their ease of use, relatively low cost and informative nature.

2. Materials and methods:

2.1. Techniques used

Indirect techniques were fluorescein diacetate (FDA) hydrolysis, chlorophyll *a* analysis and micro-Lowry protein quantification. Direct techniques included INT-Formazan staining of bacteria and diatom counts. These techniques are described below.

Fluorescein diacetate (3', 6' – diacetyl-fluorescein) (FDA) hydrolysis has been used to assess microbial activity in marine (Gurnprecht et al., 1995; Poremba, 1995) and in freshwater sediments (Battin, 1997). It has also been used to quantify biofouling on hydrogel coatings (Smith et al., 2002). Fluorescein diacetate, a colourless ester, is hydrolysed by both free (exoenzymes) and membrane bound enzymes associated with microfouling organisms. The resultant fluorescein is an acid, yellow in colour, and can be measured by spectroscopy at a wavelength of 490nm.

Chlorophyll *a* extraction and quantification has been extensively used as a surrogate indicator of the abundance of photosynthetic organisms in marine phytoplankton (Tett and Wallis, 1978; Strom et al., 2001) and on hard surfaces (Thompson et al., 1999). It is chosen for its ease of use and provides a directly comparable measure of primary productivity between different seasons and habitats.

Proteins associated with bacterial cells are routinely extracted and quantified by microbiologists (Guerlava et al., 1998; Kämpfer, 1995). Diatoms also have a considerable protein component associated with their walls (e.g. frustulins, pleuralins) and cellular components (Zurzolo and Bowler, 2001). This protein component varies according to species, nutritional state and age but can range from 6 to 70% of the dry weight of the cell (Fogg, 1975; Brown et al., 1997). Another

biofilm component, EPS, secreted by many biofilm-forming bacteria and diatoms can contain lesser quantities of protein in the form of exoenzymes, glycoproteins and amino sugars (Sutherland, 1983; Paulsen et al., 1978). This information suggests that with biofilm maturation and development protein components will increase and that subsequent quantification of this can be used as an indication of biofilm development.

Direct counts of diatoms are routinely used in marine phytoplankton studies to assess their abundance within environmental samples (e.g. Holligan and Harbour, 1977; Hannah and Boney, 1983).

INT (2-(p-iodophenyl)-3-(p-nitrophenyl)-5-phenyl tetrazolium chloride has been used to estimate the percentage of actively metabolising microorganisms in physiological and ecological studies (Smith and McFeters, 1997). The applications of the technique range from estimating microbial respiratory activity in freshwater bacterioplankton (Posch et al., 1997) to terrestrial litter environments (Stubberfield and Shaw, 1990). The reduction of INT and production of dark-red non-fluorescent crystals within the bacterial cells indicates electron transport activity, and microorganism metabolism.

2.2 Hydrogel preparation and marine deployment

The hydrogels used were transparent and contained 40% water. They were prepared in 250 mm x 200 mm poly- methyl methacrylate (PMMA) moulds to a thickness of 1-2 mm then stored in distilled water until required. The details of their preparation can be found elsewhere (Smith, 1997, Refojo, 1966). Three hydrogel sheets were prepared for this trial and were soaked in 5% benzalkonium chloride (BAC) solution for three weeks prior to the marine exposure trial. Zero time analysis of the benzalkonium chloride (BAC) levels in the hydrogels was carried out using high performance liquid chromatography (HPLC) ultra-violet detection at 214 nm (Guilfoyle et al., 1990). BAC was extracted from the hydrogels by swelling them in methanol to extract the BAC (Smith, 1997). Analysis showed that 5.4±0.19 % w/w BAC was present in each sheet with no significant differences between them.

The 3 sheets were cut into 12 smaller hydrogel samples (60 x 80 x 1 mm). These 12- samples were attached to a polymethylmethacrylate (PMMA) rack in a 3 by 4 arrangement. Each hydrogel sample was fixed to the rack using templates and stainless steel screws. For identification purposes, hydrogel samples were designated a number from 1-12, going from right to left and descending down the rack (Fig. 1). The rack was immersed in a seawater tank at University Marine Biological Station Millport (UMBS), Isle of Cumbrae, Scotland. The tank used was 20m x 10m x 2m, constructed from concrete and refilled from the Firth of Clyde over a four-hour period during local high tides. The rack was removed from the tank after 3 months to allow sufficient quantifiable fouling to occur on the hydrogels. Following rack retrieval sub-samples were removed from each 60 x 80 mm main sample for subsequent laboratory analysis.

2.3 Sub-sampling procedure and laboratory analysis

Figure 1 shows the sub-sampling scheme employed. Five core-samples (25 mm diameter) were removed from each numbered hydrogel using a precision-machined cutter, and taking care not to disrupt the biofilms on the hydrogel surfaces. One of these sub-samples was used for the quantification of BAC remaining in the

gels and the other four cores were used for each biofilm quantification technique. Samples were also taken from the PMMA rack surrounding the edges of the hydrogel samples to act as controls. Two adjacent samples were taken (Fig.1) by scraping the equivalent core-size area from the PMMA. One was used as a protein control and the other for chlorophyll *a* analysis.

2.4 BAC quantification

The amount of BAC remaining in the 12 core samples was determined using methanol extraction and quantification using HPLC analysis with ultra-violet detection at 214 nm as described previously (Guilfoyle et al., 1990).

2.5 Biofilm quantification

2.5.1 FDA analysis

Estimation of marine biofilm activity was carried out using a modification of the Adam and Duncan (2001) method. One core was cut from each hydrogel section (60 x 80 mm) and placed into individual 60 ml glass powder jars. Fifteen millimetres of 60 Mm potassium phosphate buffer pH 7.6 (8.7 g K_2HPO_4: 1.3 g KH_2PO_4) made up to 1 l in deionized water was added to each jar and 0.2 ml of 1000 µg fluorescein diacetate (3'6'- diacetyl-fluorescein, Sigma-Aldrich Co. Ltd) ml^{-1} acetone solution added to start the reaction. Jars were then placed in an orbital incubator (Gallenkamp orbital incubator, 1000 rev min^{-1}) at 10°C ± 1°C for 1 hour. Once removed from the incubator, the 25 mm diameter cores were taken out of the buffer/FDA solution and 15 ml of chloroform/methanol (2:1 v/v) added immediately to terminate the hydrolysis reaction. Jars and their contents were then shaken thoroughly by hand and the contents of each jar were filtered (Whatman, No. 2) into 100 ml conical flasks. Filtrates were measured at 490 nm on a spectrophotometer (Schimazdu UV-visible 2101PC spectrophotometer). Blanks from each treatment were used to zero the spectrophotometer before reading the sample absorbency. The concentration of fluorescein released during the assay was calculated using the calibration graph produced from 0-5 µg fluorescein ml^{-1} standards, which were prepared from a 20 µg fluorescein (sodium salt, Merck-BDH, Analar) ml^{-1} standard solution by appropriate dilution in 60 mM potassium phosphate buffer pH 7.6.

2.5.2 Protein extraction

Biofilms were removed from the 12 core sub-samples using sterile cell-scrapers and placed into separate, sterile sample tubes containing 5 ml of phosphate buffered saline (PBS). Control samples were scraped from the PMMA into 5 ml of PBS. Samples suspended in PBS were sonicated (Sonics & Materials Ultrasonic processor equipped with a 5 mm tapered microtip, 375-watt nominal power output) on ice for 3 x 60 seconds to disrupt bacterial and diatom cells and solubilise proteins. Sonicated samples were centrifuged at 13000 rpm at 4°C. Supernatant was removed and placed into another sterile tube. Subsequent precipitation and quantification of soluble proteins was carried out using a commercially available micro-Lowry protein assay kit (Sigma Diagnostics), which incorporates a protein calibration curve. Samples removed from the PMMA rack as controls were diluted 5 times following

protein precipitation because the protein levels present in these samples were potentially beyond the linear range of the assay.

2.5.3 Chlorophyll a extraction

The protocol used for chlorophyll *a* quantification followed the methods of Parsons et al. (1984). Cores used for direct counting were scraped (using a sterile scraper) into acetone-resistant test tubes containing 10 ml of acetone. 0.1 ml of magnesium carbonate was added to the sample to prevent acidification and samples placed into a dark freezer for 48 hours to stabilize the chlorophyll *a* pigments while extraction was taking place. Samples were removed after 48 hours, shaken vigorously and centrifuged at 2000 rpm, 0°C, for 4 minutes. Pigment concentration was estimated using an LKB Biochrom spectrophotometer (Model: Ultrospec 4050). 5 ml of cleared supernatant was placed into acetone washed 1-cm light path spectrophotometer cuvettes and 90% acetone used as the reference standard. Extract extinction was measured at 665 and 750 nm before and after acidification with 10% hydrochloric acid. Each 750 nm reading was subtracted from the corresponding 665 nm extinction and the equations of Nusch (1980) were used to calculate the concentration of chlorophyll *a* in the sample.

2.5.4 Bacterial staining – Laboratory method development

In recognition of the problems involved in staining bacteria on hydrogels, a staining procedure was developed for the enumeration of bacteria on these hydrophilic surfaces. Tested stains included two simple stains (aqueous methylene blue and carboyl fuchsin) and the blue fluorescent nucleic acid stain, 4', 6-diamidino-2-phenylindole dihydrochloride (DAPI). Dyes were tested in the laboratory by incubating blank hydrogels (lacking antifoulant) in static containers with three biofouling bacterial strains isolated from biofilms in the Firth of Clyde, Scotland. Gram –ve tests using glass slides showed that incubation at 20°C, for 3 days in 2216 broth (DIFCO Ltd.) yielded bacterial numbers of ca. 1×10^{10} cells cm^{-2}.

Several samples of blank hydrogel were incubated in a mixed biofouling bacterial broth and stained after 3 days, using the different stains. Hydrogels were removed from the bacterial broth and gently rinsed with sterile filtered seawater (SFSW) to remove unattached bacteria. Rinsed hydrogels were placed in petri dishes containing SFSW and 2.5% gluteraldehyde as a fixative. Fixed samples were then stained with one of the three stains. DAPI stained samples were dark incubated for 30 minutes in DAPI (0.25 mg ml^{-1}) to ensure adequate staining (Porter and Feig, 1980). Samples were then rinsed with SFSW to remove excess DAPI. Samples to be simple stained were fixed, rinsed as described and stained for 2 minutes with either aqueous methylene blue (1 mg ml^{-1}) or carboyl fuchsin (10 % v/v) Samples were carefully rinsed with distilled water to remove excess stain and examined using either bright field (simple stains) or UV fluorescence microscopy (DAPI).

DAPI-stained bacteria were obscured by intense background staining of the hydrogel by non-bound DAPI. Similarly, simple-stained bacteria were not detected under bright field due to background staining. A common method of removing background staining is the use of ethanol to remove excess stain (Allison and Sutherland, 1984). This failed; because of the nature of the hydrogels they absorb ethanol and swell cracking the biofilm on the surface of the hydrogel, with little removal of artefactual staining.

It was assumed that because of the hydrophilic nature of the hydrogels testing of similar stains would end with the same result. A stain was required which would remain colourless or nearly so when present as background staining but would react selectively with bacteria to produce a visible end product. Bacterial respiratory activity has been studied in situ by the reduction of INT (2-(p-iodophenyl)-3-(p-nitrophenyl)-5-phenyltetrazolium chloride) into water-insoluble red formazan crystals within the bacteria (Posch et al., 1997, Stubberfield and Shaw, 1990). Prior to reduction to formazan INT is only weakly coloured and was therefore, seen as a possible method to use on the hydrogel biofilms.

Blank hydrogels were incubated in bacterial broth, as described previously, and after three days, samples were rinsed gently and incubated in 10 ml of filtered seawater with 1ml of 0.2% INT (SIGMA) added. Clean hydrogel samples were also incubated with INT to ensure there was no background reduction of INT by the hydrogels in the absence of bacteria. Samples were left to incubate for 1 hour at 10°C. After the incubation period, samples were removed from the INT, rinsed gently and examined under bright-field using immersion oil. All three bacterial morphologies (rods, short rods and cocci) were clearly visible and countable in the biofilm on the hydrogel surface.

It was recognised that these laboratory samples were 'clean' with regard to a lack of confounding organic material, extensive extracellular polymeric substances and other biofilm components and, consequently, that counts from field coupons may be more difficult. It was therefore decided that indirect bacterial quantification by extraction of formazan in ethanol and subsequent spectrophotometric measurement at 458 nm, following the method of Stubberfield and Shaw (1990) might be necessary. A calibration series using different dilutions of formazan (1-(4-iodophenyl)-5-(4-nitrophenyl)-3-phenylformazan) (Sigma) in ethanol was prepared and the absorbance measured at 458 nm. In order to relate formazan concentration to potential bacterial numbers in a meaningful way, the relationship between cell concentration and formazan production was assessed for the three-biofouling strains of bacteria, BF1, BRP and BRW. This information was used to translate the levels of INT extracted from field samples into approximate bacterial abundance.

2.5.5 Diatom counts

Hydrogel sub-samples used for direct diatom counts were placed in petri dishes containing sterile filtered seawater (to prevent drying out of hydrogels and associated biofilms) and counts performed directly using phase-contrast microscopy under x 200 magnification. Ten fields of view were counted per sample. Samples used for direct diatom counting were subsequently used for chlorophyll *a* extraction and analysis.

2.6 Data analysis

Data analysis was carried out using MINITAB version 13.1. Data are presented as mean values ± 95% confidence intervals. The degree of association (interdependence) between two chosen variables was estimated using the Pearson product-moment correlation coefficient. To use this analysis it is assumed that both variables come from an underlying normal distribution (Sokal and Rohlf, 1997). Data was tested for normality using the Anderson-Darling test.

3. Results

3.1 Rack appearance and BAC levels

The rack was removed after 3 months (Fig. 2) and extensive microalgal fouling was seen on the PMMA frame in contrast with the much reduced fouling on the hydrogels. Fouling on hydrogel test pieces was visible as green colouration; this was heterogeneously distributed within individual hydrogel samples and between each of the samples on the rack. At the end of the testing period mean BAC levels for the 12-hydrogel sub-samples were 1.37 ± 0.14 % BAC w/w from a starting value of 5.4 % w/w. The diffusion of BAC from hydrogel has been measured at various temperatures and salinities and is reported elsewhere (Smith et al., 2000). The release was found to be linear over the 12 weeks, the time period of this experiment, but after this time the hydrogel was no longer releasing BAC at a sufficient rate and it was unable to prevent biofouling (Smith et al., 2002).

3.2 Biofouling quantification analyses

Patchiness of fouling on the hydrogels was reflected in the results obtained by the different techniques. Values obtained for FDA analysis of the hydrogels ranged from 0.1 to 1.6 $\mu g\ ml^{-1}\ h^{-1}$ (Fig. 3). Smith et al. (2002) found a mean value, after 12 weeks marine deployment, of 1.2 ± 0.3 $\mu g\ ml^{-1}\ h^{-1}$ on hydrogels containing BAC. Mean protein levels of 22.9 ± 9.14$\mu g\ cm^{-2}$ were obtained from the hydrogels (Fig. 4). Much higher levels of protein, 53.9 ± 22.7 $\mu g\ cm^{-2}$ were extracted from control samples taken from the PMMA frame (Fig. 4).

Direct cell counting showed that the green heterogeneous patches observed on the hydrogel test pieces at the end of the trial were attributable not to epilithic diatoms but to an unidentified filamentous green algae which was anchored at the base and growing outwards from the hydrogel surface. Relatively few of this species had reached the filament stage and cells were counted separately. The mean numbers of algal cells found on the hydrogels ranged from 6.47×10^4 cells cm^{-2} to 1.48×10^4 cells cm^{-2} with a mean value of 3.71×10^4 cells cm^{-2} (Fig. 5). Distribution of these filamentous cells was very patchy over the hydrogel samples. No diatoms were visible in any of the 12 sub-samples counted. In contrast, non-quantitative sampling of the biofilm on the PMMA frame showed that a rich and diverse diatom assemblage was present in the areas adjacent to the antifouling surfaces. Low numbers of the unidentified filamentous green algae were also found on the PMMA frame.

Levels of chlorophyll *a* extracted from the hydrogel samples and adjacent PMMA frame are presented in Fig. 6. It is clear that the levels of chlorophyll *a* on the frame surface were consistently higher than the chlorophyll *a* extracted from the biofilms on the hydrogel surfaces. Mean levels of chlorophyll *a* on the hydrogels and PMMA controls were 0.36 ± 0.15 $\mu g\ cm^{-2}$ and 5.33 ± 3.84 $\mu g\ cm^{-2}$ respectively. Comparing the chlorophyll *a* levels obtained from the hydrogel surfaces with the counts of pigmented algal cells obtained for the same samples shows that there is a poor visual relationship between the two parameters. Samples where the lowest levels of chlorophyll *a* were recorded did not have corresponding low levels of algal cells (Fig. 5). This is supported by the lack of a significant correlation between chlorophyll *a* and the number of cells counted ($p > 0.05$, $r = 0.05$, $n = 12$).

3.2.1 INT-Formazan

Hydrogel sub-samples removed at the end of the trial period were INT stained and examined for formazan coloured bacteria. Examination of the stained sub-samples showed that in those regions free of organic material bacteria were freely visible and appeared to be dominated by small bacteria (< 1.5 μm), predominantly coccoid in shape. Bacterial numbers were high, and where countable reached densities of 1.63×10^{13} cells cm^{-2}. Extensive amounts of floc material were also attached to the hydrogels. Bacteria attached to this material were stained red but were commonly impossible to count because of masking by the floc material and the extremely high numbers of bacteria present. Consequently, formazan accumulated within bacteria was ethanol extracted and the resulting absorbencies compared with the biofouling mix calibration curves to give the approximate numbers of bacteria per subsample surface area. Using this technique, the results obtained are shown in Fig. 7. This shows that a high number of bacteria were present on the hydrogel samples with a mean value of $1.38 \times 10^{12} \pm 2.98 \times 10^{12}$ cells cm^{-2}.

4.0 Discussion

The methods used in this study are commonly used by researchers assessing the fouling of surfaces in the marine environment as part of antifouling studies. However, the use of hydrogels as reservoirs for antifouling substances in the marine environment is a relatively new phenomenon and the novel nature of hydrogel structure makes some aspects of biofilm quantification on this substrate a potentially different task than from that on other solid surfaces. Accurate assessment of early stages of biofouling is very important to enable an assessment of the antifouling mechanisms in process and appraisal of the applicability of existing techniques to novel materials is needed.

In this study there was an obvious reduction in the microfouling of the BAC - impregnated hydrogels when compared with the surrounding PMMA rack. The results show that there were generally higher levels of chlorophyll *a* and protein recorded in the sub-samples taken from the PMMA frame border when compared with samples taken from the adjacent hydrogels. This indicates that BAC impregnated hydrogels work well as an antifouling substance over the exposure period, as has been recorded in previous trials (Parr et al., 1998). Biofouling development both within and between individual hydrogel samples was heterogeneous.

Differences in microfouling between hydrogel samples were not due to uneven leaching of the BAC from the hydrogels, because there was no significant difference in BAC levels between the hydrogels at the end of the exposure period. Fouling heterogeneity on hydrogels and other surfaces has important implications for the techniques ultimately used to assess biofouling on those surfaces. Before a comparison of the different methods is made, the usefulness of the individual direct and indirect techniques used to quantify fouling on the surfaces of hydrogel structures can be discussed.

Fluorescein diacetate hydrolysis has been used successfully as an estimator of microbial biomass in a variety of different habitats (Adam and Duncan, 2001) and was also used successfully in this trial for estimating fouling levels on hydrogel surfaces. The range of biofilm FDA hydrolytic activity recorded on hydrogels was similar to that recorded in a previous study which developed the application of FDA

analysis for use on hydrogel biofilms. (Smith et al., 2002). This technique detected the visibly low levels of microfouling on the hydrogels and the results also reflected the observed heterogeneity on the gels. The advantages of using FDA hydrolysis to quantify microfouling on the hydrogel surfaces include its simplicity, rapidity and sensitivity (Prieto et al., 2004). However, FDA is a non-specific method –and does not distinguish between organisms and therefore cannot reflect community composition.

Chlorophyll *a* extraction is a commonly used technique for the quantification of photosynthetic organism biomass. Results from this technique give overall estimates of the biomass of the biofilm community, but little information about the species present, from which the chlorophyll is extracted. In this instance, the chlorophyll *a* readings obtained would be assumed to reflect the abundance of unicellular diatoms present on the hydrogels. However, direct microscopy showed that the microalgal fouling on the hydrogels was different from that on the surrounding control frame. Hydrogel communities were dominated by a single species of multicellular algae and the PMMA by a diverse and natural diatom community. Microalgal community differences between the test hydrogel samples and PMMA were due to the mode of action of benzalkonium chloride which has been shown to have an algistatic effect on some marine diatoms and an algicidal effect on others (Beveridge et al., 1998). BAC levels in the hydrogels were still high enough at the end of the trial to prevent the development of a unicellular algal community, but insufficient to prevent the growth of the much more resilient multicellular green algae which dominated the photosynthetic communities on hydrogels.

Quantification of hydrogel biofilm components using protein extraction and micro-Lowry determination was a novel application of this method. It yielded consistent results with the highest levels of protein being recorded on the control PMMA rack and, as such, is a potentially useful technique to quantify biofilms on hydrogels. However, this technique requires an approximate knowledge of the protein levels likely to occur within the biofilm samples, to enable those levels to be adjusted so that they fall within the range of the protein assay method used. This problem would be further complicated if sample time-series were undertaken (a common technique in biofouling research). Effective biofilm quantification using protein analysis relies on complete and consistent protein extraction. In mixed biofilms containing diatoms and bacteria this may be hard to achieve. The long sonication times required to disrupt resilient diatom frustules and effectively liberate their protein components may result in the denaturation of proteins liberated from less resilient bacterial biofilm components. While it has some potential, biofouling researchers may see this indirect method as being too time-consuming a procedure for the routine quantification of microbial biofilm on hydrogels.

The assessment techniques utilised to directly assess bacterial fouling on hydrogels had a different set of pros and cons. Direct counting of stained bacteria on biofouled surfaces is useful because it enables direct comparisons of bacterial abundance between studies and gives an indication of the distribution of bacteria on the substrate surface and whether the antifoulant used has a specific action against certain bacterial forms. The chemical and physical nature of pHEMA hydrogels has a direct influence on the staining techniques that can be used to enumerate bacteria on these materials. In this study, the basic-staining and fluorescence (DAPI) techniques commonly used to enumerate bacteria (McFeters et al., 1999) proved to be ineffective because of the hydrophilic nature of the hydrogels which meant that, in

addition to bacterial staining, there was significant background staining which obscured the bacteria. Typical extraction techniques used to remove background staining failed because of the chemical nature of the hydrogel. Application of the INT-staining technique proved to be partially successful. In the laboratory, bacterial biofilms were stained clearly, enabling bacteria to be enumerated. Field-samples proved more problematic for direct counting, this was a consequence of the layers of organic material, which were observed to have built up on the hydrogels during the trial period. This occurred because of the mode of action of BAC-impregnated hydrogels. Benzalkonium with a bactericidal and algicidal action is released consistently over the exposed hydrogel surface for a period up to three months. During this time organic material accumulates on the hydrogel surface with no bacterial degradation. However, when the bactericidal/algicidal action of the hydrogel starts to fail as a result of reduced concentrations of BAC diffusing to the surface, bacteria exploit the abundant nutrients represented by this organic material. This means that bacteria containing INT-Formazan crystals were obscured in places by the high quantities of organic material present and necessitated ethanol extraction and comparison with the extracted INT from laboratory trials/bacteria. Similarly, Rodriquez et al. (1992) found that the INT reduction method was appropriate for single cells (or small aggregates) on filters but was not adapted for the analysis of optically dense biofilms. Where more mature bacterial biofilms on hydrogels need to be quantified, the use of the companion tetrazolium salt CTC (5-cyano-2,3-ditolyl tetrazolium chloride) may obviate some of the problems involved in conducting light microscopy on dense biofilm communities. When reduced in bacterial cells CTC forms a fluorescent formazan, which is visualised using epifluorescence microscopy (Posch et al., 1997; Smith and McFeters, 1997).

5. Conclusions

This study shows that careful consideration should be taken before a method of quantifying microfouling on pHEMA hydrogels is chosen. Direct diatom counting and the novel application of INT staining techniques are best suited for the assessment of initial biofilm formation on hydrogels, where there are lower levels of organic detritus and organisms present than are found in mature biofilms. These techniques provide important information about the general distribution and composition of the early microfouling community.

In this study, the use of the indirect techniques (FDA, chlorophyll *a* and protein analysis) was suited to quantifying mature biofilms, which had developed over a 13 week period. These methods (by their nature) sample a larger surface area of the substrate, thereby reducing the small-scale heterogeneity of fouling within individual hydrogels and enabling more reliable comparisons of the degree of fouling between different hydrogel samples to be made.

This work has demonstrated that marine biofouling on hydrogel surfaces is patchy with variable community composition. Therefore no single method of quantifying biofouling will be conclusive. The techniques used will depend on the question being addressed. If knowledge of the small-scale distribution of microfouling is required, direct-counting techniques are applicable. For the quantification of more mature biofouling, indirect techniques should be used. To obtain the maximum amount of information about the biofouling on hydrogel coatings it is necessary to use a range of quantitative techniques.

Acknowledgements

This work was grant aided by the European Commission through contract EVRI-CT-2002-40023 BRIMOM. This support is gratefully acknowledged.

References

Adam, G., Duncan, H. J., 2001. Development of a more sensitive and rapid method for the measurement of total microbial activity using Flourescein Diacetate (FDA) in a range of soils. Soil Biology Biochemistry 33, 943-951.

Allison, D.G., Sutherland, I.W., 1984. A staining technique for attached bacteria and its correlation to extracellular carbohydrate production. Journal of Microbiological Methods 2 (2), 93-99.

Bakke, R., Kommedal, R., Kalvenes, S., 2001. Quantification of biofilm accumulation by an optical approach: Journal of Microbiological Methods 44, 13 - 26.

Battin, T. J., 1997. Assessment of fluorescein diacetate hydrolysis as a measure of total esterase activity in natural stream sediment biofilms. Science of the Total Environment 198, 51 – 60.

Beveridge, C.M., Parr, A.C.S., Smith, M.J., Kerr, A., Cowling, M.J., Hodgkiess, T., 1998. The effects of benzalkonium chloride concentration on nine species of marine diatom. Environmental Pollution 103, 31-36.

Brown, M. R.W., Gilbert, P., 1993. Sensitivity of biofilms to antimicrobial agents. Journal of Applied Bacteriology Symposium Supplement 74, 87S-97S.

Brown, M.R., Jeffrey, S.W., Volkman, J.K., Dunstan, G.A., 1997. Nutritional properties of microalgae for mariculture. Aquaculture 151, 315-331.

Cowling, M. J., Hodgkiess, T, Parr, A. C. S., Smith, M. J., Kerr, A., Beveridge, C. M., Clegg, M., Menlove, R., 1998 The Effects of Biofouling on Imaging Underwater, including Possible Remedies, Proceedings Underwater Optics III, Applied Optics and Optoelectronics, Institute of Physics, Brighton, March 1998.

Dang, H., Lovell, C. R., 2000. Bacterial colonization and early succession on surfaces in marine waters as determined by amplified rRNA gene restriction analysis and sequence analysis of 16s rRNA genes. Applied Environmental Microbiology 66(2), 467 - 475.

Fogg, G.E., 1975. Algal cultures and phytoplankton ecology. The University of Wisconsin Press, Wisconsin.

Guerlava, P. V., Izac, Tholozan J. L., 1998. Comparison of different methods of cell lysis and protein emeasurments in Clostridium perfringens: Application to the cell volume determination. Current Microbiology 36,131-135.

Guilfoyle, D.E., Roos, R., Carito, S.L., 1990. An evaluation of preservative adsorption onto nylon. Journal of Parental Science and Technology 44, 314-319.

Gumprecht, G., Gerlach, H., Nehrkorn, A., 1995. FDA hydrolysis and resazurin reduction as a measure of microbial activity in sediments from the southeast Atlantic. Helogoländer Meeresuntersuchungen 49, 189-199.

Hannah, F.J., Boney, A.D., 1983. Nanophytoplankton in the Firth of Clyde, Scotland: seasonal abundance, carbon fixation and species composition. Journal of Experimental Marine Biology and Ecology 67,105-147.

Holligan, P.M., Harbour, D.S., 1977. The vertical distribution and succession of phytoplankton in the Western English Channel in 1975 and 1976. Journal of the Marine Biological Association. U. K. 57, 1075-1093.

Kerr, A., Head, R.M., Cowling, M.J., Davenport, J., Beveridge, C.M., Smith, M.J., Parr, A.C.S. and Hodgkiess, T., 1998. The early stages of marine biofouling and its effect on two types of optical sensors. Environmental International 24 (3), 331-343.

Kämpfer, P., 1995. An efficient method for preparation of extracts from gram-positive bacteria for comparison of cellular protein patterns. Journal of Microbiological Methods 21, 55 – 60.

Khoury, A. E., Nicholov, R., Soltes, S., Bruce, A.W., Reid, G., Dicosmo, F., 1992. A preliminary assessment of Pseudomonas aeruginosa biofilm development using fluorescence spectroscopy. International Biodeterioration and Biodegradation 30, 187 - 199.

Lowry, O.H., Rosebrough, N.J., Farr, A. L, Randall, R.J., 1951. Protein measurement with the Folin Phenol reagent, Journal of Biological Chemistry 193, 265-275.

Manov, D.V., Chang, G.C., Dickey, T.D., 2004. Methods for reducing biofouling of moored optical sensors. Journal of Atmospheric and Oceanic Technology 21,958-968.

McFeters, G.A., Pyle, B.H., Lisle, J.T., Broadaway, S.C., 1999. Rapid direct methods for enumeration of specific, active bacteria in water and biofilms. Journal of Applied Microbiology Symposium Supplement 85, 193S-200S.

Neu, T. R., Swerhone, G. D. W., Lawrence, J.R., 2001. Assessment of lectin-binding analysis for in-situ detection of glycoconjugates in biofilm systems: Microbiology 147, 299-313.

Nusch, E.A., 1980. Comparison of different methods for chlorophyll and phaeopigment determination. Advances in Limnology 14, 14 – 36.

Parr, A.C.S., Smith, M.J., Beveridge, C.M., Kerr, A., Cowling, M.J., Hodgkiess, T., 1998. Optical assessment of a fouling-resistant surface (PHEMA/Benzalkonium Chloride) after exposure to a marine environment. Advanced Materials for Optics. and Electronics 8, 187-193.

Parsons, R.T., Maita, Y., Lalli, C.M., 1984. A manual of chemical and biological methods for seawater analysis. New York: Pergamon Press Ltd.

Paulsen, B.S., Haug, A., Larsen, B. 1978. Structural studies of a carbohydrate containing polymer present in the mucilage tubes of the diatom *Berkeleya rutilans* (Trent.) Grun. Carbohydrate Research. 66, 103-111.

Paulsen, J.E., Oppen, E., Bakke, R.1997. Biofilm morphology in porous media, a study with microscopic and image techniques. Water Science and Technology 36(1), 1-9.

Porter, K.o.G., Feig, Y.S., 1980. The use of DAPI for identifying and counting aquatic microflora. Limnology and Oceanography 25 (5), 943-948.

Poremba, K., 1995. Hydrolytic enzymatic activity in deep-sea sediments. FEMS Microbiology and Ecology 16, 213-222.

Posch, T. J., Pernthaler, A., Alfreider, J., Psenner, R., 1997. Cell-specific respiratory activity of aquatic bacteria studied with the tetrazolium reduction method, cyto-clear slides, and image analysis. Applied Environmental Microbiology 63, 867-873.

Prieto, B., Silva, B., Lantes, O., 2004. Biofilm quantification on stone surfaces: comparison of various methods. Science of the Total Environment 333, 1-7.

Refojo, M.F., 1965. Permeation of water through some hetrogeneous hydrophilic membranes. Journal of Applied Polymer Science 10, 185-190.

Smith, J.J., McFeters, G. A., 1997. Mechanisms of INT (2-(4-iodophenyl)-3-(4-nitrophenyl)-5-phenyl tetrazolium chloride) and CTC (5-cyano-2,3,-ditolyl tetrazolium chloride) reduction in Escherichia coli K-12. Journal of Microbiological Methods 29, 161-175.

Smith, M.J, 1997. The Use of Cationic Surfactants in Marine Anti-fouling applications. *M.Sc. Thesis*, University of Glasgow.

Smith, M.J., Flowers, T.H., Parr, A.C.S., Cowling, M.J., Hodgkiess, T., 2000. Salinity and temperature effects on the release of benzalkonium chloride from hydrogel material. Polymers and Polymer Composites 8, 101-105.

Smith, M.J., Adam, G., Duncan, H.J., Cowling, M.J., 2002. The effects of cationic surfactants on marine biofilm growth on hydrogels. Estuarine, Coastal and Shelf Science 55, 361-367.
Sokal, R.B., Rohlf, F.J., 1995. Biometry. Freeman, New York.

Strathmann, M., Wingender, J., Flemming, H.C., 2002. Application of fluorescently labelled lectins for the visualization and biochemical characterization of polysaccharides in biofilms of *Pseudomonas aeruginosa*. Journal of Microbiological Methods 50, 237-248.

Strom, S.L., Brainard, M.A., Holmes, J.L.,Olson, M.B., 2001. Phytoplankton blooms are strongly impacted by microzooplankton grazing in coastal North Pacific waters. Marine Biology 138, 355-368.

Stubberfield, L.C.F., Shaw, P.J.A., 1990. A comparison of tetrazolium reduction and FDA hydrolysis with other measures of microbial activity: Journal of Microbiological Methods 12, 151-162.

Sutherland, I.W., 1983. Microbial exopolysaccharides - their role in microbial adhesion in aqueous systems. Critical Reviews in Microbiology 10, 173-200.

Tett, P., Wallis, A., 1978. The general annual cycle of chlorophyll standing crop in Loch Creran. Journal of Ecology 66, 227-239.

Thompson, R.C., Tobin, M.L., Hawkins, S.J., Norton, T.A., 1999. Problems in extraction and spectrophotometric determination of chlorophyll from epilithic microbial biofilms: towards a standard method. Journal of the Marine Biological Association U.K 79, 551-558.
Thurnheer, T., Gmür R., Guggenheim, B., 2004. Multiplex FISH analysis of a six-species bacterial biofilm. Journal of Microbiological Methods 37-47.

Wisniewski, N. and Reichart M., 2000. Methods for reducing biosensor membrane biofouling. Colloids and Surfaces B: Biointerfaces 18, 197-219.

Zurzolo, C., Bowler, C., 2001. Exploring bioinorganic pattern formation in diatoms. A story of polarized trafficking. Plant Physiology 127, 1339–1345.

Descriptions of Figures

Fig. 1. Lay out of PMMA frame containing BAC impregnated hydrogels, indicating sample labelling, with inset showing position of sub-samples taken for separate analyses. (F = FDA; I = INT; B = BAC; P = Protein; C = Chlorophyll *a*).

Fig. 2. Hydrogels in PMMA frame after 3 months marine exposure, showing the patchiness of biofilm development within and between hydrogel samples.

Fig. 3 Levels of fluorescein detected after 3 months marine exposure.

Fig. 4. Levels of protein extracted from biofilms on hydrogel sub-samples and PMMA frame after 3 months marine exposure.

Fig. 5. Number of pigmented algal cells counted on hydrogel surfaces compared with chlorophyll *a* levels obtained from the same samples.

Fig. 6. Levels of chlorophyll *a* extracted from biofilms obtained from hydrogel sub-samples and control samples taken from the PMMA frame after 3 months of marine exposure.

Fig. 7. Bacterial abundance on hydrogel field samples after 3 months marine exposure.

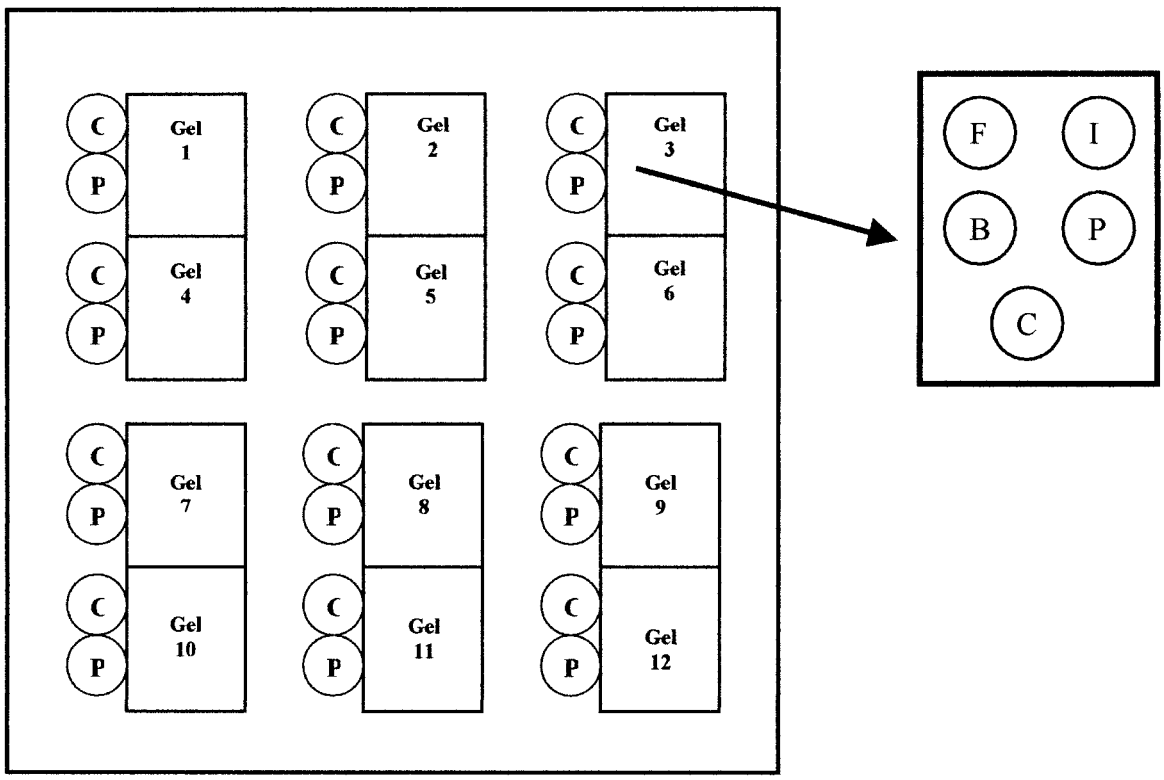
C
P
Gel 1
Gel 2
Gel 3
Gel 4
Gel 5
Gel 6
Gel 7
Gel 8
Gel 9
Gel 10
Gel 11
Gel 12
F
I
B
P
C

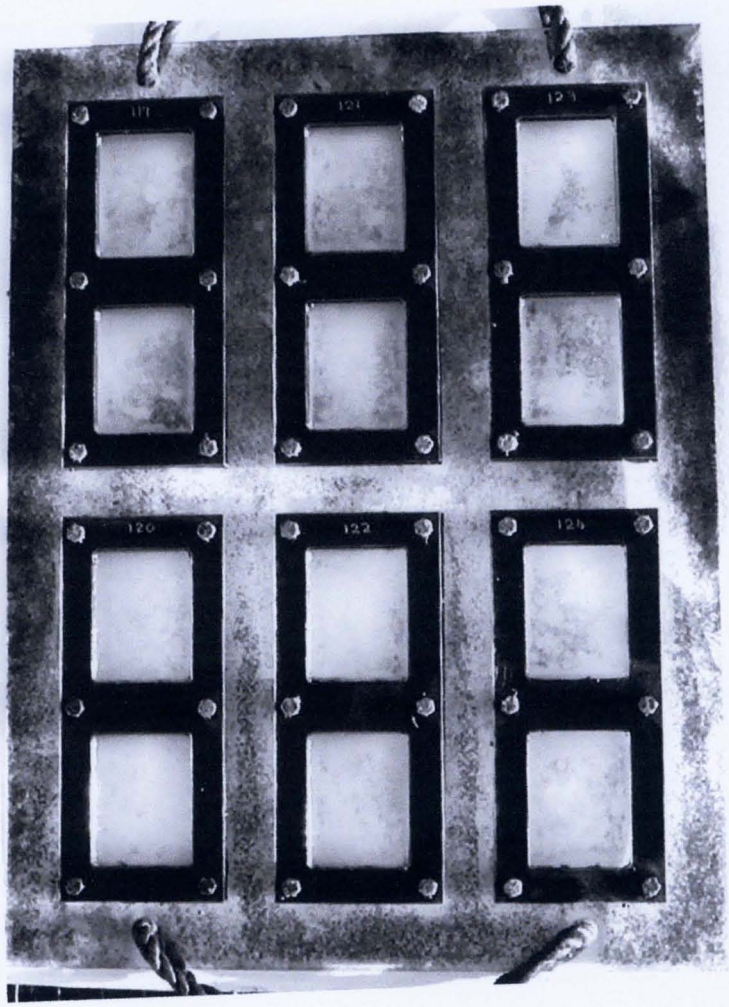
121
120
122

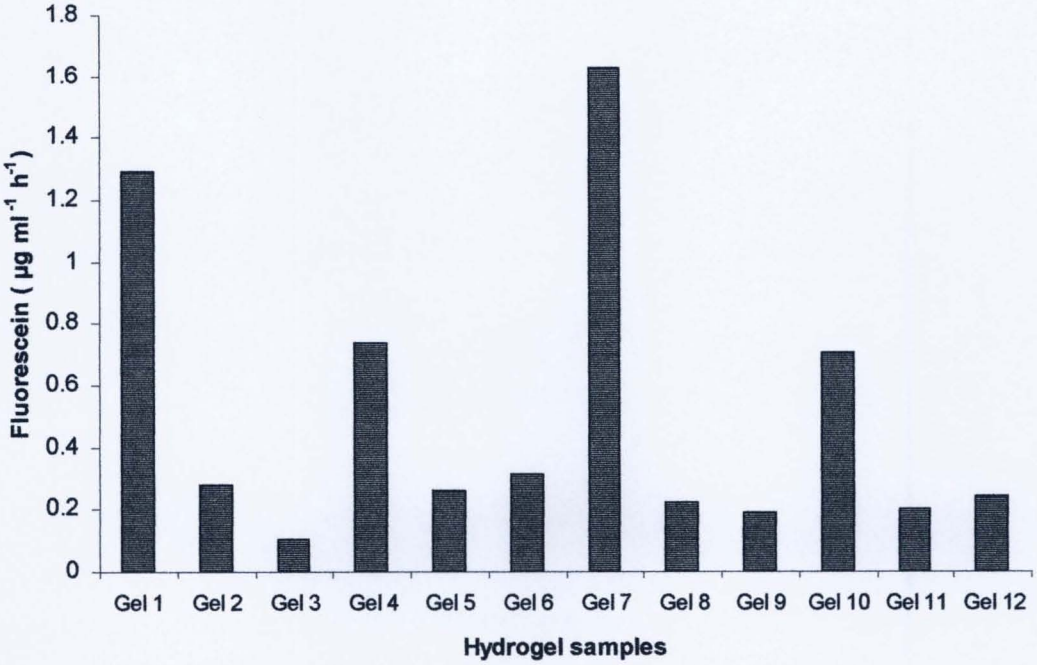
1.8
1.6
1.4
1.2
1
0.8
0.6
0.4
0.2
0
Fluorescein (µg ml-1 h-1)
Gel 1
Gel 2
Gel 3
Gel 4
Gel 5
Gel 6
Gel 7
Gel 8
Gel 9
Gel 10
Gel 11
Gel 12
Hydrogel samples

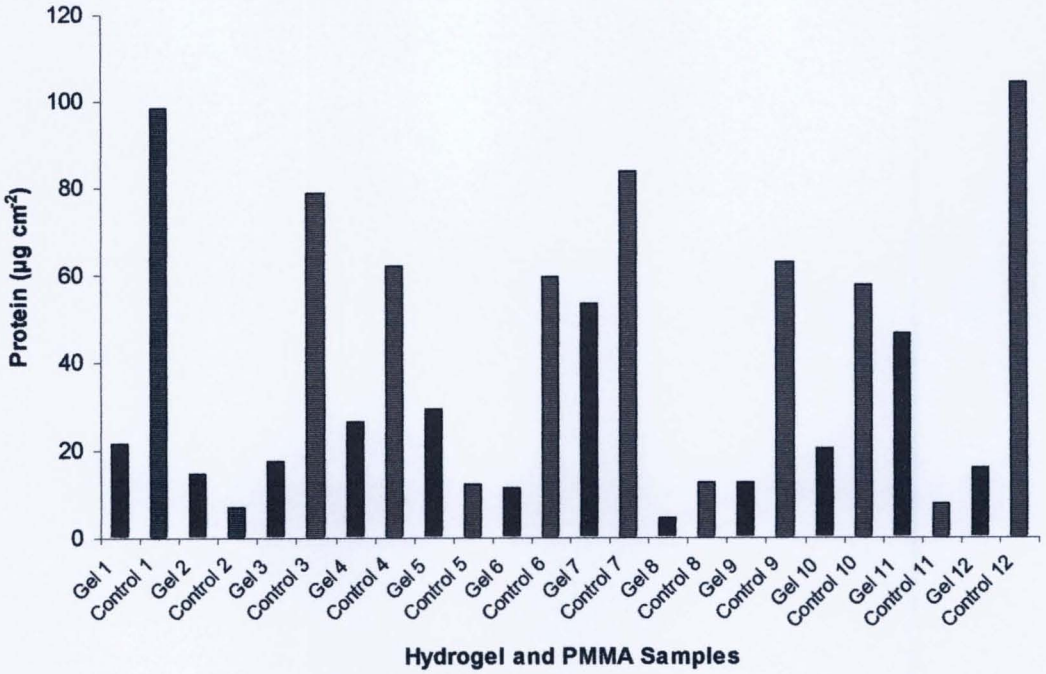
120
100
80
60
40
20
0
Protein (µg cm-2)
Gel 1
Control 1
Gel 2
Control 2
Gel 3
Control 3
Gel 4
Control 4
Gel 5
Control 5
Gel 6
Control 6
Gel 7
Control 7
Gel 8
Control 8
Gel 9
Control 9
Gel 10
Control 10
Gel 11
Control 11
Gel 12
Control 12
Hydrogel and PMMA Samples

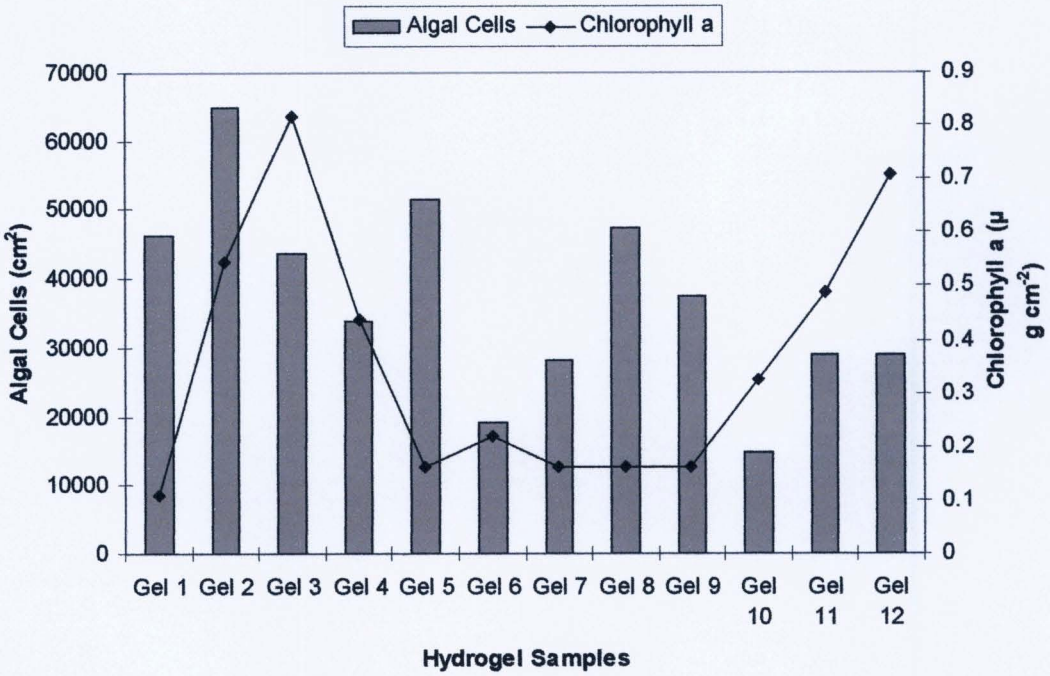
Algal Cells
Chlorophyll a
70000
60000
50000
40000
30000
20000
10000
0
0.9
0.8
0.7
0.6
0.5
0.4
0.3
0.2
0.1
0
Algal Cells (cm2)
Chlorophyll a (µ g cm-2)
Gel 1
Gel 2
Gel 3
Gel 4
Gel 5
Gel 6
Gel 7
Gel 8
Gel 9
Gel 10
Gel 11
Gel 12
Hydrogel Samples

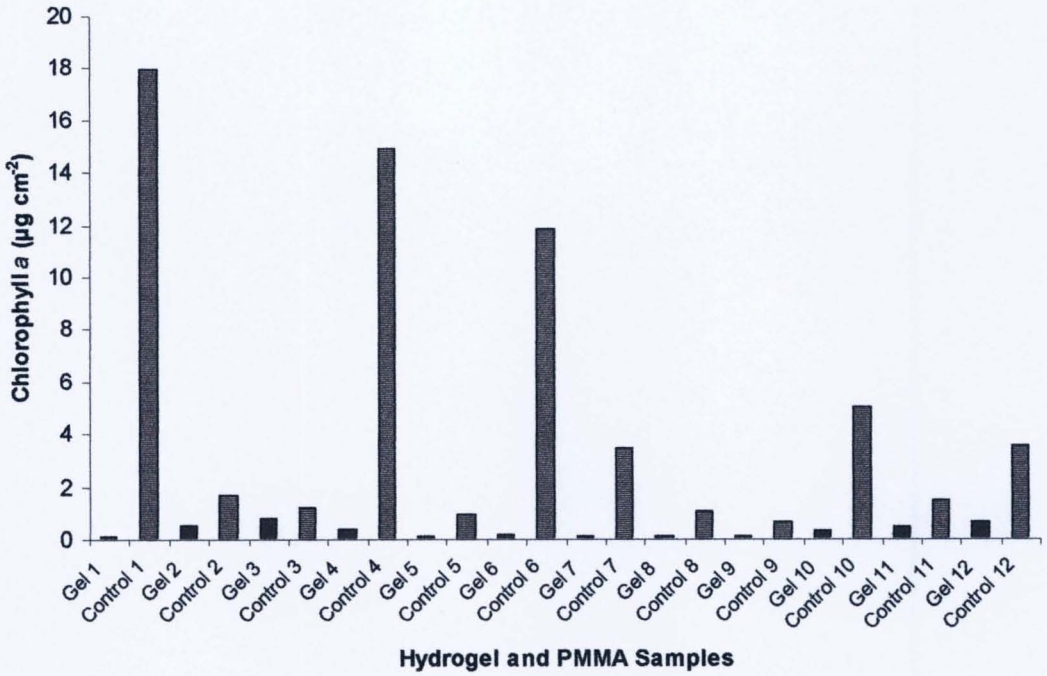
Chlorophyll a (µg cm-2)
20
18
16
14
12
10
8
6
4
2
0
Gel 1
Control 1
Gel 2
Control 2
Gel 3
Control 3
Gel 4
Control 4
Gel 5
Control 5
Gel 6
Control 6
Gel 7
Control 7
Gel 8
Control 8
Gel 9
Control 9
Gel 10
Control 10
Gel 11
Control 11
Gel 12
Control 12
Hydrogel and PMMA Samples